MULTIDISCIPLINARY APPROACHES IN EXPLORING CANCER HETEROGENEITY, TME AND THERAPY RESISTANCE: PERSPECTIVES FOR SYSTEMS MEDICINE

EDITED BY: Brigitte M. Pützer, Kanaga Sabapathy and Julio Vera González
PUBLISHED IN: Frontiers in Cell and Developmental Biology

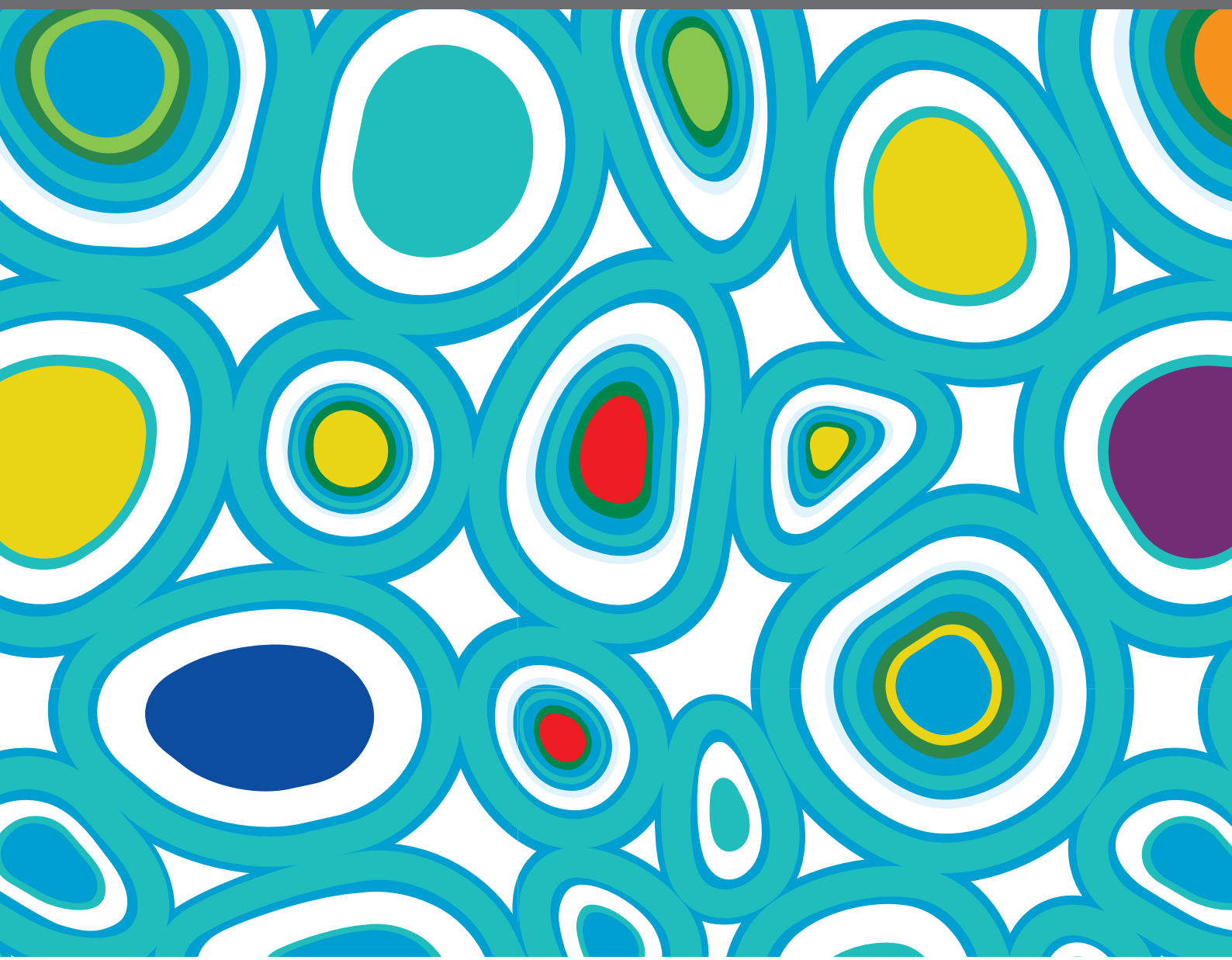

frontiers Research Topics

frontiers

Frontiers eBook Copyright Statement

The copyright in the text of individual articles in this eBook is the property of their respective authors or their respective institutions or funders. The copyright in graphics and images within each article may be subject to copyright of other parties. In both cases this is subject to a license granted to Frontiers.

The compilation of articles constituting this eBook is the property of Frontiers.

Each article within this eBook, and the eBook itself, are published under the most recent version of the Creative Commons CC-BY licence. The version current at the date of publication of this eBook is CC-BY 4.0. If the CC-BY licence is updated, the licence granted by Frontiers is automatically updated to the new version.

When exercising any right under the CC-BY licence, Frontiers must be attributed as the original publisher of the article or eBook, as applicable.

Authors have the responsibility of ensuring that any graphics or other materials which are the property of others may be included in the CC-BY licence, but this should be checked before relying on the CC-BY licence to reproduce those materials. Any copyright notices relating to those materials must be complied with.

Copyright and source acknowledgement notices may not be removed and must be displayed in any copy, derivative work or partial copy which includes the elements in question.

All copyright, and all rights therein, are protected by national and international copyright laws. The above represents a summary only. For further information please read Frontiers' Conditions for Website Use and Copyright Statement, and the applicable CC-BY licence.

ISSN 1664-8714
ISBN 978-2-88974-580-7
DOI 10.3389/978-2-88974-580-7

About Frontiers

Frontiers is more than just an open-access publisher of scholarly articles: it is a pioneering approach to the world of academia, radically improving the way scholarly research is managed. The grand vision of Frontiers is a world where all people have an equal opportunity to seek, share and generate knowledge. Frontiers provides immediate and permanent online open access to all its publications, but this alone is not enough to realize our grand goals.

Frontiers Journal Series

The Frontiers Journal Series is a multi-tier and interdisciplinary set of open-access, online journals, promising a paradigm shift from the current review, selection and dissemination processes in academic publishing. All Frontiers journals are driven by researchers for researchers; therefore, they constitute a service to the scholarly community. At the same time, the Frontiers Journal Series operates on a revolutionary invention, the tiered publishing system, initially addressing specific communities of scholars, and gradually climbing up to broader public understanding, thus serving the interests of the lay society, too.

Dedication to Quality

Each Frontiers article is a landmark of the highest quality, thanks to genuinely collaborative interactions between authors and review editors, who include some of the world's best academicians. Research must be certified by peers before entering a stream of knowledge that may eventually reach the public - and shape society; therefore, Frontiers only applies the most rigorous and unbiased reviews.
Frontiers revolutionizes research publishing by freely delivering the most outstanding research, evaluated with no bias from both the academic and social point of view. By applying the most advanced information technologies, Frontiers is catapulting scholarly publishing into a new generation.

What are Frontiers Research Topics?

Frontiers Research Topics are very popular trademarks of the Frontiers Journals Series: they are collections of at least ten articles, all centered on a particular subject. With their unique mix of varied contributions from Original Research to Review Articles, Frontiers Research Topics unify the most influential researchers, the latest key findings and historical advances in a hot research area! Find out more on how to host your own Frontiers Research Topic or contribute to one as an author by contacting the Frontiers Editorial Office: frontiersin.org/about/contact

MULTIDISCIPLINARY APPROACHES IN EXPLORING CANCER HETEROGENEITY, TME AND THERAPY RESISTANCE: PERSPECTIVES FOR SYSTEMS MEDICINE

Topic Editors:
Brigitte M. Pützer, Institute of Experimental Gene Therapy and Cancer Research, University Medicine, Germany
Kanaga Sabapathy, National Cancer Centre Singapore, Singapore
Julio Vera González, University Hospital Erlangen, Germany

Citation: Pützer, B. M., Sabapathy, K., González, J. V., eds. (2022). Multidisciplinary Approaches in Exploring Cancer Heterogeneity, TME and Therapy Resistance: Perspectives for Systems Medicine. Lausanne: Frontiers Media SA.
doi: 10.3389/978-2-88974-580-7

Table of Contents

frontiers in Cell and Developmental Biology

EDITORIAL
published: 03 February 2022
doi: 10.3389/fcell.2022.842596

Editorial: Multidisciplinary Approaches in Exploring Cancer Heterogeneity, TME and Therapy Resistance: Perspectives for Systems Medicine

Brigitte M. Pützer[1,2]* *and Kanaga Sabapathy*[3,4]

[1]Institute of Experimental Gene Therapy and Cancer Research, Rostock University Medical Center, Rostock, Germany, [2]Department Life, Light & Matter, University of Rostock, Rostock, Germany, [3]Division of Cellular and Molecular Research, Humphrey Oei Institute of Cancer Research, National Cancer Centre Singapore, Singapore, Singapore, [4]Cancer and Stem Cell Biology Program, Duke-NUS Medical School, Singapore, Singapore

Keywords: cancer heterogeneity, tumor immune microenvironment, development and homeostasis, cancer evolution, p53 family transcription factors, phenotypic plasticity, computational methods and data mining, biomarkers and personalized therapeutics

Editorial on the Research Topic

Multidisciplinary Approaches in Exploring Cancer Heterogeneity, TME and Therapy Resistance: Perspectives for Systems Medicine

OPEN ACCESS

Edited and reviewed by:
Ramani Ramchandran, Medical College of Wisconsin, United States

***Correspondence:**
Brigitte M. Pützer
brigitte.puetzer@med.uni-rostock.de

Specialty section:
This article was submitted to Molecular and Cellular Pathology, a section of the journal Frontiers in Cell and Developmental Biology

Received: *23 December 2021*
Accepted: *12 January 2022*
Published: *03 February 2022*

Citation:
Pützer BM and Sabapathy K (2022) Editorial: Multidisciplinary Approaches in Exploring Cancer Heterogeneity, TME and Therapy Resistance: Perspectives for Systems Medicine. Front. Cell Dev. Biol. 10:842596. doi: 10.3389/fcell.2022.842596

Despite significant advances that have shattered previous dogmas about the causes of tumor metastasis, the development of therapies to treat or prevent aggressive disease progression has not kept pace and remains the most important challenge. Cancer heterogeneity, to a large extent accounting for the incomplete and temporary efficacy of current anticancer measures, is still poorly understood at the molecular level. While early tumor stages are shaped by the accumulation of driver mutations, advanced cancers have a number of key adaptations or hallmarks that can contribute to metastasis (Birkbak and McGranahan, 2020).

Coherences between epithelial-mesenchymal transition (EMT) and the emergence of cancer stem cells highlight that the metastatic process is driven by epigenetic programming that involves short and long non-coding RNAs (Meier et al., 2016; Wang et al., 2016; Logotheti et al., 2020a). These events are usually cell- or tissue-specific and regulated at different developmental stages or in response to extracellular stimuli (Vanharanta and Massagué, 2013; Khan et al., 2017). Furthermore, combinatorial *de novo* activation of multiple distinct and developmentally distant transcriptional modules appears to be a recurrent mechanistic pattern (Rodrigues et al., 2018). In this regard, co-option of programs of tissue homeostasis and normal embryonic development, including off-context expression of tissue-restricted genes or reactivation of cell differentiation pathways in the cancer context (Logotheti et al., 2020b) emerge as predictors of poor patient outcome across various cancers. Another layer of heterogeneity and complexity that promotes disease progression arises from reciprocal cross-talks of cancer cell subpopulations with cellular and molecular components of the tumor microenvironment (TME) which massively influences the treatability of metastasis-prone cancer cells.

The p53 family of transcription factors (p53, p63, p73) that includes tumor suppressor proteins and their N-terminally truncated or mutant isoforms, is critically important for orchestrating the above processes. They cover a wide range of non-oncogenic and oncogenic functions by switching duties depending on the cellular and molecular background (Vikhanskaya et al., 2007; Crum and McKeon 2010;

Toh et al., 2010; Steder et al., 2013; Vera et al., 2013; Engelmann and Pützer 2014; Dulloo et al., 2015; Engelmann et al., 2015; Nemajerova et al., 2018; Melino, 2020; Wang et al., 2020; Rozenberg et al., 2021).

This Research Topic creates a conceptual framework for systems medicine approaches using information from multiple disciplines, such as developmental biology, cancer research and tumor immunology, to understand disease phenotypes based on common mechanisms and in an integrative manner. A total of 11 articles were received, of which 6 are original research and 5 are review articles.

Based on latest achievements in the field, suggesting that cancer acquires metastatic potential and evolves via co-opting gene regulatory networks of embryonic development and tissue homeostasis frequently conserved among species, Marquardt et al. focused on tumor evolution, specifically on metastatic potential in relation to organismal evolution. The authors analyzed the first appearance of tumors and the transition between non-metastatic and metastatic tumors during the evolution of phylogenetic taxa using bioinformatic tools in species-specific cancer phenotypes, multi-omics data, developmental phenotypes of knockout mice, and molecular phylogenetics. This systems-based approach provides evidence that the presence of metastasis coincides with agnatha-to-gnathostome transition, and that genes indispensable for jaw development are co-opted in tumor progression. The in-silico pipeline developed here enables prediction of putative metastatic drivers and targeting of evolutionary traits in the evolving tumor.

The relevance of lncRNAs in competing endogenous RNA (ceRNA) mechanisms and cancer regulatory networks is addressed by Zhang et al. This study highlights the effects of lncRNA somatic mutations in miRNA response elements on the expression of target mRNAs (ceM) and how this affects tumor heterogeneity. Multivariate multiple regression models showed a significant effect of 162 high-frequency mutations on the expression of ceMs and low-frequency mutations resulted in perturbation of 1624 ceMs in pan-cancer. The authors provide data underlining the impact of lncRNA mutations on changes in oncogenic functions and patient survival.

Other excellent contributions investigate context-specific mechanisms of treatment resistance, with emphasis on immunotherapy to define markers for improved responses and clinical need in different cancer settings but mainly melanoma. Considering the potentially essential role of tumor-associated B (TAB) cells in T cell-based anti-tumor immunity, Chen et al. explored the developmental changes of B cells during melanoma progression. By using seven color multiplex immunohistochemistry and automated tissue imaging, the authors analyzed the six major B cell and antibody secreting cell (ASC) subpopulations and their spatiotemporal dynamics in whole tumor sections of a large set of human melanoma samples. Their data point to a metastasis-, tumor stage-, and age-associated distribution of subpopulations with decreased memory-like TAB in metastasizing primary melanomas, but increased numbers at locoregional metastatic sites, and an enrichment for plasmablast and plasma cell-like ASC at distant metastatic sites.

The work of Lai et al. is dedicated to the improvement of dentritic cell (DC)-based vaccines in the tumor microenvironment. Authors constructed a multi-compartment Ordinary Differential Equation model representing different stages of DC immunotherapy, such as spreading and bio-distribution of intravenously injected DCs, biochemical reactions regulating DC maturation and activation, and DC-mediated T cell activation to analyze DC- and T cell-associated molecules and signaling pathway predicting the optimal targets for enhancing DC bioactivity and melanoma-specific cell therapy. Their key finding is that modulating the NF-kB inhibitor IκBα may improve differentiation of memory T (Tmem) cells.

Toy et al. uncover molecular markers of cancer radioresistance based on high-throughput gene expression data. They applied a bioinformatics approach using different methods and computational pipelines to publicly available transcriptome datasets. Results show a set of 36 differentially expressed genes primarily linked to DNA damage repair, oxidative stress, and apoptosis in common radioresistant-relevant pathways. These findings and their value as potential diagnostic markers or therapeutic targets can be validated by *in vivo* experimental studies to improve treatment outcomes.

Furthermore, several cutting-edge review articles provide an updated overview of the roles of p73, p53 and p63 as key drivers of phenotypic and functional plasticity in the context of cellular reprogramming, tissue remodeling and cancer progression, connecting intracellular events with complex and dynamic microenvironments. Focusing on published genome-wide studies, Woodstock et al. outline recent findings of a cooperative, instead of the originally known, competing interplay between p53 and Δp63, and explore how p53 family members that share common binding sites and target genes coordinate their effects on cell fate.

Laubach et al. highlight the impact of non-canonical functions of p53 family proteins in a plethora of biological processes, and refer specifically to studies that demonstrate the roles of p53, p63, and p73 in lipid and iron metabolism. Lipids are important for many cellular functions including structure, signaling, and the inflammatory response, as pointed out by recent publications. Authors discuss the similarities and differences of all three proteins in regulating these metabolic processes and their relevance to disease.

The function of p73 beyond its well-established tumor suppression effect is comprehensively addressed in the review of Maeso-Alonso et al. They summarize latest evidence for the role of p73 as a tissue architect that governs the organization and homeostasis of different microenvironments, supporting processes like multiciliogenesis, hippocampal neurogenesis, and spermatid development. This function is considered to be a conserved trait inherited from the p63/p73 hybrid-like gene ancestor at the beginning of epithelial tissue evolution tracing back to Placozoans and Cnidaria. Via integration of ChIP- and RNA-seq data, studies analyzed are further linked to their own data on p73-mediated regulation of cytoskeletal dynamics, corroborating their hypothesis.

Focusing on the structure and variegated functions of p73 isoforms, the work of Logotheti et al. characterizes the significance of TP73 in controlling development and differentiation, and how this activity can be hijacked during cancer progression or in the tumor microenvironment, with emphasis on neoneurogenesis as emerging cancer hallmark. Using melanoma as a paradigm, they provide new insight into molecular mechanisms underlying the pleiotropic effects of p73

based on the nature of p73 isoforms, the presence of interactors, the architecture of target promoters, and subcellular localization. The authors envision that dysregulation of one or more of these parameters in tumors promote aggressive metastatic stages by reactivating p73 isoforms and/or p73-regulated differentiation programs, in a spatiotemporally inappropriate manner.

Interdisciplinary work and the combination of wet- and dry-lab skills are ideal requirements for future translational research. The contributions collected in this Research Topic provide deeper insights into cancer etiology, molecular mechanisms, heterogeneity, and the role of the tumor microenvironment in metastasis. This will influence the development of individualized next-generation cancer therapeutics. Moreover, advances in biomaterial and 3D cell culture technologies like spheroids, organoids, and organs-on-chip techniques are opening new opportunities for testing patient-specific therapies.

AUTHOR CONTRIBUTIONS

BMP wrote the editorial with the input from KS.

FUNDING

This research was funded by the German Cancer Aid (Deutsche Krebshilfe 70112353), the German Research Foundation (DFG PU188/17-1), the German Federal Ministry of Education and Research e:Med MelAutim (BMBF 01ZX1905D), the European Union Structural Fund (ESF/14-BM-A55-0026/18-A01) (BMP), and by the National Research Foundation, Prime Minister's Office, Singapore under its Investigatorship Research Programme (NRF-NRFI2015-07), the National Medical Research Council of Singapore and the NCCS Cancer Fund (KS).

REFERENCES

Birkbak, N. J., and McGranahan, N. (2020). Cancer Genome Evolutionary Trajectories in Metastasis. *Cancer Cell* 37 (1), 8–19. doi:10.1016/j.ccell.2019.12.004

Crum, C. P., and McKeon, F. D. (2010). p63in Epithelial Survival, Germ Cell Surveillance, and Neoplasia. *Annu. Rev. Pathol. Mech. Dis.* 5, 349–371. doi:10.1146/annurev-pathol-121808-102117.20078223

Dulloo, I., Phang, B. H., Othman, R., Tan, S. Y., Vijayaraghavan, A., Goh, L. K., et al. (2015). Hypoxia-inducible TAp73 Supports Tumorigenesis by Regulating the Angiogenic Transcriptome. *Nat. Cell Biol* 17 (4), 511–523. doi:10.1038/ncb3130

Engelmann, D., Meier, C., Alla, V., and Pützer, B. M. (2015). A Balancing Act: Orchestrating Amino-Truncated and Full-Length P73 Variants as Decisive Factors in Cancer Progression. *Oncogene* 34 (33), 4287–4299. doi:10.1038/onc.2014.365

Engelmann, D., and Pützer, B. M. (2014). Emerging from the Shade of P53 Mutants: N-Terminally Truncated Variants of the P53 Family in EMT Signaling and Cancer Progression. *Sci. Signal.* 7 (345), re9. doi:10.1126/scisignal.2005699

Khan, F. M., Marquardt, S., Gupta, S. K., Knoll, S., Schmitz, U., Spitschak, A., et al. (2017). Unraveling a Tumor Type-specific Regulatory Core Underlying E2F1-Mediated Epithelial-Mesenchymal Transition to Predict Receptor Protein Signatures. *Nat. Commun.* 8 (1), 198. doi:10.1038/s41467-017-00268-2

Logotheti, S., Marquardt, S., Gupta, S. K., Richter, C., Edelhäuser, B. A. H., Engelmann, D., et al. (2020). LncRNA-SLC16A1-AS1 Induces Metabolic Reprogramming during Bladder Cancer Progression as Target and Co-activator of E2F1. *Theranostics* 10 (21), 9620–9643. doi:10.7150/thno.44176

Logotheti, S., Marquardt, S., Richter, C., Sophie Hain, R., Murr, N., Takan, I., et al. (2020). Neural Networks Recapitulation by Cancer Cells Promotes Disease Progression: A Novel Role of P73 Isoforms in Cancer-Neuronal Crosstalk. *Cancers* 12 (12), 3789. doi:10.3390/cancers12123789

Meier, C., Hardtstock, P., Joost, S., Alla, V., and Pützer, B. M. (2016). p73 and IGF1R Regulate Emergence of Aggressive Cancer Stem-like Features via miR-885-5p Control. *Cancer Res.* 76 (2), 197–205. doi:10.1158/0008-5472.CAN-15-1228

Melino, G. (2020). Molecular Mechanisms and Function of the P53 Protein Family Member - P73. *Biochem. Mosc.* 85 (10), 1202–1209. doi:10.1134/S0006297920100089

Nemajerova, A., Amelio, I., Gebel, J., Dötsch, V., Melino, G., and Moll, U. M. (2018). Non-oncogenic Roles of TAp73: from Multiciliogenesis to Metabolism. *Cell Death Differ.* 25 (1), 144–153. doi:10.1038/cdd.2017.178

Rodrigues, P., Patel, S. A., Harewood, L., Olan, I., Vojtasova, E., Syafruddin, S. E., et al. (2018). NF-κB-Dependent Lymphoid Enhancer Co-option Promotes Renal Carcinoma Metastasis. *Cancer Discov.* 8 (7), 850–865. doi:10.1158/2159-8290.CD-17-1211

Rozenberg, J. M., Zvereva, S., Dalina, A., Blatov, I., Zubarev, I., Luppov, D., et al. (2021). Dual Role of P73 in Cancer Microenvironment and DNA Damage Response. *Cells* 10, 3516. doi:10.3390/cells10123516

Steder, M., Alla, V., Meier, C., Spitschak, A., Pahnke, J., Fürst, K., et al. (2013). DNp73 Exerts Function in Metastasis Initiation by Disconnecting the Inhibitory Role of EPLIN on IGF1R-Akt/stat3 Signaling. *Cancer Cell* 24 (4), 512–527. doi:10.1016/j.ccr.2013.08.023

Toh, W. H., Nam, S. Y., and Sabapathy, K. (2010). An Essential Role for P73 in Regulating Mitotic Cell Death. *Cell Death Differ.* 17 (5), 787–800. doi:10.1038/cdd.2009.181

Vanharanta, S., and Massagué, J. (2013). Origins of Metastatic Traits. *Cancer Cell* 24 (4), 410–421. doi:10.1016/j.ccr.2013.09.007

Vera, J., Schmitz, U., Lai, X., Engelmann, D., Khan, F. M., Wolkenhauer, O., et al. (2013). Kinetic Modeling-Based Detection of Genetic Signatures that Provide Chemoresistance via the E2F1-p73/DNp73-miR-205 Network. *Cancer Res.* 73 (12), 3511–3524. doi:10.1158/0008-5472.CAN-12-4095

Vikhanskaya, F., Toh, W. H., Dulloo, I., Wu, Q., Boominathan, L., Ng, H. H., et al. (2007). p73 Supports Cellular Growth through C-jun-dependent AP-1 Transactivation. *Nat. Cell Biol.* 9 (6), 698–706. doi:10.1038/ncb1598

Wang, C., Teo, C. R., and Sabapathy, K. (2020). p53-Related Transcription Targets of TAp73 in Cancer Cells-Bona Fide or Distorted Reality? *Int. J. Mol. Sci.* 21 (4), 1346. doi:10.3390/ijms21041346

Wang, Y., Alla, V., Goody, D., Gupta, S. K., Spitschak, A., Wolkenhauer, O., et al. (2016). Epigenetic Factor EPC1 Is a Master Regulator of DNA Damage Response by Interacting with E2F1 to Silence Death and Activate Metastasis-Related Gene Signatures. *Nucleic Acids Res.* 44 (1), 117–133. doi:10.1093/nar/gkv885

Conflict of Interest: The authors declare that the research was conducted in the absence of any commercial or financial relationships that could be construed as a potential conflict of interest.

Publisher's Note: All claims expressed in this article are solely those of the authors and do not necessarily represent those of their affiliated organizations, or those of the publisher, the editors and the reviewers. Any product that may be evaluated in this article, or claim that may be made by its manufacturer, is not guaranteed or endorsed by the publisher.

Copyright © 2022 Pützer and Sabapathy. This is an open-access article distributed under the terms of the Creative Commons Attribution License (CC BY). The use, distribution or reproduction in other forums is permitted, provided the original author(s) and the copyright owner(s) are credited and that the original publication in this journal is cited, in accordance with accepted academic practice. No use, distribution or reproduction is permitted which does not comply with these terms.

frontiers in Cell and Developmental Biology

ORIGINAL RESEARCH
published: 07 April 2021
doi: 10.3389/fcell.2021.620248

Investigating Molecular Determinants of Cancer Cell Resistance to Ionizing Radiation Through an Integrative Bioinformatics Approach

Halil Ibrahim Toy[1,2], *Gökhan Karakülah*[1,2], *Panagiota I. Kontou*[3], *Hani Alotaibi*[1,2], *Alexandros G. Georgakilas*[4] *and Athanasia Pavlopoulou*[1,2]*

[1] Izmir Biomedicine and Genome Center, Izmir, Turkey, [2] Izmir International Biomedicine and Genome Institute, Dokuz Eylül University, Izmir, Turkey, [3] Department of Computer Science and Biomedical Informatics, University of Thessaly, Lamia, Greece, [4] DNA Damage Laboratory, Department of Physics, School of Applied Mathematical and Physical Sciences, Zografou, National Technical University of Athens, Athens, Greece

Eradication of cancer cells through exposure to high doses of ionizing radiation (IR) is a widely used therapeutic strategy in the clinical setting. However, in many cases, cancer cells can develop remarkable resistance to radiation. Radioresistance represents a prominent obstacle in the effective treatment of cancer. Therefore, elucidation of the molecular mechanisms and pathways related to radioresistance in cancer cells is of paramount importance. In the present study, an integrative bioinformatics approach was applied to three publicly available RNA sequencing and microarray transcriptome datasets of human cancer cells of different tissue origins treated with ionizing radiation. These data were investigated in order to identify genes with a significantly altered expression between radioresistant and corresponding radiosensitive cancer cells. Through rigorous statistical and biological analyses, 36 genes were identified as potential biomarkers of radioresistance. These genes, which are primarily implicated in DNA damage repair, oxidative stress, cell pro-survival, and apoptotic pathways, could serve as potential diagnostic/prognostic markers cancer cell resistance to radiation treatment, as well as for therapy outcome and cancer patient survival. In addition, our findings could be potentially utilized in the laboratory and clinical setting for enhancing cancer cell susceptibility to radiation therapy protocols.

Keywords: ionizing radiation, DNA damage repair, cancer cell radioresistance, bioinformatics, gene expression profiles, biomarkers

OPEN ACCESS

Edited by:
Brigitte M. Pützer, University Hospital Rostock, Germany

Reviewed by:
Andrew Kellett, Dublin City University, Ireland
Anna Dubrovska, Technische Universität Dresden, Germany

***Correspondence:**
Athanasia Pavlopoulou
athanasia.pavlopoulou@ibg.edu.tr

Specialty section:
This article was submitted to Molecular Medicine, a section of the journal Frontiers in Cell and Developmental Biology

Received: *22 October 2020*
Accepted: *15 March 2021*
Published: *07 April 2021*

Citation:
Toy HI, Karakülah G, Kontou PI, Alotaibi H, Georgakilas AG and Pavlopoulou A (2021) Investigating Molecular Determinants of Cancer Cell Resistance to Ionizing Radiation Through an Integrative Bioinformatics Approach. Front. Cell Dev. Biol. 9:620248. doi: 10.3389/fcell.2021.620248

INTRODUCTION

Radiation therapy or radiotherapy (RT) represents one of the optimal, most widely used modalities in the treatment of multiple cancers, either alone or combined with other curative anti-cancer modalities like chemotherapy (Delaney et al., 2005; Begg et al., 2011) or immunotherapy (Tang et al., 2014; Schoenhals et al., 2016). It is estimated that approximately 50% of all cancer patients worldwide undergo radiotherapy throughout their illness trajectory (Baskar et al., 2012).

Advances in radiotherapy contribute greatly to cancer patients' improvement of overall survival and quality of life (Baskar et al., 2012). The aim of radiotherapeutic regimens is to specifically and efficiently sensitize cancer cells to IR in order to eliminate them and

prevent cancer recurrence and relapse, minimizing at the same time the adverse effects of radiation on healthy tissue. RT affects cancer cells either directly, by inducing genomic (DNA) lesions, or indirectly, through the generation of DNA damaging intermediates through the interaction with water, like reactive oxygen/nitrogen species (ROS/RNS) and free radicals (e.g., hydrogen ion, hydroxide, etc.) (Mikkelsen and Wardman, 2003; Yamamori et al., 2012).

However, cancer cells have the capacity to develop incredible tolerability and resistance to RT, thereby evading death. Radioresistance represents a major limiting factor in the effective treatment of different types of cancers. The response of tumor cells to radiation depends both on the resistance mechanisms of the cells and also on the accelerated repopulation of the tumor bulk by cells that have developed further radioresistance (Pavlopoulou et al., 2016, 2017). As noted in previous studies, the genes that are differentially expressed (either up- or down-regulated) between radioresistant (RR) and radiosensitive (RR) cancer cells are generally implicated in DNA damage response and repair (DDR/R) pathways, apoptosis, hypoxia, or response to oxidative stress, etc. (Pavlopoulou et al., 2016, 2017). The complexity of radiation resistance mechanisms suggests the involvement of different and diverse biological mechanisms.

During the last decade, the advances in high-throughput (HTP) "omics" technologies (e.g., RNA-Seq and microarrays) enabled the generation of an enormous amount of gene expression data. Data produced with HTP technologies are stored in international public repositories such as NCBI's GEO (Gene Expression Omnibus) (https://www.ncbi.nlm.nih.gov/gds/) (Barrett et al., 2013; Clough and Barrett, 2016). GEO DataSets contains both original records and curated datasets.

Accumulated knowledge over years of research on the biological effects of radiation points toward the development of holistic approaches to "big data" analysis by employing systems biology methodologies (Unger, 2014; Beheshti et al., 2019; Spratt and Speers, 2019; Kanakoglou et al., 2020). Herein, we employed a rigorous systems biology approach to unravel the molecular determinants of resistance of cancer cells to IR, based solely on HTP data. To this end, publicly available transcriptome datasets relevant to cancer cell response to radiation were retrieved from GEO, and specifically, cancer cell lines that displayed enhanced resistance to radiation. Statistical analyses were carried out to identify the differentially expressed genes (DEGs) between radioresistant and radiosensitive tumor cells. Furthermore, functional annotation of genes allowed us to identify specific biological pathways implicated in cancer cell resistance to radiation. Our findings could be applied in the laboratory and clinical setting as biomarkers for the design of targeted and personalized radiotherapy regimens in order to effectively sensitize cancer cells to radiation, enhance tumor control and thereby minimize tumor recurrence and metastasis.

METHODS

Data Retrieval

The public repository NCBI GEO DataSets was searched extensively for gene expression datasets using relevant keywords: ("radiation therapy" or "radiotherapy") and ("cancer" or "tumor") and ("resistance" or "tolerability") and ("sensitivity" or "responsive") and ("human" or "homo sapiens"). A total of three eligible datasets were selected:

The GEO series GSE97543 (Emons et al., 2017) (**Supplementary Table 1**) includes global gene expression by microarray of both wild-type and radioresistant Dukes' type C colorectal adenocarcinoma (COAD) cell lines that were either non-irradiated or irradiated repeatedly with 2 Gray (Gy) of X-rays in order to acquire a radioresistant phenotype. The Agilent-026652 whole human genome microarray 4x44K, GPL13497 platform was used.

In GSE13280 (Marston et al., 2009) (**Supplementary Table 1**), genome-wide gene expression by microarray was performed of cell lines derived from pediatric B-precursor acute lymphoblastic leukemia (ALL) after 8 h *in vitro* exposure to 5 Gy IR. This dataset contains cell lines both resistant and responsive to radiation. The development of resistance and responsiveness to IR was assessed by measuring apoptosis in cells. The Affymetrix human genome U133A array, GPL96 platform was employed.

In GSE120798 (Gray et al., 2019) (**Supplementary Table 1**), three novel radioresistant breast cancer cell lines were established by exposing the corresponding parental cell lines MDA-MB-231 (metastatic mammary adenocarcinoma), MCF-7 (breast adenocarcinoma), and ZR-751 (luminal breast cancer) to increasing doses of X-rays for 2 and 8 h. Genome-wide gene expression analysis of both the parental and radioresistant cell lines (i.e., MDA/MDAR, MCF/MCFR, ZR/ZRR) was performed using high throughput sequencing. The NextSeq 550 (Homo sapiens), GPL21697 platform was used.

Microarray-Based Transcriptomic Data Analysis

For each microarray study, the gene expression data that represent the gene expression summary for every probe and every sample were recorded. In microarrays, many probes can map to the same Gene Symbol for various reasons, and, conversely, a probe may also map to more than one Gene Symbol if the probe sequence is not specific enough. A simple approach would be to use only the probes with one-to-one mapping for further analysis; however, this approach results in the loss of important information. To conduct an analysis based on genes and not probes, the probe identifiers were firstly converted into gene identifiers, according to Ramasamy et al. (2008) guidelines. To this end, GPL files that contained information about the gene symbols that correspond to probe IDs were used in order to resolve the "many-to-many" relationships between probes and genes by averaging the expression profiles for genes with more than one probe (Ramasamy et al., 2008). We identified the Gene Symbols with the usage of the HUGO Gene Nomenclature Committee (Braschi et al., 2019) and the National Center for Biotechnology Information (NCBI) GENE (Sayers et al., 2020).

The two-sample *t*-test was employed to identify genes differentially expressed between the case (RR) and control (RS) groups. However, a disadvantage of the *t*-test in the analysis of microarray data is that if most of the experiments in a given

study contain a relatively small number of samples per group, the assumption of normality is untenable. To resolve this, the statistical method *t*-test with bootstrap was used (Efron and Tibshirani, 1993). Bootstrap provides an ideal method to generate accurate estimates of the standard errors when no formula for the sampling distribution is available or when available formulas make inappropriate assumptions (e.g., small sample size, non-normal distribution). In this study, bootstrap analysis was conducted with 1,000 replicates, a relatively high number, in order to generate accurate estimates of the standard errors.

A typical microarray experiment measures the expression of several thousand genes simultaneously across different conditions. When investigating for potential DEGs between two conditions, each gene is treated independently, and the *t*-test is performed on each gene separately. The incidence of false positives (i.e., genes falsely declared as DEGs) is proportional to the number of tests performed and the critical significance level (*p*-value cut-off). In order to account for multiple comparisons, a correction method proposed by Benjamini and Hochberg (1995) which controls False Discovery Rate (FDR) was applied. FDR-controlling procedures have greater power (i.e., they can discover more statistically significant differences), at the expense of increased Type I error rate. Genes with adjusted *p*-value (or *q*-value) less or equal to 0.05 were considered as statistically significant in this study. For all statistical analyses, the Stata 13 statistical software package (StataCorp, 2013) was used. For the creation of heatmaps from microarray data, the average linkage clustering with Euclidean distance clustering method implemented in Heatmapper (http://heatmapper.ca/) was utilized.

RNA-Seq-Based Transcriptomic Data Analysis

For the RNA-Seq based transcriptome analysis, the following pipeline was utilized. The FASTQ files were extracted from the respective Sequence Read Archive (SRA) files containing raw RNA-Seq reads by using the SRA Tool Kit v.2.9.0 (Alnasir and Shanahan, 2015) with the *"fastq-dump –gzip –skip-technical –readids –dumpbase –clip –split-3"* command. The raw RNA-Seq reads in FASTQ files were aligned to the human reference genome GRCh38 (Ensembl version 97) by employing the splice junction aligner HISAT2 v.2.1.0 (Kim et al., 2015) with *"hisat2 -p -dta -x {input.index} -U {input.fq} -S {out.sam}"* parameters. The generated SAM file was converted to the respective binary BAM file by using SAM Tools v.1.9.0 (Li et al., 2009) with *"samtools sort -@ 10 -o {output.bam} {input.sam}"* commands. String Tie v.1.3.5 (Pertea et al., 2015) was utilized with *"stringtie -e -B -p -G {input.gtf} -A {output.tab} -o {output.gtf} -l {input.label}{input.bam}"* parameters for the measurement of gene expression levels. The reconstructed transcripts and transcript abundances were reported in the output GTF file. In order to detect differentially expressed genes between RR and RS samples, we utilized the EdgeR package v3.28.0 (Robinson et al., 2010) of the R statistical computation environment v.3.6.1 (https://www.r-project.org). We firstly applied the trimmed mean of M-values (TMM) normalization (Robinson and Oshlack, 2010) implemented in EdgeR to the count data and we employed generalized linear models with "cell lines," "resistance," and "time" as factors. Then, estimating dispersion was computed with the *estimateDisp* function, and differential expression analysis between the two RNA-Seq groups (RR and RS) was performed using the *glmFit* and *glmLRT* functions of the EdgeR package v3.28.0 (Robinson et al., 2010) of the R statistical computation environment v.3.6.1 (https://www.r-project.org). In order to detect statistically significant differentially expressed genes, the threshold for the absolute $\log_2$-fold change was set at two ($|\log_2 FC \geq 2|$), and for the FDR (Benjamini and Hochberg, 1995)-corrected *p*-value at 0.05. All statistical calculations for the RNASeq data were performed by using the R software environment. The *pheatmap* package of R (https://CRAN.R-project.org/package=pheatmap) was utilized to generate a heatmap from RNA-Seq data.

Pathway Enrichment Analysis

To assign biological role(s) to the genes under study that are associated with biological pathways, gene set enrichment analysis (GSEA), or functional enrichment analysis, was conducted. GSEA is a method to identify biological processes or pathways that are over-represented in a large set of genes. To this end, WebGestalt (WEB-based GEne SeT AnaLysis Toolkit) (Zhang et al., 2005; Liao et al., 2019) was employed to identify statistically significant over-represented WikiPathways (Kutmon et al., 2016) cancer terms in the sets of genes; the threshold for the FDR-corrected *p*-value was set at 10^{-3}, and hypergeometric distribution analysis was used.

Functional Interactions Networks

The associations among the molecules under study were investigated and visualized with the usage of STRING (Search Tool for Retrieval of Interacting Genes/Proteins) v11.0 (Szklarczyk et al., 2019), a database of either known or predicted, direct or indirect, gene/protein associations derived from diverse resources. The highest confidence interaction score ($\geq$0.9) was chosen to display the associations amongst genes/proteins in the generated network.

Survival Analysis

The prognostic potential of the 36 radiogenes was investigated in three types of cancers, namely, breast invasive carcinoma (BRCA), colon adenocarcinoma (COAD), and acute myeloid leukemia (LAML), a type of haematologic cancer like ALL, through the web-based tool GEPIA (Gene Expression Profiling Interactive Analysis) (Tang et al., 2017) version 2 (http://gepia2.cancer-pku.cn/#index), based on data acquired from The Cancer Genome Atlas (TCGA) (https://tcga-data.nci.nih.gov). The cancer patient cohort is divided into the high-risk and low-risk categories; the cut-offs for low and high gene expression level patient cohorts were set at 50%.

Tissue-Wise Differential Gene Expression Analysis

GEPIA2 (Tang et al., 2017), which contains gene expression data from cancer and corresponding normal tissues from

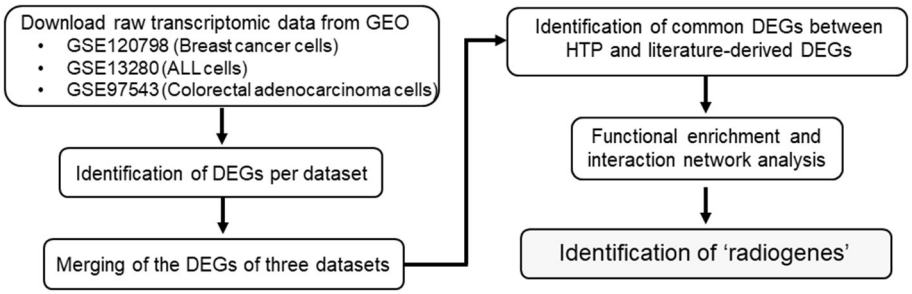

FIGURE 1 | Flowchart diagram of the overall methodology employed in this study. Three eligible transcriptome datasets were retrieved from NCBI's GEO. Genes differentially expressed (DEGs) between the radioresistant and radiosensitive cancer cells were identified per dataset. The DEGs of the three analyzed datasets were integrated and compared with an earlier own study on cancer cell radioresistance-related genes/proteins derived from literature research. Functional enrichment analysis of the common genes was performed to obtain the so-called "radiogenes".

TCGA (https://tcga-data.nci.nih.gov) and the Genotype-Tissue Expression (GTEx) (https://gtexportal.org/home/), respectively, was used to investigate the differential expression patterns of the radiogenes under study in BRCA, COAD, and LAML cancer-normal tissue; $|\log FC| \geq 2$ and FDR-corrected p-value ≤ 0.05.

RESULTS

The overall procedure for data collection and analysis followed in the present study is described illustratively in **Figure 1**.

Identification of Differential Expression Patterns in Radioresistance vs. Radiosensitive Cancer Cells

The two techniques for transcriptome profiling, RNA-Seq and microarray, have large inherent differences. RNA-Seq is considered "superior" since it allows the detection of low abundance transcripts and novel transcript isoforms (Marioni et al., 2008). For this reason, we applied different statistical methods for RNA-Seq (Li, 2019) and microarray (Kontou et al., 2018) data processing and analysis.

The number of differentially expressed genes (DEGs) found between radioresistant and radiosensitive cancer cells (**Figure 2**) for each dataset is 6372 (GSE120798), 782 (GSE13280), and 541 (GSE97543), respectively (**Supplementary Table 2**). The pathways over-represented in the DEGs of the three datasets are related primarily to DDR/R and cell survival (**Figure 3**).

Differential gene expression analysis was performed for the three parental breast cancer cell lines in GSE120798 (Gray et al., 2019) against their radioresistant derivatives, to identify those genes that are significantly dysregulated in response to radiation stress. A total of 11 samples were compared; one biological replicate for each condition (**Supplementary Table 1**). The number of detected DEGs (Gray et al., 2019) is remarkably higher as compared to the ones derived from microarray gene expression data (**Supplementary Table 2**). This discrepancy is likely due to the ability of RNA-Seq to detect and quantify, even rare, transcripts without *a priori* knowledge of a given gene (Metzker, 2010). Accordingly, the number of enriched pathways is also greater in this dataset (**Figure 3**). Three DDR/R pathways were found to be enriched in the DEGs, including the generic "DNA Damage Response" pathway. Two pathways are specifically implicated in IR-induced DNA damage response, namely "DNA IR-Double Strand Breaks (DSBs) and cellular response via ATM," and "DNA IR-damage and cellular response via ATR." Ataxia telangiectasia mutated (ATM) and ataxia telangiectasia and Rad3-related (ATR) proteins are evolutionarily conserved proteins that have a critical regulatory role in DDR and maintenance of genome integrity (Marechal and Zou, 2013; Awasthi et al., 2015). Furthermore, the "PI3K-AKT-mTOR signaling pathway and therapeutic opportunities" was shown to be over-represented in the set of DEGs; increased activity of PI3K in the radioresistant cells of this transcriptome dataset was also observed by Gray et al. (2019). Phosphatidylinositol-3-kinase (PI3K)/AKT/mammalian target of rapamycin (PI3K/AKT/mTOR) signaling is critical to many aspects of tumor cell growth and survival (Porta et al., 2014) and therefore could be likely involved in the survival of irradiated cancer cells.

Differential expression analysis was also carried out of the irradiated COAD cells in the GSE97543 dataset (Emons et al., 2017). A total of six samples were compared; three biological replicates for the wild-type (radiosensitive) cell lines and three for the radioresistant cells (**Supplementary Table 1**). The notch signaling pathway is significantly over-represented (**Figure 3**) in the DEGs of this dataset (**Supplementary Table 2**). Notch signaling is suggested to confer a selective survival advantage on tumors (Capaccione and Pine, 2013). Hence, the Notch network could be implicated in the resistance and survival of the COAD cells to irradiation. Regarding the over-represented DDR/R pathways, one pathway is related to processing IR-induced DNA lesions through ATR signaling and the other to mismatch repair (MMR), which is responsible for detecting and repairing mismatched nucleotides (Iyer et al., 2006; Larrea et al., 2010). MMR reaction is initiated by binding of the MSH2 (MutS homolog 2)/MSH6 heterodimer to the mismatched DNA; both *MSH2* and *MSH6* were found differentially expressed in the radioresistant COAD cells. The MutS homologs MSH2 and MSH6 form a heterodimer that binds to short insertion/deletion

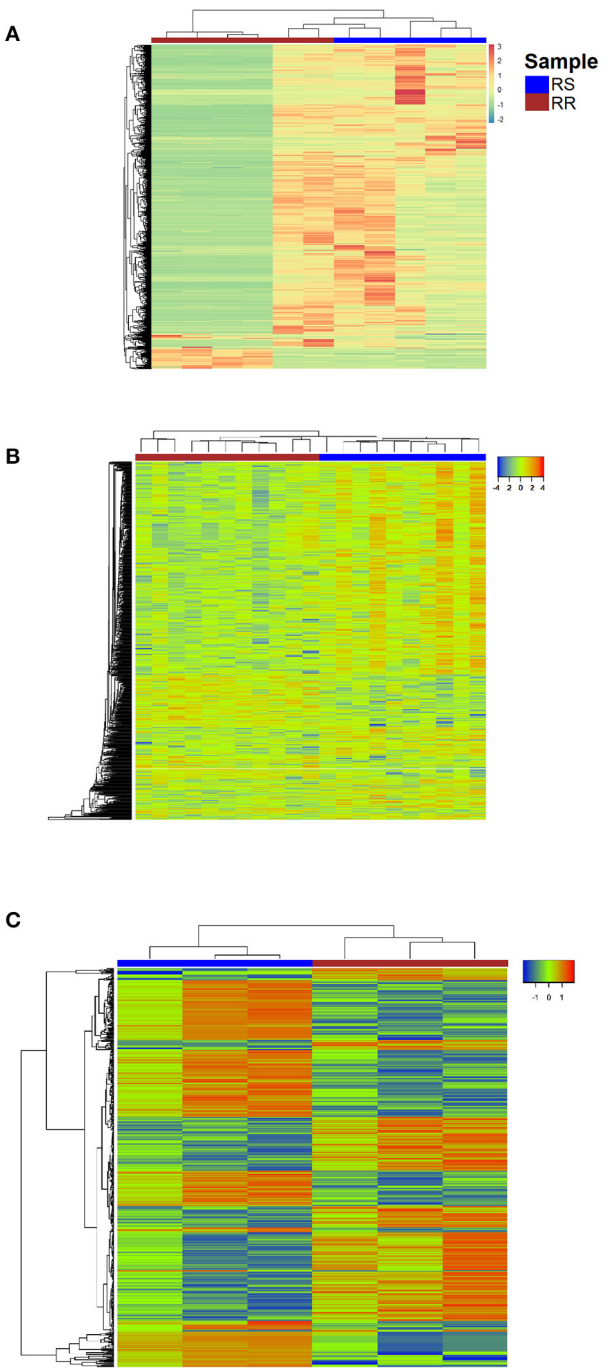

FIGURE 2 | Heatmap representing color-coded expression levels of DEGs for the datasets **(A)** GSE120798 (breast cancer), **(B)** GSE13280 (ALL), **(C)** GSE97543 (COAD); columns correspond to samples and rows correspond to genes. RR, Radioresistant; RS, Radiosensitive.

DNA mispairs (Habraken et al., 1996; Edelbrock et al., 2013). The MMR proteins also function in signaling DNA damage (Duckett et al., 1996b; Modrich, 1997). Earlier studies have shown that MSH2 is also involved in the processing of the biologically significant clustered DNA damages, as well as the execution of apoptosis induced by IR (Holt et al., 2009).

In GSE13280 (Marston et al., 2009), the gene expression profiles of radioresistant and radiosensitive ALL cell lines (eleven replicates for each condition) were compared (**Supplementary Table 1**) for the identification of DEGs (**Supplementary Table 2**). The enriched transforming growth factor beta (TGFB) signaling pathway (**Figure 3**), like the Notch network (Capaccione and Pine, 2013), is implicated in several aspects of cancer initiation, promotion, and progression (Syed, 2016). Hence, the Notch- and TGFB-mediated signaling pathways might render ALL cells less vulnerable to IR-induced apoptosis by exerting their cellular pro-survival effect.

Identification of Cancer Cell Radioresistance–Related Genes

The procedure we followed to identify an optimal number of cancer cell radioresistance–related genes is illustrated in **Supplementary Figure 1**. A list of 175 bio molecules (**Supplementary Table 3**) was proposed in a previous study by Pavlopoulou et al. (2017) to be implicated in tumor cell radioresistance. These genes/proteins were manually collected through a comprehensive and thorough literature search. The DEGs identified in each of the three transcriptome datasets were merged; a list of 7,185 genes was compiled (**Supplementary Table 3**). Those genes were compared to the literature-derived molecules, and 88 genes were found in common (**Supplementary Table 3**). In order to identify an optimal number of genes implicated in radioresistance, we performed functional enrichment analysis of these genes. The pathways over-represented in the 88 genes (**Figure 4**) are related to DDR/R, similar to those detected in the DEGs of the individual datasets (**Figure 3**), as well as to apoptosis. Signaling pathways mediated by the cardinal tumor suppressor TP53 are also related to radioresistance (**Figure 4**). Collectively, 36 genes were found to be implicated in cancer-associated biological pathways listed in **Table 1**, 26 of those up-regulated and 10 down-regulated in RR cancer cells. The products of the 36 genes also form a highly connected network (**Figure 5**), with high-confidence interactions, suggesting that these proteins associate, either functionally or physically, to confer cellular resistance to IR. Therefore, we propose 36 interconnected pivotal genes, henceforth referred to as "radiogenes," which participate in radioresistance-relevant pathways and mechanisms.

Differentially Expressed Radiogenes in Cancer vs. Normal Tissue

Collectively, 19 radiogenes, found to be differentially expressed in the three radioresistant vs. the radiosensitive cancer cell lines (**Table 1**), are consistently deregulated in their corresponding cancer-matched normal tissues with the same direction (i.e., up- or down-regulated) (**Supplementary Figure 2**). This finding could be utilized in personalized tumor treatment for the selective eradication of cancer cells by applying radiotherapy without harming the adjacent healthy tissue at the same time.

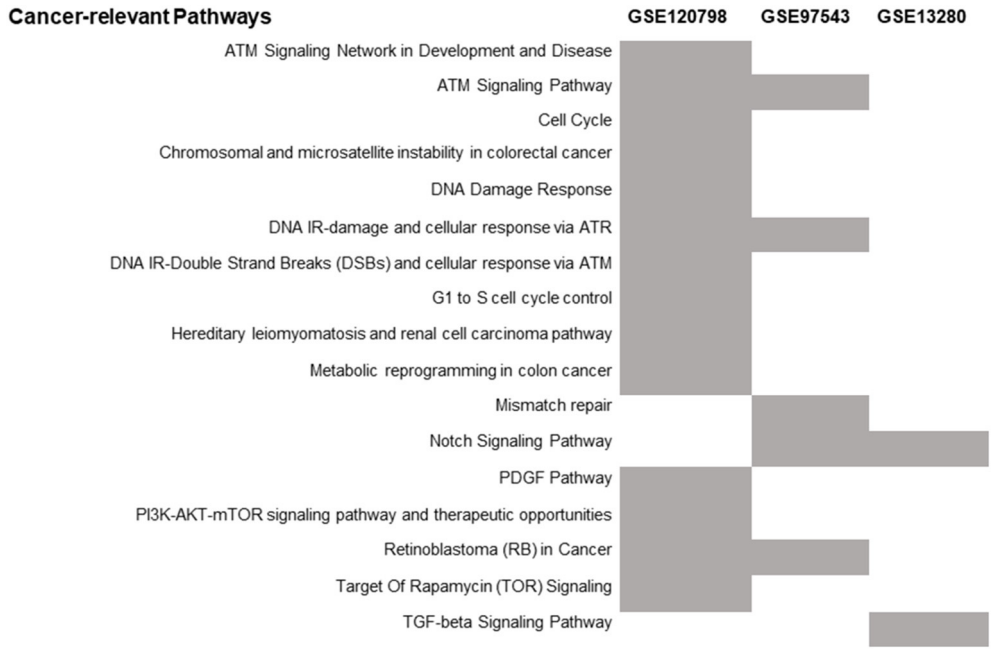

FIGURE 3 | Distribution of the over-represented cancer-related WikiPathways in the DEGs of each transcriptome dataset. The enriched pathways are indicated by gray.

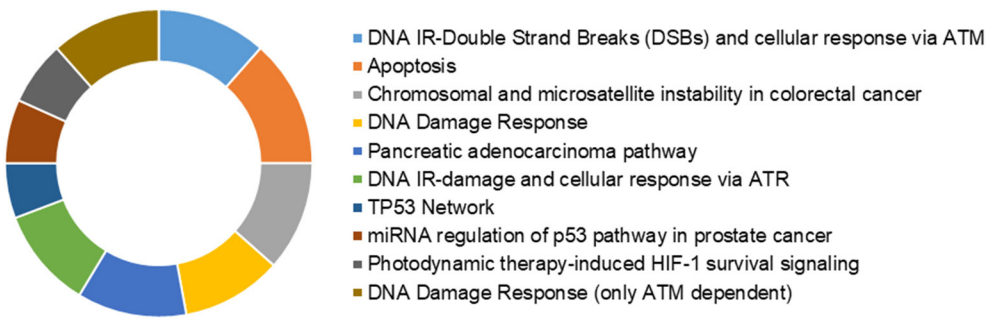

FIGURE 4 | Donut chart depicting the over-represented cancer-relevant pathways across the 88 common genes.

Radiogenes Are Potential Cancer Prognostic Markers

The differential expression of the radiogenes can also predict the clinical outcome of cancer patients. In particular, a statistically significant association was found between *CHEK1*, *MAP2K1*, and *PLK1* overexpression and worse overall survival in breast invasive carcinoma patients, indicated by pooled hazard ratio (HR) values higher than 1 and *p*-values lower than 0.05. Conversely, a significant relationship was observed between high expression of *NFKBIA*, which is otherwise underexpressed in radioresistant breast cancer cells, and favorable prognosis, indicated by an HR value < 1 (**Supplementary Figure 3**).

DISCUSSION

Cancer cells confer resistance to irradiation through diverse mechanisms including enhanced DNA damage repair capacity, activation of cell survival signaling pathways, inhibition of apoptotic pathways, and induced autophagy.

DDR/R is a complex entangled process consisting of recognition (or detection, or sensing), signaling, and repair of DNA damage (Rouse and Jackson, 2002). Ionizing radiation usually generates a variety of DNA lesions, including abasic (apurinic/apyrimidinic) sites, oxidized bases, crosslinks between thymine and cytosine bases, DNA single-strand breaks (SSBs), and DNA double-strand breaks (DSBs) (Sutherland et al., 2000). In the case of SSBs, only one strand of the double stranded DNA helix is severed. SSBs are recognized and processed by base excision repair (BER) and nucleotide excision repair (NER) mechanisms (Caldecott, 2008). DSB is the most detrimental type of DNA lesions since both strands of the double helix are broken. DSBs are repaired mainly through homologous recombination (HR) if cells are present in the S/G2 cell-cycle phase or, the less accurate, non-homologous end joining (NHEJ) (Budman and Chu, 2005). Those different types of DNA lesions can be formed

TABLE 1 | Gene symbol and expression status of the 36 differentially expressed radiogenes (radioresistant vs. radiosensitive cancer cells).

Gene	Expression status	Cell line
AKT1	Up	BC
ATM	Up	BC
BAX	Down	BC; ALL
BBC3	Down	BC
BCL2	Up	BC
BIRC5	Up	BC
BRCA1	Up	BC
BRCA2	Up	BC
CASP3	Down	BC
CCND1	Up	BC
CHEK1	UP	BC
EGLN1	Up	BC
HIF1A	Up	BC; ALL
JAK1	Down	BC
JUN	Up	BC
MAP2K1	UP	BC
MAP2K2	Up	BC
MCL1	Up	BC
MSH2	Up	BC; COAD
NBN	Up	BC
NFKB1	Up	BC
NFKBIA	Down	BC
PARP1	Up	BC
PLK1	Up	BC
PMAIP1	Down	BC
PRKDC	Up	BC
PTEN	Down	BC
RELA	Up	BC
RNF8	Up	BC
SOD2	Up	BC; ALL
STAT1	Down	BC
STAT3	Up	BC
TERF2	Up	BC
TP53	Down	BC
UBE2D3	Down	ALL
XIAP	Up	BC

ALL, acute lymphoblastic leukemia; BC, breast cancer; COAD, colorectal adenocarcinoma.

Those radiogenes found to be differentially expressed between TCGA-derived cancer tissue and corresponding GTEx matched normal tissue are italicized.

either separately or in close vicinity (a few nm), resulting in clustered DNA lesions or locally multiply damaged sites (MDS). Clustered DNA damage, the hallmark of IR, is considered the most severe type of genomic damage because of its complexity. This complex DNA damage includes both DSBs and non-DSBs, usually referred to as oxidatively-clustered DNA lesions (OCDLs), occurring within a DNA region of 15–20 bp. The corresponding DNA damage repair mechanisms are recruited by the cell in response to clustered damaged sites. However, harnessing the corresponding DNA repair machinery to the clustered damaged sites is quite challenging since the presence of a lesion in one strand can delay significantly the simultaneous processing of another lesion on the complementary strand. Furthermore, OCDLs can be rapidly converted into *de novo* DSBs by a DNA glycosylase during the repair. As a result, unrepaired MDS can lead to increasing levels of genotoxic damage, triggering also systemic responses (Nikitaki et al., 2016). Clustered DNA lesions, if not properly processed, could contribute to increased genomic instability in the form of chromosomal aberrations (e.g., deletions and inversions) and microsatellite instability, leading eventually to carcinogenesis. Therefore, the induction of clustered DNA damage increases the cytotoxic effect of radiation, especially in highly proliferating cancer cells. Radioresistant cancer cells though can counteract this effect through their ability to respond to and repair complex/clustered DNA damage more efficiently without avoiding necessarily increased genomic instability, as compared to their radiosensitive counterparts (Hada and Georgakilas, 2008; Georgakilas et al., 2013; Mavragani et al., 2017, 2019; Bukowska and Karwowski, 2018). The radiogenes identified in the present study are implicated in diverse mechanisms underlying the acquisition of radioresistance in cancer cells.

Among the 36 "radiogenes", *ATM*, *BRCA1/2*, *CHEK1*, *CCND1*, *MSH2*, *NBN*, *PARP1*, *PLK1*, *PRKDC,* and *RNF8*, which are consistently up-regulated across the radioresistant cancer cell lines (**Table 1**) and the corresponding cancer tissue (**Supplementary Figure 2**), are crucially implicated in different stages of DDR/R. In particular, ATM plays a protagonistic role in the initial stage of DDR/R, that is, DNA damage detection and stress-response signaling (Iliakis et al., 2003; Yang et al., 2004). ATM signaling is activated by a wide variety of DNA lesions, as well as DNA replication stress (Marechal and Zou, 2013; Burger et al., 2019). Mutations in ATM result in the genetic disorder ataxia-telangiectasia (AT), which is characterized by the high sensitivity of AT patients to IR and cancer predisposition (Gatti et al., 1988). Checkpoint kinase 1 (CHEK1), which acts downstream of ATM, is a core regulator of cell cycle checkpoint signaling in DNA damage response (Flaggs et al., 1997; Patil et al., 2013). Cyclin D1 (CCND1) was demonstrated to induce post-DNA damage cell cycle arrest and apoptosis in different types of cancers (Cai et al., 2012; Smith et al., 2016). PRKDC is a serine/threonine DNA-activated protein kinase involved in DSB recognition and DNA damage repair through NHEJ (Soubeyrand et al., 2003). Notably, ATM and PRKDC were found to affect greatly cancer cell response to IR through genome-wide genetic screening in a recent study by Francica et al. (2020). Moreover, BRCA1 and BRCA2 are largely involved in cell cycle control and maintenance of genomic stability in response to DNA damage (Deng, 2006; Gudmundsdottir and Ashworth, 2006). Another radiogene, *NBN (nibrin)*, encodes one of the three components of the MRN complex (MRE11A-RAD50-NBN), which is implicated in the recognition and repair of DSBs (Lamarche et al., 2010). NBN is mutated in patients with Nijmegen breakage syndrome (NBS), and cells from NBS patients are hypersensitive to IR (Taalman et al., 1983). In addition, a functional link between ATM and NBN proteins has been demonstrated by Zhao et al. (2000). Also, the MMR protein MSH2 (MutS homolog 2) is

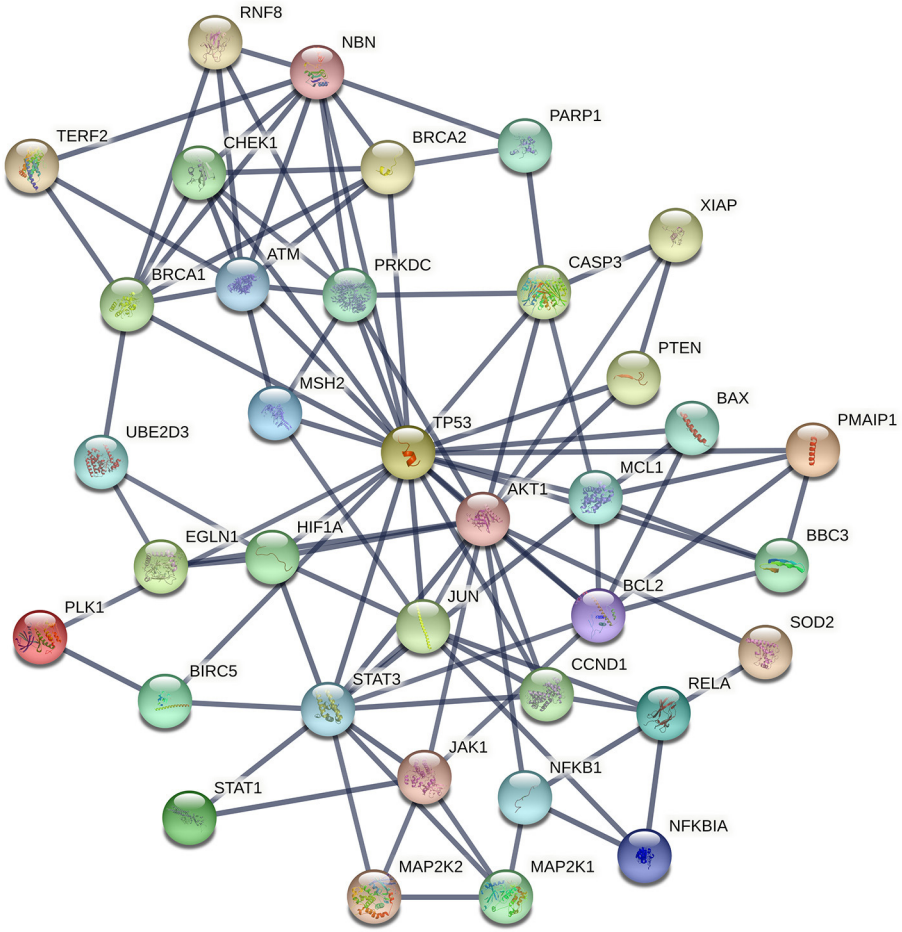

FIGURE 5 | STRING interaction network of the products of the 36 radiogenes. The nodes represent proteins and the edges indicate different modes of interactions with a confidence score ≥ 0.9.

suggested to contribute to radioresistance via SSB processing (Li et al., 2016). Moreover, RNF8 (ring finger protein 8) protein catalyzes the mono-ubiquitination of histones H2A and H2B during DNA damage, thereby facilitating DNA damage repair and activation of cell cycle checkpoint (Kolas et al., 2007; Ma et al., 2011); RNF8 is associated with radioresistance in human nasopharyngeal cancer cells (Wang et al., 2015). The protein encoded by the radiogene *PLK1 (Polo-like kinase 1)* is involved in cell cycle resumption following DNA damage-induced checkpoint arrest (Hyun et al., 2014; Bruinsma et al., 2017). It has been demonstrated that inhibition of *PLK1* renders glioblastoma and non-small cell lung cancer cells sensitive to IR (Pezuk et al., 2013; Van den Bossche et al., 2019). Of particular note, pharmacological inhibitors of the BER enzyme PARP1 [poly(ADP-ribose) polymerase 1], such as niraparib, olaparib, and rucaparib, are widely used for targeted cancer therapy (Sulai and Tan, 2018; Patel et al., 2020). Importantly, *CHEK1* and *PLK1* were found to be poor prognostic biomarkers for the survival of breast cancer patients (**Supplementary Figure 3**), further supporting that enhanced DNA damage repair mechanisms in cancer cells play a catastaltic role in efficient radiotherapy (Pavlopoulou et al., 2016, 2017). Therefore, DDR/R might represent a primary "danger" signal, leading eventually to the activation of downstream signaling cascades and pro-survival mechanisms (Nikitaki et al., 2015).

The apoptotic pathway is also affected by the cellular response to radiation-induced genomic damage in cancers, as we suggest in this study. Radioresistant cancer cells have developed the ability to evade apoptosis prompted by their response to extreme and repair-resistant DNA damage, mainly due to deregulation of key pro-apoptotic molecules like TP53 (Fridman and Lowe, 2003; Haupt et al., 2003), PTEN (Lu et al., 2016), PMAIP1 (mediator of damage-induced p53-mediated apoptosis) (Oda et al., 2000), BBC3 (TP53-upregulated modulator of apoptosis) (Han et al., 2001; Nakano and Vousden, 2001), BAX (BCL2-associated X protein) (Pawlowski and Kraft, 2000), as well as anti-apoptotic proteins like MCL1 (Fujise et al., 2000; Glaser et al., 2012), BCL2 (Akl et al., 2014), BIRC5 (Chiou et al., 2003), and XIAP (X-linked inhibitor of apoptosis) (Duckett et al., 1996a; Deveraux and Reed, 1999). In a consistent manner, in this study, the pro-apoptotic genes were shown to be up-regulated, whereas the anti-apoptotic genes are down-regulated

in radioresistant cancer cells (**Table 1**). Of those, BCL2, which is down-regulated in radioresistant breast cancer cells and tissue (**Table 1**, **Supplementary Figure 2**), can suppress apoptosis by inhibiting the activity of caspases indispensable for apoptosis, such as caspase-3 (CASP3) (Porter and Janicke, 1999; Swanton et al., 1999). Of note, aberrant activation of the Notch signaling pathway was demonstrated to inhibit TP53-mediated damage response and promote breast carcinogenesis by preventing apoptosis (Stylianou et al., 2006), suggesting a link between pro-survival and apoptotic mechanisms. PTEN was also found to promote apoptosis and cell cycle arrest via PI3K/AKT-dependent and -independent signaling (Weng et al., 2001).

The radiogene *NFKB1*, which transactivates several pro-inflammatory genes (Liu et al., 2017), was found to be overexpressed in radioresistant breast cancer cells and tissue (**Table 1**, **Supplementary Figure 2**). Furthermore, the members of the NFKB1 family, NFKBIA and RELA, can act either as inducers or inhibitors of apoptosis, respectively (Sonenshein, 1997; Barkett and Gilmore, 1999), consistent with their expression status in RR cells (**Table 1**; over- and under-expressed). The well-known NFKB1 inhibitor alpha (NFKBIA) was shown to be a favorable predictor in breast cancer patients (**Supplementary Figure 3**). Moreover, NFKB1, together with the inflammatory factors HIF1A (hypoxia-inducible factor 1) and STAT3, both of which were found to be up-regulated in radioresistant breast cancer cells (**Table 1**) and HIF1A overexpressed in breast cancer tissue (**Supplementary Figure 2**), are critically implicated in cancer radioresistance and radiation-induced inflammatory responses (Multhoff and Radons, 2012). On the other hand, STAT1, found down-regulated in the same cell lines (**Table 1**), as opposed to STAT3, elicits pro-apoptotic and anti-proliferative responses and promotes anti-cancer immunity (Avalle et al., 2012).

Suppression of *UBE2D3*, which is down-regulated in radioresistant ALL cells (**Table 1**), was demonstrated in a study by Wang et al. (2013) to decrease radiosensitivity of human breast cancer cells by promoting telomere maintenance. In addition, UBE2D3 is negatively correlated with TERF2 (telomeric repeat binding factor 2), the latter of which is primarily involved in telomere maintenance (Kim et al., 2009) and is down-regulated in radioresistance (**Table 1**).

Radiation can also exert its genotoxic and cytotoxic effects through the indirect and systemic induction of severe oxidative stress and the production of ROS in the organism (Kryston et al., 2011). The radiogene *HIF1A* plays a pivotal cytoprotective role against oxidative stress (Li et al., 2019) by inhibiting autophagy and cell death (Pouyssegur et al., 2006). Moreover, the superoxide scavenging enzyme SOD2 (superoxide dismutase 2), found overexpressed both in radioresistant breast cancer and ALL cells (**Table 1**), at normal expression levels provides a cytoprotective effect. Thus, SOD2 can likely exert a protective effect on RR cancer cells by controlling potential ROS-mediated DNA damage via catalyzing the reduction of superoxide into less genotoxic molecules like oxygen (Wang et al., 2018).

Notably, in this study, pro-survival pathways (**Figure 3**) like Notch signaling, were found to be implicated both in solid and blood cancers, probably by mediating survival of cancer cells to radiation-induced clustered/complex DNA damage (Marston et al., 2009; Capaccione and Pine, 2013). Moreover, the PI3K/AKT/mTOR signaling pathway is suggested to be important in regulating cell survival in response to different types of cellular stress (Hung et al., 2012; Porta et al., 2014), including genotoxic stress. Hence, pro-survival pathways could be considered as potential therapeutic targets in cancer (Porta et al., 2014).

A major limitation of this study, particularly for the two solid cancers datasets, is the lack of patient-derived tumor tissue, as well as cancer stem cells, which constitute a subpopulation in solid tumors that display stem-like characteristics (Pavlopoulou et al., 2016). Instead, the respective experimental studies relied on the use of commercial cancer cell lines; of particular note, the ALL cells were derived from "real" patients. However, the extent to which the individual cancer cell lines can capture the cellular and genomic complexity of tumors is questioned. Further research is needed to determine whether the results derived from the cancer cell lines investigated in this study or other studies could be extrapolated to their corresponding tissues of origin, like breast tumor tissue and colorectal adenocarcinoma. Nevertheless, it is suggested that large panels of cancer cell lines can faithfully capture the genomic heterogeneity of cancers (Sakellaropoulos et al., 2019; Vougas et al., 2019). Beyond the discussed limitations, the over- or under-expressions of the radiogenes in radioresistant phenotypes have been verified, to a great extent, by independent experimental biochemical studies available in the literature. In addition, the clinical implications of those genes are further supported by the patient survival results (**Supplementary Figure 3**).

CONCLUSION

In the present study, we employed an integrative bioinformatics approach to analyze transcriptomic data regarding the molecular determinants of cancer cell radioresistance. On the basis of our findings, both solid and hematologic cancer cells likely depend on similar mechanisms to confer resistance to IR (i.e., DDR/R and cell survival). Moreover, we identified 36 functionally associated radiogenes that participate in radioresistance-associated pathways. Most of those radiogenes were also shown to be differentially regulated in the corresponding cancer tissues. Moreover, several of the radiogenes were found to have potential prognostic value for the clinical outcome of cancer patients. However, the availability of clinically derived cancer tissues would provide a more reliable source for conducting research on the response of cancer patients to radiation. The overall data presented herein can be particularly useful for clinicians in selecting suitable targets (e.g., DDR/R inhibitors) for appropriate combination therapy using IR. In conclusion, we suggest that this bioinformatics premise can be harnessed as a first step in the rational design of *in vivo* experimental studies or in personalized medicine for optimizing tumor response and cancer cell susceptibility to therapeutic ionizing radiation and

reduction of the total effective radiation dose administered to the patient.

DATA AVAILABILITY STATEMENT

The original contributions presented in the study are included in the article/**Supplementary Material**; further inquiries can be directed to the corresponding author/s.

AUTHOR CONTRIBUTIONS

AP conceived the study. AP and AGG designed and supervised the study. HIT, GK, PK, and AP performed the experiments and analyzed the data. HIT, GK, PK, HA, AGG, and AP wrote the manuscript. All authors reviewed and approved of the final manuscript.

FUNDING

HIT acknowledges YÖK (Yükseköğretim Kurulu) and TÜBİTAK 2211-C scholarship. PK was co-financed by Greece and the European Union (European Social Fund- ESF) through the Operational Programme "Human Resources Development, Education and Lifelong Learning" in the context of the project "Reinforcement of Postdoctoral Researchers - 2 nd Cycle" (MIS-5033021), implemented by the State Scholarships Foundation (IKY).

SUPPLEMENTARY MATERIAL

The Supplementary Material for this article can be found online at: https://www.frontiersin.org/articles/10.3389/fcell.2021.620248/full#supplementary-material

Supplementary Figure 1 | Schematic workflow outlining the selection of radiogenes. Venn diagram comparing the high-throughput (HTP) and literature-derived cancer radioresistance-associated genes. Functional enrichment and interaction network analysis of the common 88 genes resulted in 36 genes. Red, up-regulated genes; Green, down-regulated genes.

Supplementary Figure 2 | Differential expression patterns of radiogenes in the corresponding cancer tissue; BRCA, breast invasive carcinoma; COAD, colon adenocarcinoma; LAML, acute myeloid leukemia. The red box represents cancer tissue samples and the gray box indicates normal samples.

Supplementary Figure 3 | Kaplan-Meier curves depicting the prognostic value of radiogenes for overall survival in invasive breast carcinoma **(A)** *CHEK1*, **(B)** *PLK1*, **(C)** *MAP2K1* and **(D)** *NFKBIA*. The HR "HR(high)" and the corresponding p-values "p(HR)" are shown. The 95% confidence intervals (CI) are denoted by dotted lines. The number of high-risk and low-risk patients are indicated by "n(high)" and "n(low)," respectively.

Supplementary Table 1 | Samples from each transcriptomic dataset analyzed in this study.

Supplementary Table 2 | List of the differentially expressed genes (DEGs) of each of the three transcriptome datasets and the DEGs common among datasets. Log_2FC of radioresistant vs. radiosensitive differentially expressed genes in GSE120798 (breast cancer) cell lines; cut-off $|log_2FC \geq 2|$.

Supplementary Table 3 | List of the merged DEGs from each dataset, literature-derived genes/proteins and common molecules.

REFERENCES

Akl, H., Vervloessem, T., Kiviluoto, S., Bittremieux, M., Parys, J. B., De Smedt, H., et al. (2014). A dual role for the anti-apoptotic Bcl-2 protein in cancer: mitochondria versus endoplasmic reticulum. *Biochim. Biophys. Acta* 1843, 2240–2252. doi: 10.1016/j.bbamcr.2014.04.017

Alnasir, J., and Shanahan, H. P. (2015). Investigation into the annotation of protocol sequencing steps in the sequence read archive. *Gigascience* 4:23. doi: 10.1186/s13742-015-0064-7

Avalle, L., Pensa, S., Regis, G., Novelli, F., and Poli, V. (2012). STAT1 and STAT3 in tumorigenesis: a matter of balance. *JAKSTAT* 1, 65–72. doi: 10.4161/jkst.20045

Awasthi, P., Foiani, M., and Kumar, A. (2015). ATM and ATR signaling at a glance. *J. Cell Sci.* 128, 4255–4262. doi: 10.1242/jcs.169730

Barkett, M., and Gilmore, T. D. (1999). Control of apoptosis by Rel/NF-kappaB transcription factors. *Oncogene* 18, 6910–6924. doi: 10.1038/sj.onc.1203238

Barrett, T., Wilhite, S. E., Ledoux, P., Evangelista, C., Kim, I. F., Tomashevsky, M., et al. (2013). NCBI GEO: archive for functional genomics data sets–update. *Nucleic Acids Res.* 41, D991–D995. doi: 10.1093/nar/gks1193

Baskar, R., Lee, K. A., Yeo, R., and Yeoh, K. W. (2012). Cancer and radiation therapy: current advances and future directions. *Int. J. Med. Sci.* 9, 193–199. doi: 10.7150/ijms.3635

Begg, A. C., Stewart, F. A., and Vens, C. (2011). Strategies to improve radiotherapy with targeted drugs. *Nat. Rev. Cancer* 11, 239–253. doi: 10.1038/nrc3007

Beheshti, A., McDonald, J. T., Miller, J., Grabham, P., and Costes, S. V. (2019). GeneLab database analyses suggest long-term impact of space radiation on the cardiovascular system by the activation of FYN through reactive oxygen species. *Int. J. Mol. Sci.* 20:661. doi: 10.3390/ijms20030661

Benjamini, Y., and Hochberg, Y. (1995). Controlling the false discovery rate: a practical and powerful approach to multiple testing. *J. R. Stat. Soc. Ser. B* 57, 289–300. doi: 10.1111/j.2517-6161.1995.tb02031.x

Braschi, B., Denny, P., Gray, K., Jones, T., Seal, R., Tweedie, S., et al. (2019). Genenames.org: the HGNC and VGNC resources in 2019. *Nucleic Acids Res.* 47, D786–D792. doi: 10.1093/nar/gky930

Bruinsma, W., Aprelia, M., Garcia-Santisteban, I., Kool, J., Xu, Y. J., and Medema, R. H. (2017). Inhibition of Polo-like kinase 1 during the DNA damage response is mediated through loss of Aurora A recruitment by Bora. *Oncogene* 36, 1840–1848. doi: 10.1038/onc.2016.347

Budman, J., and Chu, G. (2005). Processing of DNA for nonhomologous end-joining by cell-free extract. *EMBO J.* 24, 849–860. doi: 10.1038/sj.emboj.7600563

Bukowska, B., and Karwowski, B. T. (2018). The clustered DNA lesions - types, pathways of repair and relevance to human health. *Curr. Med. Chem.* 25, 2722–2735. doi: 10.2174/0929867325666180226110502

Burger, K., Ketley, R. F., and Gullerova, M. (2019). Beyond the trinity of ATM, ATR, and DNA-PK: multiple kinases shape the DNA damage response in concert with RNA metabolism. *Front. Mol. Biosci.* 6:61. doi: 10.3389/fmolb.2019.00061

Cai, C. K., Zhao, G. Y., Tian, L. Y., Liu, L., Yan, K., Ma, Y. L., et al. (2012). miR-15a and miR-16-1 downregulate CCND1 and induce apoptosis and cell cycle arrest in osteosarcoma. *Oncol. Rep.* 28, 1764–1770. doi: 10.3892/or.2012.1995

Caldecott, K. W. (2008). Single-strand break repair and genetic disease. *Nat. Rev. Genet.* 9, 619–631. doi: 10.1038/nrg2380

Capaccione, K. M., and Pine, S. R. (2013). The Notch signaling pathway as a mediator of tumor survival. *Carcinogenesis* 34, 1420–1430. doi: 10.1093/carcin/bgt127

Chiou, S. K., Jones, M. K., and Tarnawski, A. S. (2003). Survivin - an anti-apoptosis protein: its biological roles and implications for cancer and beyond. *Med. Sci. Monit.* 9, PI25–PI29.

Clough, E., and Barrett, T. (2016). The gene expression omnibus database. *Methods Mol. Biol.* 1418, 93–110. doi: 10.1007/978-1-4939-3578-9_5

Delaney, G., Jacob, S., Featherstone, C., and Barton, M. (2005). The role of radiotherapy in cancer treatment: estimating optimal utilization from a review of evidence-based clinical guidelines. *Cancer* 104, 1129–1137. doi: 10.1002/cncr.21324

Deng, C. X. (2006). BRCA1: cell cycle checkpoint, genetic instability, DNA damage response and cancer evolution. *Nucleic Acids Res.* 34, 1416–1426. doi: 10.1093/nar/gkl010

Deveraux, Q. L., and Reed, J. C. (1999). IAP family proteins–suppressors of apoptosis. *Genes Dev.* 13, 239–252. doi: 10.1101/gad.13.3.239

Duckett, C. S., Nava, V. E., Gedrich, R. W., Clem, R. J., Van Dongen, J. L., Gilfillan, M. C., et al. (1996a). A conserved family of cellular genes related to the baculovirus iap gene and encoding apoptosis inhibitors. *EMBO J.* 15, 2685–2694 doi: 10.1002/j.1460-2075.1996.tb00629.x

Duckett, D. R., Drummond, J. T., Murchie, A. I., Reardon, J. T., Sancar, A., Lilley, D. M., et al. (1996b). Human MutSalpha recognizes damaged DNA base pairs containing O6-methylguanine, O4-methylthymine, or the cisplatin-d(GpG) adduct. *Proc. Natl. Acad. Sci. U. S. A.* 93, 6443–6447. doi: 10.1073/pnas.93.13.6443

Edelbrock, M. A., Kaliyaperumal, S., and Williams, K. J. (2013). Structural, molecular and cellular functions of MSH2 and MSH6 during DNA mismatch repair, damage signaling and other noncanonical activities. *Mutat. Res.* 743–744, 53–66. doi: 10.1016/j.mrfmmm.2012.12.008

Efron, B., and Tibshirani, R. (1993). *An Introduction to the Bootstrap*. Boca Raton, FL: Chapman & Hall/CRC.

Emons, G., Spitzner, M., Reineke, S., Moller, J., Auslander, N., Kramer, F., et al. (2017). Chemoradiotherapy resistance in colorectal cancer cells is mediated by Wnt/beta-catenin signaling. *Mol. Cancer Res.* 15, 1481–1490. doi: 10.1158/1541-7786.MCR-17-0205

Flaggs, G., Plug, A. W., Dunks, K. M., Mundt, K. E., Ford, J. C., Quiggle, M. R., et al. (1997). Atm-dependent interactions of a mammalian chk1 homolog with meiotic chromosomes. *Curr. Biol.* 7, 977–986. doi: 10.1016/S0960-9822(06)00417-9

Francica, P., Mutlu, M., Blomen, V. A., Oliveira, C., Nowicka, Z., Trenner, A., et al. (2020). Functional radiogenetic profiling implicates ERCC6L2 in non-homologous end joining. *Cell Rep.* 32:108068. doi: 10.1016/j.celrep.2020.108068

Fridman, J. S., and Lowe, S. W. (2003). Control of apoptosis by p53. *Oncogene* 22, 9030–9040. doi: 10.1038/sj.onc.1207116

Fujise, K., Zhang, D., Liu, J., and Yeh, E. T. (2000). Regulation of apoptosis and cell cycle progression by MCL1. Differential role of proliferating cell nuclear antigen. *J. Biol. Chem.* 275, 39458–39465. doi: 10.1074/jbc.M006626200

Gatti, R. A., Berkel, I., Boder, E., Braedt, G., Charmley, P., Concannon, P., et al. (1988). Localization of an ataxia-telangiectasia gene to chromosome 11q22-23. *Nature* 336, 577–580. doi: 10.1038/336577a0

Georgakilas, A. G., O'Neill, P., and Stewart, R. D. (2013). Induction and repair of clustered DNA lesions: what do we know so far? *Radiat. Res.* 180, 100–109. doi: 10.1667/RR3041.1

Glaser, S. P., Lee, E. F., Trounson, E., Bouillet, P., Wei, A., Fairlie, W. D., et al. (2012). Anti-apoptotic Mcl-1 is essential for the development and sustained growth of acute myeloid leukemia. *Genes Dev.* 26, 120–125. doi: 10.1101/gad.182980.111

Gray, M., Turnbull, A. K., Ward, C., Meehan, J., Martinez-Perez, C., Bonello, M., et al. (2019). Development and characterisation of acquired radioresistant breast cancer cell lines. *Radiat. Oncol.* 14:64. doi: 10.1186/s13014-019-1268-2

Gudmundsdottir, K., and Ashworth, A. (2006). The roles of BRCA1 and BRCA2 and associated proteins in the maintenance of genomic stability. *Oncogene* 25, 5864–5874. doi: 10.1038/sj.onc.1209874

Habraken, Y., Sung, P., Prakash, L., and Prakash, S. (1996). Binding of insertion/deletion DNA mismatches by the heterodimer of yeast mismatch repair proteins MSH2 and MSH3. *Curr. Biol.* 6, 1185–1187. doi: 10.1016/S0960-9822(02)70686-6

Hada, M., and Georgakilas, A. G. (2008). Formation of clustered DNA damage after high-LET irradiation: a review. *J. Radiat. Res.* 49, 203–210. doi: 10.1269/jrr.07123

Han, J., Flemington, C., Houghton, A. B., Gu, Z., Zambetti, G. P., Lutz, R. J., et al. (2001). Expression of bbc3, a pro-apoptotic BH3-only gene, is regulated by diverse cell death and survival signals. *Proc. Natl. Acad. Sci. U. S. A.* 98, 11318–11323. doi: 10.1073/pnas.201208798

Haupt, S., Berger, M., Goldberg, Z., and Haupt, Y. (2003). Apoptosis - the p53 network. *J. Cell Sci.* 116 (Pt 20), 4077–4085. doi: 10.1242/jcs.00739

Holt, S. M., Scemama, J. L., Panayiotidis, M. I., and Georgakilas, A. G. (2009). Compromised repair of clustered DNA damage in the human acute lymphoblastic leukemia MSH2-deficient NALM-6 cells. *Mutat. Res.* 674, 123–130. doi: 10.1016/j.mrgentox.2008.09.014

Hung, C. M., Garcia-Haro, L., Sparks, C. A., and Guertin, A. D. (2012). mTOR-dependent cell survival mechanisms. *Cold Spring Harb. Perspect. Biol.* 4:a008771. doi: 10.1101/cshperspect.a008771

Hyun, S. Y., Hwang, H. I., and Jang, Y. J. (2014). Polo-like kinase-1 in DNA damage response. *BMB Rep.* 47, 249–255. doi: 10.5483/BMBRep.2014.47.5.061

Iliakis, G., Wang, Y., Guan, J., and Wang, H. (2003). DNA damage checkpoint control in cells exposed to ionizing radiation. *Oncogene* 22, 5834–5847. doi: 10.1038/sj.onc.1206682

Iyer, R. R., Pluciennik, A., Burdett, V., and Modrich, P. L. (2006). DNA mismatch repair: functions and mechanisms. *Chem. Rev.* 106, 302–323. doi: 10.1021/cr0404794

Kanakoglou, D. S., Michalettou, T. D., Vasileiou, C., Gioukakis, E., Maneta, D., Kyriakidis, K. V., et al. (2020). Effects of high-dose ionizing radiation in human gene expression: a meta-analysis. *Int. J. Mol. Sci.* 21:1938. doi: 10.3390/ijms21061938

Kim, D., Langmead, B., and Salzberg, S. L. (2015). HISAT: a fast spliced aligner with low memory requirements. *Nat. Methods* 12, 357–360. doi: 10.1038/nmeth.3317

Kim, H., Lee, O. H., Xin, H., Chen, L. Y., Qin, J., Chae, H. K., et al. (2009). TRF2 functions as a protein hub and regulates telomere maintenance by recognizing specific peptide motifs. *Nat. Struct. Mol. Biol.* 16, 372–379. doi: 10.1038/nsmb.1575

Kolas, N. K., Chapman, J. R., Nakada, S., Ylanko, J., Chahwan, R., Sweeney, F. D., et al. (2007). Orchestration of the DNA-damage response by the RNF8 ubiquitin ligase. *Science* 318, 1637–1640. doi: 10.1126/science.1150034

Kontou, P. I., Pavlopoulou, A., and Bagos, P. G. (2018). Methods of analysis and meta-analysis for identifying differentially expressed genes. *Methods Mol. Biol.* 1793, 183–210. doi: 10.1007/978-1-4939-7868-7_12

Kryston, T. B., Georgiev, A. B., Pissis, P., and Georgakilas, A. G. (2011). Role of oxidative stress and DNA damage in human carcinogenesis. *Mutat. Res.* 711, 193–201. doi: 10.1016/j.mrfmmm.2010.12.016

Kutmon, M., Riutta, A., Nunes, N., Hanspers, K., Willighagen, E. L., Bohler, A., et al. (2016). WikiPathways: capturing the full diversity of pathway knowledge. *Nucleic Acids Res.* 44, D488–D494. doi: 10.1093/nar/gkv1024

Lamarche, B. J., Orazio, N. I., and Weitzman, M. D. (2010). The MRN complex in double-strand break repair and telomere maintenance. *FEBS Lett.* 584, 3682–3695. doi: 10.1016/j.febslet.2010.07.029

Larrea, A. A., Lujan, S. A., and Kunkel, T. A. (2010). SnapShot: DNA mismatch repair. *Cell* 141:730.e1. doi: 10.1016/j.cell.2010.05.002

Li, D. (2019). "Statistical methods for rna sequencing data analysis," in *Computational Biology*, ed H. Husi (Brisbane, QLD: Codon Publications).

Li, H., Handsaker, B., Wysoker, A., Fennell, T., Ruan, J., Homer, N., et al. (2009). The sequence alignment/map format and SAMtools. *Bioinformatics* 25, 2078–2079. doi: 10.1093/bioinformatics/btp352

Li, H. S., Zhou, Y. N., Li, L., Li, S. F., Long, D., Chen, X. L., et al. (2019). HIF-1alpha protects against oxidative stress by directly targeting mitochondria. *Redox Biol.* 25:101109. doi: 10.1016/j.redox.2019.101109

Li, Z., Pearlman, A. H., and Hsieh, P. (2016). DNA mismatch repair and the DNA damage response. *DNA Repair* 38, 94–101. doi: 10.1016/j.dnarep.2015.11.019

Liao, Y., Wang, J., Jaehnig, E. J., Shi, Z., and Zhang, B. (2019). WebGestalt 2019: gene set analysis toolkit with revamped UIs and APIs. *Nucleic Acids Res.* 47, W199–W205. doi: 10.1093/nar/gkz401

Liu, T., Zhang, L., Joo, D., and Sun, S. C (2017). NF-kappaB signaling in inflammation. *Signal Transduct. Target Ther.* 2:17023. doi: 10.1038/sigtrans.2017.23

Lu, X. X., Cao, L. Y., Chen, X., Xiao, J., Zou, Y., and Chen, Q. (2016). PTEN inhibits cell proliferation, promotes cell apoptosis, and induces cell cycle arrest via downregulating the PI3K/AKT/hTERT pathway in lung adenocarcinoma A549 cells. *Biomed. Res. Int.* 2016:2476842. doi: 10.1155/2016/2476842

Ma, T., Keller, J. A., and Yu, X. (2011). RNF8-dependent histone ubiquitination during DNA damage response and spermatogenesis. *Acta Biochim. Biophys. Sin.* 43, 339–345. doi: 10.1093/abbs/gmr016

Marechal, A., and Zou, L. (2013). DNA damage sensing by the ATM and ATR kinases. *Cold Spring Harb. Perspect. Biol.* 5:a012716. doi: 10.1101/cshperspect.a012716

Marioni, J. C., Mason, C. E., Mane, S. M., Stephens, M., and Gilad, Y. (2008). RNA-seq: an assessment of technical reproducibility and comparison with gene expression arrays. *Genome Res.* 18, 1509–1517. doi: 10.1101/gr.079558.108

Marston, E., Weston, V., Jesson, J., Maina, E., McConville, C., Agathanggelou, A., et al. (2009). Stratification of pediatric ALL by *in vitro* cellular responses to DNA double-strand breaks provides insight into the molecular mechanisms underlying clinical response. *Blood* 113, 117–126. doi: 10.1182/blood-2008-03-142950

Mavragani, I. V., Nikitaki, Z., Kalospyros, S. A., and Georgakilas, A. G. (2019). Ionizing radiation and complex DNA damage: from prediction to detection challenges and biological significance. *Cancers* 11:1789. doi: 10.3390/cancers11111789

Mavragani, I. V., Nikitaki, Z., Souli, M. P., Aziz, A., Nowsheen, S., Aziz, K., et al. (2017). Complex DNA damage: a route to radiation-induced genomic instability and carcinogenesis. *Cancers* 9:91. doi: 10.3390/cancers9070091

Metzker, M. L. (2010). Sequencing technologies - the next generation. *Nat. Rev. Genet.* 11, 31–46. doi: 10.1038/nrg2626

Mikkelsen, R. B., and Wardman, P. (2003). Biological chemistry of reactive oxygen and nitrogen and radiation-induced signal transduction mechanisms. *Oncogene* 22, 5734–5754. doi: 10.1038/sj.onc.1206663

Modrich, P. (1997). Strand-specific mismatch repair in mammalian cells. *J. Biol. Chem.* 272, 24727–24730. doi: 10.1074/jbc.272.40.24727

Multhoff, G., and Radons, J. (2012). Radiation, inflammation, and immune responses in cancer. *Front. Oncol.* 2:58. doi: 10.3389/fonc.2012.00058

Nakano, K., and Vousden, K. H. (2001). PUMA, a novel proapoptotic gene, is induced by p53. *Mol. Cell* 7, 683–694. doi: 10.1016/S1097-2765(01)00214-3

Nikitaki, Z., Mavragani, I. V., Laskaratou, D. A., Gika, V., Moskvin, V. P., Theofilatos, K., et al. (2016). Systemic mechanisms and effects of ionizing radiation: a new "old" paradigm of how the bystanders and distant can become the players. *Semin. Cancer Biol.* 37–38, 77–95. doi: 10.1016/j.semcancer.2016.02.002

Nikitaki, Z., Michalopoulos, I., and Georgakilas, A. G. (2015). Molecular inhibitors of DNA repair: searching for the ultimate tumor killing weapon. *Future Med. Chem.* 7, 1543–1558. doi: 10.4155/fmc.15.95

Oda, E., Ohki, R., Murasawa, H., Nemoto, J., Shibue, T., Yamashita, T., et al. (2000). Noxa, a BH3-only member of the Bcl-2 family and candidate mediator of p53-induced apoptosis. *Science* 288, 1053–1058. doi: 10.1126/science.288.5468.1053

Patel, M., Nowsheen, S., Maraboyina, S., and Xia, F. (2020). The role of poly(ADP-ribose) polymerase inhibitors in the treatment of cancer and methods to overcome resistance: a review. *Cell Biosci.* 10:35. doi: 10.1186/s13578-020-00390-7

Patil, M., Pabla, N., and Dong, Z. (2013). Checkpoint kinase 1 in DNA damage response and cell cycle regulation. *Cell. Mol. Life Sci.* 70, 4009–4021. doi: 10.1007/s00018-013-1307-3

Pavlopoulou, A., Bagos, P. G., Koutsandrea, V., and Georgakilas, A. G. (2017). Molecular determinants of radiosensitivity in normal and tumor tissue. A bioinformatic approach. *Cancer Lett.* 403, 37–47. doi: 10.1016/j.canlet.2017.05.023

Pavlopoulou, A., Oktay, Y., Vougas, K., Louka, M., Vorgias, C. E., and Georgakilas, A. G. (2016). Determinants of resistance to chemotherapy and ionizing radiation in breast cancer stem cells. *Cancer Lett.* 380, 485–493. doi: 10.1016/j.canlet.2016.07.018

Pawlowski, J., and Kraft, A. S. (2000). Bax-induced apoptotic cell death. *Proc. Natl. Acad. Sci. U. S. A.* 97, 529–531. doi: 10.1073/pnas.97.2.529

Pertea, M., Pertea, G. M., Antonescu, C. M., Chang, T. C., Mendell, J. T., and Salzberg, S. L. (2015). StringTie enables improved reconstruction of a transcriptome from RNA-seq reads. *Nat. Biotechnol.* 33, 290–295. doi: 10.1038/nbt.3122

Pezuk, J. A., Brassesco, M. S., Morales, A. G., de Oliveira, J. C., de Oliveira, H. F., Scrideli, C. A., et al. (2013). Inhibition of polo-like kinase 1 induces cell cycle arrest and sensitizes glioblastoma cells to ionizing radiation. *Cancer Biother. Radiopharm.* 28, 516–522. doi: 10.1089/cbr.2012.1415

Porta, C., Paglino, C., and Mosca, A. (2014). Targeting PI3K/Akt/mTOR signaling in cancer. *Front. Oncol.* 4:64. doi: 10.3389/fonc.2014.00064

Porter, A. G., and Janicke, R. U. (1999). Emerging roles of caspase-3 in apoptosis. *Cell Death Differ.* 6, 99–104. doi: 10.1038/sj.cdd.4400476

Pouyssegur, J., Dayan, F., and Mazure, N. M. (2006). Hypoxia signalling in cancer and approaches to enforce tumour regression. *Nature* 441, 437–443. doi: 10.1038/nature04871

Ramasamy, A., Mondry, A., Holmes, C. C., and Altman, D. G. (2008). Key issues in conducting a meta-analysis of gene expression microarray datasets. *PLoS Med.* 5:e184. doi: 10.1371/journal.pmed.0050184

Robinson, M. D., McCarthy, D. J., and Smyth, K. G. (2010). edgeR: a bioconductor package for differential expression analysis of digital gene expression data. *Bioinformatics* 26, 139–140. doi: 10.1093/bioinformatics/btp616

Robinson, M. D., and Oshlack, A. (2010). A scaling normalization method for differential expression analysis of RNA-seq data. *Genome Biol.* 11:R25. doi: 10.1186/gb-2010-11-3-r25

Rouse, J., and Jackson, S. P. (2002). Interfaces between the detection, signaling, and repair of DNA damage. *Science* 297, 547–551. doi: 10.1126/science.1074740

Sakellaropoulos, T., Vougas, K., Narang, S., Koinis, F., Kotsinas, A., Polyzos, A., et al. (2019). A deep learning framework for predicting response to therapy in cancer. *Cell Rep.* 29, 3367–3373.e4. doi: 10.1016/j.celrep.2019.11.017

Sayers, E. W., Beck, J., Brister, J. R., Bolton, E. E., Canese, K., Comeau, D. C., et al. (2020). Database resources of the national center for biotechnology information. *Nucleic Acids Res.* 48, D9–D16. doi: 10.1093/nar/gkz899

Schoenhals, J. E., Seyedin, S. N., Tang, C., Cortez, M. A., Niknam, S., Tsouko, E., et al. (2016). Preclinical rationale and clinical considerations for radiotherapy plus immunotherapy: going beyond local control. *Cancer J.* 22, 130–137. doi: 10.1097/PPO.0000000000000181

Smith, D., Mann, D., and Yong, K. (2016). Cyclin D type does not influence cell cycle response to DNA damage caused by ionizing radiation in multiple myeloma tumours. *Br. J. Haematol.* 173, 693–704. doi: 10.1111/bjh.13982

Sonenshein, G. E. (1997). Rel/NF-kappa B transcription factors and the control of apoptosis. *Semin. Cancer Biol.* 8, 113–119. doi: 10.1006/scbi.1997.0062

Soubeyrand, S., Pope, L., Pakuts, B., and Hache, R. J. (2003). Threonines 2638/2647 in DNA-PK are essential for cellular resistance to ionizing radiation. *Cancer Res.* 63, 1198–1201.

Spratt, D. E., and Speers, C. (2019). RadioGx: a new preclinical tool to model intrinsic radiosensitivity. *Cancer Res.* 79, 6076–6078. doi: 10.1158/0008-5472.CAN-19-3277

StataCorp (2013). *Stata Statistical Software: Release 13*. College Station, TX: StataCorp LP.

Stylianou, S., Clarke, R. B., and Brennan, K. (2006). Aberrant activation of notch signaling in human breast cancer. *Cancer Res.* 66, 1517–1525. doi: 10.1158/0008-5472.CAN-05-3054

Sulai, N. H., and Tan, A. R. (2018). Development of poly(ADP-ribose) polymerase inhibitors in the treatment of BRCA-mutated breast cancer. *Clin. Adv. Hematol. Oncol.* 16, 491–501.

Sutherland, B. M., Bennett, P. V., Sidorkina, O., and Laval, J. (2000). Clustered DNA damages induced in isolated DNA and in human cells by low doses of ionizing radiation. *Proc. Natl. Acad. Sci. U. S. A.* 97, 103–108. doi: 10.1073/pnas.97.1.103

Swanton, E., Savory, P., Cosulich, S., Clarke, P., and Woodman, P. (1999). Bcl-2 regulates a caspase-3/caspase-2 apoptotic cascade in cytosolic extracts. *Oncogene* 18, 1781–1787. doi: 10.1038/sj.onc.1202490

Syed, V. (2016). TGF-beta signaling in cancer. *J. Cell Biochem.* 117, 1279–1287. doi: 10.1002/jcb.25496

Szklarczyk, D., Gable, A. L., Lyon, D., Junge, A., Wyder, S., Huerta-Cepas, J., et al. (2019). STRING v11: protein-protein association networks with increased coverage, supporting functional discovery in genome-wide experimental datasets. *Nucleic Acids Res.* 47, D607–D613. doi: 10.1093/nar/gky1131

Taalman, R. D., Jaspers, N. G., Scheres, J. M., de Wit, J., and Hustinx, T. W. (1983). Hypersensitivity to ionizing radiation, *in vitro*, in a new chromosomal breakage disorder, the Nijmegen breakage syndrome. *Mutat. Res.* 112, 23–32. doi: 10.1016/0167-8817(83)90021-4

Tang, C., Wang, X., Soh, H., Seyedin, S., Cortez, M. A., Krishnan, S., et al. (2014). Combining radiation and immunotherapy: a new systemic therapy for solid tumors? *Cancer Immunol. Res.* 2, 831–838. doi: 10.1158/2326-6066.CIR-14-0069

Tang, Z., Li, C., Kang, B., Gao, G., Li, C., and Zhang, Z. (2017). GEPIA: a web server for cancer and normal gene expression profiling and interactive analyses. *Nucleic Acids Res*. 45, W98–W102. doi: 10.1093/nar/gkx247

Unger, K. (2014). Integrative radiation systems biology. *Radiat. Oncol*. 9:21. doi: 10.1186/1748-717X-9-21

Van den Bossche, J., Domen, A., Peeters, M., Deben, C., De Pauw, I., Jacobs, J., et al. (2019). Radiosensitization of non-small cell lung cancer cells by the Plk1 inhibitor volasertib is dependent on the p53 status. *Cancers* 11:1893. doi: 10.3390/cancers11121893

Vougas, K., Sakellaropoulos, T., Kotsinas, A., Foukas, G. P., Ntargaras, A., Koinis, F., et al. (2019). Machine learning and data mining frameworks for predicting drug response in cancer: an overview and a novel *in silico* screening process based on association rule mining. *Pharmacol. Ther*. 203:107395. doi: 10.1016/j.pharmthera.2019.107395

Wang, M., Chen, X., Chen, H., Zhang, X., Li, J., Gong, H., et al. (2015). RNF8 plays an important role in the radioresistance of human nasopharyngeal cancer cells *in vitro*. *Oncol. Rep*. 34, 341–349. doi: 10.3892/or.2015.3958

Wang, W., Yang, L., Hu, L., Li, F., Ren, L., Yu, H., et al. (2013). Inhibition of UBE2D3 expression attenuates radiosensitivity of MCF-7 human breast cancer cells by increasing hTERT expression and activity. *PLoS ONE* 8:e64660. doi: 10.1371/journal.pone.0064660

Wang, Y., Branicky, R., Noe, A., and Hekimi, S. (2018). Superoxide dismutases: dual roles in controlling ROS damage and regulating ROS signaling. *J. Cell Biol*. 217, 1915–1928. doi: 10.1083/jcb.201708007

Weng, L., Brown, J., and Eng, C. (2001). PTEN induces apoptosis and cell cycle arrest through phosphoinositol-3-kinase/Akt-dependent and -independent pathways. *Hum. Mol. Genet*. 10, 237–242. doi: 10.1093/hmg/10.3.237

Yamamori, T., Yasui, H., Yamazumi, M., Wada, Y., Nakamura, Y., Nakamura, H., et al. (2012). Ionizing radiation induces mitochondrial reactive oxygen species production accompanied by upregulation of mitochondrial electron transport chain function and mitochondrial content under control of the cell cycle checkpoint. *Free Radic. Biol. Med*. 53, 260–270. doi: 10.1016/j.freeradbiomed.2012.04.033

Yang, J., Xu, Z. P., Huang, Y., Hamrick, H. E., Duerksen-Hughes, P. J., and Yu, Y. N. (2004). ATM and ATR: sensing DNA damage. *World J. Gastroenterol*. 10, 155–160. doi: 10.3748/wjg.v10.i2.155

Zhang, B., Kirov, S., and Snoddy, J. (2005). WebGestalt: an integrated system for exploring gene sets in various biological contexts. *Nucleic Acids Res*. 33, W741–W748. doi: 10.1093/nar/gki475

Zhao, S., Weng, Y. C., Yuan, S. S., Lin, Y. T., Hsu, H. C., Lin, S. C., et al. (2000). Functional link between ataxia-telangiectasia and Nijmegen breakage syndrome gene products. *Nature* 405, 473–477. doi: 10.1038/35013083

Conflict of Interest: The authors declare that the research was conducted in the absence of any commercial or financial relationships that could be construed as a potential conflict of interest.

Copyright © 2021 Toy, Karakülah, Kontou, Alotaibi, Georgakilas and Pavlopoulou. This is an open-access article distributed under the terms of the Creative Commons Attribution License (CC BY). The use, distribution or reproduction in other forums is permitted, provided the original author(s) and the copyright owner(s) are credited and that the original publication in this journal is cited, in accordance with accepted academic practice. No use, distribution or reproduction is permitted which does not comply with these terms.

frontiers in Cell and Developmental Biology

ORIGINAL RESEARCH
published: 17 May 2021
doi: 10.3389/fcell.2021.658346

Oncogenic Landscape of Somatic Mutations Perturbing Pan-Cancer lncRNA-ceRNA Regulation

Yuanfu Zhang[1†], Peng Han[2,3†], Qiuyan Guo[4†], Yangyang Hao[1], Yue Qi[1], Mengyu Xin[1], Yafang Zhang[5], Binbin Cui[2]* and Peng Wang[1]**

[1] College of Bioinformatics Science and Technology, Harbin Medical University, Harbin, China, [2] Department of Colorectal Surgery, Harbin Medical University Cancer Hospital, Harbin, China, [3] Heilongjiang Cancer Research Institute, Harbin, China, [4] Department of Gynecology, The First Affiliated Hospital of Harbin Medical University, Harbin, China, [5] Department of Anatomy, Harbin Medical University, Harbin, China

OPEN ACCESS

Edited by:
Kanaga Sabapathy,
National Cancer Centre Singapore, Singapore

Reviewed by:
Emenike K. Onyido,
Swansea University Medical School, United Kingdom
Ashish Lal,
National Institutes of Health (NIH), United States

***Correspondence:**
Peng Wang
wpgqy@163.com
Binbin Cui
13351112888@163.com
Yafang Zhang
yafangzhang2008@aliyun.com

†These authors share first authorship

Specialty section:
This article was submitted to Molecular Medicine, a section of the journal Frontiers in Cell and Developmental Biology

Received: 25 January 2021
Accepted: 19 April 2021
Published: 17 May 2021

Citation:
Zhang Y, Han P, Guo Q, Hao Y, Qi Y, Xin M, Zhang Y, Cui B and Wang P (2021) Oncogenic Landscape of Somatic Mutations Perturbing Pan-Cancer lncRNA-ceRNA Regulation. Front. Cell Dev. Biol. 9:658346. doi: 10.3389/fcell.2021.658346

Competing endogenous RNAs (ceRNA) are transcripts that communicate with and co-regulate each other by competing for the binding of shared microRNAs (miRNAs). Long non-coding RNAs (lncRNAs) as a type of ceRNA constitute a competitive regulatory network determined by miRNA response elements (MREs). Mutations in lncRNA MREs destabilize their original regulatory pathways. Study of the effects of lncRNA somatic mutations on ceRNA mechanisms can clarify tumor mechanisms and contribute to the development of precision medicine. Here, we used somatic mutation profiles collected from TCGA to characterize the role of lncRNA somatic mutations in the ceRNA regulatory network in 33 cancers. The 31,560 mutation sites identified by TargetScan and miRanda affected the balance of 70,811 ceRNA regulatory pathways. Putative mutations were categorized as high or low based on mutation frequencies. Multivariate multiple regression revealed a significant effect of 162 high-frequency mutations in six cancer types on the expression levels of target mRNAs (ceMs) through the ceRNA mechanism. Low-frequency mutations in multiple cancers perturbing 1624 ceM have been verified by Student's *t*-test, indicating a significant mechanism of changes in the expression level of oncogenic genes. Oncogenic signaling pathway studies involving ceMs indicated functional heterogeneity of multiple cancers. Furthermore, we identified that lncRNA, perturbing ceMs associated with patient survival, have potential as biomarkers. Our collective findings revealed individual differences in somatic mutations perturbing ceM expression and impacting tumor heterogeneity.

Keywords: ceRNA, somatic mutation, prognosis, functional analysis, oncogenic pathway

INTRODUCTION

In recent years, novel, post-transcriptional regulatory mechanisms of competing endogenous RNAs (ceRNAs) have been revealed. RNA molecules, including messenger RNAs (mRNAs), long noncoding RNAs (lncRNAs), circular RNAs, and pseudogene transcripts, can function as competing endogenous RNAs (ceRNAs) to indirectly regulate the expression of relevant target genes by competing with each other for microRNAs (miRNAs) (Salmena et al., 2011). These ceRNAs harbor miRNA response elements (MREs) that bind to miRNA through complementary

sequences and can induce degradation or inhibition of the expression of target genes. In addition, the combination of miRNAs and target genes was a complex network; one miRNA can regulate multiple genes and one gene can be regulated by multiple miRNAs.

LncRNAs were once regarded as byproducts of gene transcription (Quinn and Chang, 2016). However, they are crucial in post-transcriptional regulation through the ceRNA mechanism (Chen et al., 2019) and are dramatic factors that contribute to biological growth and development, aging, diseases, and multiple cancers (Rinn and Chang, 2012; Schmitt and Chang, 2016). For example, MALAT1, which is highly expressed in most cancers, regulates the cell cycle (Tripathi et al., 2013), and PCA3 is an important molecular marker in the early stage of cancer (Lemos et al., 2019). Somatic mutations, which occur in cells other than germ cells and are not inherited, are the substantial cause of most tumors (Jia and Zhao, 2017). Mutation in an miRNA response elements (MRE) of lncRNA can weaken, enhance, or prevent binding to the original miRNA, resulting in an imbalance in the ceRNA regulatory network and altered expression of the relevant target genes (Thomas et al., 2011; Thomson and Dinger, 2016).

The development of sequencing technologies has enabled the identification of somatic mutations associated with tumors (Martincorena and Campbell, 2015). Genetic variations affecting miRNA gene expression have been described (Civelek et al., 2013; Siddle et al., 2014), as has the expression of coding genes whose 3′ untranslated regions are targeted by miRNAs (Gamazon et al., 2012; Lu and Clark, 2012). Genetic polymorphisms affecting the regulation of human ceRNAs have been reported (Li M. J. et al., 2017). However, few studies have explored the effects of somatic mutations on ceRNA mechanisms.

Here, we used mutation and RNA-seq profiles from The Cancer Genome Atlas (TCGA) (Tomczak et al., 2015) database to conduct a systematic investigation concerning the effects of lncRNA mutations on the expression of target mRNAs via the ceRNA mechanism in pan-carcinoma. We also studied the impact of significant mutations on oncogenic mechanisms and patient survival.

MATERIALS AND METHODS

Data Collection

Information concerning RNA-seq and somatic mutation profiles of 33 cancers were obtained from The Cancer Genome Atlas (Tomczak et al., 2015) (TCGA)[1] database. The GRCh38 v29 version of the human genome annotation data from GENCODE (Harrow et al., 2012)[2], including the position and sequence information of lncRNAs, was used to annotate somatic mutation profiles. Sequences of miRNA and annotation information were obtained from the miRBase (Kozomara and Griffiths-Jones, 2014)[3] database. Interaction data of miRNA and target genes (mRNA) that were validated using established experimental methods including the luciferase reporter assay, PCR, and western blotting were collected from miRTarBase (Chou et al., 2018) V8.0[4]. Hallmark (Hanahan and Weinberg, 2011) gene sets were collected from the Molecular Signatures Database (MSigDB Liberzon et al., 2011)[5].

Construction of Somatic Mutation-miRNA-lncRNA (ceL)-mRNA (ceM) Unit

Among the numerous somatic mutations in the pan-cancer genome, lncRNA mutations was the focus of this study. We, respectively, define the lncRNA and mRNA involved in the ceRNA regulatory mechanism as ceL and ceM. Sequences approximately 7 nucleotide (nt) upstream and downstream of the lncRNA somatic mutation sites were extracted using the lncRNA annotation from GENCODE, which will be used to construct mutation and control sequences. Considering that the TargetScan (Friedman et al., 2009) software does not recognize short sequences, it was necessary to extract longer upstream nucleotide sequences (14 nt) to offset this impact. TargetScan and miRanda (Betel et al., 2008) (e.g., the miRanda algorithm) are miRNA target gene prediction tools, and therefore were used to predict the miRNA-target relationships of control sequences with strict thresholds of score > 160 and energy < -20 for miRanda and context score < -0.4 for TargetScan. We defined the lncRNA and mRNA involved in the imbalance of ceRNA regulatory mechanism as ceL and ceM, respectively. We selected "mutation-miRNA-lncRNA (ceL)" units with varying binding affinities between the mutation and control sequences, and regarded loss, down, gain, and up as the four conditions of altered lncRNA and miRNA binding affinity (Li M. J. et al., 2017). We further searched for candidate mRNAs (ceMs) controlled by the same miRNA from the miRNA-target gene data of miRTarBase as the last element to construct the somatic mutation-miRNA-ceL-ceM (SMILM) unit. In this context, "putative mutations" are defined as mutations effecting original ceRNA regulation mechanism. This definition has been used in a previous study of genetic associations with ceRNA regulation in the human genome (Li et al., 2020).

Classification and Definition of Mutations

Somatic mutations do not occur frequently. We defined a site at which at least two samples displayed a mutation as a high-frequency (HF) mutation site. The remaining mutations were defined as low-frequency (LF) mutation sites. The altered binding affinity of lncRNA and miRNA binding was divided into four states (gain, up, loss, and down). Gain, up, loss, and down were scored as +1, +0.5, −1, and −0.5, respectively. The functional score of each mutation was calculated by summing the states of all mutated miRNAs associated with it. For LF mutations, we focused on the mRNAs (ceMs) affected by somatic mutations

[1]https://portal.gdc.cancer.gov/

[2]https://www.gencodegenes.org/

[3]http://www.mirbase.org/ftp.shtml

[4]http://mirtarbase.cuhk.edu.cn/php/index.php

[5]http://software.broadinstitute.org/gsea/msigdb

through ceRNA regulatory mechanisms. The possible expression tendency of the mRNA was defined as "up" means that the sum of the mutation scores that regulate this mRNA is greater than zero, "down" means the opposite of "up," and "none" means that the sum of the mutation scores that regulate this mRNA is equal to zero.

Multivariate Multiple Regression Analyses

Different experimental tools were used for identification of SMILM units mediated by HF mutations (HF-SMILM) and LF mutations (LF-SMILM). In the HF-SMILM unit, multivariate multiple regression models were used to validate whether the expression level normalized by Fragments PerKilobase Million (FPKM) of ceL and ceM conformed to target prediction results (Valente et al., 2014). The fold-change values were used to evaluate the extent of expression changes between two groups of samples. For each SMILM unit, we considered the expression levels of lncRNA (El) and mRNA (Em) as two independent response variables. As a predictor, the genotype (Gt) of an individual was used as the driving variable. Synergistic factors such as the residual expression of miRNAs might also affect the response variables. At the same time, we assumed that the error vector $\varepsilon = (\varepsilon_1, \varepsilon_2)'$ followed a multivariate Gaussian distribution with an expected value of zero and an unknown covariance matrix. The multivariate multiple regression model constructed for the SMILM unit is:

$$(El, Em) = Gt + MIr + \varepsilon \quad (1)$$

We used this equation to validate all the SMILM units. We defined ηl and ηm as the regression coefficients of the driving variable Gt. The influence of Gt changes on the expression of ceL and ceM was quantified using the regression coefficients ηl and ηm, and the statistical significance of the model was obtained. Since ceL and ceM present a competitive relationship in the ceRNA mechanism, we required that ceL expression changes with genotype and ceM expression changes with genotype followed opposite tendencies ($\eta l \times \eta m < 0, p-\text{value} < 0.05$) (Li M. J. et al., 2017).

LF-SMILM unit data were split based on the characterization by ceM, obtaining the somatic mutations, lncRNA, miRNA, and samples corresponding to each ceM. We divided cancer samples into mutated and non-mutated samples according to whether the sample had mutations that affected the expression of specific mRNA (ceM) through the ceRNA mechanism. Student's *t*-test was used to compare the ceM expression changes in the two categories of sample. The ceMs with p-value < 0.05 were retained due to significant changes in their expression affected by putative mutations.

Construction of ceRNA Regulatory Network

In the SMILM unit validated by multivariate multiple regression models, the mutated lncRNA (ceL), miRNA, and target gene mRNA (ceM) constitute a two-level regulatory relationship. Therefore, we used Cytoscape (Shannon et al., 2003) to visualize this regulatory relationship in significant SMILM units [mutations-miRNA-lncRNA (ceL)-mRNA (ceM)] (Long et al., 2019).

Functional Enrichment Analysis Connecting Oncogenic Signaling Pathways

We obtained ceMs whose expression were significantly affected by somatic mutations through the ceRNA mechanism. To assess the role of these ceMs in various cancers, we used the compareCluster function in the R package clusterProfiler to perform functional analyses on multiple pan-cancer gene sets, using threshold pvalueCutoff = 0.05. Seventeen oncogenic signaling pathways (Malumbres and Barbacid, 2003; Reya and Clevers, 2005; Wade et al., 2013; Moradi-Marjaneh et al., 2018; Ayuk and Abrahamse, 2019; Soleimani et al., 2019, 2020) were collected from articles published between 2008 and 2019. The overlapping signal path was filtered out based on enrichment results.

Survival Analysis

We used the Cox proportional hazards model (Fisher and Lin, 1999) to estimate whether the expression of ceMs regulated by lncRNA mutations according to the ceRNA mechanism was related to patient survival. Hazard ratios (HRs) < 1 and $p < 0.05$ indicated significant relationships between ceM and reduced risk of death. An HR > 1 indicated the converse. Based on the predicted results, each sample was categorized as one of four types: including "None" means no mutation disrupts the expression of the target gene, "Up-regulated" means the presence of mutations that cause only upregulation of target gene expression, "Down-regulated" means the presence of mutations that cause only downregulation of target gene expression, and "Unknown" means that both mutations resulting in up- and down-regulation of the expression of the target gene are present. The R package for survival was used to create survival curves (Rich et al., 2010). The fitted results were visualized using a ggsurvplot. A p-value < 0.05 was considered to represent a significant difference in survival.

RESULTS

Global Mutation Map Reveals Heterogeneity of Different Tumors

We evaluated samples from the TCGA database collection for which somatic mutation data were available, producing a global map of somatic mutation sample distribution. The map contained 7604 samples with lncRNA mutations in 10,489 samples from 33 cancers (**Figure 1A** and **Supplementary Table 1**). We examined the distribution of mutations on chromosomes. The lncRNA mutations in multiple cancer types aggregated differently on chromosomes, especially in kidney renal papillary cell carcinoma (KIPR), acute myeloid leukemia (LAML), pheochromocytoma and paraganglioma (PCPG), thymoma (THYM), and uveal melanoma (UVM),

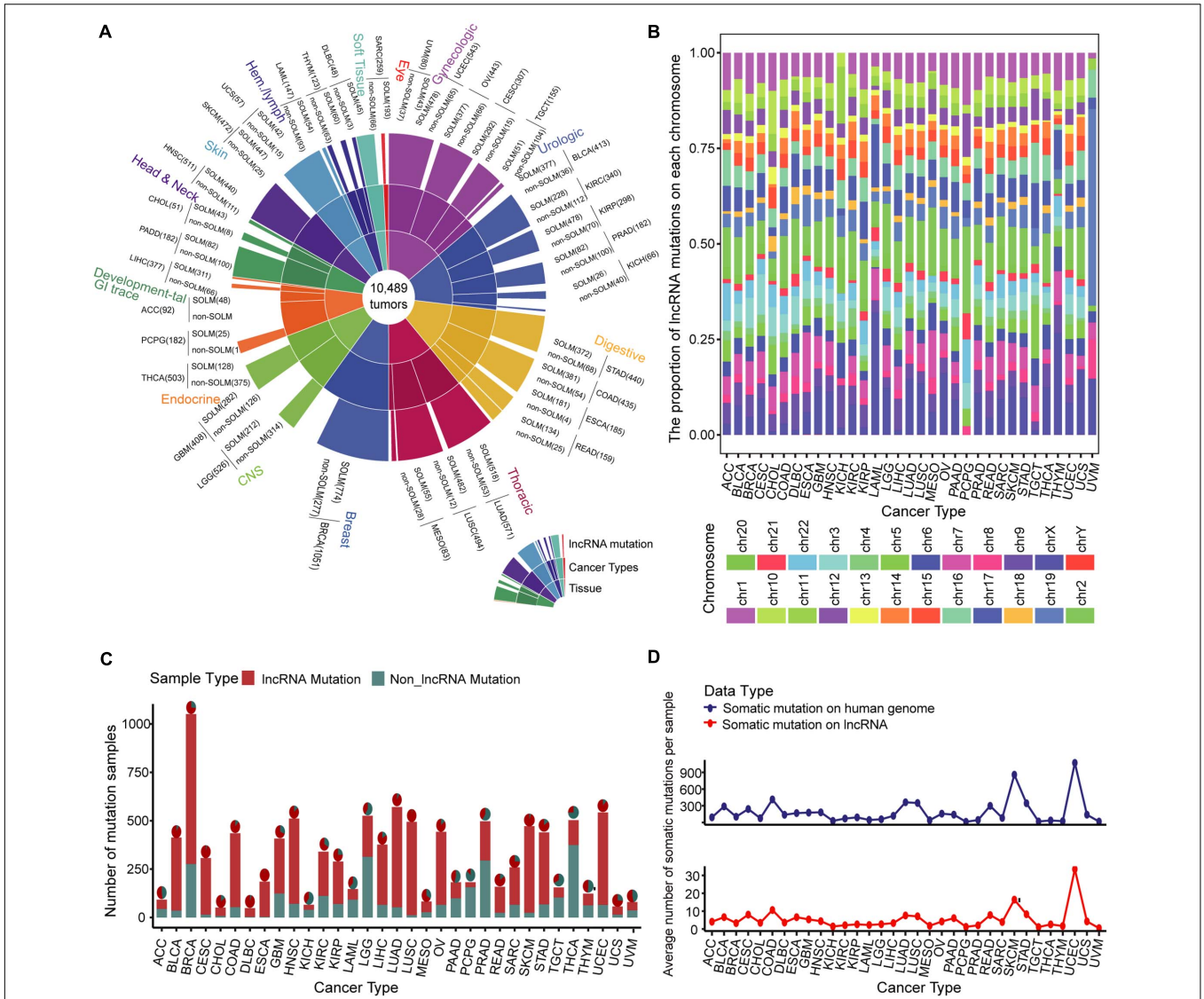

FIGURE 1 | Landscape of somatic mutations across 33 cancer types. **(A)** Global map of lncRNA mutations in different tissues and cancers. **(B)** Bar plot of the proportion of lncRNA mutations on each chromosome in multiple cancer types. Twenty-two pairs of homologous chromosomes and two sex chromosomes are marked with distinct colors. **(C)** Samples with lncRNA somatic mutations are marked in red in 33 cancer type samples. The pie chart illustrates the proportion of lncRNA mutations in all somatic mutations. **(D)** Average numbers of somatic mutations per sample on the entire genome and lncRNA are presented by line chart across 33 cancer types.

compared to those in other tumors (**Figure 1B**). These findings indicate that the distribution specificity of lncRNA mutations on chromosomes may be the underlying cause of cancer functional heterogeneity. Of all renal cell carcinoma subtypes, the KIPR subtype of kidney cancer has different molecular characteristics and poor survival (Cancer Genome Atlas Research Network, Linehan et al., 2016; Ricketts et al., 2018). Lung adenocarcinoma (LUAD) and lung squamous cell carcinoma (LUSC) lung cancer subtypes displayed similar mutation distribution profiles on chromosomes, suggesting that cancers in the same tissue site have a similar distribution of mutations on chromosomes. Breast invasive carcinoma (BRCA), kidney chromophobe (KICH), kidney renal clear cell carcinoma (KIRC), and thyroid carcinoma (THCA) displayed large sample sizes but relatively few lncRNA mutations, suggesting that mutations in lncRNAs have a strong distribution preference among various cancers (**Figures 1C,D**). LncRNA mutations had low frequencies in the range of 1 to 10%, suggesting that the rates of lncRNA mutations vary among cancer types (**Supplementary Figure 1**). These findings were consistent with previous studies showing that mutation frequency fluctuates significantly in pan-cancer, and that the mutation rate of some cancers is greatly increased due to missing repair pathways or chromosome integrity checkpoints (Martincorena and Campbell, 2015). We also assessed numbers of mutations per lncRNA in cancer types. A set of lncRNAs with a high mutation frequency was evident for multiple cancers (**Supplementary Figure 2**). The

lncRNAs XIST, TTN-AS1, STRA6LP, and TSIX had high numbers of mutations in most cancers, which play an important role in the oncogenic mechanism. The lncRNA XIST can regulate X chromosome silent transcription and act as an miRNA sponge upregulating SOD2 to inhibit the development of non-small cell lung cancer (Chen et al., 2016; Liu et al., 2019). TTN-AS1 is an miRNA sponge that regulates cancer development through a ceRNA mechanism (Wang Y. et al., 2020).

Significant Mechanism of lncRNA Mutation Perturbing ceRNA Regulation

We developed a pipeline to assess the effect of somatic mutations perturbing lncRNA-ceRNA regulation in pan-cancer (**Figure 2A**). To examine the influence of lncRNA mutations on miRNA binding sites according to TargetScan (Friedman et al., 2009) and miRanda (Betel et al., 2008), we used pan-cancer mutation profiles from TCGA. In total, we identified 31,560 putative somatic mutation sites for 33 cancer types in 3,124 putative miRNA target genes (putative lncRNAs). These mutated lncRNAs showed different binding affinities to 2437 miRNAs compared to wild type sequences across 33 cancers (**Figure 2B**). Considering that the larger numbers of putative mutations in several cancers are due to larger numbers of initial mutations, the proportions of putative mutations compared with the original lncRNA mutations were examined, which reflected the contribution of the mutations-miRNA-ceRNA mechanism in the carcinogenic process across the 33 cancers. PCPG, which had lower number of mutations and average number of mutations per sample, had the highest percentage of putative lncRNA mutations to original somatic mutations on lncRNA (**Figure 2C**), suggesting that the contribution of the mutations-miRNA-ceRNA mechanism in the oncogenic process is not determined simply by numbers of mutations. Next, for each putative lncRNA (ceL), we found other experimentally verified mRNAs (ceM) targeted by the same miRNA and established a minimal miRNA-ceRNA regulation unit, which we termed the somatic mutation-miRNA-ceL-ceM (SMILM) unit. Taken together, these results reveal significant mechanisms by which mutations perturb gene expression.

The frequency of somatic mutations is lower compared with genetic variations, and an appropriate number of mutation and control samples to explain the relationship between ceL and the corresponding ceM expression in SMILM units is not available (Li M. J. et al., 2017). Therefore, we defined mutations in at least two samples of the same cancer as high-frequency mutations (HF mutations, n = 831), and the rest as low-frequency mutations (LF mutations, n = 32,823) (**Figure 2D**). For these two categories of mutations, we separately applied multiple regression and Student's t-test to jointly model the contribution of mutations on ceRNA expression variation (see section Materials and Methods).

Statistical Identification Portrays ceRNA Expression Fluctuation Landscape

ceRNA Expression Variation Driven by HF-Mutation

Next, we used a regression model to examine the effect of HF mutations on ceRNA expression levels. We found that only six cancer types, including colon adenocarcinoma (COAD), head and neck squamous cell carcinoma (HNSC), LUSC, skin cutaneous melanoma (SKCM), STAD, and uterine corpus endometrial carcinoma (UCEC), had putative HF mutations that passed the regression test and identified 293 ceL and ceM genes whose expression levels were significantly correlated with genotypic changes (**Figure 3A**). Several factors affecting the effectiveness of ceRNAs have been reported, including the expression levels of miRNAs and ceRNAs, as well as binding affinity to miRNA target sites (Ebert and Sharp, 2010; Mukherji et al., 2011; Salmena et al., 2011). Since miRNA expression variation has been considered in the regression model, we focused on ceRNA-centric factors. We further required a consistent direction between the regression coefficient ηl and the changes in the functional prediction score from TargetScan and miRanda. Accordingly, we redefined 162 SMILIM units, in which ceL and ceM expression variations displayed opposite and consistent orientations with the target prediction results (**Figure 3A**). Among 742 putative transition and transversion mutations, 17 mutations were identified to disturb the ceRNA regulation. In addition, three of 59 putative indel mutations were found to disturb the ceRNA regulation. Compared to the original HF mutations, the verified somatic mutations were drastically reduced (**Figure 3B**). It is likely that ceM expression changes rely not only on a minimal SMILM unit, but also on the interaction of the ceRNA network and other regulatory factors, such as transcription factors (TFs) and DNA methylation.

The majority of ηl and ηm were concentrated between -10 and 10 in the 162 significant SMILM units, suggesting an important effect of these somatic mutations on ceM expression and ceRNA regulation compared with genetic variation (Li M. J. et al., 2017; **Figure 3C**). The mutation-ceRNA regulatory relationship was a complex network, where a single mutation affected the affinity to bind multiple miRNAs and thus disturbed the expression of multiple mRNAs (**Figures 3D,E** and **Supplementary Figure 3**). For example, an indel (chr17: 80340219C) of COAD enhanced the binding affinity of hsa-miR-7110-5p in lncRNA AC124319.3 (ENSG00000280248; p-value = 3.57E-3, ηl = -8.03), which competed with TPM3 (p-value = 6.43E-5, ηm = 0.79; **Figures 3E,F**). Further, one-sample t-test confirmed that the expression levels of AC124319.3, hsa-miR-7110-5p, and TPM3 in non-mutated samples were statistically different from the average expression of mutant samples (**Figure 3G**), suggesting that the expression level of miRNA, as a key link with the ceRNA regulatory pathway, is an important factor in identifying the imbalance in the ceRNA mechanism. Taken together, these results suggest that the presence of somatic mutations in lncRNAs could affects the expression of target genes through a ceRNA regulatory pathway.

Individual Differences in ceM Expression Variation Produced by LF-Mutation

For SMILM units disturbed by LF mutations, we focused on the target ceMs determined by the operability of the experiment and the important role of protein-coding genes in physiological function. To assess the carcinogenic function of LF-SMILM units, we extracted target ceMs involved in cancer hallmarks, which are

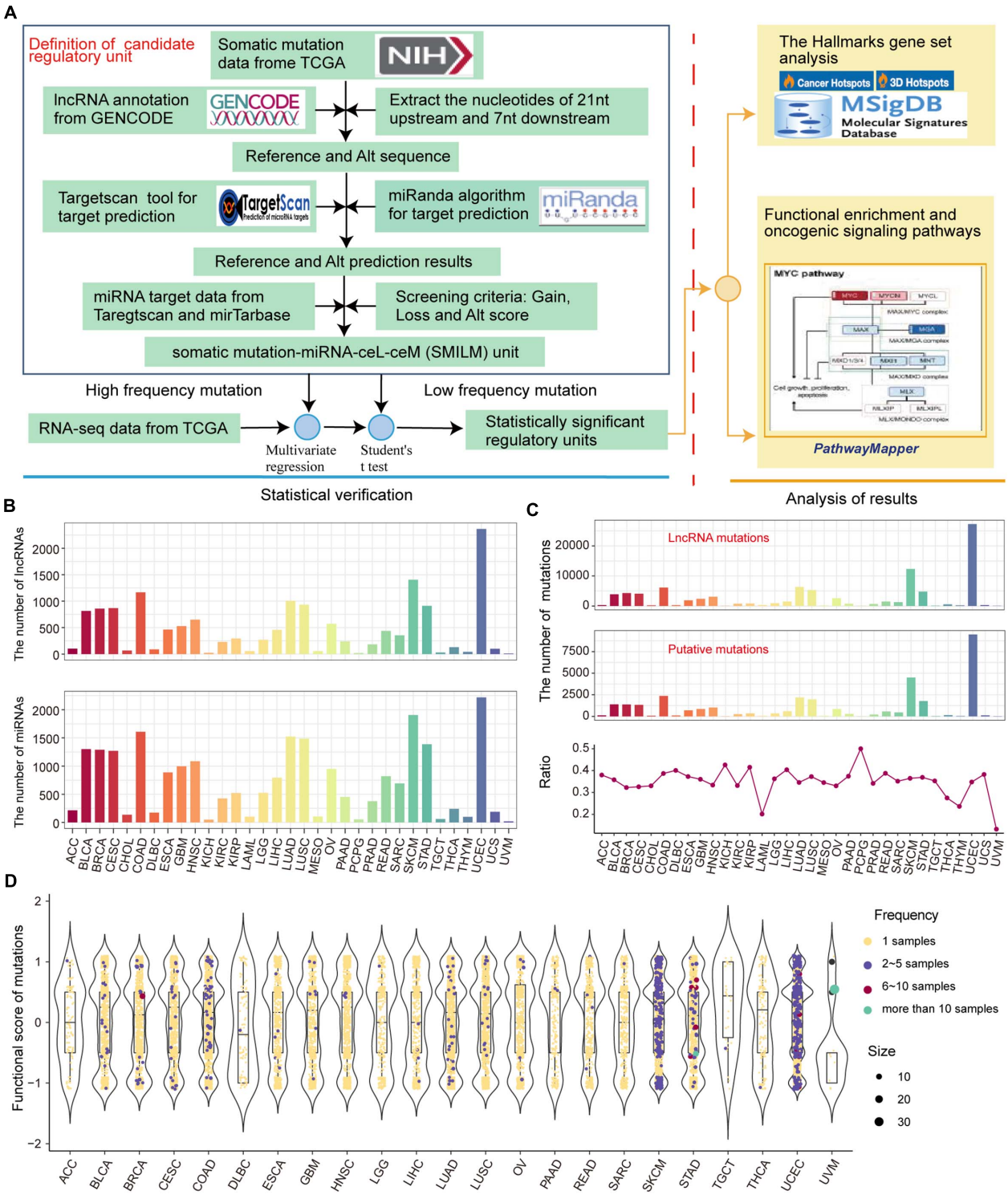

FIGURE 2 | Predicting somatic mutations on lncRNAs that potentially impact the ceRNA mechanism. **(A)** Workflow for SMILM unit construction, unit verification, and functional pathway analysis. **(B)** Numbers of lncRNAs and miRNAs affected by somatic mutations in different cancers. **(C)** Numbers of putative somatic mutations in SMILM units across 33 cancers is shown in a line chart. Proportions of putative mutations in each cancer type as a percentage of the original somatic mutations on lncRNA are shown by bar plot. **(D)** Functional scores of putative mutations in each cancer. Blue, red, green, and purple denote numbers of samples in which a particular mutation occurs.

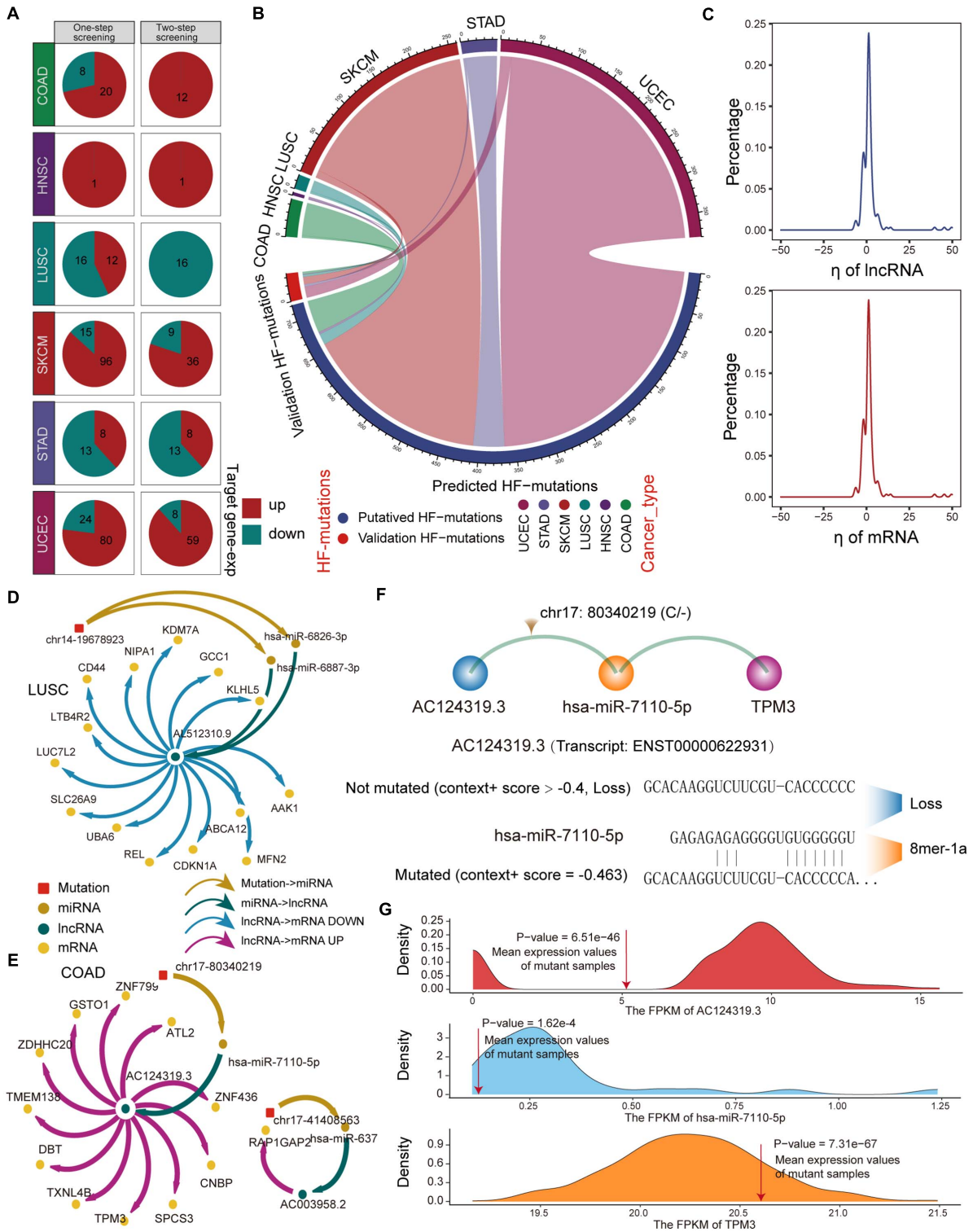

FIGURE 3 | Regression model to identify HF-SMILM units. **(A)** HF-SMILM units that passed one-step and two-step screening in six cancer types. Directions of change in the expression of ceM in the HF-SMILM unit affected by the mutation are marked by blue and red. **(B)** Circle diagram of proportions of putative mutations in these six cancers before and after the regression test. **(C)** Distribution of regression coefficients of ceL and ceM in the multiple regression analysis of the HF-SMILM units. **(D)** Regulatory network of HF-SMILM units that passed regression test in LUSC. Unique identifiers used by nodes and interactions in the network. **(E)** Same as in **(D)** but for HF-SMILM units that passed regression test in COAD. **(F)** Binding affinity changes of AC124319.3 and hsa-miR-7110-5p before and after the chr17: 80340219 (C/–) mutation in AC124319.3. **(G)** The density curve reflects the distribution of genes expression for COAD and the average expression level of the genes in the mutant sample was marked with a red line. The one-sample *t*-test was used to calculate statistical significance.

important biological processes in cancer development (Agarwal et al., 2015). We divided the expression changes of the target ceM into up, down, and none (**Figure 4A**, see **Supplementary Methods**). Our data suggest that lncRNA mutations amplify and depress the expression of protein-coding genes (ceMs) through the ceRNA mechanism in multiple cancers to comprehensively impact the carcinogenic process of the hallmarks.

We statistically verified the expression variation of hallmark ceMs affected by LF mutations through the ceRNA mechanism. We found that the expression levels of 1624 ceMs occurring in 32 cancer types were significantly different between the corresponding mutant and control samples and were regulated by 2849 ceL. Cancers with a high number of samples or high lncRNA mutations displayed a small number of identified ceMs (**Figure 4B**), suggesting that the contribution of mutation-miRNA-ceRNA mechanism is heterogeneous in pan-cancer. Fold change as a measure of change in ceMs expression was found to be clustered between 0.8 and 1.2 (**Figure 4C**), suggesting that simple statistical metrics mask individualized differences in the expression of mutant interference ceMs. We also found that variation in the expression of target ceM was highly correlated with the change in target prediction score in STAD and Sarcoma (SARC) (**Figures 4D,E**). This evidence suggests that a ceM could be affected by multiple SMILM units, which have different regulatory effects on the expression of ceM determined by individual differences in putative mutations. Together, these data indicate that individual mutation differences are an important cause of fluctuations in the expression of ceMs.

ceM Oncogenic Pathways Reveal Pan-Cancer Functional Heterogeneities

CeMs confirmed to be affected by LF mutations in pan-cancer were collected for gene set enrichment analysis (GSEA) (Subramanian et al., 2005) weighing by fold change of ceM expression. We found significantly enriched hallmark gene sets in ceM genes only in COAD and UCEC. Allograft rejection and inflammation response pathways were enriched in ceMs with upregulated expression in both COAD and UCEC (**Figures 5A,B**), revealing a high similarity in the effects of lncRNA mutations through ceRNA mechanisms in COAD and UCEC. Further, we integrated all ceMs perturbed by HF and LF mutations to analyze the effect of mutation-miRNA-ceRNA mechanism on cellular functions in pan-cancer by KEGG functional enrichment analysis. We found only 21 cancers with significantly enriched functional pathways, primarily involved in energy metabolism, cell metastasis, apoptosis, and functions related to cancer complications (**Figure 5C** and **Supplementary Figure 4**), indicating that the mutations-miRNA-ceRNA mechanism is widely involved in the development of cancers.

We compiled and reviewed 17 oncogenic signaling pathways verified in articles published between 2008 and 2019 (**Supplementary Table 2**). We only identified eight oncogenic signaling pathways in the KEGG functional enrichment results of eight cancer types (**Supplementary Figure 5**). These include the p53 signaling pathway (Wade et al., 2013), phosphoinositide 3-kinase (PI3K)-AKT signaling pathway, mitogen-activated protein kinase (MAPK) signaling pathway (Soleimani et al., 2019), Ras signaling pathway (Malumbres and Barbacid, 2003), Toll-like receptor (TLR) signaling pathway (Moradi-Marjaneh et al., 2018), mammalian target of rapamycin (mTOR) signaling pathway (Ayuk and Abrahamse, 2019), Wnt signaling pathway (Reya and Clevers, 2005) and NF-kappa B (NF-kB) signaling pathway (Soleimani et al., 2020). Regarding these oncogenic signaling pathways, ceMs of UCEC, adrenocortical carcinoma (ACC), and COAD function in the p53 signaling pathway, ceMs of UCEC, and esophageal carcinoma (ESCA) function in the Ras-MAPK and mTOR signaling pathways, and ceMs of brain lower grade glioma (LGG), lymphoid neoplasm diffuse large B-cell lymphoma (DLBC), LUSC, COAD, and UCEC function in the PI3K-AKT signaling pathway (**Figure 5D** and **Supplementary Figure 6**). These findings suggest that pan-cancer ceMs regulate oncogenic signaling pathways in a flexible manner with certain similarities. The ceMs in COAD were mainly enriched in the p53, TLR, and NF-kB oncogenic signaling pathways, which regulate cell cycle arrest, DNA repair, apoptosis, proinflammatory effects, inflammation, and survival. Furthermore, the ceMs in UCEC regulated cell cycle arrest and apoptosis in the p53 pathway, proliferation and apoptosis in the Ras-MAPK pathway, lipid biosynthesis and autophagy in the mTOR pathway, and angiogenesis and DNA repair in the PI3K-Akt pathway. These results indicate that pan-cancer, where the same oncogenic pathways are regulated through the mutations-miRNA-ceRNA mechanism, is heterogeneous in specific functions. The MDM2 and MDM4 ceMs in COAD and UCEC were found to be important for the stabilization and activation of p53 and could serve as important targets for anti-cancer therapy (Toledo and Wahl, 2007; Wade et al., 2010). The NF-κB signaling pathway is a typical proinflammatory signal transduction pathway and an important target for novel anti-carcinogenic drugs (Lawrence, 2009). mTOR is critical in the pathway and promotes cancer proliferation and metabolism upon overactivation, which is also an important target for cancer therapy (Tian et al., 2019). Taken together, these results suggest that functional variations in pan-cancer that are disturbed by somatic mutations through the ceRNA mechanism may lead to tumor-specific phenotypes.

Survival Analysis Reveals Biomarker lncRNA in Pan-Cancer

We evaluated the impact of ceMs that participate in the carcinogenic signaling pathway on the survival of cancer patients. Several genes (ceMs) in five cancer types had a significant hazard ratio (HR) value according to Cox proportional hazard model, suggesting a relationship between patient prognosis and lncRNA mutations (**Supplementary Figure 7**). The Kaplan–Meier method was used to plot survival-related ceMs (**Figures 6A–C** and **Supplementary Figures 8A,B**). We found that samples resulting in the upregulation of EREG in COAD had poor overall survival and that such samples were enriched in stage IV (**Figure 6A**). It is intriguing to note that according to Kaplan–Meier analysis, there was no significant difference in the survival of BCL2L1 between mutant and control samples (**Figure 6A**), which may be attributed to the weak effect of

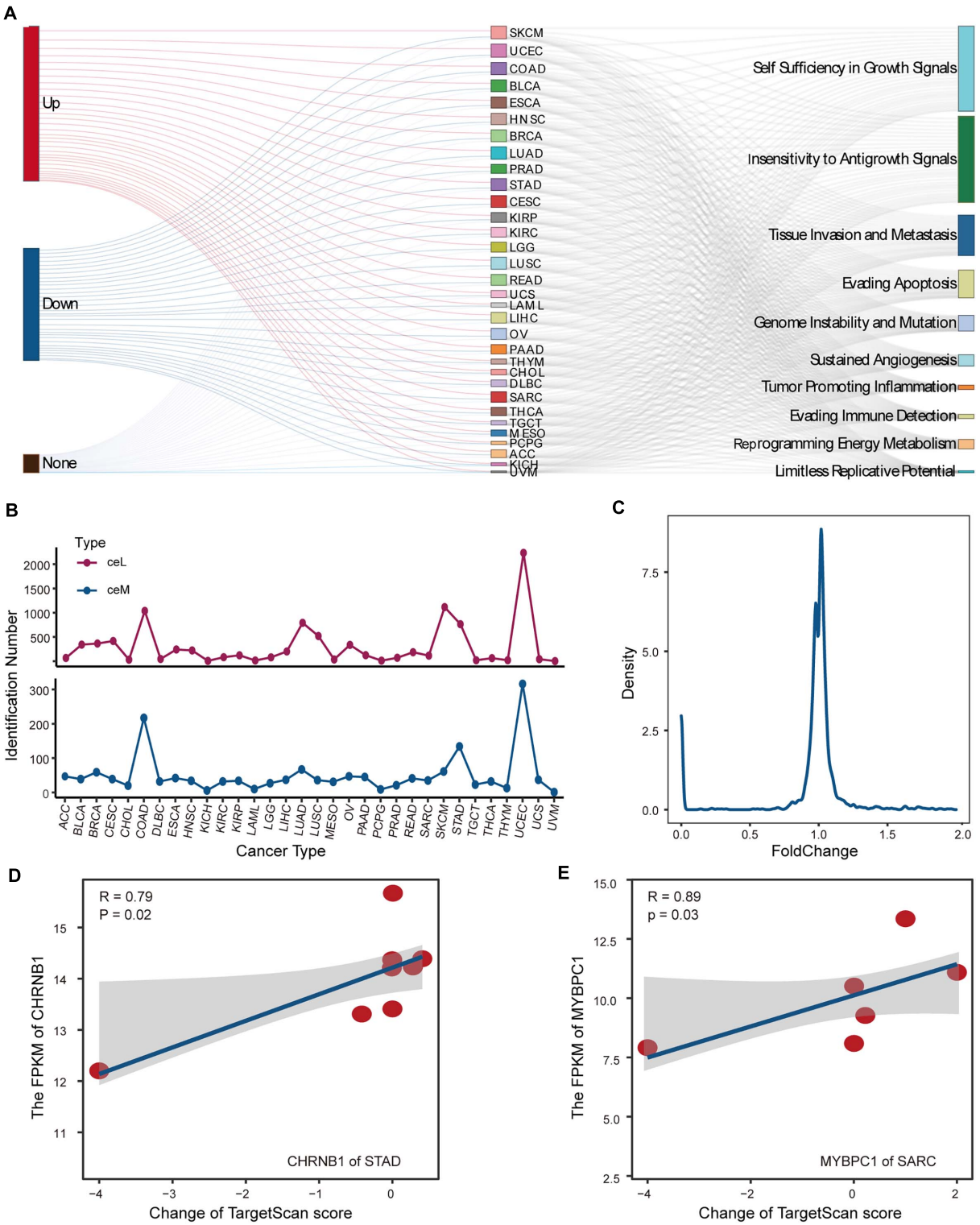

FIGURE 4 | Analysis and detection of LF-mutations. **(A)** Sankey diagram demonstrating the possible effects of putative LF-mutations on the corresponding ceM expression and the contribution of these ceMs to the 10 classical hallmark gene sets. **(B)** Numbers of ceM and ceL that passed the statistical test in pan-cancer. **(C)** Line plot illustrating the density distribution of fold change of all ceM that passed the statistical test in pan-cancer. **(D)** Relationship between expression of CHRNB1 in STAD and the corresponding lncRNA-miRNA target prediction scores shown by scatter plots with plotting of fitted curves. **(E)** Same as in **(D)** but for the expression of MYBPC1 in SRAC.

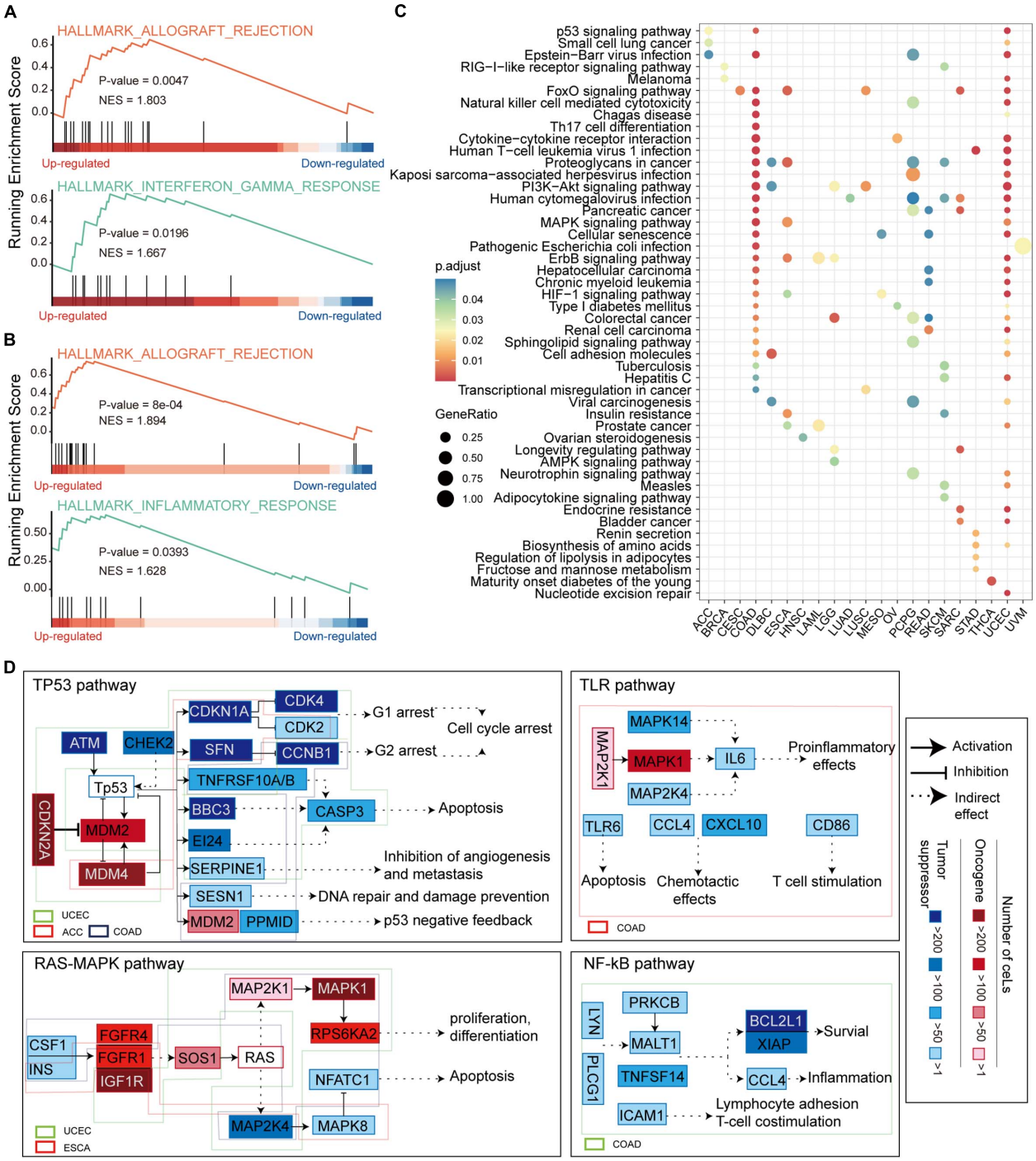

FIGURE 5 | Functional enrichment analysis of ceMs. **(A)** Enrichment of allograft rejection and inflammation response pathways on ceMs for COAD. **(B)** Same as in **(A)** but for UCEC. **(C)** Dot plot illustrating the top five pathways from functional enrichment results of ceMs for pan-cancer. **(D)** Signaling pathways affected by ceM mapped to illustrate the function mechanism of ceM in pan-cancer. Oncogenic and suppressor genes are shown in red and blue, respectively. Use of three categories to represent the relationships between two genes: activation, inhibition, and indirect effect.

mutations on ceM expression in several samples. FGFR1, a proven independent prognostic risk factor in patients with resected esophageal squamous cell carcinoma (Wang Y. et al., 2019), was significantly differentially expressed in mutant ESCA samples (*p*-value = 7.56e-04), and high expression of FGFR1 was associated with poorer patient prognosis (**Figure 6B**). We found that "unknown" samples that perturb MAPK1 expression in UCEC had a better prognosis and the least proportion was

in stage IV (**Figure 6C**). Previous studies have suggested that MAPK1 regulates the metastasis and invasion of cervical cancer through a ceRNA mechanism (Li W. et al., 2017). These results indicate an important contribution of the lncRNA mutation-ceRNA mechanism to the overall survival of cancer patients.

LncRNAs that regulate prognosis-related ceM expression can be critical factors in cancers. High-frequency mutated lncRNAs regulating prognosis-related ceM expression were screened for the identification of cancer-related biomarkers (**Supplementary Table 3**, **Supplementary Figures 8C,D**, and **Figures 6D–F**). TTN-AS1 (ENSG00000237298) was identified as a potential biomarker involved in the regulation of both EREG and BCL2L1 (**Figure 6D**). TTN-AS1 has been proven to be associated with the prognosis of COAD and regulate apoptosis and invasion in osteosarcoma (Fu et al., 2019), lung adenocarcinoma (Jia et al., 2019) and colorectal cancer (Wang Y. et al., 2020) via the ceRNA mechanism. The lncRNA GSN-AS1 (ENSG00000235865) regulates BCL2L1 (**Figures 6D,E**), which has been proven to be an important prognostic marker for luminal subtype breast cancer (Yang et al., 2016). lncRNA XIST (ENSG00000229807), TTN-AS1 (ENSG00000237298), and TSIX (ENSG00000270641), which regulate MAPK1 and ERBB3 in UCEC (**Figure 6F**), were shown to be miRNA sponges that control apoptosis via the ceRNA mechanism (Bu et al., 2018; Fu et al., 2019; Li et al., 2020). Taken together, these results suggest that several potential biomarker lncRNAs regulate the expression of protein-coding genes through the ceRNA mechanism to affect patient survival.

DISCUSSION

In this study, we integrated mutation data from 33 cancer types with RNA-seq profiles from TCGA to explore the association between somatic mutations in lncRNA and the regulatory mechanism of ceRNA. Using multivariate multiple regression and statistical analyses, we identified 162 significant HF-SMILM units and many ceMs perturbed by LF mutations from pan-cancers. The mutations-miRNA-ceRNA mechanism appeared to be dynamic, with individual differences in the regulation of ceRNA expression due to mutation specificity. In addition, we characterized the function of ceMs in pan-cancer through oncogenic signaling pathway studies and survival analysis, identifying biomarker lncRNAs that regulate the expression of ceM associated with patient survival. These findings provide a new perspective to explain the role of lncRNA mutations in post-transcriptional gene regulation.

Although we used both TargetScan and miRanda tools to predict potential SMILM units with rigorous screening of scores and energetics, it is also possible that our lncRNA mutation-miRNA detection missed target sites not predicted by either tool. Alternatively, we considered the union or intersection of multiple miRNA-target prediction algorithms, including PITA (Kertesz et al., 2007) and RNAhybrid (Kruger and Rehmsmeier, 2006); however, unions might introduce many false positives and intersections might introduce false negatives. Our current standards provide a reasonable and reliable reference for further functional research, and experimental methods such as CLIP-seq and RIP-seq can be used to overcome these shortcomings. Another potential limitation of our study is that we only considered one competing unit for detection in a complex ceRNA regulatory network. Changes in the expression of a node gene in the ceRNA regulatory network perturbs the balance of the entire network (Levine et al., 2007). The cascade effect caused by miRNA redistribution and ceRNA competition from a global perspective requires building a more complex algorithm to more accurately describe the complete response of the entire network.

It is certainly a significant idea that we consider lncRNA somatic mutations in terms of the ceRNA regulatory mechanism. The effects of genetic variation on ceRNA regulation have been revealed by previous studies (Cheng et al., 2015; Ghanbari et al., 2015; Li M. J. et al., 2017), and a large database of correlations has emerged (Li et al., 2014). However, few studies have addressed somatic mutations (Wang P. et al., 2020). Previous studies have focused on the perturbation of ceRNA mechanisms by genetic variations (Gamazon et al., 2012; Ghanbari et al., 2015; Li M. J. et al., 2017; Wang P. et al., 2020). For example, one of our prior studies determined the effect of somatic mutations of lncRNA on ceRNA mechanisms in pan-cancers (Wang P. et al., 2020). Li et al. have explored the genetic associations with ceRNA regulation in the human genome. These studies focused on methodology development and dataset construction on how to connect genomic variations and ceRNA expression. Thus, further studies evaluating the effects of mutations on ceRNA expression and downstream function are needed. Our research aimed to provide new insights into the oncogenic mechanism from the perspective of somatic mutations perturbing the ceRNA mechanism. Further, we expanded the scope of our analysis to study the effect of mutations on perturbing biological networks, functions, and clinical phenotypes. We believe that our analysis will be helpful for dissecting disease pathology caused by personalized mutations and further contribute to precision medicine.

Despite the limitations of our study, our findings reveal one of the underlying causes of changes in the physiological functions in cancer, which will help advance the development of precision medicine. Using mutation and transcriptome data from multiple cancers, we found many cancer-specific SMILM units and identified ceMs affected by ceLs. These results complement recent studies on the mechanism by which lncRNA mutations perturb ceRNA (Bhattacharya and Cui, 2016; Wang P. et al., 2020). By verifying the HF-mutation SMILM unit, we discovered the mutation-mediated ceRNA expression fluctuation mechanism. We also found individual differences in changes in the expression of ceM. The diverse distribution of HF and LF mutations in different cancers and genes was consistent with the genetic heterogeneity of different cancers. Thus, we performed a specific investigation on specific cancer types and genes based on the background of tumor heterogeneity. This strategy has been previously used to characterize individual disease pathologies caused by cancer-specific or gene-specific mutations (Lawrence et al., 2013; Zack et al., 2013; ICGC/TCGA Pan-Cancer Analysis of Whole Genomes Consortium, 2020). We believe that our exhaustive analysis will be helpful for dissecting disease pathology

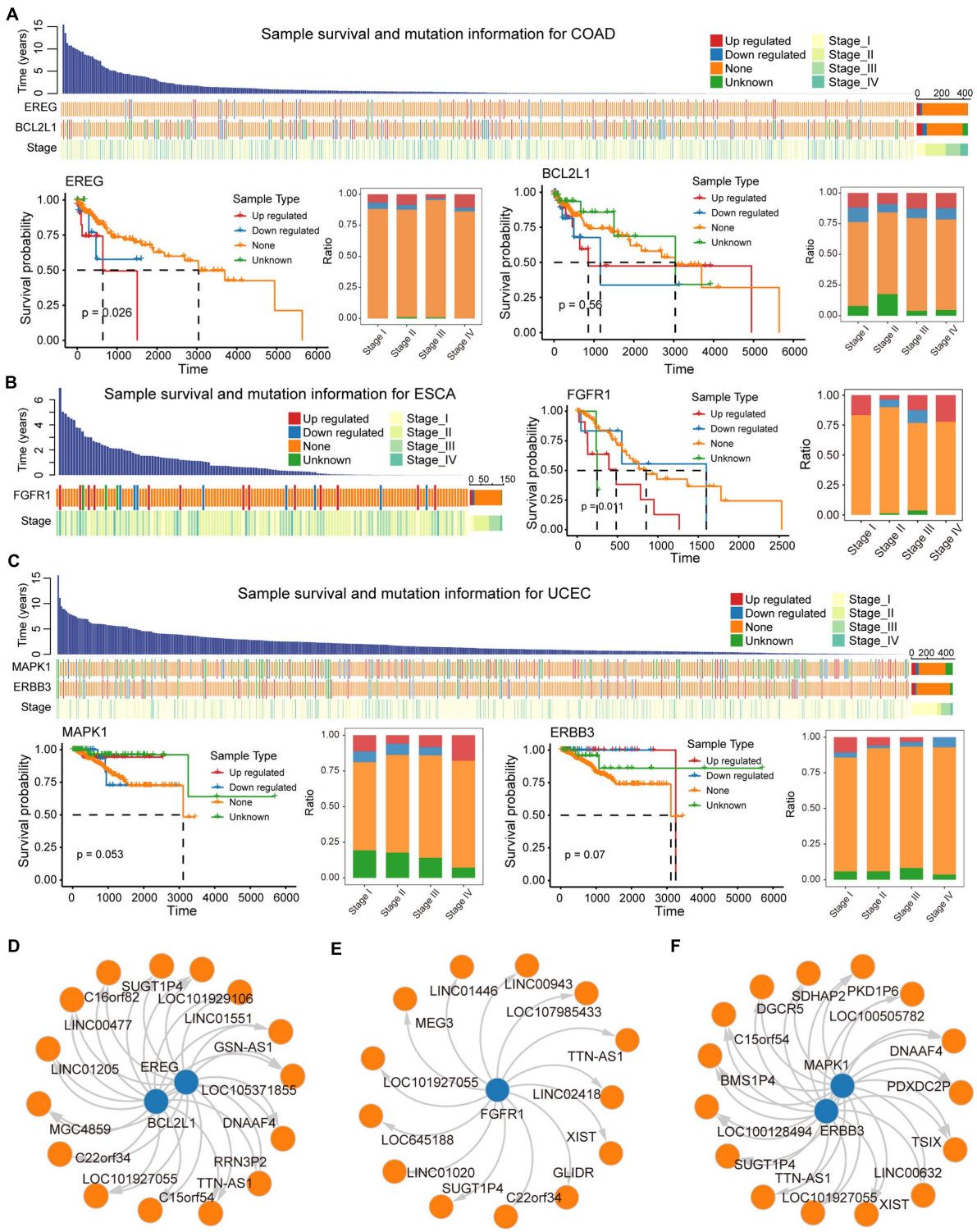

FIGURE 6 | Biomarker lncRNAs (ceL) regulate mRNA (ceM) through the ceRNA mechanism. **(A)** Waterfall plot illustrating effects (Up-regulated, Down-regulate, None, and Unknown) of mutations in each sample for COAD on ceM expression, and include information such as patient survival time and clinical stage of each sample. Survival predictions and relationships to clinical staging for four sample types classified, respectively, based on the genes EREG and BCL2L1 were presented by survival curves and bar plot. **(B)** Same as in **(A)** but for ESCA, and the gene FGFR1. **(C)** The same as in **(A)** but for UCEC, and the genes MAPK1 and ERBB3. **(D–F)** The relationship between biomarker lncRNAs and regulated ceM for COAD, ESCA, and UCEC.

caused by personalized mutations and contribute to precision medicine. Importantly, we performed functional enrichment and oncogenic signature pathway studies, as well as survival analysis of ceMs from multiple cancers. We identified that pan-cancer has functional heterogeneity in mutation-ceRNA mechanisms, primarily enriched in cell proliferation and apoptosis, DNA repair, and immune regulation. Furthermore, FLT1 of LUSC, ITGB1 of DLBC, MDM4, and CDKN1A of ACC, MAPK1, and ERBB3 of UCEC, FGFR1 of ESCA, and EREG and BCL2L1 of COAD have been strongly associated with patient survival in their respective cancers. Furthermore, the biomarker lncRNAs, which regulate the above genes and are mutated with HF, contribute to the development of clinical research.

With the rapid development of high-throughput technologies, an increasing number of large biological data sets can be obtained at the whole-transcriptome level. This makes it difficult to dissect the individual pathologies behind the fast-growing datasets. Although many novel biomarkers have been identified by *in vivo* or *in vitro* experimental methods, identifying new disease-biomarker associations based on traditional, one-by-one experimental studies are expensive, complex, and time-consuming. To overcome these problems, a bioinformatics strategy has been used in previous studies to dissect gene regulation and revealed valuable results (Du et al., 2013; Li et al., 2015; Wang P. et al., 2015). We believe that our analyses will provide novel insights into mutations affecting lncRNA-associated regulatory mechanisms at the transcriptional level. Both the method and predictions could serve as helpful references for future experimental and functional dissections of lncRNAs.

CONCLUSION

Our study provides a global landscape of the effects of lncRNA somatic mutations on the ceRNA mechanism in pan-cancer. Our findings extend existing knowledge on the relevance of lncRNA mutations in functions related to cancer via the ceRNA mechanism. The integration of mutation and RNA expression data from tumor samples enhances the interpretation of the identified SMILMs, helping to improve the reliability of the predictions; thus, this approach may provide more precise theoretical guidance for experimental studies and clinical applications.

DATA AVAILABILITY STATEMENT

The datasets presented in this study can be found in online repositories. The names of the repository/repositories and accession number(s) can be found in the article/ **Supplementary Material**.

AUTHOR CONTRIBUTIONS

PW, BC, and YaZ conceived and designed the experiments. YuZ, PH, QG, and YH analyzed data. YQ and MX collected the data. YuZ, PH, and QG validated the method and data. YuZ and PH wrote this manuscript. All authors read and approved the final manuscript.

FUNDING

This work was supported by the National Natural Science Foundation of China (32070622, 81702766, 82072640, and 81902646), Heilongjiang Provincial Natural Science Foundation (LH2020H046), Postdoctoral Science Foundation of China (2020M670922), and Postdoctoral Foundation of Heilongjiang Province (LBH-Z19077).

SUPPLEMENTARY MATERIAL

The Supplementary Material for this article can be found online at: https://www.frontiersin.org/articles/10.3389/fcell.2021.658346/full#supplementary-material

REFERENCES

Agarwal, V., Bell, G. W., Nam, J. W., and Bartel, D. P. (2015). Predicting effective microRNA target sites in mammalian mRNAs. *eLife* 4:e05005. doi: 10.7554/eLife.05005.028

Ayuk, S. M., and Abrahamse, H. (2019). mTOR signaling pathway in cancer targets photodynamic therapy in vitro. *Cells* 8:431. doi: 10.3390/cells8050431

Betel, D., Wilson, M., Gabow, A., Marks, D. S., and Sander, C. (2008). The microRNA.org resource: targets and expression. *Nucleic Acids Res.* 36, D149–D153. doi: 10.1093/nar/gkm995

Bhattacharya, A., and Cui, Y. (2016). SomamiR 2.0: a database of cancer somatic mutations altering microRNA-ceRNA interactions. *Nucleic Acids Res.* 44, D1005–D1010. doi: 10.1093/nar/gkv1220

Bu, Y., Zheng, D., Wang, L., and Liu, J. (2018). LncRNA TSIX promotes osteoblast apoptosis in particle-induced osteolysis by down-regulating miR-30a-5p. *Connect. Tissue Res.* 59, 534–541. doi: 10.1080/03008207.2017.1413362

Cancer Genome Atlas Research Network, Linehan, W. M., Spellman, P. T., Ricketts, C. J., Creighton, C. J., Fei, S. S., et al. (2016). Comprehensive molecular characterization of papillary renal-cell carcinoma. *N. Engl. J. Med.* 374, 135–145. doi: 10.1056/NEJMoa1505917

Chen, C. K., Blanco, M., Jackson, C., Aznauryan, E., Ollikainen, N., Surka, C., et al. (2016). Xist recruits the X chromosome to the nuclear lamina to enable chromosome-wide silencing. *Science* 354, 468–472. doi: 10.1126/science.aae0047

Chen, Y., Lin, Y., Bai, Y., Cheng, D., Bi, Z., and Long Noncoding, A. (2019). RNA (lncRNA)-associated competing endogenous RNA (ceRNA) network identifies eight lncRNA biomarkers in patients with osteoarthritis of the knee. *Med. Sci. Monit.* 25, 2058–2065. doi: 10.12659/MSM.915555

Cheng, D. L., Xiang, Y. Y., Ji, L. J., and Lu, X. J. (2015). Competing endogenous RNA interplay in cancer: mechanism, methodology, and perspectives. *Tumour. Biol.* 36, 479–488. doi: 10.1007/s13277-015-3093-z

Chou, C. H., Shrestha, S., Yang, C. D., Chang, N. W., Lin, Y. L., Liao, K. W., et al. (2018). miRTarBase update 2018: a resource for experimentally validated microRNA-target interactions. *Nucleic Acids Res.* 46, D296–D302. doi: 10.1093/nar/gkx1067

Civelek, M., Hagopian, R., Pan, C., Che, N., Yang, W. P., Kayne, P. S., et al. (2013). Genetic regulation of human adipose microRNA expression and its

consequences for metabolic traits. *Hum. Mol. Genet.* 22, 3023–3037. doi: 10.1093/hmg/ddt159

Du, Z., Fei, T., Verhaak, R. G., Su, Z., Zhang, Y., Brown, M., et al. (2013). Integrative genomic analyses reveal clinically relevant long noncoding RNAs in human cancer. *Nat. Struct. Mol. Biol.* 20, 908–913. doi: 10.1038/nsmb.2591

Ebert, M. S., and Sharp, P. A. (2010). Emerging roles for natural microRNA sponges. *Curr. Biol.* 20, R858–R861. doi: 10.1016/j.cub.2010.08.052

Fisher, L. D., and Lin, D. Y. (1999). Time-dependent covariates in the Cox proportional-hazards regression model. *Annu. Rev. Public Health* 20, 145–157. doi: 10.1146/annurev.publhealth.20.1.145

Friedman, R. C., Farh, K. K., Burge, C. B., and Bartel, D. P. (2009). Most mammalian mRNAs are conserved targets of microRNAs. *Genome Res.* 19, 92–105. doi: 10.1101/gr.082701.108

Fu, D., Lu, C., Qu, X., Li, P., Chen, K., Shan, L., et al. (2019). LncRNA TTN-AS1 regulates osteosarcoma cell apoptosis and drug resistance via the miR-134-5p/MBTD1 axis. *Aging* (*Albany NY*) 11, 8374–8385. doi: 10.18632/aging.102325

Gamazon, E. R., Ziliak, D., Im, H. K., LaCroix, B., Park, D. S., Cox, N. J., et al. (2012). Genetic architecture of microRNA expression: implications for the transcriptome and complex traits. *Am. J. Hum. Genet.* 90, 1046–1063. doi: 10.1016/j.ajhg.2012.04.023

Ghanbari, M., Franco, O. H., de Looper, H. W., Hofman, A., Erkeland, S. J., and Dehghan, A. (2015). Genetic variations in microRNA-binding sites affect microRNA-mediated regulation of several genes associated with cardiometabolic phenotypes. *Circ. Cardiovasc. Genet.* 8, 473–486. doi: 10.1161/CIRCGENETICS.114.000968

Hanahan, D., and Weinberg, R. A. (2011). Hallmarks of cancer: the next generation. *Cell* 144, 646–674. doi: 10.1016/j.cell.2011.02.013

Harrow, J., Frankish, A., Gonzalez, J. M., Tapanari, E., Diekhans, M., Kokocinski, F., et al. (2012). GENCODE: the reference human genome annotation for The ENCODE Project. *Genome Res.* 22, 1760–1774. doi: 10.1101/gr.135350.111

ICGC/TCGA Pan-Cancer Analysis of Whole Genomes Consortium (2020). Pan-cancer analysis of whole genomes. *Nature* 578, 82–93. doi: 10.1038/s41586-020-1969-6

Jia, P., and Zhao, Z. (2017). Impacts of somatic mutations on gene expression: an association perspective. *Brief Bioinform.* 18, 413–425.

Jia, Y., Duan, Y., Liu, T., Wang, X., Lv, W., Wang, M., et al. (2019). LncRNA TTN-AS1 promotes migration, invasion, and epithelial mesenchymal transition of lung adenocarcinoma via sponging miR-142-5p to regulate CDK5. *Cell Death Dis.* 10:573. doi: 10.1038/s41419-019-1811-y

Kertesz, M., Iovino, N., Unnerstall, U., Gaul, U., and Segal, E. (2007). The role of site accessibility in microRNA target recognition. *Nat. Genet.* 39, 1278–1284. doi: 10.1038/ng2135

Kozomara, A., and Griffiths-Jones, S. (2014). miRBase: annotating high confidence microRNAs using deep sequencing data. *Nucleic Acids Res.* 42, D68–D73. doi: 10.1093/nar/gkt1181

Kruger, J., and Rehmsmeier, M. (2006). RNAhybrid: microRNA target prediction easy, fast and flexible. *Nucleic Acids Res.* 34, W451–W454. doi: 10.1093/nar/gkl243

Lawrence, M. S., Stojanov, P., Polak, P., Kryukov, G. V., Cibulskis, K., Sivachenko, A., et al. (2013). Mutational heterogeneity in cancer and the search for new cancer-associated genes. *Nature* 499, 214–218. doi: 10.1038/nature12213

Lawrence, T. (2009). The nuclear factor NF-kappaB pathway in inflammation. *Cold Spring Harb. Perspect. Biol.* 1:a001651. doi: 10.1101/cshperspect.a001651

Lemos, A. E. G., Matos, A. D. R., Ferreira, L. B., and Gimba, E. R. P. (2019). The long non-coding RNA PCA3: an update of its functions and clinical applications as a biomarker in prostate cancer. *Oncotarget* 10, 6589–6603. doi: 10.18632/oncotarget.27284

Levine, E., Zhang, Z., Kuhlman, T., and Hwa, T. (2007). Quantitative characteristics of gene regulation by small RNA. *PLoS Biol.* 5:e229. doi: 10.1371/journal.pbio.0050229

Li, J. H., Liu, S., Zhou, H., Qu, L. H., and Yang, J. H. (2014). starBase v2.0: decoding miRNA-ceRNA, miRNA-ncRNA and protein-RNA interaction networks from large-scale CLIP-Seq data. *Nucleic Acids Res.* 42, D92–D97. doi: 10.1093/nar/gkt1248

Li, L., Lv, G., Wang, B., and Kuang, L. (2020). XIST/miR-376c-5p/OPN axis modulates the influence of proinflammatory M1 macrophages on osteoarthritis chondrocyte apoptosis. *J. Cell Physiol.* 235, 281–293. doi: 10.1002/jcp.28968

Li, M. J., Zhang, J., Liang, Q., Xuan, C., Wu, J., Jiang, P., et al. (2017). Exploring genetic associations with ceRNA regulation in the human genome. *Nucleic Acids Res.* 45, 5653–5665. doi: 10.1093/nar/gkx331

Li, W., Liang, J., Zhang, Z., Lou, H., Zhao, L., Xu, Y., et al. (2017). MicroRNA-329-3p targets MAPK1 to suppress cell proliferation, migration and invasion in cervical cancer. *Oncol. Rep.* 37, 2743–2750. doi: 10.3892/or.2017.5555

Li, Y., Shao, T., Jiang, C., Bai, J., Wang, Z., Zhang, J., et al. (2015). Construction and analysis of dynamic transcription factor regulatory networks in the progression of glioma. *Sci. Rep.* 5:15953. doi: 10.1038/srep15953

Liberzon, A., Subramanian, A., Pinchback, R., Thorvaldsdottir, H., Tamayo, P., and Mesirov, J. P. (2011). Molecular signatures database (MSigDB) 3.0. *Bioinformatics* 27, 1739–1740. doi: 10.1093/bioinformatics/btr260

Liu, J., Yao, L., Zhang, M., Jiang, J., Yang, M., and Wang, Y. (2019). Downregulation of LncRNA-XIST inhibited development of non-small cell lung cancer by activating miR-335/SOD2/ROS signal pathway mediated pyroptotic cell death. *Aging* (*Albany NY*) 11, 7830–7846. doi: 10.18632/aging.102291

Long, J., Xiong, J., Bai, Y., Mao, J., Lin, J., Xu, W., et al. (2019). Construction and investigation of a lncRNA-associated ceRNA regulatory network in cholangiocarcinoma. *Front. Oncol.* 9:649. doi: 10.3389/fonc.2019.00649

Lu, J., and Clark, A. G. (2012). Impact of microRNA regulation on variation in human gene expression. *Genome Res.* 22, 1243–1254. doi: 10.1101/gr.132514.111

Malumbres, M., and Barbacid, M. (2003). RAS oncogenes: the first 30 years. *Nat. Rev. Cancer* 3, 459–465. doi: 10.1038/nrc1097

Martincorena, I., and Campbell, P. J. (2015). Somatic mutation in cancer and normal cells. *Science* 349, 1483–1489. doi: 10.1126/science.aab4082

Moradi-Marjaneh, R., Hassanian, S. M., Fiuji, H., Soleimanpour, S., Ferns, G. A., Avan, A., et al. (2018). Toll like receptor signaling pathway as a potential therapeutic target in colorectal cancer. *J. Cell Physiol.* 233, 5613–5622. doi: 10.1002/jcp.26273

Mukherji, S., Ebert, M. S., Zheng, G. X., Tsang, J. S., Sharp, P. A., and van Oudenaarden, A. (2011). MicroRNAs can generate thresholds in target gene expression. *Nat. Genet.* 43, 854–859. doi: 10.1038/ng.905

Quinn, J. J., and Chang, H. Y. (2016). Unique features of long non-coding RNA biogenesis and function. *Nat. Rev. Genet.* 17, 47–62. doi: 10.1038/nrg.2015.10

Reya, T., and Clevers, H. (2005). Wnt signalling in stem cells and cancer. *Nature* 434, 843–850. doi: 10.1038/nature03319

Rich, J. T., Neely, J. G., Paniello, R. C., Voelker, C. C., Nussenbaum, B., and Wang, E. W. (2010). A practical guide to understanding Kaplan-Meier curves. *Otolaryngol. Head Neck Surg.* 143, 331–336. doi: 10.1016/j.otohns.2010.05.007

Ricketts, C. J., De Cubas, A. A., Fan, H., Smith, C. C., Lang, M., Reznik, E., et al. (2018). The cancer genome atlas comprehensive molecular characterization of renal cell carcinoma. *Cell Rep.* 23, 313–326.e5. doi: 10.1016/j.celrep.2018.03.075

Rinn, J. L., and Chang, H. Y. (2012). Genome regulation by long noncoding RNAs. *Annu. Rev. Biochem* 81, 145–166. doi: 10.1146/annurev-biochem-051410-092902

Salmena, L., Poliseno, L., Tay, Y., Kats, L., and Pandolfi, P. P. (2011). A ceRNA hypothesis: the Rosetta Stone of a hidden RNA language? *Cell* 146, 353–358. doi: 10.1016/j.cell.2011.07.014

Schmitt, A. M., and Chang, H. Y. (2016). Long noncoding RNAs in cancer pathways. *Cancer Cell* 29, 452–463. doi: 10.1016/j.ccell.2016.03.010

Shannon, P., Markiel, A., Ozier, O., Baliga, N. S., Wang, J. T., Ramage, D., et al. (2003). Cytoscape: a software environment for integrated models of biomolecular interaction networks. *Genome Res.* 13, 2498–2504. doi: 10.1101/gr.1239303

Siddle, K. J., Deschamps, M., Tailleux, L., Nedelec, Y., Pothlichet, J., Lugo-Villarino, G., et al. (2014). A genomic portrait of the genetic architecture and regulatory impact of microRNA expression in response to infection. *Genome Res.* 24, 850–859. doi: 10.1101/gr.161471.113

Soleimani, A., Rahmani, F., Ferns, G. A., Ryzhikov, M., Avan, A., and Hassanian, S. M. (2020). Role of the NF-kappaB signaling pathway in the pathogenesis of colorectal cancer. *Gene* 726:144132. doi: 10.1016/j.gene.2019.144132

Soleimani, A., Rahmani, F., Saeedi, N., Ghaffarian, R., Khazaei, M., Ferns, G. A., et al. (2019). The potential role of regulatory microRNAs of RAS/MAPK

signaling pathway in the pathogenesis of colorectal cancer. *J. Cell Biochem.* 120, 19245–19253. doi: 10.1002/jcb.29268

Subramanian, A., Tamayo, P., Mootha, V. K., Mukherjee, S., Ebert, B. L., Gillette, M. A., et al. (2005). Gene set enrichment analysis: a knowledge-based approach for interpreting genome-wide expression profiles. *Proc. Natl. Acad. Sci. U.S.A* 102, 15545–15550. doi: 10.1073/pnas.0506580102

Thomas, L. F., Saito, T., and Saetrom, P. (2011). Inferring causative variants in microRNA target sites. *Nucleic Acids Res.* 39:e109. doi: 10.1093/nar/gkr414

Thomson, D. W., and Dinger, M. E. (2016). Endogenous microRNA sponges: evidence and controversy. *Nat. Rev. Genet.* 17, 272–283. doi: 10.1038/nrg.2016.20

Tian, T., Li, X., and Zhang, J. (2019). mTOR signaling in cancer and mTOR inhibitors in solid tumor targeting therapy. *Int. J. Mol. Sci* 20:755. doi: 10.3390/ijms20030755

Toledo, F., and Wahl, G. M. (2007). MDM2 and MDM4: p53 regulators as targets in anticancer therapy. *Int. J. Biochem. Cell Biol.* 39, 1476–1482. doi: 10.1016/j.biocel.2007.03.022

Tomczak, K., Czerwinska, P., and Wiznerowicz, M. (2015). The Cancer Genome Atlas (TCGA): an immeasurable source of knowledge. *Contemp. Oncol.* (*Pozn*) 19, A68–A77. doi: 10.5114/wo.2014.47136

Tripathi, V., Shen, Z., Chakraborty, A., Giri, S., Freier, S. M., Wu, X., et al. (2013). Long noncoding RNA MALAT1 controls cell cycle progression by regulating the expression of oncogenic transcription factor B-MYB. *PLoS. Genet.* 9:e1003368. doi: 10.1371/journal.pgen.1003368

Valente, G., Castellanos, A. L., Vanacore, G., and Formisano, E. (2014). Multivariate linear regression of high-dimensional fMRI data with multiple target variables. *Hum. Brain Mapp.* 35, 2163–2177. doi: 10.1002/hbm.22318

Wade, M., Li, Y. C., and Wahl, G. M. (2013). MDM2, MDMX and p53 in oncogenesis and cancer therapy. *Nat. Rev. Cancer* 13, 83–96. doi: 10.1038/nrc3430

Wade, M., Wang, Y. V., and Wahl, G. M. (2010). The p53 orchestra: Mdm2 and Mdmx set the tone. *Trends Cell Biol.* 20, 299–309. doi: 10.1016/j.tcb.2010.01.009

Wang, P., Li, X., Gao, Y., Guo, Q., Ning, S., Zhang, Y., et al. (2020). LnCeVar: a comprehensive database of genomic variations that disturb ceRNA network regulation. *Nucleic Acids Res.* 48, D111–D117. doi: 10.1093/nar/gkz887

Wang, P., Ning, S., Zhang, Y., Li, R., Ye, J., Zhao, Z., et al. (2015). Identification of lncRNA-associated competing triplets reveals global patterns and prognostic markers for cancer. *Nucleic Acids Res.* 43, 3478–3489. doi: 10.1093/nar/gkv233

Wang, Y., Jiang, F., Xiong, Y., Cheng, X., Qiu, Z., and Song, R. (2020). LncRNA TTN-AS1 sponges miR-376a-3p to promote colorectal cancer progression via upregulating KLF15. *Life Sci.* 244:116936. doi: 10.1016/j.lfs.2019.116936

Wang, Y., Wu, Y., Li, J., Lai, Y., Zhou, K., and Che, G. (2019). Prognostic and clinicopathological significance of FGFR1 gene amplification in resected esophageal squamous cell carcinoma: a meta-analysis. *Ann. Transl. Med.* 7:669. doi: 10.21037/atm.2019.10.69

Yang, F., Lv, S. X., Lv, L., Liu, Y. H., Dong, S. Y., Yao, Z. H., et al. (2016). Identification of lncRNA FAM83H-AS1 as a novel prognostic marker in luminal subtype breast cancer. *Onco Targets Ther.* 9, 7039–7045. doi: 10.2147/OTT.S110055

Zack, T. I., Schumacher, S. E., Carter, S. L., Cherniack, A. D., Saksena, G., Tabak, B., et al. (2013). Pan-cancer patterns of somatic copy number alteration. *Nat. Genet.* 45, 1134–1140. doi: 10.1038/ng.2760

Conflict of Interest: The authors declare that the research was conducted in the absence of any commercial or financial relationships that could be construed as a potential conflict of interest.

Copyright © 2021 Zhang, Han, Guo, Hao, Qi, Xin, Zhang, Cui and Wang. This is an open-access article distributed under the terms of the Creative Commons Attribution License (CC BY). The use, distribution or reproduction in other forums is permitted, provided the original author(s) and the copyright owner(s) are credited and that the original publication in this journal is cited, in accordance with accepted academic practice. No use, distribution or reproduction is permitted which does not comply with these terms.

frontiers in Cell and Developmental Biology

ORIGINAL RESEARCH
published: 21 May 2021
doi: 10.3389/fcell.2021.677944

Spatiotemporal Analysis of B Cell- and Antibody Secreting Cell-Subsets in Human Melanoma Reveals Metastasis-, Tumor Stage-, and Age-Associated Dynamics

*Minyi Chen[1], Franziska Werner[1], Christine Wagner[1], Martin Simon[1], Erika Richtig[2], Kirsten D. Mertz[3,4], Johannes Griss[5] and Stephan N. Wagner[1]**

[1] Laboratory of Molecular Dermato-Oncology and Tumor Immunology, Department of Dermatology, Medical University of Vienna, Vienna, Austria, [2] Department of Dermatology, Medical University of Graz, Graz, Austria, [3] Cantonal Hospital Baselland, Institute of Pathology, Liestal, Switzerland, [4] University of Basel, Basel, Switzerland, [5] Department of Dermatology, Medical University of Vienna, Vienna, Austria

OPEN ACCESS

Edited by:
Brigitte M. Pützer, University Hospital Rostock, Germany

Reviewed by:
Li-Peng Hu, Shanghai Jiao Tong University, China
Weijuan Yao, Peking University Health Science Centre, China

***Correspondence:**
Stephan N. Wagner
stephan.wagner@meduniwien.ac.at

Specialty section:
This article was submitted to Molecular Medicine, a section of the journal Frontiers in Cell and Developmental Biology

Received: *08 March 2021*
Accepted: *27 April 2021*
Published: *21 May 2021*

Citation:
Chen M, Werner F, Wagner C, Simon M, Richtig E, Mertz KD, Griss J and Wagner SN (2021) Spatiotemporal Analysis of B Cell- and Antibody Secreting Cell-Subsets in Human Melanoma Reveals Metastasis-, Tumor Stage-, and Age-Associated Dynamics. Front. Cell Dev. Biol. 9:677944. doi: 10.3389/fcell.2021.677944

Background: The role of tumor-associated B cells in human cancer is only starting to emerge. B cells typically undergo a series of developmental changes in phenotype and function, however, data on the composition of the B cell population in human melanoma are largely absent including changes during tumor progression and their potential clinical significance.

Methods: In this study, we compared the number and distribution of six major B cell and antibody secreting cell subpopulations outside tertiary lymphoid structures in whole tumor sections of 154 human cutaneous melanoma samples (53 primary tumors without subsequent metastasis, 44 primary tumors with metastasis, 57 metastatic samples) obtained by seven color multiplex immunohistochemistry and automated tissue imaging and analysis.

Results: In primary melanomas, we observed the highest numbers for plasmablast-like, memory-like, and activated B cell subtypes. These cells showed a patchy, predominant paratumoral distribution at the invasive tumor-stroma margin. Plasma cell-like cells were hardly detected, germinal center- and transitional/regulatory-like B cells not at all. Of the major clinicopathologic prognostic factors for primary melanomas, metastasis was associated with decreased memory-like B cell numbers and a higher age associated with higher plasmablast-like cell numbers. When we compared the composition of B cell subpopulations in primary melanomas and metastatic samples, we found a significantly higher proportion of plasma cell-like cells at distant metastatic sites and a higher proportion of memory-like B cells at locoregional than distant metastatic sites. Both cell types were detected mainly in the para- and intratumoral stroma.

Conclusion: These data provide a first comprehensive and comparative spatiotemporal analysis of major B cell and antibody secreting cell subpopulations in human melanoma and describe metastasis-, tumor stage-, and age-associated dynamics, an important premise for B cell-related biomarker and therapy studies.

Keywords: tumor-associated B cells, memory B cells, plasma cells, human melanoma, tumor microenvironment, multiplex immunohistochemistry, spatiotemporal dynamics

INTRODUCTION

The tumor immune microenvironment critically regulates tumor initiation, progression and response to therapy (reviewed in Binnewies et al., 2018). Though B cells constitute a significant part of this microenvironment, the exploration of their role in human cancer has just begun (reviewed in Fridman et al., 2021).

Syngeneic mouse cancer models have shown that tumor-associated B cells (TAB) and antibody secreting cells (ASC), such as plasmablasts, can promote tumor progression (de Visser et al., 2005; Ammirante et al., 2010) and inhibit (Affara et al., 2014; Shalapour et al., 2015, 2017; Gunderson et al., 2016) but also support anti-tumor T cell-dependent therapy responses (Lu et al., 2020). In melanoma, syngeneic mouse models revealed both pro- as well as anti-tumorigenic effects of B cells (reviewed in Fremd et al., 2013), while advanced models such as genetically engineered mouse models or xenotransplantation models suffer from inadequate tumor infiltration by B cells or other immune cells of the tumor microenvironment (Hooijkaas et al., 2012). These data underline the importance of studies in human tissue samples.

In human melanoma, phenotypic analysis showed that the tumor microenvironment contains $CD20^+$ TAB (reviewed in Ladányi, 2015) and $CD138^+$ or IgA^+CD138^+ ASC, which are primarily found at the invasive tumor-stroma margin (Erdag et al., 2012; Bosisio et al., 2016; Griss et al., 2019). However, existing data on their impact on disease progression and outcome are inconsistent. Initial studies on the association of TAB numbers in primary human melanomas with patient survival employed CD20-immunostaining and reported on higher numbers in histological subtypes with a worse prognosis (Hillen et al., 2008) or on the association of higher percentages of $CD20^+$ TAB within tumor-infiltrating lymphocytes with a worse patient prognosis (Martinez-Rodriguez et al., 2014). These data were supported by observations from melanoma metastases where a 7-marker protein signature, including CD20, negatively predicted overall and recurrence-free patient survival (Meyer et al., 2012). Also in other human cancer types, including ductal carcinoma *in situ* of the breast, pancreatic ductal carcinoma and non-small cell lung, colorectal, oral hypopharynx, prostate and metastatic ovarian cancers, reports do exist that correlate infiltration with $CD20^+$ or $CD19^+$ TAB with poor patient disease outcome, tumor recurrence and/or progression (reviewed in Mohammed et al., 2013; Woo et al., 2014; Dong et al., 2006; Wouters and Nelson, 2018).

These studies, however, are contrasted by several other independent reports showing higher numbers or densities of $CD20^+$ TAB to be associated with improved patient survival, such as in melanoma metastases (Erdag et al., 2012) and primary cutaneous melanomas (Ladányi et al., 2011; Garg et al., 2016). These data are in line with reports from other human cancer types, including (triple-negative) inflammatory breast, epithelial and high-grade serous ovarian, non-small cell lung, early cervical squamous cell, metastatic colorectal, gastric, hepatocellular, pancreatic ductal, esophageal, biliary tract, muscle invasive bladder, oral hypopharynx, tongue squamous cell cancers, soft tissue sarcoma and mesothelioma, where high intratumoral $CD20^+$ or $CD19^+$ TAB numbers or densities alone or sometimes together with $CD3^+$ or $CD8^+$ T cells are associated with a favorable disease outcome (Linnebacher and Maletzki, 2012; Bindea et al., 2013; Lao et al., 2016; Schwartz et al., 2016; Wouters and Nelson, 2018; Helmink et al., 2020; Fridman et al., 2021).

In studies including additional expression of CD138, a marker associated with plasma cell differentiation, high CD20 together with CD138 expression correlated with a higher tumor grade in epithelial ovarian cancer and immune cell-associated CD138 expression alone with poorer overall and cancer-specific patient survival (Lundgren et al., 2016). Similarly, infiltration of $CD20^+$ TAB with CD138 expression into primary operable ductal invasive breast cancer was associated with poorer cancer-specific survival (Mohammed et al., 2013) and plasma cell enrichment in G1/2 papillary/acinar adenocarcinomas described as an independent negative prognostic factor (Kurebayashi et al., 2016). In contrast, a favorable prognostic effect was described for $CD138^+$ cell infiltration in colorectal, esophageal and gastric cancers (reviewed in Wouters and Nelson, 2018; Fridman et al., 2021). In human melanoma metastases, increased $CD138^+$ plasma cell counts showed a trend to better patient survival (Erdag et al., 2012) and patients with primary melanomas of > 2 mm in thickness and enriched for sheets/clusters of $CD138^+$ IgA-expressing plasma cells had a worse overall survival. In contrast, plasma cell-sparse melanomas had a significantly better survival than plasma cell-rich tumors and a trend toward a better survival than plasma cell-negative tumors (Bosisio et al., 2016).

Together, these data clearly pinpoint the presence of TAB and ASC in different human cancers, cancer subtypes and tumor stages, but indicate that these B cells may play varied roles. An attractive hypothesis for the varied roles of B cells is the presence of different TAB and ASC subpopulations. However, such data are lacking, mainly because of the limited ability to apply complex marker combinations required to identify such B cell phenotypes. We have recently shown that B cells from human melanoma are not only essential to sustain inflammation and $CD8^+$ T cell numbers in the tumor microenvironment but also can directly augment T cell activation by immune checkpoint blockade

(Griss et al., 2019). We were also the first to report increased B cell numbers to predict improved response and survival of melanoma patients receiving immune checkpoint blockade. These data were most recently supported and extended by independent analyses of melanoma tertiary lymphoid structures (TLS), where tumor-associated B cells are thought to be educated (Cabrita et al., 2020; Helmink et al., 2020). Together, these and our studies describe B cells to play an unexpected essential role in T cell-based anti-tumor immunity and the responsible B cell phenotypes to typically having undergone antigen-dependent activation and class switch recombination (Griss et al., 2019; Helmink et al., 2020). Despite their presumably high relevance for anti-tumor immune responses and immunotherapeutic strategies, data on the presence of these B cell subpopulations and their distribution in human melanoma are mostly missing so far.

Here we present a systematic comparative spatiotemporal analysis for six different antigen-experienced B cell and antibody secreting cell subpopulations in a series of 154 human melanoma samples. Using seven color multiplex immunohistochemistry and automated tissue imaging and analysis of whole tumor sections (Griss et al., 2019), we detected metastasis-, tumor stage-, and age-associated dynamics in the composition of these subpopulations.

MATERIALS AND METHODS

Patient Cohorts

Whole tissue sections were obtained from cutaneous primary melanomas of caucasian patients who underwent surgery between 2002 and 2016 at the Cantonal Hospital Baselland, Liestal, Switzerland, and between 2004 and 2020 at the Department of Dermatology, Medical University of Graz, Austria. Tumor samples from Graz were provided by the Biobank Graz of the Medical University. All tumors were obtained with informed patients' consent and the pathology files retrieved as approved by the local Ethics Committees (EKNZ vote BASEC 2016-01499 for Liestal; 32-238 ex 19/20 for Graz).

Histological diagnoses were made by board-certified pathologists from the Cantonal Hospital Baselland, Liestal, and board-certified dermatologists at the Department of Dermatology, Medical University of Graz, in some cases together with external board-certified pathologists. Diagnoses were reviewed by two authors of this study, a board-certified pathologist (KM) and a board-certified dermatologist (SW). The respective clinicopathologic information was recorded in **Tables 1**, **2**. As desmoplastic melanomas show a distinct clinical behavior, they were not included into this study (Lens et al., 2005).

The cohort included 97 patients with primary cutaneous melanoma, aged between 19 and 93 years at the time of first diagnosis. 53 patients presented without metastasis within a follow-up of a maximum 194 months interval (mean: 84 months, **Table 1**). 44 patients developed metastasis within a follow-up of a maximum 231 months interval (mean: 54 months, **Table 2**). From 10 of the latter patients, additional 16 metastatic

TABLE 1 | Clinical and histopathological summary of melanoma patients with primary tumors without subsequent metastasis.

No. of patients		**53**
Follow-up (months)	Mean	84
	Median	98
	Range	8–194
Age	Mean	64
	Median	68
	Range	31–93
Breslow depth (thickness in mm)	Mean	2.49
	Median	1.75
	Range	0.36–10
Location	Extremities	20
	Head/neck	3
	Trunk	30
Ulceration	Present	23
	Absent	30
Histotype*	SSM	40
	NM	8
	ALM	4
	NOS	1
Sex	Male	33
	Female	20

**SSM, superficial spreading melanoma; NM, nodular melanoma; ALM, acral lentiginous melanoma; NOS, not otherwise specified.*

TABLE 2 | Clinical and histopathological summary of melanoma patients with primary tumors with subsequent metastasis.

No. of patients		**44**
Follow-up (months)*	Mean	54
	Median	32
	Range	0–231
Age	Mean	65
	Median	68
	Range	19–91
Breslow depth (thickness in mm)**	Mean	4.71
	Median	2.65
	Range	0.7–17
Location**	Extremities	15
	Head/neck	7
	Trunk	21
Ulceration**	Present	24
	Absent	19
Histotype***	SSM	20
	NM	19
	ALM	2
	LMM	1
	NOS	2
Sex	Male	30
	Female	14

**Seven samples without follow-up information (after metastasis).*

***Five samples without exact information about Breslow depth, one about location, one about ulceration.*

****SSM, superficial spreading melanoma; NM, nodular melanoma; ALM, acral lentiginous melanoma; LMM, lentigo maligna melanoma; NOS, not otherwise specified.*

samples were collected at the time of first diagnosis. These early metastatic samples almost exclusively consisted of locoregional skin and clinically detectable (macroscopic) nodal metastases, where tumor deposits had completely replaced lymph node tissue or could be histologically clearly separated from remains of the lymphatic tissue.

None of these patients received local or systemic antitumor treatment before surgery of the primary tumor.

Seven Color Multiplex Immunohistochemical Staining for TAB and ASC Subpopulations

Tumor tissue analysis and read-out were approved by the Ethics Committee of the Medical University of Vienna (ethics vote 1999/2019). Four micrometer sections from formalin-fixed paraffin-embedded blocks were used. Staining parameters for each primary antibody were optimized using human tonsil tissue and representative study samples. The complete multiplex immunostaining procedure was designed as previously described (Carstens et al., 2017; Gorris et al., 2018; Griss et al., 2019). Antibodies used in stainings were against: CD19 (1:250 dilution, Abcam, clone EPR5906, catalogue number #134114), CD20 (1:2000, Agilent, clone L26, M0755), CD38 (1:450, Agilent, clone AT13/5, M7077), CD138 (1:450, Agilent, clone MI15, M7228), CD27 (1:500, Abcam, clone EPR8569, #ab 131254), CD5 (1:500, Novocastra, clone 4C7, CD5-4C7-L-CE).

Tissue sections were subjected to six rounds of immunohistochemical staining after dewaxing. Each round of staining started with a 30 min heat-induced antigen retrieval step with either citrate buffer (pH 6.0) or Tris-EDTA buffer (pH 9.0), respectively, a subsequent 30 min fixation step with neutral 7.5% formaldehyde (SAV Liquid Production) and a 15 min blocking step using 20% normal goat serum (Agilent, X0907), followed by successive incubations with primary antibody, biotinylated anti-mouse or -rabbit secondary antibody, Streptavidin-HRP (Dako, K5003) and Opal fluorophore dye (Akoya Biosciences). Each antibody was assigned to one of the fluorophores Opal 520, Opal 540, Opal 570, Opal 620, Opal 650, and Opal 690 (Akoya; FP1487001KT, FP1494001KT, FP1488001KT, FP1495001KT, FP1496001KT and FP1497001KT) diluted in 1X Plus Amplification Diluent (Akoya, FP1498). After six rounds of antibody stainings, nuclei were counterstained with DAPI (Akoya, FP1490) and slides mounted with PermaFluor fluorescence mounting medium (Thermo Fisher Scientific, TA-030-FM). Stainings with single primary antibodies were run in parallel to control for false positive (incomplete stripping of antibody-tyramide complexes) and false negative results (antigen masking by multiple antibodies, "umbrella-effect") as well as for spillover effects (detection of fluorophores in adjacent channels) as described by us before (Griss et al., 2019). Reproducibility was controlled by a reference slide in each run, antibody batches were not changed in this study. Negative controls included concentration-matched isotype stainings and stainings without primary antibodies (Kaufman et al., 2013). To detect $CD19^{low}$ plasma cell-like ASC, the concentration of the primary anti-CD19 antibody was adapted to allowing for detection of cellular patterns and frequencies obtained by $CD138^+$ pooled IgA/IgG^+ stainings on human tonsil and melanoma (Griss et al., 2019).

Automated Acquisition and Quantification of TAB and ASC Subpopulations

Multiplexed slides of the whole tumor sections were scanned on a Vectra 3 Automated Quantitative Pathology Imaging System (version 3.0.5., Akoya) and, after spectral unmixing, analyzed with inForm® Tissue Finder™ (version 2.4.1, Akoya) as described (Carstens et al., 2017; Gorris et al., 2018; Griss et al., 2019). An unstained representative tumor section was used to determine autofluorescence. Tumor areas with closely packed clusters of lymphoid cells (e.g., TLS) did not allow for an unambiguous allocation of fluorophore signals to a single cell and were excluded from our analysis as were tumor areas of ulceration. If any, remaining lymphatic tissue in early locoregional nodal metastases was also excluded.

We identified TAB and ASC subpopulations in whole tumor sections by differential CD19, CD20, CD38, CD138, CD27 and CD5 expression as described by us before (Griss et al., 2019): (i) $CD19^+$ $CD20^-$ $CD38^+$ $CD138^-$ as plasmablast-like, (ii) $CD19^+$ $CD20^-$ $CD138^+$ as plasma cell-like, (iii) $CD19^+$ $CD20^+$ $CD38^-$ $CD138^-$ $CD27^{var}$ as memory-like B cells, (iv) $CD20^+$ $CD38^+$ $CD138^-$ $CD5^-$ as germinal center-like B cells, (v) $CD19^+$ $CD20^-$ $CD38^-$ $CD138^-$ $CD27^+$ as activated B cells, (vi) $CD20^+$ $CD19^-$ $CD138^-$ $CD5^+$ as transitional/regulatory-like B cells and (vii) other cells (**Figure 1**). The CD19 staining was optimized for detection of $CD19^{low}$ plasma cell-like cells (see above) and these cells could be detected at significant numbers, still they may be slightly underrepresented. As expression of CD27 can be downregulated on tumor-infiltrating B cells (Nielsen et al., 2012; Hegde et al., 2016), also activated B cells may be underrepresented. All phenotyping and subsequent quantifications were performed blinded to the sample identity.

Statistical Analysis

Cell-level data (i.e., intensities per channel for the cell compartments "membrane," "cytoplasm" and "nucleus") were exported from inForm® Tissue Finder™ as text files and processed using R (version 4.0.3). Intensity thresholds were manually adjusted after manual inspection of every slide. Based on these thresholds, markers were defined as positive or negative and cells assigned to specific phenotypes based on the above marker combinations.

RESULTS

Experimental Strategy

TAB in primary human melanomas show a rather patchy and inhomogeneous infiltration pattern with sometimes predominant paratumoral, intratumoral or mixed distribution (Garg et al., 2016). We therefore decided to analyze whole tissue sections of 154 human cutaneous melanoma samples from four different cohorts representing different stages of melanoma

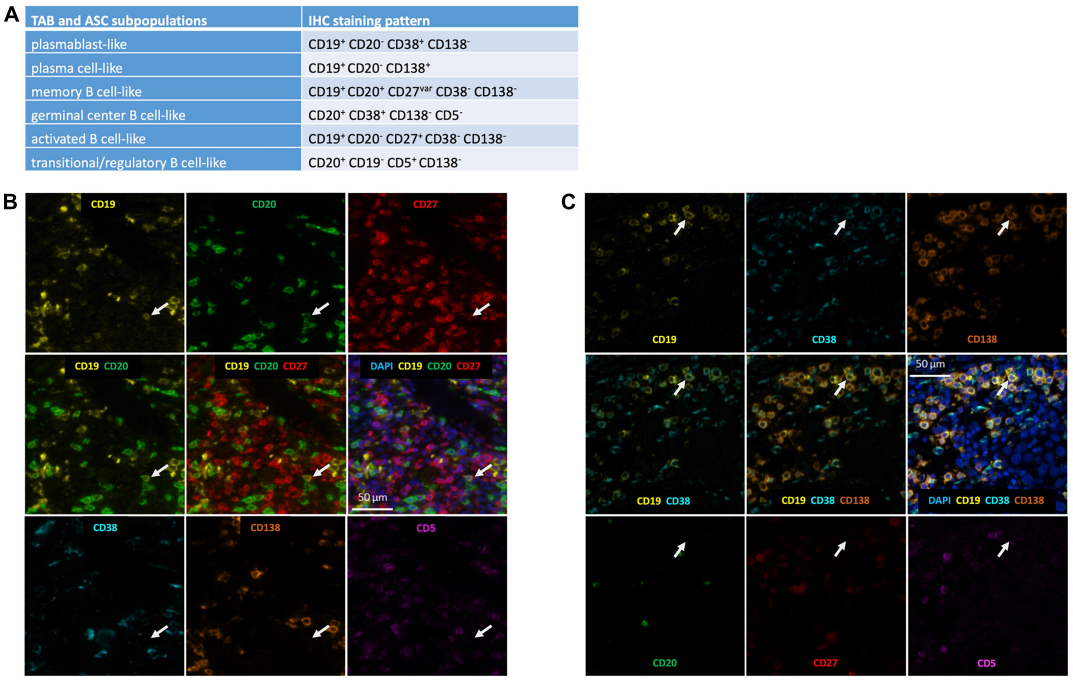

FIGURE 1 | Detection of TAB and ASC subpopulations in human melanoma. **(A)** Marker combinations used to identify TAB and ASC subpopulations by seven color multiplex immunostaining. Identification of **(B)** a $CD19^+CD20^+CD27^+$ memory-like TAB and **(C)** a $CD19^+CD38^+CD138^+$ plasma cell-like ASC. Serial images for the different markers: positive markers are given in the upper row; composite images of positive markers are given in the middle row, together with DAPI nuclear staining in the middle right; negative markers are given in the lower row. Arrows depict the same cell being representative for the respective TAB and ASC subpopulation. Scale bars represent 50 µm.

progression by seven color multiplex immunohistochemistry and automated tissue imaging and analysis for the presence and distribution of six different B cell subpopulations (activated, memory-like, germinal center-like and transitional/regulatory-like TAB as well as plasmablast-like and plasma cell-like ASC) outside TLS.

We first determined the absolute frequencies of each TAB and ASC subpopulations in tumor samples from 97 primary human melanomas and their association with the most important categorical clinicopathologic parameters.

For an association with disease progression, we compared the composition of the TAB/ASC population in primary tumor samples to that in 16 early locoregional and 41 late distant melanoma metastases. Data for the composition of the TAB/ASC population at distant metastatic samples were taken from own published data that have been collected with exactly the same staining, imaging and analysis approach in melanoma skin metastases (Griss et al., 2019).

Frequencies of Distinct B Cell and Antibody Secreting Cell Subpopulations in Primary Melanomas Are Associated With Prognostic Clinicopathologic Parameters

In line with previous reports on $CD20^+$ TAB (Garg et al., 2016), TAB and ASC subpopulations showed a rather patchy, predominant paratumoral distribution at the invasive tumor-stroma margin and sometimes an intratumoral as well as a mixed intratumoral and paratumoral infiltration pattern. We therefore decided to use whole tumor sections to stain 97 cutaneous primary human melanomas samples for the presence of six different B cell subpopulations outside TLS. We found TAB and ASC subpopulations in 65 of 97 primary melanoma samples (67%, **Table 3**). These subpopulations could be classified as activated and memory-like TAB as well as plasmablast-like and plasma cell-like ASC (**Figure 1**). Germinal center-like and transitional/regulatory-like TAB were not detected. Frequencies were highest for plasmablast-like ASC, followed by memory-like and activated TAB subpopulations. Plasma cell-like ASC were detected only at very low numbers (**Table 3**).

We then compared primary melanoma samples for metastasis, the single most important prognostic factor for melanoma patients, and observed that primary melanomas with metastasis contained a lower number of TAB and ASC containing tumors than primary melanomas without metastasis (**Table 3** and **Figure 2**). Primary tumors with subsequent metastasis contained significantly less memory-like TAB (mean 5.9 ± 14.5 vs. 2.7 ± 9.5 cells/mm^2, $p = 0.02$, CI 95% = −0.75 to 0, Bonferroni corrected Wilcoxon Rank Sum test) and a trend toward a decreased frequency of plasmablast-like cells (mean 7.7 ± 18.3 vs. 2.5 ± 6.5, $p = 0.17$, CI 95% = −0.41 to 0, Bonferroni corrected Wilcoxon Rank Sum test) compared to tumor samples without metastasis (**Table 3** and **Figure 2**).

TABLE 3 | Summary of multiplex immunohistochemistry staining results in primary melanoma samples.

	Primary melanomas without metastasis	Primary melanomas with metastasis
No. of samples	53	44
No. of samples with TAB and/or ASC subpopulations	41	24
No. of cells/mm^2 tumor area		
Activated TAB, range:	0–56	0–38
Mean:	4.0 ± 9.3	2.2 ± 6.3
Memory-like TAB*, range:	0–73	0–49
Mean:	5.9 ± 14.5	2.7 ± 9.5
Plasmablast-like ASC, range:	0–103	0–29
Mean:	7.7 ± 18.3	2.5 ± 6.5
Plasma cell-like ASC, range:	0–5	0–7
Mean:	0.6 ± 1.1	0.4 ± 1.1

$p \leq 0.05$ between primary melanomas without vs. with metastasis.

When we stratified primary melanoma samples for other prognostically important categorical clinicopathologic parameters, we found primary tumor samples from patients with higher age (above the median of 68 years) to contain significantly higher frequencies of plasmablast-like ASC (mean 9.4 ± 20 vs. 2.0 ± 5.3 cells/mm^2; $p = 0.05$, CI 95% = 0 to 1.3, Bonferroni corrected Wilcoxon Rank Sum test), but not for the other three TAB and ASC subpopulations (**Figure 3**). Differences for Breslow depth, ulceration and sex were not found (**Figure 3**).

The increased frequency of plasmablast-like ASC in primary melanomas of patients with higher age was somewhat surprising in view of the reported decrease of mature B cell numbers with age (reviewed in Crooke et al., 2019). We therefore screened each individual tumor sample for the frequency of plasmablast-like ASC and found a small subgroup of primary melanomas with considerably high frequencies. When we then compared the top 10% primary melanomas with highest frequencies of plasmablast-like ASC ($n = 10$) vs. the rest of tumor samples, we found this subgroup significantly driven by higher age and—to a minor degree—by higher Breslow depth ($p < 0.01$ and $p = 0.09$, respectively, ANCOVA), but not by sex or the presence of ulceration.

Thus, a decreased frequency of memory-like TAB is associated with metastasis of primary melanomas and an increased frequency of plasmablast-like cells with higher age.

Frequencies of Distinct B Cell and Antibody Secreting Cell Subpopulations Are Associated With Different Stages of Melanoma Disease

We next hypothesized that the observed changes in the frequency of TAB and ASC subpopulations with metastasis may also give a hint on changes in the frequency or composition of TAB and ASC subpopulations in further stages of melanoma progression. We thus compared primary tumors with locoregional and distant metastatic tumor sites.

Therefore, an additional 16 early locoregional metastases were stained by multiplex immunohistochemistry for TAB and ASC subpopulations. In nodal tumor samples, tumor deposits had completely replaced lymph node tissue or could be histologically clearly separated from the remaining lymphatic tissue. In the rare cases where some lymphatic tissue was left, we also observed infiltration of the subcapsular region. In tumor samples from early locoregional metastases, TAB and ASC subpopulations were detected primarily in stromal septa within the tumor and paratumorally at the invasive tumor-stroma margin, a pattern comparable to that reported previously for distant metastatic sites (Griss et al., 2019).

To compare these data from primary tumors and early locoregional metastatic sites with those from late distant metastatic sites, we used our own published data that had been generated in distant melanoma metastases by exactly the same staining, imaging and analysis approach (Griss et al., 2019). This data set provides relative frequencies of exactly the same TAB and ASC subpopulations and we compared these to the relative frequencies obtained in the present study. To allow analysis for the several TAB and ASC subpopulations within individual tumor samples, we included into this comparison tumor samples with only ≥50 B cell counts as determined by CD20- and/or CD19-immunoreactivity (for sample numbers see legend **Figure 4**).

While the relative counts for activated TAB did not change between primary tumors, locoregional and distant metastatic sites, we observed significant changes for memory-like TAB and plasma cell-like ASC (Bonferroni corrected $p < 0.01$ for both, Kruskal-Wallis Test). Memory-like TAB at locoregional metastatic sites showed comparable relative counts to primary tumors that did not metastasize but were increased compared to primary tumors with subsequent metastasis and distant metastatic sites (Bonferroni corrected $p = 0.08$ and $p < 0.001$, CI 95% –0.46 to –0.02 and 0.19 to 0.46, respectively, Wilcoxon rank sum test) (**Figure 4**). Plasma cell-like ASC exhibited highest relative counts at distant metastatic sites, these counts were significantly higher than in primary tumors and locoregional metastases (Bonferroni corrected $p < 0.01$ for both, CI 95% –0.47 to –0.17, –0.4 to –0.14, respectively, Wilcoxon rank sum test, **Figure 4**).

Thus, during disease progression memory-like TAB show highest frequencies at early locoregional metastatic sites whereas plasma cell-like ASC preferentially accumulate at late distant metastatic sites.

DISCUSSION

TAB and ASC occur in many human cancers but may play varied functional roles dependent on cancer type, genetic and histological subtypes and tumor stages. There is now substantial data that B cells may play an essential role in T cell-based anti-tumor immunity in human melanoma (Griss et al., 2019; Cabrita et al., 2020) by sustaining inflammation and CD8$^+$ T cell numbers in the tumor microenvironment and directly augmenting T cell activation by immune checkpoint

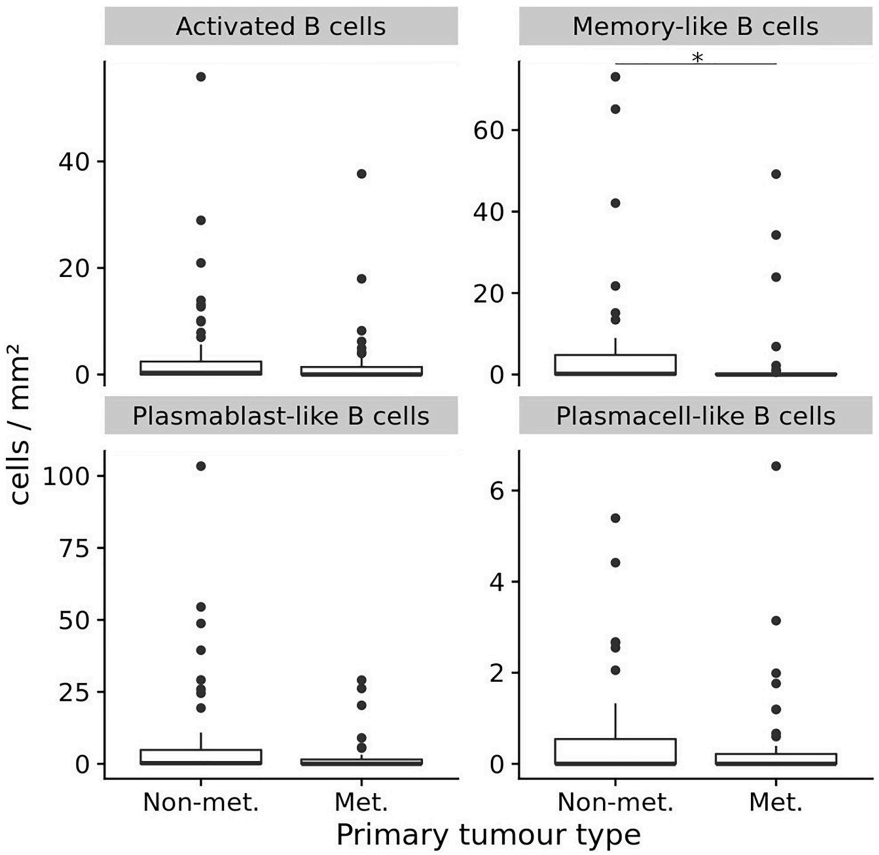

FIGURE 2 | The frequencies (cells/mm^2) of four different TAB and ASC subpopulations in primary human melanomas and their association with metastasis. Box plots comparing primary tumors that did not metastasize (Non-met.) within a mean follow-up of 84 months vs. those that metastasized (Met.) with a mean follow-up of 54 months. FDRs are 0.02 for memory-like TAB and 0.17 for plasmablast-like ASC. In boxplots lower and upper hinges correspond to first and third quartiles and center lines to medians. Upper whiskers extend to the largest value within 1.5 times the interquartile range. Outliers are shown as black circles. *$p \leq 0.05$.

blockade (Griss et al., 2019). While different TAB and ASC subtypes have been suggested to exert these immunostimulatory functions, reported candidate subtypes are typically antigen-activated and somatically recombined (Griss et al., 2019; Helmink et al., 2020). Beside activated TAB, such subtypes include germinal-center and memory B cells as well as plasmablasts and plasma cells and we have now performed a systematic analysis for the presence of these TAB and ASC subtypes in human melanoma samples comprising different stages of tumor progression. Using seven color multiplex immunohistochemistry and an automated tissue imaging and analysis approach, we identified (i) in primary melanomas highest numbers for plasmablast-like ASC, followed by memory-like and activated TAB, whereas plasma cell-like ASC were detected at comparably very low numbers; (ii) high frequencies of plasmablast-like ASC in primary melanomas to be driven by higher age and, to a lesser extent, by Breslow depth; (iii) an association of metastasis of primary melanomas with decreased counts of memory-like TAB; and (iv) increased relative frequencies for memory-like TAB at locoregional metastatic sites and a preferential enrichment for plasma cell-like ASC at distant metastatic sites.

Activated and memory-like TAB as well as plasmablast- and plasma cell-like ASC have been described by us before in distant human metastatic lesions and this study now confirms their presence also in regional metastatic and in primary melanoma sites. Similar to their distribution in distant metastases, TAB and ASC subpopulations in regional metastases were present in stromal septa within the tumor and at the invasive tumor stroma margin. In primary tumors, TAB and ASC subpopulations showed a rather patchy, predominant paratumoral distribution at the invasive tumor-stroma margin and sometimes an intratumoral as well as a mixed intratumoral and paratumoral infiltration pattern. These patterns are comparable to those reported previously for CD20$^+$ B cells in primary melanomas and other cancer types (Bindea et al., 2013; Garg et al., 2016). Also similar to CD20$^+$ TAB, the frequencies of distinct TAB and ASC subpopulations in primary human melanomas did not correlate with tumor thickness and ulceration, but with decreased metastasis (Garg et al., 2016). Thus our study further supports the meanwhile prevailing view of an anti-tumorigenic role of B cells in primary human melanoma (reviewed in Fridman et al., 2021) and provides the first evidence for diminution of a distinct TAB subpopulation, namely

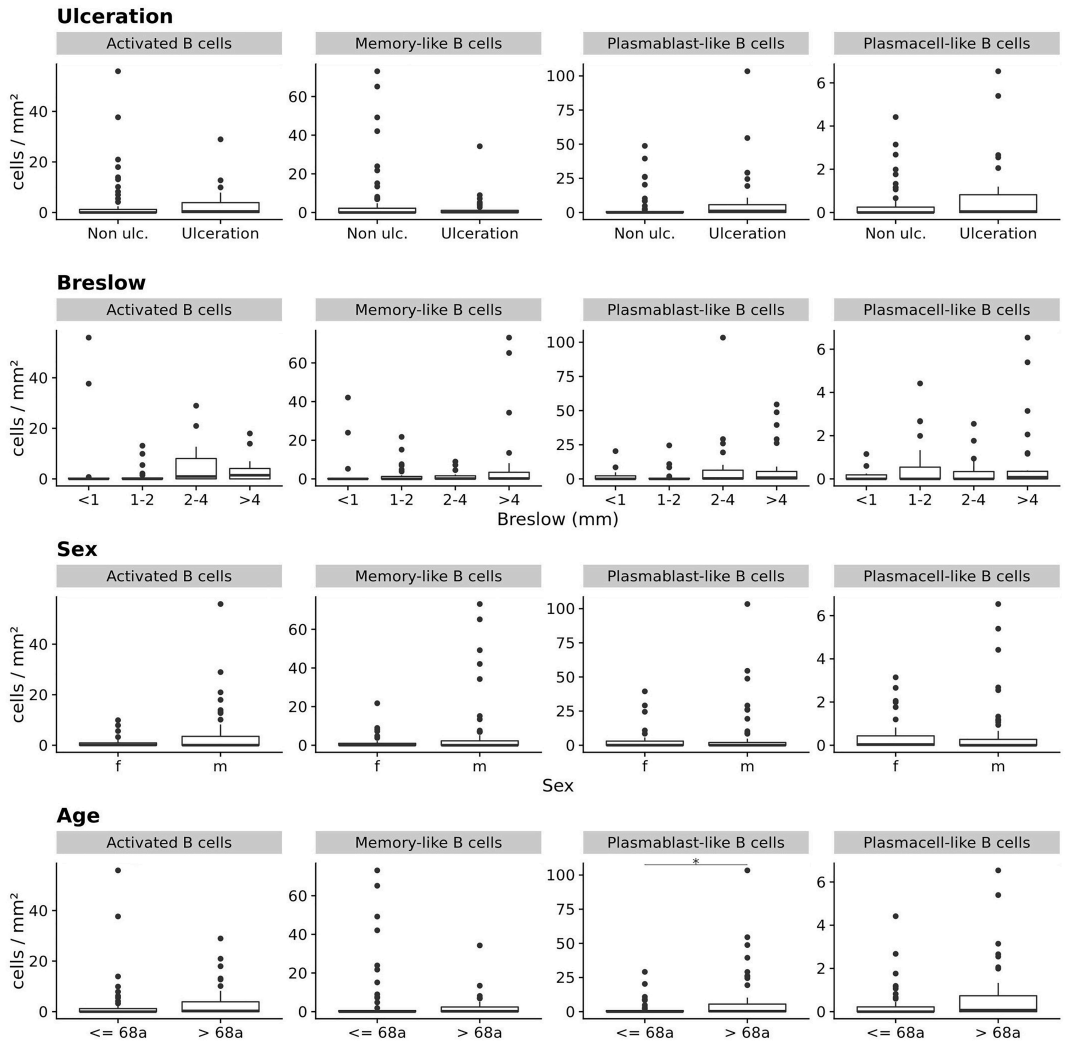

FIGURE 3 | The frequencies (cells/mm^2) of four different TAB and ASC subpopulations in primary human melanomas and their association with categorial prognostic clinicopathologic parameters. Box plots comparing primary tumors with and without ulceration, with increasing Breslow depths, for sex and age (from top to bottom). FDR is 0.05 for plasmablast-like ASC and age (median = 68 years). In boxplots lower and upper hinges correspond to first and third quartiles and center lines to medians. Upper whiskers extend to the largest value within 1.5 times the interquartile range. Outliers are shown as black circles. *$p \leq 0.05$.

memory-like B cells in primary tumors with documented metastasis. Memory B cells are critical to the induction of adaptive B cell responses not only to foreign but also to tumor antigens (Seifert and Küppers, 2016). A recent report has highlighted their potential therapeutic role in metastatic human melanoma where memory B cells have been associated with TLS (Helmink et al., 2020) and, together with other antigen-experienced and somatically recombined TAB and ASC subpopulations, linked to response of metastatic disease to immune checkpoint blockade (Griss et al., 2019; Cabrita et al., 2020; Helmink et al., 2020). The demonstrated detection of this B cell subpopulation particularly in TLS of metastatic locoregional nodal sites (Helmink et al., 2020) is also in line with our observation of increased memory-like TAB counts at locoregional sites, which consisted mainly of lymph nodes in our study cohort.

Plasmablast-like cells showed the highest frequency of TAB and ASC subpopulations in primary melanomas. These frequencies, however, were mainly driven by a subgroup of melanoma patients with increased age and Breslow depth. Human B cell populations are known to change quantitatively and qualitatively with increasing age and these changes have a clear impact on anti-tumor immune cell functions, best documented by the increased cancer susceptibility of older adults. In contrast to switched memory B cells, naive B cells and unswitched mature B cells in peripheral blood significantly decrease with age, a phenomenon that is linked to intrinsic mechanisms like decreased mRNA stability of transcription factor E47, which results in decreased induction of activation-induced cytidine deaminase and impaired ability to undergo class switch recombination and antibody secretion (Frasca et al., 2011). These intrinsic mechanisms are complemented

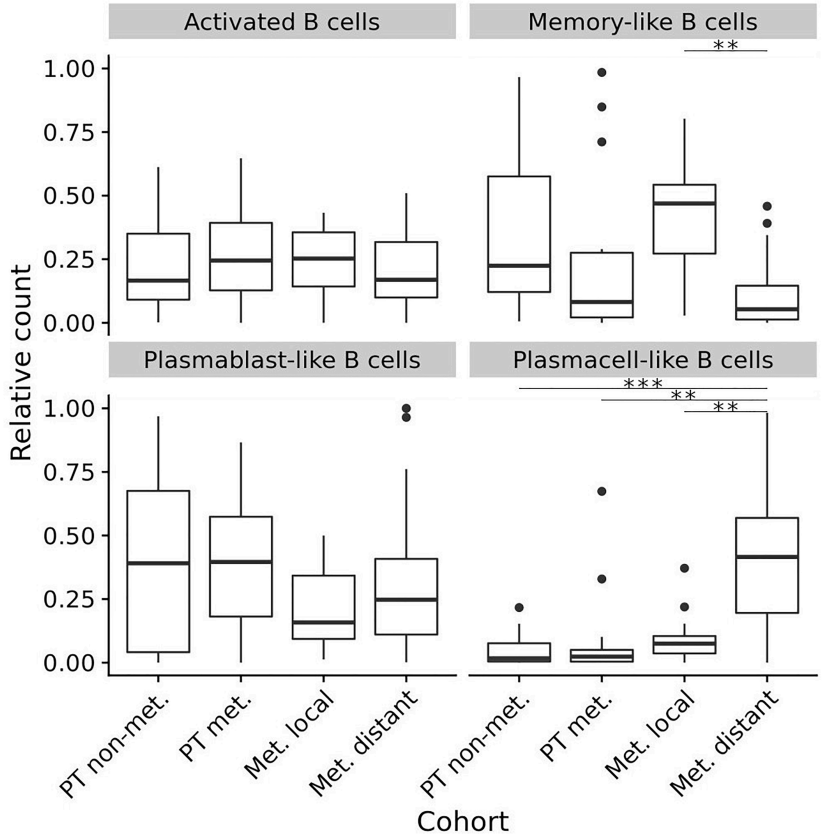

FIGURE 4 | Composition (relative frequencies) of four different TAB and ASC subpopulations in different stages of human melanoma disease. Box plots comparing primary tumors that did not metastasize (PT non-met., $n = 22$) with primary tumors that metastasized (PT met., $n = 14$), early locoregional metastatic sites (Met. local, $n = 15$) and late distant metastatic sites (Met. distant, $n = 33$). FDRs (adjusted) for memory-like TAB at early locoregional metastatic sites are 0.08 and 0.001 compared to primary tumors that metastasized and late distant metastatic sites, respectively. FDRs (adjusted) for plasma cell-like ASC at late distant metastatic sites are < 0.001 compared to primary tumors that did not metastasize, and 0.001 compared to both primary tumors that metastasized as well as early locoregional metastatic sites. In boxplots lower and upper hinges correspond to first and third quartiles and center lines to medians. Upper whiskers extend to the largest value within 1.5 times the interquartile range. Outliers are shown as black circles. $^{**}p < 0.01$, $^{***}p < 0.001$.

by additional extrinsic factors such as defects in T cell help to B cells or increased numbers of regulatory T cells in the peripheral blood (Wagner et al., 2018) as well as structural and functional changes in secondary lymphoid organs of the elderly (reviewed in Crooke et al., 2019). All these intrinsic and extrinsic factors argue against B cell maturation within germinal centers of secondary or tertiary lymphoid structures as a mechanism underlying the increased frequencies of plasmablast-like ASC in a subgroup of primary melanomas. In line with this assumption, we could hardly detect any mature TLS in hematoxylin & eosin or multiplex immunohistochemical stains in this subgroup (own unpublished data). An alternative source for plasmablasts in primary melanomas could be the B1 cell population which can differentiate into short lived IgM + plasmablasts outside germinal centers. Though B1 cells also undergo age-associated changes such as a decrease of numbers in peripheral blood, sub-analyses have shown that with advancing age spontaneous antibody secretion by B1 cells is modified, but not necessarily reduced in terms of the number of IgG-secreting B1 cells and the amount of IgM secretion per cell (Rodriguez-Zhurbenko et al., 2019). B1 cells express substantial levels of the transcription factor BLIMP1, which decrease with age, and of the transcription factor PAX5, which increase with age (Rodriguez-Zhurbenko et al., 2019). As high BLIMP1 levels are required particularly for plasma cell differentiation, one is tempting to speculate that the reduced BLIMP1 levels at higher age could still be sufficient to induce plasmablasts which need significantly less BLIMP1 for differentiation (Nutt et al., 2015). Consistently, the subgroup of primary melanomas with highest numbers of plasmablast-like ASC did not contain somehow comparable numbers of plasma cell-like ASC. Furthermore, recent mouse data indicate that Pax5 downregulation is not required for plasmablast development but is rather essential for accumulation and optimal IgG secretion of long-lived plasma cells with progressing age (Crooke et al., 2019; Liu et al., 2020).

$CD138^+$ IgA^+ plasma cells have been described in human primary melanomas particularly of >2 mm in thickness, where plasma cell-rich tumors—as identified by staining for CD138—had a worse overall survival than plasma-sparse ones

(Bosisio et al., 2016). Consistent with our data, both $CD138^+$ and $CD138^+$ IgA^+ plasma cells were detected in only a small number of primary melanomas from two independent cohorts (Bosisio et al., 2016). While we could not address an association with overall survival in our study, numbers of plasma cell-like ASC in our study could be associated neither with metastasis nor with prognostic markers such as Breslow depth or the presence of ulceration as reported for $CD138^+$ plasma cells (Bosisio et al., 2016). This may be due to the smaller sample size in our study, particularly of tumors with >2mm in thickness, and/or due to different staining and tissue evaluation approaches. These include the usage of multiple markers vs. a single marker for detection of plasma cells. While staining for CD138 alone, which is not exclusively expressed on plasma cells, may have led to overestimation of cell numbers, we cannot exclude a slight underestimation in our study, though we have optimized our CD19 immunostaining approach for detection of $CD19^{low}$ plasma cell-like cells. Additional differences are the evaluation of whole tissue samples vs. selected tissue areas and the use of a quantitative automated read-out vs. application of a semiquantitative visual scoring system. Interestingly, the rather low number of plasma cell-like ASC at primary melanoma sites was paralleled by a low number in locoregional metastatic sites but contrasted by a significant enrichment at distant metastatic sites, which comprised skin metastases in our study cohort. An attractive explanation for this observation may provide the reported neogenesis of TLS particularly in human melanoma skin metastases (Cipponi et al., 2012) together with the recent reports on an association of mature TLS (Cabrita et al., 2020; Helmink et al., 2020; Petitprez et al., 2020) with clonal B cell expansion, increased B cell receptor diversity and higher numbers of plasmablasts/plasma cells (Cabrita et al., 2020; Helmink et al., 2020). While some earlier reports describe the presence of TLS-associated cell types such as high endothelial venules (Dieu-Nosjean et al., 2008) and $LAMP3^+$ mature dendritic cells (Ladányi et al., 2007) in primary human melanomas, a systematic analysis of numbers, areas, localization and maturation states of TLS at different tumor stages is still lacking.

CONCLUSION

Together, this study significantly widens the knowledge of the spectrum of B cell subpopulations and their spatiotemporal dynamics in human melanoma. Our data show a rather inhomogeneous distribution along different stages of human melanoma progression with numbers of memory-like TAB which decrease in primary melanomas that metastasize, but increase at locoregional metastatic sites, and with numbers of plasma cell-like ASC which increase at distant metastatic sites. These variations may have important implications for the biology of human melanoma as well as for the development of B cell-related biomarker and therapy studies.

DATA AVAILABILITY STATEMENT

Datasets generated for this study are available to any qualified researcher on request to the corresponding author, without undue reservation.

ETHICS STATEMENT

The patients/participants provided their written informed consent to tumor sample collection. Tumor sample collection and the studies involving these tumor samples were reviewed and approved by the Ethikkommission Nordwest- und Zentralschweiz (vote BASEC 2016-01499) and the Ethikkommission der Medizinischen Universität Graz (32-238 ex 1103 19/20). Tumor tissue analysis and read-out was additionally approved by the Ethics Committee of the Medical University of Vienna (ethics vote 1999/2019).

AUTHOR CONTRIBUTIONS

JG and SW: conception and design. ER, KM, MC, MS, and SW: clinical data collection and assembly, patient materials. MC, FW, CW, MS, and SW: multiplex immunostaining, automated imaging acquisition, and data read out. JG: statistics. All authors contributed to the manuscript writing and final approval of the manuscript.

FUNDING

This work received support from the Austrian Science Fund (FWF) Project P30325-B28 and IPPTO Project No. DOC 59-B33 to SW.

ACKNOWLEDGMENTS

We thank Lorenzo Cerroni, Alexandra Rodlauer-Kriegl, Ariane Aigelsreiter, Vivien Kriegl, and Monika Weiss for searching, providing or processing human tumor samples and the respective clinicopathologic information. Parts of the tumor samples used in this project have been provided by the Biobank Graz of the Medical University of Graz, Austria.

REFERENCES

Affara, N. I., Ruffell, B., Medler, T. R., Gunderson, A. J., Johansson, M., Bornstein, S., et al. (2014). B cells regulate macrophage phenotype and response to chemotherapy in squamous carcinomas. *Cancer Cell* 25, 809–821. doi: 10.1016/j.ccr.2014.04.026

Ammirante, M., Luo, J.-L., Grivennikov, S., Nedospasov, S., and Karin, M. (2010). B-cell-derived lymphotoxin promotes castration-resistant prostate cancer. *Nature* 464, 302–305. doi: 10.1038/nature08782

Bindea, G., Mlecnik, B., Tosolini, M., Kirilovsky, A., Waldner, M., Obenauf, A. C., et al. (2013). Spatiotemporal dynamics of intratumoral immune cells reveal the immune landscape in human cancer. *Immunity* 39, 782–795. doi: 10.1016/j.immuni.2013.10.003

Binnewies, M., Roberts, E. W., Kersten, K., Chan, V., Fearon, D. F., Merad, M., et al. (2018). Understanding the tumor immune microenvironment (TIME) for effective therapy. *Nat. Med.* 24, 541–550. doi: 10.1038/s41591-018-0014-x

Bosisio, F. M., Wilmott, J. S., Volders, N., Mercier, M., Wouters, J., Stas, M., et al. (2016). Plasma cells in primary melanoma. Prognostic significance and possible role of IgA. *Mod. Pathol.* 29, 347–358. doi: 10.1038/modpathol.2016.28

Cabrita, R., Lauss, M., Sanna, A., Donia, M., Skaarup Larsen, M., Mitra, S., et al. (2020). Tertiary lymphoid structures improve immunotherapy and survival in melanoma. *Nature* 577, 561–565. doi: 10.1038/s41586-019-1914-8

Carstens, J. L., Correa de Sampaio, P., Yang, D., Barua, S., Wang, H., Rao, A., et al. (2017). Spatial computation of intratumoral T cells correlates with survival of patients with pancreatic cancer. *Nat. Commun.* 8:15095. doi: 10.1038/ncomms15095

Cipponi, A., Mercier, M., Seremet, T., Baurain, J.-F., Théate, I., van den Oord, J., et al. (2012). Neogenesis of lymphoid structures and antibody responses occur in human melanoma metastases. *Cancer Res.* 72, 3997–4007. doi: 10.1158/0008-5472.CAN-12-1377

Crooke, S. N., Ovsyannikova, I. G., Poland, G. A., and Kennedy, R. B. (2019). Immunosenescence and human vaccine immune responses. *Immun. Ageing* 16:25. doi: 10.1186/s12979-019-0164-9

de Visser, K. E., Korets, L. V., and Coussens, L. M. (2005). De novo carcinogenesis promoted by chronic inflammation is B lymphocyte dependent. *Cancer Cell* 7, 411–423. doi: 10.1016/j.ccr.2005.04.014

Dieu-Nosjean, M.-C., Antoine, M., Danel, C., Heudes, D., Wislez, M., Poulot, V., et al. (2008). Long-term survival for patients with non–small-cell lung cancer with intratumoral lymphoid structures. *J. Clin. Oncol.* 26, 4410–4417. doi: 10.1200/JCO.2007.15.0284

Dong, H. P., Elstrand, M. B., Holth, A., Silins, I., Berner, A., Trope, C. G., et al. (2006). NK- and B-cell infiltration correlates with worse outcome in metastatic ovarian carcinoma. *Am. J. Clin. Pathol.* 125, 451–458. doi: 10.1309/15B66DQMFYYM78CJ

Erdag, G., Schaefer, J. T., Smolkin, M. E., Deacon, D. H., Shea, S. M., Dengel, L. T., et al. (2012). Immunotype and immunohistologic characteristics of tumor-infiltrating immune cells are associated with clinical outcome in metastatic melanoma. *Cancer Res.* 72, 1070–1080. doi: 10.1158/0008-5472.CAN-11-3218

Frasca, D., Diaz, A., Romero, M., Landin, A. M., and Blomberg, B. B. (2011). Age effects on B cells and humoral immunity in humans. *Ageing Res. Rev.* 10, 330–335. doi: 10.1016/j.arr.2010.08.004

Fremd, C., Schuetz, F., Sohn, C., Beckhove, P., and Domschke, C. (2013). B cell-regulated immune responses in tumor models and cancer patients. *Oncoimmunology* 2:e25443. doi: 10.4161/onci.25443

Fridman, W. H., Petitprez, F., Meylan, M., Chen, T. W.-W., Sun, C.-M., Roumenina, L. T., et al. (2021). B cells and cancer: to B or not to B? *J. Exp. Med.* 218:e20200851. doi: 10.1084/jem.20200851

Garg, K., Maurer, M., Griss, J., Brüggen, M.-C., Wolf, I. H., Wagner, C., et al. (2016). Tumor-associated B cells in cutaneous primary melanoma and improved clinical outcome. *Hum. Pathol.* 54, 157–164. doi: 10.1016/j.humpath.2016.03.022

Gorris, M. A. J., Halilovic, A., Rabold, K., van Duffelen, A., Wickramasinghe, I. N., Verweij, D., et al. (2018). Eight-color multiplex immunohistochemistry for simultaneous detection of multiple immune checkpoint molecules within the tumor microenvironment. *J. Immunol.* 200, 347–354. doi: 10.4049/jimmunol.1701262

Griss, J., Bauer, W., Wagner, C., Simon, M., Chen, M., Grabmeier-Pfistershammer, K., et al. (2019). B cells sustain inflammation and predict response to immune checkpoint blockade in human melanoma. *Nat. Commun.* 10:4186. doi: 10.1038/s41467-019-12160-2

Gunderson, A. J., Kaneda, M. M., Tsujikawa, T., Nguyen, A. V., Affara, N. I., Ruffell, B., et al. (2016). Bruton tyrosine kinase–dependent immune cell cross-talk drives pancreas cancer. *Cancer Discov.* 6, 270–285. doi: 10.1158/2159-8290.CD-15-0827

Hegde, P. S., Karanikas, V., and Evers, S. (2016). The where, the when, and the how of immune monitoring for cancer immunotherapies in the era of checkpoint inhibition. *Clin. Cancer Res.* 22, 1865–1874. doi: 10.1158/1078-0432.CCR-15-1507

Helmink, B. A., Reddy, S. M., Gao, J., Zhang, S., Basar, R., Thakur, R., et al. (2020). B cells and tertiary lymphoid structures promote immunotherapy response. *Nature* 577, 549–555. doi: 10.1038/s41586-019-1922-8

Hillen, F., Baeten, C. I. M., van de Winkel, A., Creytens, D., van der Schaft, D. W. J., Winnepenninckx, V., et al. (2008). Leukocyte infiltration and tumor cell plasticity are parameters of aggressiveness in primary cutaneous melanoma. *Cancer Immunol. Immunother.* 57, 97–106. doi: 10.1007/s00262-007-0353-9

Hooijkaas, A., Gadiot, J., Morrow, M., Stewart, R., Schumacher, T., and Blank, C. U. (2012). Selective BRAF inhibition decreases tumor-resident lymphocyte frequencies in a mouse model of human melanoma. *Oncoimmunology* 1, 609–617. doi: 10.4161/onci.20226

Kaufman, H. L., Kirkwood, J. M., Hodi, F. S., Agarwala, S., Amatruda, T., Bines, S. D., et al. (2013). The Society for Immunotherapy of Cancer consensus statement on tumour immunotherapy for the treatment of cutaneous melanoma. *Nat. Rev. Clin. Oncol.* 10, 588–598. doi: 10.1038/nrclinonc.2013.153

Kurebayashi, Y., Emoto, K., Hayashi, Y., Kamiyama, I., Ohtsuka, T., Asamura, H., et al. (2016). Comprehensive immune profiling of lung adenocarcinomas reveals four immunosubtypes with plasma cell subtype a negative indicator. *Cancer Immunol. Res.* 4, 234–247. doi: 10.1158/2326-6066.CIR-15-0214

Ladányi, A. (2015). Prognostic and predictive significance of immune cells infiltrating cutaneous melanoma. *Pigment Cell Melanoma Res.* 28, 490–500. doi: 10.1111/pcmr.12371

Ladányi, A., Kiss, J., Mohos, A., Somlai, B., Liszkay, G., Gilde, K., et al. (2011). Prognostic impact of B-cell density in cutaneous melanoma. *Cancer Immunol. Immunother.* 60, 1729–1738. doi: 10.1007/s00262-011-1071-x

Ladányi, A., Kiss, J., Somlai, B., Gilde, K., Fejös, Z., Mohos, A., et al. (2007). Density of DC-LAMP+ mature dendritic cells in combination with activated T lymphocytes infiltrating primary cutaneous melanoma is a strong independent prognostic factor. *Cancer Immunol. Immunother.* 56, 1459–1469. doi: 10.1007/s00262-007-0286-3

Lao, X.-M., Liang, Y.-J., Su, Y.-X., Zhang, S.-E., Zhou, X., and Liao, G.-Q. (2016). Distribution and significance of interstitial fibrosis and stroma-infiltrating B cells in tongue squamous cell carcinoma. *Oncol. Lett.* 11, 2027–2034. doi: 10.3892/ol.2016.4184

Lens, M. B., Newton-Bishop, J. A., and Boon, A. P. (2005). Desmoplastic malignant melanoma: a systematic review. *Br. J. Dermatol.* 152, 673–678. doi: 10.1111/j.1365-2133.2005.06462.x

Linnebacher, M., and Maletzki, C. (2012). Tumor-infiltrating B cells. *Oncoimmunology* 1, 1186–1188. doi: 10.4161/onci.20641

Liu, G. J., Jaritz, M., Wöhner, M., Agerer, B., Bergthaler, A., Malin, S. G., et al. (2020). Repression of the B cell identity factor Pax5 is not required for plasma cell development. *J. Exp. Med.* 217:e20200147. doi: 10.1084/jem.20200147

Lu, Y., Zhao, Q., Liao, J.-Y., Song, E., Xia, Q., Pan, J., et al. (2020). Complement Signals Determine Opposite Effects of B Cells in Chemotherapy-Induced Immunity. *Cell* 180, 1081–1097.e24. doi: 10.1016/j.cell.2020.02.015

Lundgren, S., Berntsson, J., Nodin, B., Micke, P., and Jirström, K. (2016). Prognostic impact of tumour-associated B cells and plasma cells in epithelial ovarian cancer. *J. Ovarian Res.* 9, 21. doi: 10.1186/s13048-016-0232-0

Martinez-Rodriguez, M., Thompson, A. K., and Monteagudo, C. (2014). A significant percentage of CD20-positive TILs correlates with poor prognosis in patients with primary cutaneous malignant melanoma. *Histopathology* 65, 726–728. doi: 10.1111/his.12437

Meyer, S., Fuchs, T. J., Bosserhoff, A. K., Hofstädter, F., Pauer, A., Roth, V., et al. (2012). A seven-marker signature and clinical outcome in malignant melanoma: a large-scale tissue-microarray study with two independent patient cohorts. *PLoS One* 7:e38222. doi: 10.1371/journal.pone.0038222

Mohammed, Z. M. A., Going, J. J., Edwards, J., Elsberger, B., and McMillan, D. C. (2013). The relationship between lymphocyte subsets and clinico-pathological determinants of survival in patients with primary operable invasive ductal breast cancer. *Br. J. Cancer* 109, 1676–1684. doi: 10.1038/bjc.2013.493

Nielsen, J. S., Sahota, R. A., Milne, K., Kost, S. E., Nesslinger, N. J., Watson, P. H., et al. (2012). CD20 + tumor-infiltrating lymphocytes have an atypical CD27 - memory phenotype and together with CD8 + T cells promote favorable prognosis in ovarian cancer. *Clin. Cancer Res.* 18, 3281–3292. doi: 10.1158/1078-0432.CCR-12-0234

Nutt, S. L., Hodgkin, P. D., Tarlinton, D. M., and Corcoran, L. M. (2015). The generation of antibody-secreting plasma cells. *Nat. Rev. Immunol.* 15, 160–171. doi: 10.1038/nri3795

Petitprez, F., de Reyniès, A., Keung, E. Z., Chen, T. W.-W., Sun, C.-M., Calderaro, J., et al. (2020). B cells are associated with survival and immunotherapy response in sarcoma. *Nature* 577, 556–560. doi: 10.1038/s41586-019-1906-8

Rodriguez-Zhurbenko, N., Quach, T. D., Hopkins, T. J., Rothstein, T. L., and Hernandez, A. M. (2019). Human B-1 cells and B-1 cell antibodies change with advancing age. *Front. Immunol.* 10:483. doi: 10.3389/fimmu.2019.00483

Schwartz, M., Zhang, Y., and Rosenblatt, J. D. (2016). B cell regulation of the anti-tumor response and role in carcinogenesis. *J. Immunother. Cancer* 4:40. doi: 10.1186/s40425-016-0145-x

Seifert, M., and Küppers, R. (2016). Human memory B cells. *Leukemia* 30, 2283–2292. doi: 10.1038/leu.2016.226

Shalapour, S., Font-Burgada, J., Di Caro, G., Zhong, Z., Sanchez-Lopez, E., Dhar, D., et al. (2015). Immunosuppressive plasma cells impede T-cell-dependent immunogenic chemotherapy. *Nature* 521, 94–98. doi: 10.1038/nature14395

Shalapour, S., Lin, X.-J., Bastian, I. N., Brain, J., Burt, A. D., Aksenov, A. A., et al. (2017). Inflammation-induced IgA+ cells dismantle anti-liver cancer immunity. *Nature* 551, 340–345. doi: 10.1038/nature24302

Wagner, A., Garner-Spitzer, E., Jasinska, J., Kollaritsch, H., Stiasny, K., Kundi, M., et al. (2018). Age-related differences in humoral and cellular immune responses after primary immunisation: indications for stratified vaccination schedules. *Sci. Rep.* 8:9825. doi: 10.1038/s41598-018-28111-8

Woo, J. R., Liss, M. A., Muldong, M. T., Palazzi, K., Strasner, A., Ammirante, M., et al. (2014). Tumor infiltrating B-cells are increased in prostate cancer tissue. *J. Transl. Med.* 12:30. doi: 10.1186/1479-5876-12-30

Wouters, M. C. A., and Nelson, B. H. (2018). Prognostic significance of tumor-infiltrating B cells and plasma cells in human cancer. *Clin. Cancer Res.* 24, 6125–6135. doi: 10.1158/1078-0432.CCR-18-1481

Conflict of Interest: The authors declare that the research was conducted in the absence of any commercial or financial relationships that could be construed as a potential conflict of interest.

Copyright © 2021 Chen, Werner, Wagner, Simon, Richtig, Mertz, Griss and Wagner. This is an open-access article distributed under the terms of the Creative Commons Attribution License (CC BY). The use, distribution or reproduction in other forums is permitted, provided the original author(s) and the copyright owner(s) are credited and that the original publication in this journal is cited, in accordance with accepted academic practice. No use, distribution or reproduction is permitted which does not comply with these terms.

frontiers in Cell and Developmental Biology

ORIGINAL RESEARCH
published: 02 June 2021
doi: 10.3389/fcell.2021.682619

A Systems-Based Key Innovation-Driven Approach Infers Co-option of Jaw Developmental Programs During Cancer Progression

Stephan Marquardt[1†], Athanasia Pavlopoulou[2,3†], Işıl Takan[2,3], Prabir Dhar[1], Brigitte M. Pützer[1,4] and Stella Logotheti[1]*

[1] Institute of Experimental Gene Therapy and Cancer Research, Rostock University Medical Center, Rostock, Germany, [2] İzmir Biomedicine and Genome Center, İzmir, Turkey, [3] İzmir International Biomedicine and Genome Institute, Dokuz Eylül University, İzmir, Turkey, [4] Department Life, Light & Matter, University of Rostock, Rostock, Germany

OPEN ACCESS

Edited by:
Renjie Chai,
Southeast University, China

Reviewed by:
Amélie E. Coudert,
Université Paris Diderot, France
Miriam Gaggianesi,
University of Palermo, Italy

***Correspondence:**
Stella Logotheti
Styliani.Logotheti@med.uni-rostock.de

† These authors have contributed equally to this work and share first authorship

Specialty section:
This article was submitted to Molecular Medicine, a section of the journal Frontiers in Cell and Developmental Biology

Received: *18 March 2021*
Accepted: *11 May 2021*
Published: *02 June 2021*

Citation:
Marquardt S, Pavlopoulou A, Takan I, Dhar P, Pützer BM and Logotheti S (2021) A Systems-Based Key Innovation-Driven Approach Infers Co-option of Jaw Developmental Programs During Cancer Progression. Front. Cell Dev. Biol. 9:682619. doi: 10.3389/fcell.2021.682619

Cancer acquires metastatic potential and evolves via co-opting gene regulatory networks (GRN) of embryonic development and tissue homeostasis. Such GRNs are encoded in the genome and frequently conserved among species. Considering that all metazoa have evolved from a common ancestor via major macroevolutionary events which shaped those GRNs and increased morphogenetic complexity, we sought to examine whether there are any key innovations that may be consistently and deterministically linked with metastatic potential across the metazoa clades. To address tumor evolution relative to organismal evolution, we revisited and retrospectively juxtaposed seminal laboratory and field cancer studies across taxa that lie on the evolutionary lineage from cnidaria to humans. We subsequently applied bioinformatics to integrate species-specific cancer phenotypes, multiomics data from up to 42 human cancer types, developmental phenotypes of knockout mice, and molecular phylogenetics. We found that the phenotypic manifestations of metastasis appear to coincide with agnatha-to-gnathostome transition. Genes indispensable for jaw development, a key innovation of gnathostomes, undergo mutations or methylation alterations, are aberrantly transcribed during tumor progression and are causatively associated with invasion and metastasis. There is a preference for deregulation of gnathostome-specific versus pre-gnathostome genes occupying hubs of the jaw development network. According to these data, we propose our systems-based model as an *in silico* tool the prediction of likely tumor evolutionary trajectories and therapeutic targets for metastasis prevention, on the rationale that the same genes which are essential for key innovations that catalyzed vertebrate evolution, such as jaws, are also important for tumor evolution.

Keywords: cancer evolution, metastasis, jaw development, epithelial-mesenchymal transition, gnathostomes, cyclostomes, tumor evolutionary trajectories, prediction model

INTRODUCTION

Despite advances in cancer management, manifestation of lesions with metastatic potential signals the terminal stage of disease. The term "metastatic potential" may include any combination of cancer phenotypes that enable metastatic dissemination including motility, immune evasion, and ability to survive in circulation and proliferate at distant sites (Birkbak and McGranahan, 2020). Cancer progression is governed by mechanisms distinct from those of initiation (Logotheti et al., 2020). While at early stages cancer cells accumulate driver mutations, at advanced stages, they do not acquire additional, metastasis-specific mutations (Rodrigues et al., 2018), but rather hijack programs of tissue-homeostasis and normal embryonic development and reactivate them in an unusual place, at the wrong time (Logotheti et al., 2020). Metastasis is promoted by aberrant gene regulation, and metastatic transcriptional programs arise from *de novo* combinatorial activation of multiple distinct and developmentally distant transcriptional modules (Rodrigues et al., 2018). We and others have shown that cancer progression is facilitated by ectopic activation of genes that have tissue-restricted profiles (Rousseaux et al., 2013; Richter et al., 2019), or are involved in placenta (Costanzo et al., 2018) and embryonic development (Billaud and Santoro, 2011) including, but not limited to, neuronal development and function (Logotheti et al., 2020). For instance, we have recently provided compelling evidence that genes involved in neuronal development and neurological function are reactivated in tumors and predict poor patient outcomes across various cancers. Tumors co-opt genes essential for the development of distinct anatomical parts of the nervous system, with a frequent preference for cerebral cortex and the neural crest-derived enteric nerves function (Logotheti et al., 2020). In this respect, co-option, the evolutionary process through which a biological function within a specific context may be alternatively used in another context to support a novel function, emerges as a recurrent and prevailing pattern during tumor progression (Billaud and Santoro, 2011).

The gene regulatory networks (GRN) of embryonic development and tissue homeostasis are encoded in the genomes of animal species and define their attributes and morphogenetic complexity (Levine and Davidson, 2005). Considering that tumors can progress to metastatic stages by co-opting such gene programs, it is reasonable to conjure that the metastatic potential largely depends on the gene reservoir of the species on which tumors grow. For example, lesions growing on animals as simple as cnidarians will plausibly usurp the GRNs controlling their corresponding attributes, while mammal tumors have access to GRNs underlying more sophisticated body plans. From a phylogenetic point of view, all metazoa have evolved from a common ancestor via major macroevolutionary events, which advanced the animal body plans, and GRNs which are associated with these events are conserved across species (Levine and Davidson, 2005). Given that these GRNs can be inevitably at the disposal of cancerous tumors, we wondered whether the same key innovations through which the species evolved may have been, in parallel, exploited by the primary tumor, in order to evolve toward metastatic stages. The term "key innovation," as used herein, refers to any novel phenotypic trait that facilitates adaptive radiation and evolutionary success of a taxonomic group (Hunter, 1998), as well as the respective genes and/or GRNs that support establishment of this trait. The epithelial-mesenchymal transition (EMT), that is the hierarchical GRN which controls neural crest, a vertebrate-specific multipotent embryonic cell population which generates several body anatomical structures (Martik and Bronner, 2017) is a representative example of co-option of key innovations toward enhancing metastatic potential. Indeed, the same EMT factors mediating differentiation and migration of neural crest are also ectopically reactivated during tumor progression (Kerosuo and Bronner-Fraser, 2012; Fürst et al., 2019).

All metazoa can develop tumors (Domazet-Lošo et al., 2014), but major differences in their prevalence and metastatic potential are observed across phyla. The "big-bang" of tumor formation is traced to Cnidaria and correlates with the emergence of multicellularity. All cancer-associated genes are conserved in Cnidaria, and *Hydra* tumor cells have an invasive capacity (Domazet-Lošo et al., 2014). However, the aforementioned phylogenetic origin of tumor formation does not coincide with the phenotypic manifestations of aggressiveness, since Cnidaria neither form true metastases nor die of cancer (Domazet-Lošo et al., 2014). Thus, it remains enigmatic how species with lethal cancers have non-metastatic common ancestors, as well as if there are any key innovations that may be linked with increased prevalence of metastasis across the metazoa clades. We hypothesized that if certain key innovations increase organismal fitness of a given species population, they will likely undergo positive selection, despite the risk of being co-opted by the tumors later on in the life of the individuals of the respective population. To explore whether organisms that inherited key innovations from a common ancestor consistently manifest metastatic potential, in contrast to the ones which lack them, we applied phylogeny, that is, the evolutionary history of species in relation to oncogeny (Dawe, 1969). Herein, we revisited and retrospectively juxtaposed cancer reports across taxa on the same evolutionary lineage with mammals, from cnidarians to humans, and then integrated cancer phenotypes of these species with high-throughput data from up to 42 human cancer types, data on developmental phenotypes of knockout mice, and phylogenetic comparative methods. This multidisciplinary meta-analysis allowed us to infer that phenotypic manifestation of metastasis coincides with agnatha-to-gnathostome transition. Genes essential for jaw development, which is a key innovation of gnathostomes, are deregulated in tumor cells and are causatively associated with tumor progression.

MATERIALS AND METHODS

Identification of Jaw-Indispensable Genes

To identify those genes that are indispensable for the development of cartilaginous jaws (JIGs), we screened the Mouse

Genome Informatics (MGI) database (Bult et al., 2019) for genes the knockout of which leads to mouse phenotypes with jaw-related defects, as recently described (Logotheti et al., 2020), using the terms "cartilage," "jaws," "mandible/mandibular," "maxilla," and "micrognathia." Their human orthologs were identified and the official HUGO gene nomenclature committee (HGNC) (Gray et al., 2015) gene symbols were used (**Supplementary Table 2**).

Orthologs Search

The HGNC symbols of the 305 jaw-indispensable genes (JIG; **Supplementary Table 2**) were used initially to retrieve the corresponding, well-annotated, gnathostome (*Homo sapiens*, *Mus musculus*, *Gallus gallus*, *Xenopus laevis*, *Danio rerio*, and *Callorhinchus milli*) protein sequences from the publicly available non-redundant sequence database NCBI RefSeq (O'Leary et al., 2016). The canonical or longest known transcripts per protein were selected. For obtaining orthologous sequences from the agnatha genera under study (Petromyzon, Branchiostoma, Ciona, Strongylocentrotus, and Hydra), the retrieved gnathostome sequences were used as probes to iteratively search the agnathan genomes available in NCBI RefSeq and GenBank (Sayers et al., 2019), by applying reciprocal BLASTp and BLASTn (Altschul et al., 1990) with default parameters; an in-house Python script was employed (available on request). The protein domain organization of the novel sequences was explored through SMART v.8.0 (Letunic and Bork, 2018).

To identify the "true orthologs" of each JIG/protein, phylogenetic trees (a total of 305) of the homologous, gnathostome and agnathan, protein sequences were constructed. To this end, the amino acid sequences of the homologous proteins were aligned using Clustal Omega, version 1.2.4 (Sievers and Higgins, 2014a,b) and the resulting multiple sequence alignment was provided as input to the software package MEGA version 10. 1 (Kumar et al., 2018) in order to perform phylogenetic analyses, by employing a neighbor-joining (NJ) and a maximum likelihood (ML) method. The expected number of amino acid substitutions per position was estimated with the JTT model (Jones et al., 1992). The robustness of the inferred phylogenetic trees was evaluated by bootstrapping (100 pseudo-replicates). Only those agnathan sequences that clustered with the known gnathostome sequences under study were considered as "true orthologs." A characteristic example is shown in **Supplementary Figure 1**.

Functional Interaction Networks and Gene Set Enrichment Analysis

The associations among the jaw-indispensable human genes/protein products were investigated in the STRING v11.0 database (Szklarczyk et al., 2019), by selecting a high confidence interaction score ($\geq$0.9). Moreover, Cytoscape v3.8.0 (Shannon et al., 2003), was employed for network processing, visualization and statistical analysis. For the Gene Set Enrichment Analysis, the GSEA-P 2.0 software (Broad Institute, Cambridge, MA, United States) (Subramanian et al., 2005) was used. Enriched hallmark and Gene Ontology terms were plotted against the negative log10 of their individual FDR value ($<$0.05).

Meta-Analyses of Mutation and Methylation Data From Human Tumors

We juxtaposed the datasets of PanCancer and GENCODEv32 using Ensembl gene IDs and filtered for protein coding genes with a transcript support level TSL $<$ 3, to generate a comprehensive dataset of 19,617 transcripts. Recently identified cancer driver genes and frequently mutated genes were also used (Bamford et al., 2004; Kandoth et al., 2013; Bailey et al., 2018). As control gene lists, we generated 100 lists of 305 random genes by sampling the 19,313 transcripts (without JIGs) without replacement (available on request). The Cancer Gene Census (CGC) list of 723 genes (including two non-coding) was downloaded from the COSMIC (Catalogue of Somatic Mutations in Cancer) website (Bamford et al., 2004) and juxtaposed with JIGs or random lists. For evaluating stochastic events, we calculated the percentage of events by chance ($x\% = 100 \times k/19{,}313$ coding genes without JIGs, $k = 721$ CGC, 299 cancer drivers, 127 frequently mutated) and performed Chi-squared test (stochastic events) or z-test (random gene lists). The number of patients affected by gene mutations and the number of mutations per gene were retrieved from the GDC data portal (Jensen et al., 2017) after uploading the respective gene list. DiseaseMeth database (Xiong et al., 2017) was used to detect the differentially methylated JIGs in several cancer types. All results were downloaded and data for the different cancer types were pooled.

Transcriptome Analysis in CCLE, TCGA, and GEO Databases

Cancer Cell Line Encyclopedia (CCLE) and The Cancer Genome Atlas (TCGA) transcriptomic data were analyzed as recently described (Logotheti et al., 2020). For identifying differentially regulated transcripts in metastatic versus primary lesions or normal tissue, transcriptome data from the Gene Expression Omnibus (GEO) database (Clough and Barrett, 2016) (study numbers: GSE21510, GSE2509, GSE25976, GSE43837, GSE468, GSE6919, GSE7929, GSE7930, GSE8401) were analyzed by GEO2R. Cox regression analysis was performed by R software using the *coxph* function in the *survival* package.

Statistical Analysis

Unless otherwise stated, statistics were performed by Student's t-test; p values less than 0.05 were considered as significant ($^{*}p < 0.05$, $^{**}p < 0.01$, $^{***}p < 0.001$). All statistical tests were two-sided.

RESULTS

Key Innovations in Relation With Tumor Characteristics Across Phylogenetic Taxa: Available Resources and Considerations

As a framework for comparing tumors among metazoa, we used the one proposed by Dawe, one of the pioneers to address oncogeny in relation to phylogeny. The framework is

the phylogenetic tree *per se* and the comparisons are made by ascending the bifurcating tree, in a direction from the last common ancestor to the more recent taxon, by recording changes which occurred proximal to the divergent branches at each node (Dawe, 1969). In line with this, we selected that taxon in each bifurcation of the phylogenetic tree in which an indispensable hallmark macroevolutionary trait occurred first, and was conserved throughout the descendant lineage, up to mammals and humans (Hickman et al., 2001). Porifera was the baseline taxonomic group of our study panel, since sponges do not develop apparent tumors (Domazet-Lošo et al., 2014). In the case of Protochordates, due to their nodal position between invertebrates and vertebrates (Delsuc et al., 2006), both children taxa (Cephalochordates and Urochordates) were included in the analysis.

We extensively searched publicly available databases, for peer-reviewed cancer reports on representatives of these taxa. A degree of inherent heterogeneity due to diverse experimental methods across these reports should be assumed. Notwithstanding, these records are, to date, the best available source of information on tumor characteristics of these taxa. They remain fundamental, especially given that in some species, experimental carcinogenesis protocols cannot be applied, due to animal ethics restrictions and/or because they do not represent conventional laboratory animal models. To eliminate potential bias by comparing pathology reports on isolated cases, we particularly emphasized on studies which (a) followed-up large populations of animals over ample periods of time, and (b) provided a clear number of subjects, histological characterizations, and wherever possible, experimental validations. Another comprehensive source of information is the "Registry of Tumors in Lower Animals" (RTLA), i.e., an official repository of validated tumor reports from a large number of invertebrates and cold blooded vertebrates (Harshbarger, 1969), and the "Overall five year progress report for the registry of tumors in lower animals from September 30, 2002 through September 30, 2007" (personal communication, Dr. P.J. Daschner). We also considered parameters that are particularly important for metastasis, mainly (a) the circulatory system, which offers cancer cells a means for energy supply and migration to secondary sites (Hanahan and Weinberg, 2011) and (b) the immune system, which reflects the innate ability of an organism to detect and eliminate malignant cells and represents a major evolutionary pressure in the tumor microenvironment (Angelova et al., 2018). All chordates have a closed circulatory system (Hickman et al., 2001). Adaptive immunity first occurred in cyclostomes (Cooper and Alder, 2006), whereas all their ancestors possess only innate immunity (Langlet and Bierne, 1982; Cooper and Alder, 2006; Maciel and Oviedo, 2018). Overall, tumors across the selected taxa, in association with aggressiveness, immunity and the circulatory system can be overviewed in **Figure 1** and **Supplementary Table 1**.

Tumor Landscape in Pre-vertebrates

According to available reports (**Supplementary Table 1**), Cnidaria are the most ancient organisms known to develop naturally occurring tumors. Although tumors in Hydra polyps reduce capacity for egg production and rate of population growth, they are non-lethal for the affected individuals (Domazet-Lošo et al., 2014). Platyhelminthes develop spontaneous, non-lethal tumors (Harshbarger, 1969; Tascedda and Ottaviani, 2014), while their exposure to carcinogen type 1A cadmium leads to benign tumors and impairment of their regenerative ability, especially in combination with inactivation of tumor-suppressor genes (Van Roten et al., 2018). No tumors have been reported in Nemertea. Nematodes develop germline cell-derived tumors (Kirienko et al., 2010). Cancer in Molluscs is manifested as a leukemia-like, disseminated neoplasia (DN), and as germinal cell-derived gonadal neoplasia (Barber, 2004; Carballal et al., 2015). Importantly, DN in *Mya arenaria* populating the coast of North America, is a horizontally transmissible form of cancer, whereby the cancer clone, which likely arose in a single individual, is spread to host clams, and bears a genotype distinct from the host genotypes (Metzger et al., 2015). Nevertheless, such deadly tumors are restricted to bivalvia, and, to date, have not been described in other pre-vertebrate taxa on the same evolutionary lineage. Indeed, Echinoderms are resistant to chemical-induced oncogenesis (Wellings, 1969), and either lack spontaneous tumor lesions (Wellings, 1969) or develop non-invasive/non-lethal, pigmented lesions (Fontaine, 1969). Similarly, the protochordates either appear to be cancer-free (Urochordates) (Dawe, 1969; Wellings, 1969) or form benign tumors (Cephalochordates) (Wellings, 1969). Overall, with the exception of Molluscs, tumors in pre-vertebrates are not associated with lethal outcomes (**Figure 1**).

Emergence of Metastasis Coincides With Agnatha-Gnathostomes Split Within the Vertebrate Clade

Cyclostomes, the only living jawless vertebrates (agnatha) (Gess et al., 2006), comprise a monophyletic group (Heimberg et al., 2010), including Petromyzontia (lampreys) and Myxinoidei (hagfishes). Until 70's, only one case of cyclostome cancer had been reported in RTLA. Following this singleton report, Falkmer and colleagues addressed cyclostome tumor pathology in an extensive, thorough and well-controlled manner (Falkmer et al., 1976, 1978; Falkmer, 1998) and, up to this day, this seminal work remains the most comprehensive source of information for carcinogenesis on this enigmatic, though basal, vertebrate superclass. In particular, Falkmer screened, for tumor incidence, two large populations of lampreys caught in Ume/Ricklean rivers, and hagfishes caught inside and outside the Gullmar fjord. In a population of 6,000 lampreys, only one individual (0.017%) presented highly differentiated primary hepatocellular carcinoma. In contrast, tumors were detected in the hagfish population inside the fjord, and this percentage was significantly enhanced versus the tumor-bearing individuals in the open-sea control group (**Figure 2**). Of the 27,300 hagfishes captured within a 5-year period (1972–1976), up to 5.8% exhibited liver neoplasms (adenomas and carcinomas). This percentage was significantly higher compared to the tumor-bearing individuals (2.8%) in the control, open-sea population of 1,183 hagfishes caught outside the fjord. Although the affected hagfishes developed high- or low-differentiation tumors, they showed

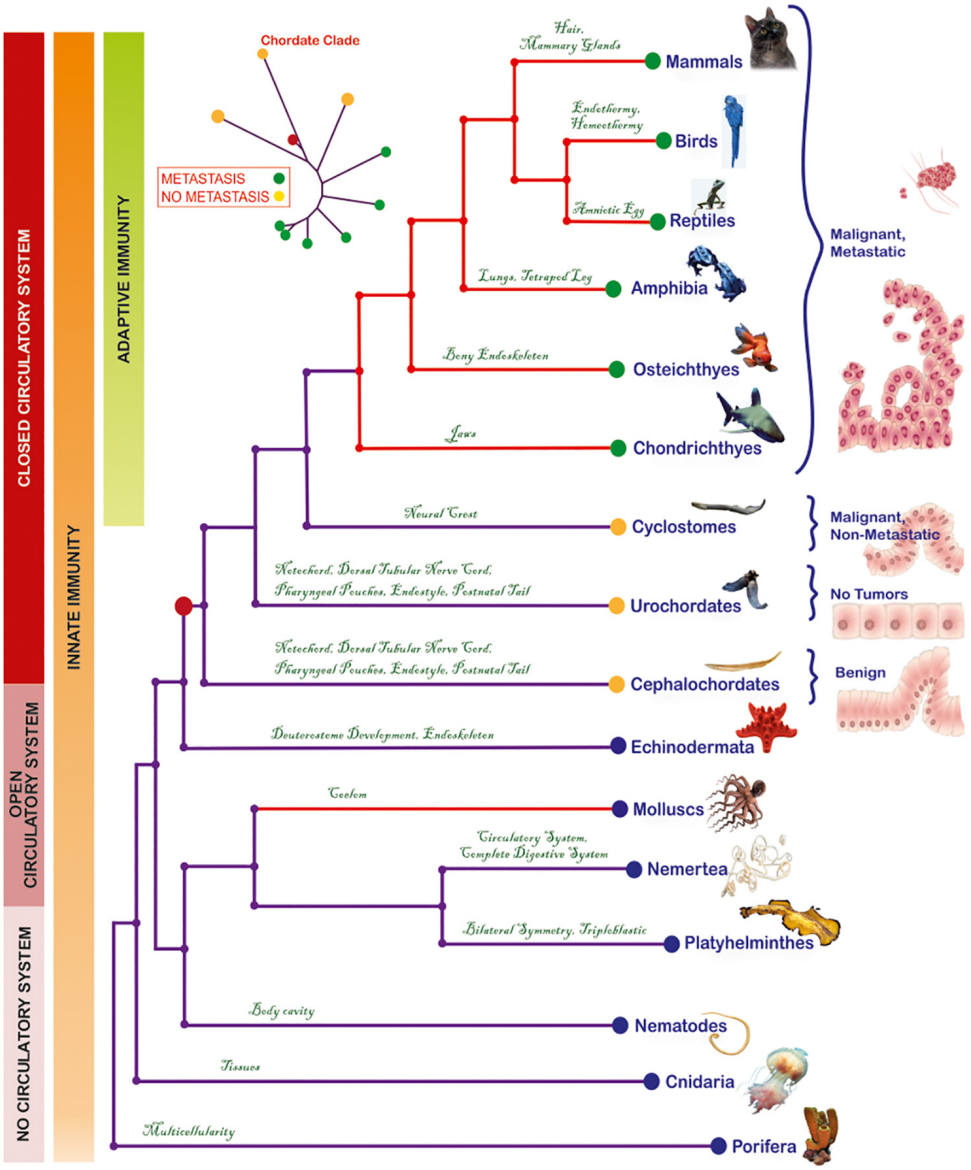

FIGURE 1 | Phylogenetic tree depicting the evolutionary relationships of metazoa and the emergence of metastasis in the cyclostome-to-chondrichthyes transition. Each phylogenetic group has manifested, for the first time, a key innovation that was conserved throughout the lineage. Red-colored clades indicate groups with lethal cancer types. Based on information derived from histological analyses, tumors were classified into benign (corresponding to initiation), malignant/non-metastatic (corresponding to promotion) or malignant, metastatic (corresponding to progression). Invasive and metastatic tumors have been reported from Chondrichthyes to mammals. The mollusks present contagious invasive cancer, while the urochordates are cancer-resistant. The red dot on the tree represents the common chordate ancestor, which gave rise to both, metastatic (green dots) and non-metastatic species (yellow dots). Model of the progression from a normal cell to metastatic cancer was modified from a previous illustration (Iacobuzio-Donahue et al., 2012). The origins of a closed circulatory system and of acquired immunity are also presented.

no macroscopic signs of metastasis (Falkmer et al., 1976, 1978; Falkmer, 1998). This increased cancer incidence was attributed to a combination of polychlorinated biphenyls (PCBs) and dichlorodiphenyltrichloromethylmethane (DDT), two anthropogenic organochloride contaminants which entered the fjord via washout. Due to parasitism of hagfishes on PCB/DDT-contaminated fishes, the organochlorides bioaccumulated in their liver or pancreatic islets, eventually triggering oncogenesis at these sites (Falkmer et al., 1978). The fact that despite their exposure to confirmed carcinogens (Lauby-Secretan et al., 2013; Loomis et al., 2015; Abu-Helil and van der Weyden, 2019), a percentage developed malignant tumors, but none of the 28,483 study individuals developed metastasis, leads to the suggestion that these animals may be metastasis-refractory or metastasis-incapable. Nevertheless, metastatic capability is evident in all descendant lineages. In particular, in Chondrichthyes, at least

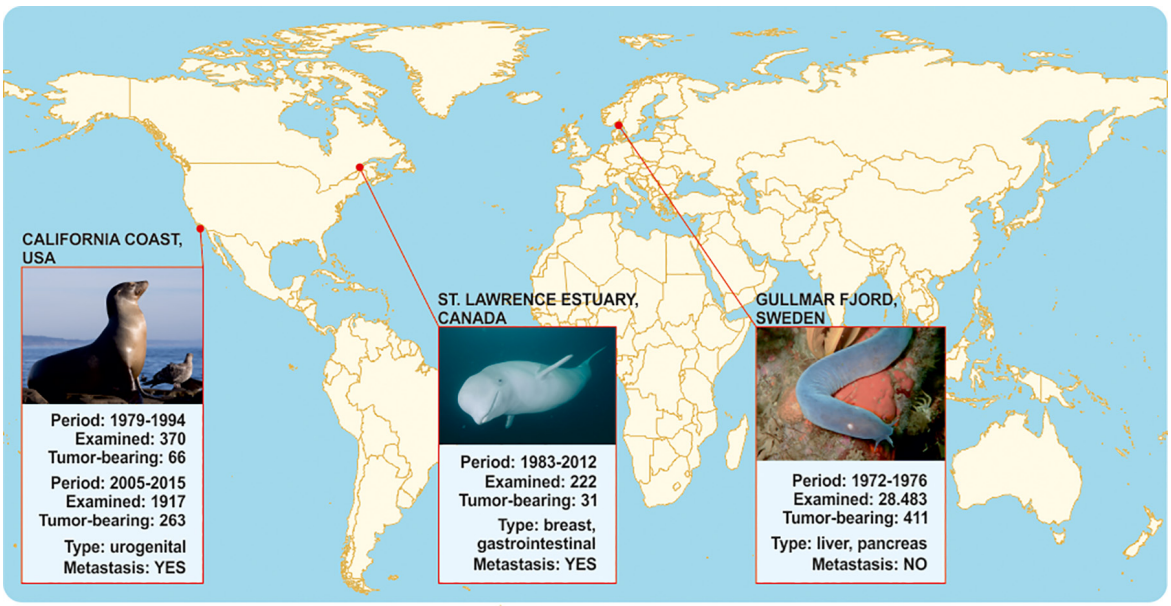

FIGURE 2 | Comparative epidemiology data on metastases in agnathan versus gnathostome representatives that inhabit comparable carcinogen-contaminated aquatic environments. No metastases have been reported in hagfishes inside and outside Gullmar fjord. On the contrary, toothed belugas in Quebec as well as California sea lions that inhabit environments polluted with similar organochlorides are susceptible to metastatic tumors.

50 cases of spontaneous cancer, including invasive (Wellings, 1969) and metastatic (Schlumberger and Lucke, 1948; Ostrander et al., 2004) tumors, have been recorded; in Osteichthyes, the tumor incidence increases and metastatic cases become more frequent (Schlumberger and Lucke, 1948; Wellings, 1969; Couch and Harshbarger, 1985; Groff, 2004); in amphibia (Stacy and Parker, 2004), reptiles (Abu-Helil and van der Weyden, 2019), birds (Abu-Helil and van der Weyden, 2019), and mammals (Albuquerque et al., 2018), there is an increased prevalence of invasive and metastatic cancers (Albuquerque et al., 2018). Collectively, a retrospective overview of tumor reports suggests the consistent occurrence of metastases in chondrichthyes and their descendants, providing hints that the establishment of metastatic potential coincides with the agnatha-to-gnathostome transition within the vertebrate clade (**Figure 1**).

The complicated life-cycle of cyclostomes, as well as ethical considerations regarding their research (Shimeld and Donoghue, 2012), challenge the application of experimental carcinogenesis protocols on adult individuals to simulate Falkmer's field study on a laboratory scale (Shimeld and Donoghue, 2012). Hence, as a surrogate test for corroborating associations between agnatha-to-gnathostome transition and metastatic potential, we sought to juxtapose Falkmer's nodal tumor pathology reports on adult cyclostomes to those of gnathostome representatives living in comparable PCB/DDT-contaminated environments (**Figure 2**). In particular, Beluga whales and California sea lions inhabit aquatic environments with persistent organic pollutants similar to those reported for the Gullmar fjord, and show unusually high cancer prevalence among marine mammals (Deming et al., 2018), which has been associated with exposure to carcinogens (Ylitalo et al., 2005; Randhawa et al., 2015; Lair et al., 2016). As shown in **Figure 2**, in an isolated population of about 900 toothed belugas (*Delphinapterus leucas*) living in the heavily industrialized St Lawrence Estuary of Quebec, Canada, cancer was reported as one of the most frequent causes of death (14%, 31/222 animals) in 222 carcasses found stranded or drifting, from 1983 to 2012. Tumors were often metastatic and fatal, and associated with the gastrointestinal tract (adenocarcinoma of the gastrointestinal mucosa, salivary gland and cholangiocellular carcinoma) and mammary glands. Exposure to carcinogens has been associated to increased cancer incidence (Lair et al., 2016), since living and dead beluga tissues were heavily contaminated by agricultural and industrial contaminants, including PCB/DDTs and their metabolites (Martineau et al., 2002). Similarly, between 1979 and 2015, necropsies of 2,287 sea lions beached-off central California coast in United States revealed high cancer incidence, where the predominant neoplasms were poorly differentiated urogenital carcinomas, with frequent local invasions and widespread metastases (Lipscomb et al., 2000; Deming et al., 2018). Metastasis was diagnosed in 18% (66/370) of necropsied animals from 1979 to 1994. From 2005 to 2015, 14% (263/1917) of cases had cancers, the vast majority of which were metastatic (Lipscomb et al., 2000; Deming et al., 2018), localized in the urogenital tissues and associated with organochloride bioaccumulation (Ylitalo et al., 2005; Randhawa et al., 2015). Hence, in similar carcinogenic environments, gnathostome species appear susceptible to aggressive cancers in contrast to the metastasis-refractory Gullmar fjord hagfishes. Similarly, organochloride pollutants have been correlated with risk of metastasis in human breast cancer patients (Koual et al., 2019). The aforementioned observations suggest that gnathostomes might be more prone to metastasis than agnatha

upon exposure to carcinogenic pollutants. If this is indeed the case, then macroevolutionary gains of gnathostomes, such as the cartilaginous jaws, emerge as a key innovation possibly associated with metastasis.

JIGs Undergo Frequent Mutations and DNA Methylation Alterations in Human Cancers

Agnatha-to-gnathostomes transition was promoted by the evolution of a cartilaginous skull, along with the establishment of jaws. These novelties facilitated the emergence of a complex brain and senses, that, together with the pharyngeal cartilage, allowed gnathostomes to shift to active predation, intermittent feeding and behavioral diversification (Kaucka and Adameyko, 2019). They highlight vertebrates' evolutionary success and, thus, are conserved from chondrichthyes to human (Kaucka and Adameyko, 2019). Based on the observation that the phenotypic manifestations of metastasis coincide with the evolutionary time point of occurrence of gnathostome key innovations, we used computational methods to unravel links between jaw formation and metastatic potential. We postulated that if our hypothesis is valid, then genes supporting formation of cartilaginous jaws would tend to be deregulated during cancer progression. To identify genes essential for the development of cartilaginous jaws, we screened the Mouse Genome Informatics (MGI) database for knockout-mice phenotypes that encompass jaw-related defects. In this way, 305 JIG were identified, all of which exhibit highly conserved human orthologs (**Supplementary Table 2**). The term "JIG," as used herein, refers to any gene which, if impaired, leads to abnormal jaw embryonic development. Notably, as indicated by the calculated ratios of jaws phenotypes to all affected phenotypes (**Supplementary Table 2**), JIGs are not functionally restricted only to jaw development, however mutation in even one of them leads to jaw malformations. GSEA revealed JIGS' involvement in skeletal system and cartilage development, appendage morphogenesis, and pattern specification (**Figure 3A**); molecular functions such as DNA binding, transactivation activity and signaling receptor binding (**Figure 3B**); and hallmark processes like Wnt-beta, TGF-beta and NOTCH signaling, and EMT (**Figure 3C**). STRING analysis indicated that 173 of these factors form a highly interconnected network (**Figure 3D**). Altogether, these data suggest that JIGs interact either physically or functionally within the context of jaw formation, to create a network, to which we, hereafter, refer to as jaw-developmental network (JDN).

Next, we examined whether JIGs undergo frequent genetic and/or epigenetic alterations in tumors. First, we juxtaposed three distinct lists of identified cancer gene drivers and mutations (Bamford et al., 2004; Kandoth et al., 2013; Bailey et al., 2018) with the list of JIGs to determine the number of JIGs that are mutated across human cancer types. To ensure that the association is non-random, we compared to 100 control lists each encompassing an equal number of 305 random, unrelated genes (available on request). A significant enrichment of CGC factors was observed among the JIGs 16.7%, or 51 genes) relative to random gene lists of the same size (3.5 $\pm$ 1.2%) and relative to the expected value (3.7%, or 721 of 19,313 coding genes from GENCODEv32, $p < 0.001$) (**Figure 4A**, left). The same tendency was observed when JIGs were juxtaposed to 299 driver genes and mutations identified from a comprehensive PanCancer and PanSoftware analysis spanning 9,423 tumor exomes by employing 26 computational tools (Bailey et al., 2018). JIGs represent 8.9% (27 genes) of the identified cancer drivers versus 1.0 $\pm$ 0.6% of random genes ($p < 0.001$) (**Figure 4A**, middle). Similar results were obtained when the same analysis was performed versus a group of 127 significantly mutated genes which have been identified as oncogenesis drivers across 12 major cancer types, whereby most tumors bear two to six of these mutations (Kandoth et al., 2013). A significant enrichment of JIGs for 18 of these genes (5.9% compared to expected 0.6%, which is 127 in 19,313 coding genes) was observed, as opposed to the random genes (0.5 $\pm$ 0.4%, $p < 0.001$) (**Figure 4A**, right). Overall, compared to the control lists, JIGs are highly enriched in cancer driver genes and mutations (**Figure 4A** and **Supplementary Table 3**). Then, using gene mutation data from PanCan cohort, we calculated the mutation frequency for all JIGs across human cancer types, and found a significant increase compared to control lists (**Figure 4B**). To further assess whether JIGs tend to be epigenetically altered in cancer, we meta-analyzed data of the DiseaseMeth 2.0 database (**Figure 4C**), and found frequent alterations of DNA methylation in JIGs, while hypomethylation was the most prevalent type of aberration in tumors versus normal tissue controls (131 JIGs hypomethylated, 47 hypermethylated, 47 hypo-/hyper-methylated, $\chi^2 = 62.72$, $p < 0.001$). Collectively, JIGs appear to undergo mutations and/or perturbations of DNA methylation patterns in cancer.

JIGs Are Transcriptionally Deregulated in Aggressive Stages and Predict Cancer Patient Outcomes

To further explore potential links between jaw development and cancer progression, we checked invasive cancer cell lines and patient tumors for changes in JIG transcriptional activity. In this regard, based on a recently described approach (Logotheti et al., 2020), we classified all cell lines of the Cancer Cell Line Encyclopedia (CCLE; Barretina et al., 2012), which includes gene expression data of 962 cell lines, into highly-invasive and less-invasive types, according to the levels of E-cadherin, N-cadherin, Vimentin, ZEB1, and SNAI1, which constitute reliable markers for EMT and tumor progression (Khan et al., 2017). Then, we examined whether JIGs are differentially expressed in highly- versus less-invasive cells across 24 common cancer types. We found that, compared to the control lists, a significantly higher number of JIGs is differentially expressed in high- versus low-aggressive cells (1.8-fold higher, $z = 8.89$, $p < 0.001$), where more JIGs are upregulated (JIGs vs. control: 100 vs. 39.1 $\pm$ 6.6 genes) than downregulated (39 vs. 40.4 $\pm$ 6.5 genes, $p < 0.003$, **Figure 5A** and **Supplementary Table 3**). These results indicate a non-stochastic tendency for enhanced transcription of JIGs in highly invasive states.

Additionally, to evaluate the clinical relevance of these findings, we meta-analyzed gene expression data in 35 different

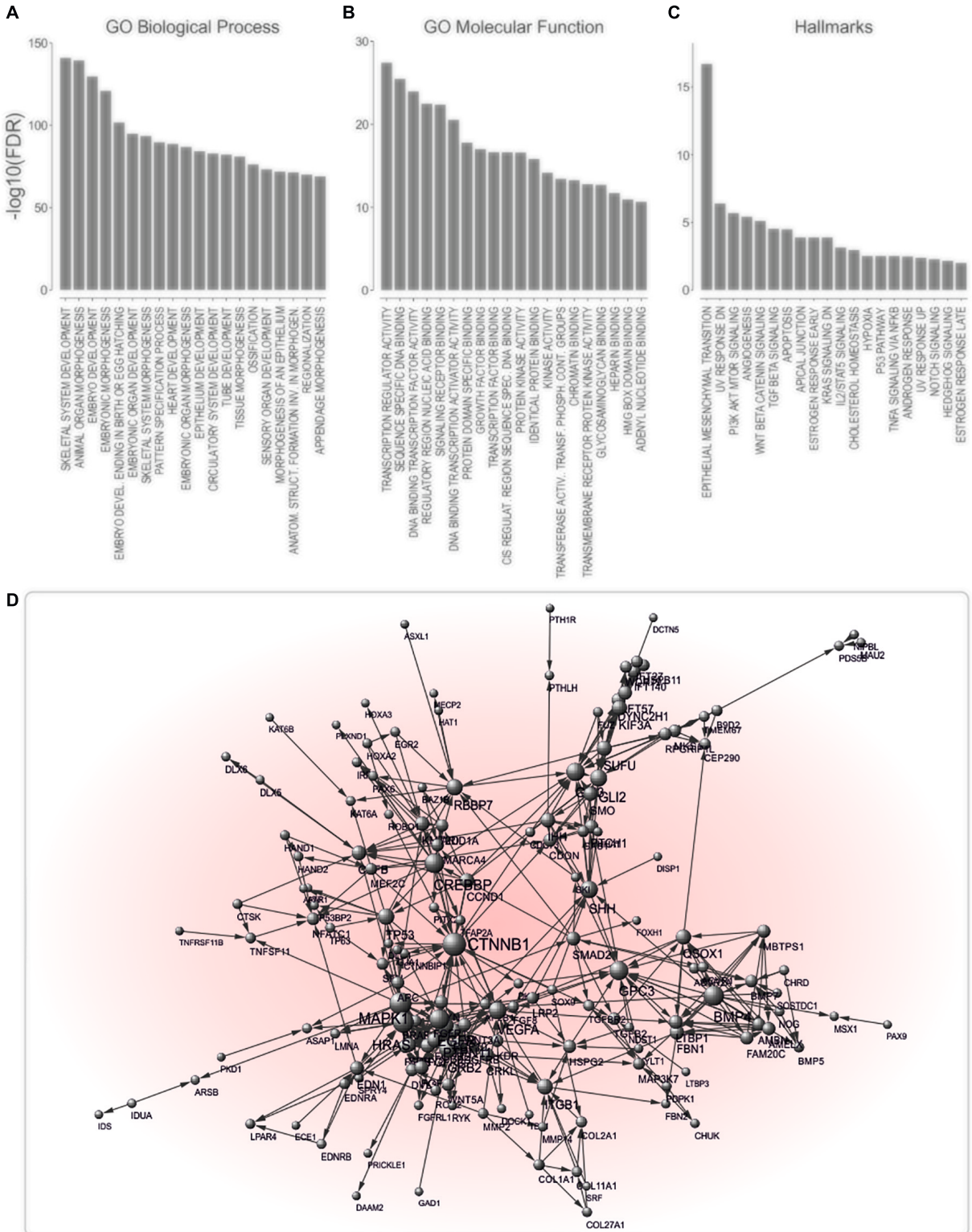

FIGURE 3 | JIGs exhibit a high degree of interconnectedness. **(A–C)** Analysis of enriched GO biological processes: **(A)** GO molecular functions, **(B)** and hallmark processes, **(C)** indicates a role of JIGs in the development and EMT, mainly via affecting transcriptional regulation. **(D)** Interaction network of JIGs (interaction confidence score ≥ 0.9) shows that 173 of 305 genes/proteins are highly interconnected. The nodes represent genes/proteins and the connecting edges functional associations. Node sizes reflect node degree.

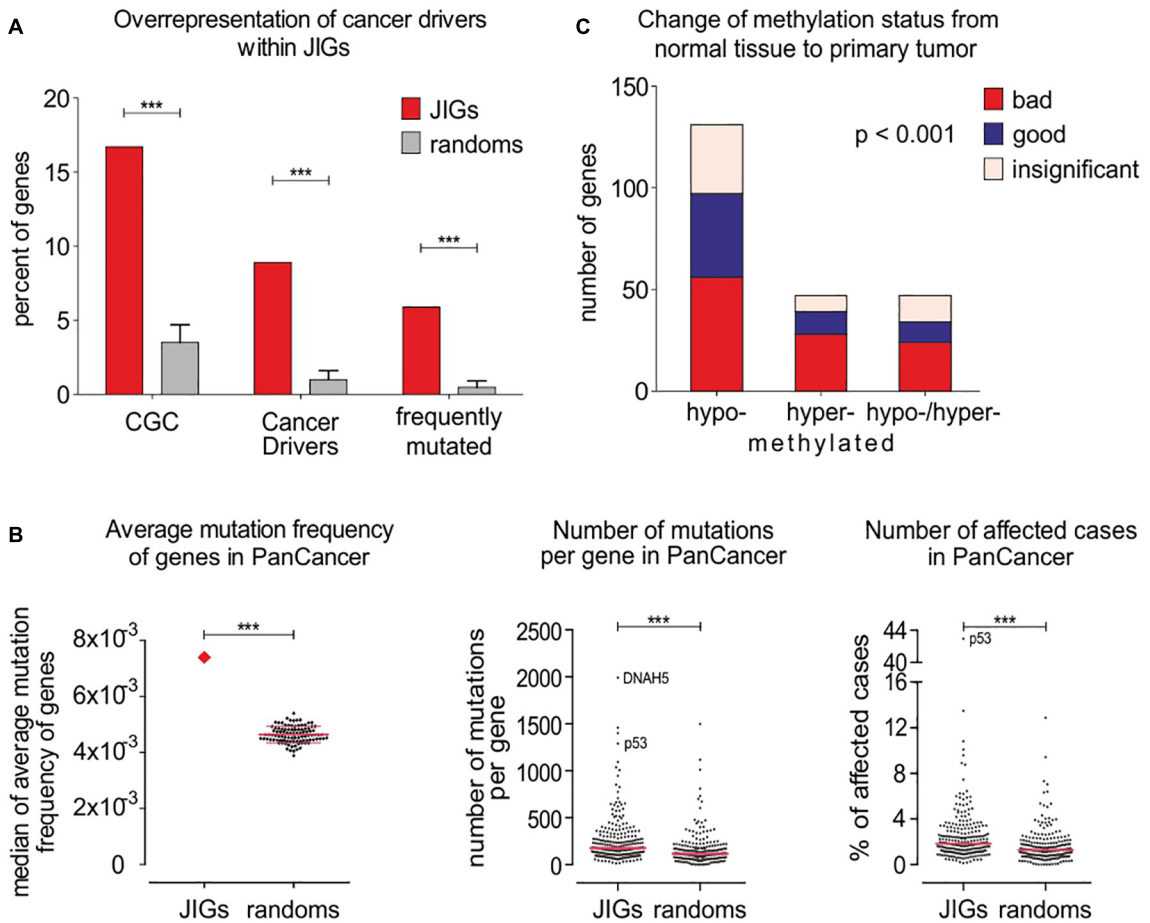

FIGURE 4 | JIGs undergo frequent gene mutations and epigenetic alterations across cancer types. **(A)** JIG enrichments in known and frequently mutated cancer drivers as indicated versus controls were 16.7% vs. 3.5 ± 1.2% ($p < 0.001$), **(left)**; 8.9% vs. 1.0 ± 0.6% ($p < 0.001$), **(middle)**; and 5.9% vs. 0.5 ± 0.4% ($p < 0.001$), **(right)**.**(B)** The average mutation frequency of JIGs is higher in PanCan cohort versus genes of the random lists **(left)**. This entails a higher number of mutations per individual JIG **(center)** and a higher number of patients exhibiting mutations in JIGs **(right)**. Pink lines: medians. **(C)** Almost 74% (225/305) of JIGs undergo aberrant DNA methylation in 42 cancer types versus normal control tissues, whereby 131 are significantly hypomethylated, 47 are hypermethylated, and 47 are either hypomethylated or hypermethylated in a cancer type-dependent manner. Cox regression analysis on PanCan TCGA cohort data showed that more hypo- than hyper- methylated JIGs are correlated with either poor ("bad," red color) or favorable ("good," blue color) patient outcomes. Bars represent SEM.

cancer types from PanCan TCGA cohort (Liu et al., 2018). Interestingly, correlation analyses implied that a large fraction of JIGs are co-expressed in patient tumors, with a tendency to preserve their crosstalks. In particular, relative to the control lists JIGs demonstrated increased value of (i) median expression correlation (MEC) per gene (JIG vs. control: 0.039 ± 0.045 vs. 0.008 ± 0.003, $z = 6.99$, $p < 0.001$, **Figure 5B**, red-boxed diagram), and (ii) more and greater positive correlation areas per gene (13.72 ± 13.05 vs. 3.04 ± 5.39, $z = 33.6$, $p < 0.001$, **Figure 5B**, green-boxed diagram). Using Cox regression, we deciphered all genes associated with patient survival, and subsequently determined the percentage of significant prognostic factors among JIGs. Overall, 227 JIGs correlated with patient outcomes, and showed a higher ratio of poor versus favorable prognostic factors (1.64:1, $\chi^2 = 13.33$, $p < 0.001$) compared to the corresponding ratio of the control lists (1.25:1, $\chi^2 = 2.79$, $p = 0.095$, correspondingly). We also found that 118 JIGs are both, deregulated in highly aggressive states in CCLE and correlated with patient outcomes in PanCan, with a ratio of 1.68:1 for poor versus favorable prognostic factors ($\chi^2 = 7.63$, $p < 0.006$) as opposed to the corresponding 0.93:1 ratio of the control lists ($\chi^2 = 0.1$, $p = 0.755$, **Figure 5C** and **Supplementary Table 3**). Collectively, JIGs appear to become deterministically deregulated in highly invasive cells, with frequent transactivation events, and predict poor patient outcomes. Similar alterations in JIGs also occur in metastatic lesions. In particular, we additionally compared these data with transcriptomes of primary versus metastatic lesions from breast, colon, hepatocellular, medulloblastoma, melanoma, and prostate cancers, that were retrieved from the GEO database (Clough and Barrett, 2016). We found that more JIGs that were poor prognostic factors in PanCan cohort are deregulated in metastases, as opposed to the corresponding favorable factors (1.85:1, $\chi^2 = 15.21$, $p < 0.001$, **Figure 5D** and **Supplementary Table 3**).

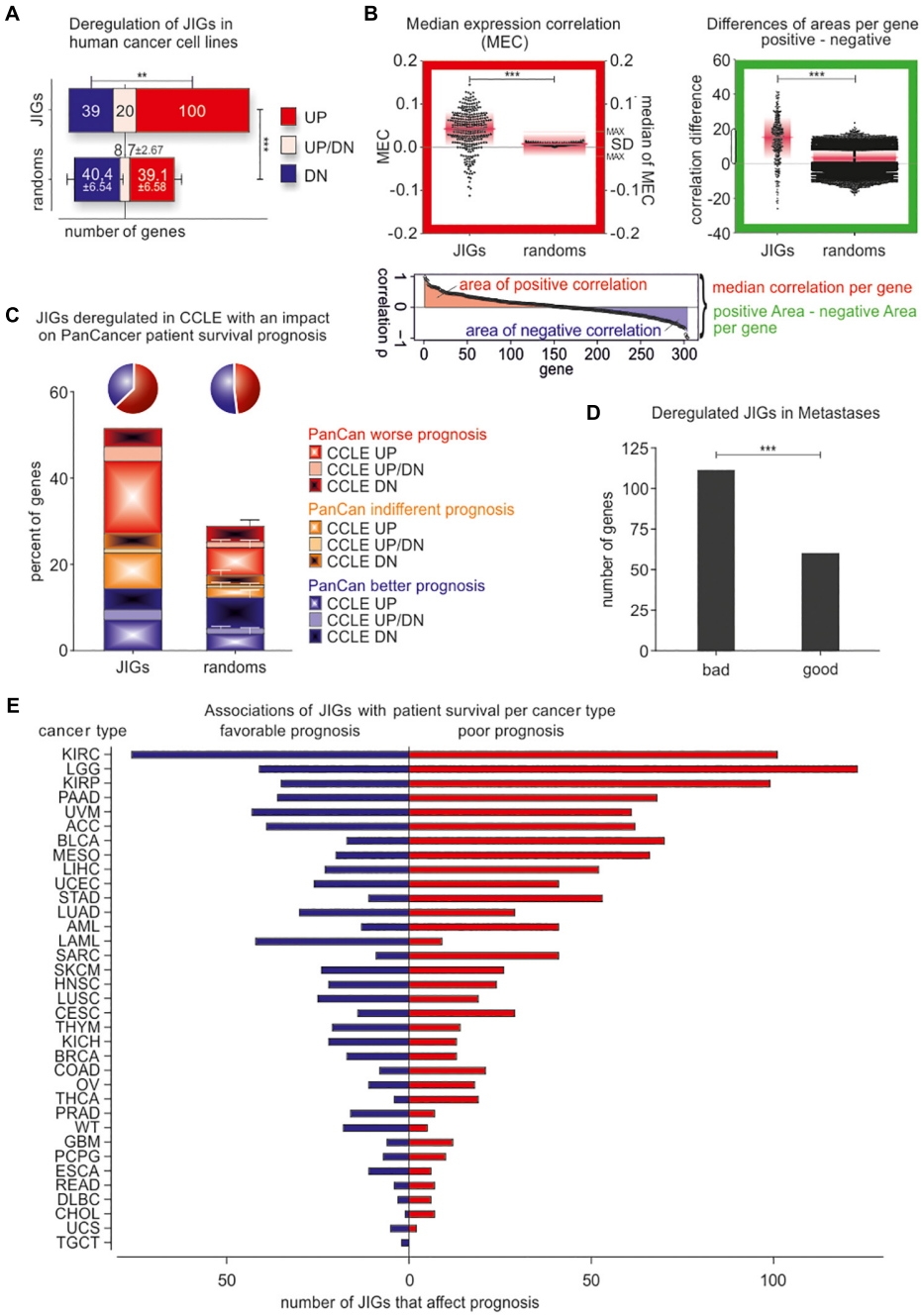

FIGURE 5 | JIGs are transcriptionally deregulated in invasive/metastatic stages and predict clinical outcomes in a cancer type-dependent manner. **(A)** JIG transcripts are deregulated in the highly invasive versus the less-invasive CCLE cell lines, and the total percentage is 1.8-fold higher than the corresponding percentage of control lists. Red: upregulated, blue: downregulated, pink: cancer type-dependent deregulation. Error bars represent mean with SD. **(B)** *Red-boxed diagram:* median expression correlation (MEC) in PanCan and SD of MEC (pink boxes) are higher among JIGs compared to random lists (shown are the 100 medians of MEC with maximal SD). *Green-boxed diagram:* the differences of positive versus negative area of correlation per gene show (a) a significantly larger span and (b) over all a higher positive value compared to 100 random gene lists. Pink lines represent the median, pink boxes represent SD. **(C)** Cox regression analysis of JIGs on the survival of the TCGA PanCan cohort. 227 JIGs correlated with patient outcomes, of which 141 predicted worse and 86 better outcomes. Among 159 deregulated JIGs in highly-aggressive states across several cancer types of CCLE, 118 JIGs (74.2%) influence patient prognosis. Of those, 74 (62.7%) (pie chart, blue) had an adverse effect, 51 were exclusively upregulated in aggressive states of CCLE (CCLE UP, plain red), while additional 10 JIGs were upregulated in some as well as downregulated in other cancer types (CCLE UP/DN, plain pink). Only 44 JIGs differentially expressed in CCLE (dashed blue, plain blue, and dashed pink) had a beneficial effect on survival prognosis (pie chart, green). **(D)** Transcriptional deregulation of JIGs in metastases versus primary tumor or normal tissue, and correlation with JIGs that affect patient prognosis in PanCan. JIG deregulations in 6 metastatic cancer types are more correlated with poor outcomes (1.85:1). **(E)** Survival analysis for JIGs across different TCGA cancers. The prognostic potential of JIGs depends on the cancer type. In the majority of cancer types, more JIGs are associated with poor prognosis and less with favorable prognosis. No cancer tissue was found unaffected by JIGs.

TABLE 1 | Effects of JIGs on cancer patient prognosis (in descending order of total number of JIGs that affect each cancer type).

Abbreviation	Cancer type	Number of JIGs associated with poor prognosis	Number of JIGs associated with favorable prognosis
KIRC	Kidney renal clear cell carcinoma	115	87
LGG	Brain Lower Grade Glioma	130	49
KIRP	Kidney renal papillary cell carcinoma	112	46
PAAD	Pancreatic adenocarcinoma	89	47
UVM	Uveal Melanoma	75	52
ACC	Adrenocortical carcinoma	77	49
MESO	Mesothelioma	88	25
BLCA	Bladder Urothelial Carcinoma	89	21
LIHC	Liver hepatocellular carcinoma	75	29
STAD	Stomach adenocarcinoma	72	21
UCEC	Uterine Corpus Endometrial Carcinoma	54	33
LUAD	Lung adenocarcinoma	46	40
AML	Acute Myeloid Leukemia	60	23
SKCM	Skin Cutaneous Melanoma	42	39
LAML	Acute Myeloid Leukemia	18	58
LUSC	Lung squamous cell carcinoma	40	34
SARC	Sarcoma	55	17
KICH	Kidney Chromophobe	34	35
HNSC	Head and Neck squamous cell carcinoma	34	33
CESC	Cervical squamous cell carcinoma and endocervical adenocarcinoma	39	25
BRCA	Breast invasive carcinoma	26	32
THYM	Thymoma	19	33
OV	Ovarian serous cystadenocarcinoma	31	19
THCA	Thyroid carcinoma	41	9
COAD	Colon adenocarcinoma	33	16
ESCA	Esophageal carcinoma	15	25
GBM	Glioblastoma multiforme	24	15
PCPG	Pheochromocytoma and Paraganglioma	21	16
PRAD	Prostate adenocarcinoma	10	26
WT	Wilms Tumor	7	29
READ	Rectum adenocarcinoma	24	8
DLBC	Lymphoid Neoplasm Diffuse Large B-cell Lymphoma	14	11
CHOL	Cholangiocarcinoma	17	3
UCS	Uterine Carcinosarcoma	7	11
TGCT	Testicular Germ Cell Tumors	1	5

Next, we estimated the effect of each JIG on prognosis for individual cancer types, using Cox regression (**Figure 5E**, **Table 1**, and **Supplementary Table 4**). We found that all JIGs correlate with patient outcomes and that a single JIG can affect prognosis of at least three cancer types. Although there were JIGs implicated in as many as 16 cancer types, no single JIG was universally associated with prognosis in all 35 cancers. Rather, their effect is cancer type-dependent. The top-ten most impacted cancer types, ranked by the total number of JIGs affecting, either beneficially (left) or detrimentally (right), the disease outcome are KIRC, LGG, KIRP, PAAD, UVM, ACC, MESO, BLCA, LIHC, and STAD.

Gnathostome-Specific JIGs Are Preferably Deregulated During Cancer Progression

The developmental origin of the cartilaginous jaw consists a turning point in vertebrate evolutionary history and is attributed to the neural crest (Sauka-Spengler and Bronner-Fraser, 2008), and especially to the cranial neural crest cells, from which cartilage is exclusively formed (Martik and Bronner, 2017). Evolutionary Developmental (Evo-Devo) biology studies comparing embryonic programs in jawless versus early jawed chordates indicate that instead of appearing *de novo*, jaws have rather arisen through the co-option of an ancient developmental pre-pattern (Cerny et al., 2010), in association with corresponding changes in the underlying GRNs. Jaw evolution was driven by incorporation of new genes into a pre-existing dorso-ventral patterning program, which altered the identity of jaw-forming chondrocytes (Cerny et al., 2010). For instance, some transcription factors are components of neural crest GRNs in both, jawed and jawless vertebrates, while other transcription factors are cranial neural crest-specific and included in gnathostomes, but missing from lampreys' GRNs (Martik and Bronner, 2017).

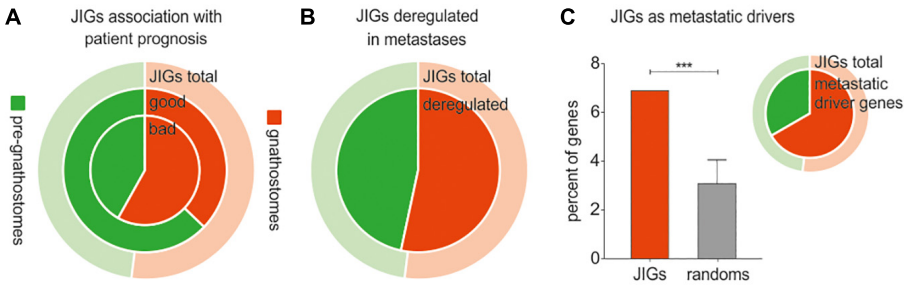

FIGURE 6 | Cancer progression and metastasis are associated with deregulation of evolutionarily younger JIGs. Red indicates gnathostome-specific, green indicates pre-gnathostome orthologs. In all pie charts, the outer, ring represents the composition of the total 305 JIGs in gnathostome-specific (light red) and pre-gnathostome (light green) JIGs. **(A)** Cox regression analysis of JIGs in PanCan revealed that 51.6% of gnathostome-specific orthologs predict worse and only 20.1% better prognosis (ratio 2.56:1) versus 40.4 and 37.0% (ratio 1.09:1) in pre-gnathostome genes. **(B)** In metastasis, a slightly higher number of gnathostome-specific JIGs is deregulated compared to the pre-gnathostomes (inner circle). **(C)** Estimation of gnathostome versus pre-gnathostome genes that are deregulated in a setting of xenograft experimental evolution. Diagram: among the 700 genes which were identified as drivers of tumor evolution, significant enrichment of JIGs was found (6.89%, or 21 genes) as compared to random lists (3.08 ± 0.98%). Pie: of the 21 deregulated JIGs, 14 (66.7%) were of gnathostome and 7 (33.4%) of pre-gnathostome origin.

According to the abovementioned Evo-Devo concepts, the JDN components do not have a similar evolutionary age. It is rather plausible that gene homologs which arose in gnathostomes might have got interconnected with a network that pre-existed in agnatha, perhaps to support morphological novelty. Motivated by this, we questioned whether invasive cancer cells show preference to "usurp" the pre-existing genes or the ones that were incorporated to the JDN after the divergence of jawed vertebrates from cyclostomes. In this respect, we approximated the evolutionary age of all JIGs (**Supplementary Table 5**) and assessed the effects of pre-gnathostome versus gnathostome-specific orthologs on cancer progression. Importantly, to eliminate bias in the estimation of the JIGs' evolutionary age from partially sequenced animal genomes, we included only model organisms with well-annotated genomes. We found that of 305 JIGs, 159 JIGs probably originated in jawed vertebrates, since no "true orthologs" of their corresponding proteins could be detected in jawless species, whereas the other 146 JIGs are of pre-gnathostome origin. Cox regression analysis in PanCan revealed that a higher number of gnathostome-specific JIGs is associated with poor patient outcomes, as opposed to the pre-gnathostome JIGs with an almost equal distribution (82:32 vs. 59:54, $\chi^2 = 8.56$, $p < 0.002$, **Figure 6A**). Consistently, a tendency toward transcriptional deregulation of gnathostome-specific versus pre-gnathostome JIGs was observed in metastases compared to primary tumors ($\chi^2 = 1.09$, $p < 0.296$, **Figure 6B**). We also performed a similar meta-analysis on data produced in a mouse experimental setting, where a tumor's evolution from initiation to metastasis has been simulated *in vivo* via sequential xenografting (Chen et al., 2015). We estimated gnathostome versus pre-gnathostome genes that are deregulated in a setting of xenograft experimental evolution, where a tumor's full-life history from initiation to metastasis was simulated by transforming the immortalized human breast epithelial cell line with *HRAS* and performing sequential xenografting in mice until metastases were observed (Chen et al., 2015). Among the 700 genes which underwent driver expression changes, on the basis that their expression was exclusively increasing or decreasing (Chen et al., 2015), we found that JIGs are significantly enriched ($z = 3.9$, $p < 0.001$), while their majority tends to be of gnathostome rather than pre-gnathostome origin (14:7, $\chi^2 = 1.71$, $p = 0.19$, **Figure 6C** and **Supplementary Table 3**). Collectively, the strong correlations of gnathostome-specific genes with poor and metastatic outcomes, as well as with drivers of experimental tumor evolution underscore a preference for deregulation of evolutionarily younger JIGs toward tumor progression.

Deregulated Expression of JDN Components During Cancer Progression Is More Pronounced in the Gnathostome-Specific Hubs

JIGs appear to form a highly interconnected network (**Figure 3D**). In biological networks, the most highly connected nodes, the so-called "hubs," are considered biologically significant and more relevant to the overall function of the network (Barabási et al., 2011; Kontou et al., 2016; Pavlopoulos et al., 2018). The intra-modular hubs are central to a given network module, with the highest number of connections to the neighboring nodes, whereas inter-modular hubs are intermediate between two or more modules. Taking this into account, we sought to investigate whether gnathostome-specific genes that are deregulated in cancer also occupy hub positions in the JDN. First we identified, through STRING network analysis, 60 nodes representing intra- and inter-modular hubs (**Figure 7A**). By approximating their evolutionary age, we found that these hubs correspond largely to gnathostome-specific versus pre-gnathostome orthologs (**Figure 7B** and **Supplementary Table 5**). Upon comparison of these 60 hubs to CCLE-derived data, we found that 33 (55.0%) of them are deregulated in highly invasive cancer cells, 25 of which are of gnathostome-, and 8 of pre-gnathostome origin ($\chi^2 = 7.76$, $p = 0.005$).

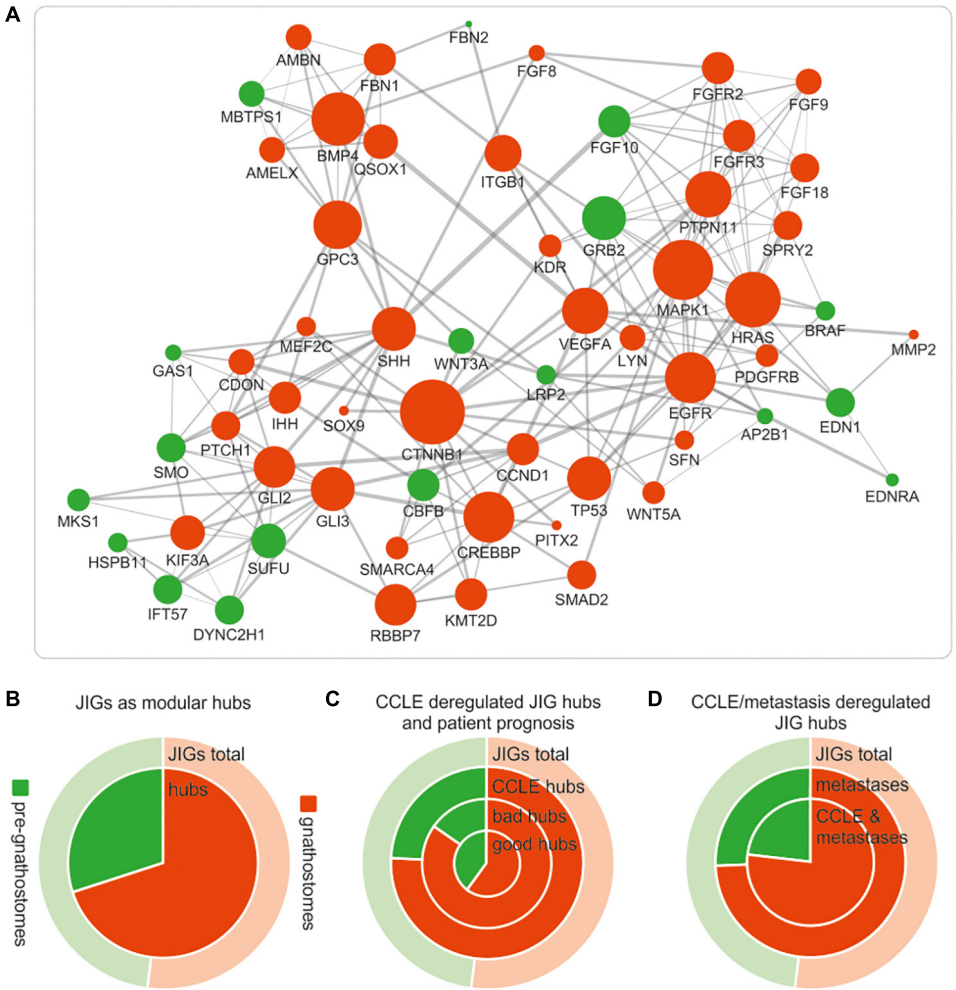

FIGURE 7 | Deregulations of gnathostome-specific hubs of the JDN are more frequent associated with invasive and metastatic stages, as opposed to pre-gnathostome hubs. **(A)** Functional interaction network (confidence interaction score ≥ 0.9) of the gnathostome-specific and pre-gnathostome JIG hubs. The size of the nodes is proportional to the node degree in the "original" JDN network in **Figure 3d**. The 60 nodes that represent intra- and inter-modular hubs in the original network appear to be interconnected and form a rather dense network. **(B)** The gnathostome-specific genes make up 52% (159) of all 305 JIGs (outer ring "JIG total," red), whilst the proportion of gnathostome hubs is significantly enriched in relation to the pre-gnathostome (inner circle "hubs," red). **(C)** More gnathostome-specific hubs that are deregulated in CCLE cells are correlated with worse prognosis in PanCan cohort (ring "bad hubs," red). In contrast, more pre-gnathostome hubs tend to correlate with favorable than poor prognosis (compare ring "bad hubs" with inner circle "good hubs," green). **(D)** More gnathostome-specific hubs are found deregulated, compared to the pre-gnathostome ones, in metastatic lesions (inner ring). This preference is more pronounced for hubs commonly deregulated in metastatic samples and CCLE cells (inner circle).

Notably, all 33 JDN hubs predicted by this approach are indeed causatively linked with invasiveness and/or metastasis in a cancer type-dependent manner, according to experimental evidence in the preclinical setting (**Supplementary Table 6**). In particular, studies using *in vitro* cell lines, mouse xenografts and/or patient samples underscore that most of the hubs promote tumor progression and metastasis. Further data curation in the clinical trials database showed that for several of these hubs, molecular modifiers have been developed and entered clinical trials, either as monotherapies or as combination regimens. In addition, screenings in the drugs.com online pharmaceutical encyclopedia and the publicly available database of the United States Food and Drug Administration (FDA) indicated that small molecules targeting six of these hubs are already approved and marketed drugs for the treatment of aggressive and metastatic cancers. Indeed, as shown in **Supplementary Table 6**, our model was able to identify EGFR which is targeted by approved drugs such as cetuximab, dacomitinib and erlotinib; members of the VEGF (VEGFA/KDR) pathway which are targeted by, for example, bevacizumab, pazopanib or sorafenib; members of the FGFR family of receptors, which are targeted by erdafitinib or pemigatinib; and effectors of the hedgehog signaling pathway (SMO, SHH) which are targeted by glasdegib, sonidegib or vismodegib. Other factors, such as GLI2, GLI3, CDON, MEF2C, PITX, SFN, SPRY2, WNT3A and WNT5A (**Supplementary Table 6**), show

a consistent metastasis-promoting role across several cancer types in preclinical studies, which provides a foundation for the development of molecular modifiers against them and their introduction to clinical trials.

Regarding the age of the hubs of JDN in relation with tumor invasiveness, our studies indicate that among the 60 JDN hubs, the evolutionarily younger ones tend to be more frequently deregulated in aggressive states. The tendency for deregulation of gnathostome-specific hubs as compared to the pre-gnathostome hubs is clinically relevant for cancer patients. We found that more gnathostome-specific hubs are correlated with worse than favorable prognosis (17:10 hubs, correspondingly), whereas the opposite applies for the pre-gnathostome hubs (4:9, $\chi^2 = 2.47$, $p = 0.116$, **Figure 7C**). In addition, aberrant transcription of more gnathostome-specific than pre-gnathostome hub JIGs was observed in metastatic versus primary tumors (35:12 = 2.92, $\chi^2 = 11.26$, $p < 0.001$, **Figure 7D**). This effect is particularly observed among those hubs that are deregulated in highly invasive cancer cell lines (25:8 = 3.13, $\chi^2 = 8.76$, $p = 0.003$, **Figure 7D**). Overall, there is a preference for transcriptional deregulation of gnathostome-specific hubs in the invasive and metastatic stages. Taken together, these results indicate a prevalence of gnathostome-specific genes in occupying hub positions in JDN. However, at the same time, these are preferentially exploited by cancer cells over pre-gnathostome hubs to promote cancer aggressiveness.

DISCUSSION

Cancer is considered an evolutionary and ecological process (Merlo et al., 2006). A neoplasm consists of genetically and epigenetically heterogeneous cell populations that compete for space and resources, evade immune surveillance and cooperate to disseminate to secondary organs. The fitness of cell subpopulations is further shaped by their interactions with cellular and molecular components of the tumor microenvironment. The fittest, or "evolutionarily successful," cell variants are those acquiring capabilities which increase the probability to obtain metastatic potential (Merlo et al., 2006). Darwinian laws apply to both, the tumors and the organisms on which tumors grow. Somatic selection occurs along with organismal selection, following "a mirror within a mirror"-like pattern: heterogeneous cell subpopulations of a growing tumor undergo selection of the fittest within a population of organisms which is under constant evolutionary pressure. Although the timeframe for clonal selection of tumor cells (in months or years) is significantly more narrow than for species selection (millions of years), it is reasonable to envisage that, at a given evolutionary time point, the attributes encoded in the genome of a specific species can be accessed by its cancerous tumor.

Herein, we provide compelling evidence that metastasis is phenotypically manifested within the gnathostome clade, and that genes which are essential for jaw development, a hallmark macroevolutionary trait of gnathostomes, are co-opted during cancer progression. Genes supporting jaw developmental programs tend to undergo mutational and epigenetic changes, with frequent transactivations in invasive and metastatic stages, and a preference for enhanced transcription of the gnathostome-specific versus the ancient ones. These data strongly suggest that the same genes/gene interactions underlying key innovations are also preferentially co-opted within the tumor context toward aggressive outcomes. Certain structures which provide selective advantages at an organismal level, such as placenta development (Costanzo et al., 2018), neural crest formation (Kerosuo and Bronner-Fraser, 2012), and jaw development (this study) may be "hacked" by cancer cells to improve their own fitness, manifested as metastatic potential. The preference of invasive cancer cells to usurp evolutionarily newer hubs of the JDN further reinforces this notion. This observation also implies that there might be a trade-off between the vulnerability to metastasis and the conservation of key innovations that are indispensable for vertebrate fitness and, thus, cannot undergo secondary losses.

Successful prediction of the likely paths of tumor progression is valuable for diagnostic, prognostic, and treatment purposes, but effective models are still not in place (Diaz-Uriarte and Vasallo, 2019). For establishing such prediction models and designing drugs that target events of tumor evolution (Amirouchene-Angelozzi et al., 2017), it is essential to unveil parallels between organismal and clonal selection. Based on our findings, we introduce a systems-based, key innovation-driven model, as an *in silico* tool for prediction of putative prometastatic drivers, on the rationale that genes that are crucial for evolution of a species might be important for tumor evolution. The fact that the results derived using this model are in agreement with the bulk of preclinical studies and with clinical interventions (see **Supplementary Table 6** for details) underscores both, the prediction accuracy of this approach and the translational value of these candidates. In particular, our computational model predicted 33 hub JIGs that are deregulated in highly invasive cell lines of CCLE, consistently with experimental *in vitro*, *in vivo* and/or in patient evidence that these genes mainly support cancer progression. Several of these gene targets have already been translated to marketed drugs, while other factors predicted by this model might represent promising novel targets, since they show consistent metastasis-inducing effects across several cancers. New molecular entities able to inhibit these candidates can be developed and be further assessed in the clinical setting for their potential to prevent metastatic progression or disease recurrence. Out of these 33 hubs, 25 are of gathostome- versus 8 of pregnathostome-origin, indicating a pronounced tendency of cancer cells to usurp the evolutionarily-younger hubs of the JDN network in order to evolve to aggressive stages. Hence, taking into account that a tumor may progress by usurping genes specifically related with vertebrate key-innovations, this model may hold a potential to facilitate the prediction of tumor evolutionary trajectories.

A main future challenge is to design comprehensive experimental settings, where associations between key innovations and metastasis could be investigated at the mechanistic and molecular level, in parallel with corresponding cancer phenotypes. Studies in primitive metastasis-competent taxa versus the incompetent ones could facilitate reconstruction

of the evolutionary history of metastasis by identifying which molecular events that catalyzed gnathostome evolution have also consistently benefited the evolution of primary tumors toward more aggressive stages. Advantageously, a well-established Evo-Devo study system of gnathostomes versus pre-gnathostomes, amenable to experimental and genetic manipulations at embryonic stages (Kuratani et al., 2002; Cerny et al., 2010; Jandzik et al., 2015), could be repurposed for cancer research. This *in vivo* system is comprised of three chordata species of the same evolutionary lineage, presenting progressively aggressive cancer phenotypes from the most ancient to the most recent: amphioxus, the most basal extant chordate, with benign tumors; the metastasis-incompetent jawless lampreys; and the metastasis-competent jawed zebrafish. By comparing lamprey and amphioxus development with that of zebrafish, and other vertebrates like frog and salamander, Evo-Devo specialists attempt to reconstruct genetic and developmental changes underlying the major events in vertebrate evolution (Kuratani et al., 2002; Cerny et al., 2010; Jandzik et al., 2015). Subjecting this system into carcinogenic treatments and comparatively examining the developing lesions in conjunction with genetic and functional changes might provide a glimpse into conserved pathways which are consistently recapitulated in metastases. For instance, it could be investigated whether absence of certain gnathostome-specific genes/gene interactions in the jawless organisms hinders activation of prometastatic cascades in their respective tumors, as opposed to their jawed counterparts. Moreover, studies on cancer-resistant pre-vertebrates, such as echinoderms, urochordates and cephalochordates, could also be considered to dissect their cancer resilience in relation with their hallmark attributes, for instance their increased regeneration ability (Somorjai et al., 2012).

Our key innovation-driven model underscores a preference of invasive tumors for usurping evolutionarily newer features. Otherwise, a recent concept, known as "atavistic model," asserts that neoplasms rely on re-expression of ancestral traits and reverse evolution from multicellularity (MC) to unicellularity (UC; Bussey et al., 2017), which is likely promoted by upregulation of UC genes, disruption of interconnectedness between UC and MC genes (Trigos et al., 2017) and loss-of-function mutations on MC genes (Chen et al., 2015). Furthermore, recent studies show that metastatic competence arises from heterogeneous cancer cell populations without the need for acquisition of additional mutations, and is benefited from further selection of tumor-initiating mutations that seed primary tumorigenesis (Jacob et al., 2015). By unifying these notions, we propose that tumor initiation may be triggered by mutations in evolutionarily old genes governing processes at the "dawn" of multicellularity, such as cell proliferation and genomic stability (Lineweaver et al., 2014). Such alterations in ancient genes may confer genetic heterogeneity (Chen et al., 2015), which is the driving force of evolution. Subsequently, tumor progression may be enabled via selection of clones that entail crosstalks between tumor-initiating mutations already acquired at primary tumor cells and evolutionarily-young genes that support gnathostome key-innovations. Future studies could uncover if such crosstalks guide recurrent routes to metastasis, thereby providing a foundation for the rational design of strategies that prevent cancer evolution.

DATA AVAILABILITY STATEMENT

The datasets presented in this study can be found in online repositories. The names of the repository/repositories and accession number(s) can be found in the article/**Supplementary Material**.

AUTHOR CONTRIBUTIONS

SL, SM, and BP conceived the project and designed experiments. SM developed bioinformatics pipelines and analyzed high-throughput data. AP and IT designed and performed phylogenomics and network analyses. PD and SL performed literature research. SL, SM, and AP analyzed and interpreted data. IT and SM prepared the figures. SL drafted the manuscript. SL, AP, and BP reviewed and edited the manuscript. All authors read and approved the final manuscript.

FUNDING

This work was supported by funding from the German Federal Ministry of Education and Research e:Med-MelAutim (BMBF grant 01ZX1905D), German Cancer Aid (Deutsche Krebshilfe grant 70112353), and Deutsche Forschungsgemeinschaft (DFG grant PU 188/17-1). IT acknowledges the YÖK (Yükseköğretim Kurulu) scholarship.

ACKNOWLEDGMENTS

All contributors to this study are included in the list of authors.

SUPPLEMENTARY MATERIAL

The Supplementary Material for this article can be found online at: https://www.frontiersin.org/articles/10.3389/fcell.2021.682619/full#supplementary-material

Supplementary Figure 1 | Maximum likelihood-based tree of protein sequences of the p53 family. A characteristic example of the well-studied *p53* gene family, where distinct orthologs of the three members of this family (i.e., TP53, TP63 and TP73) were found exclusively in gnathostome species. The agnathan p53 homologs occupy a basal position in this phylogenetic tree, suggesting that a primordial *TP53/63/73* gene might have existed in jawless species which after a series of duplications gave rise to the functionally divergent *TP53*, *TP63* and *TP73* genes in jaw-bearing vertebrates.

Supplementary Table 1 | Taxa under study in correlation with their tumor characteristics, their circulatory and immune systems, the level of body organization and their ability to develop metastatic or lethal cancers.

Supplementary Table 2 | Mouse gene knockouts which present jaws abnormalities. The human orthologs are included. The ratio of the jaw-related

phenotypes to all developmental phenotypes affected by each gene knockout is also shown.

Supplementary Table 3 | Associations of each JIG with genetic and epigenetic alterations in tumors, survival of PanCan patients, and expression in highly invasive or metastatic stages. Column annotations: CGC = included in the Cancer Gene Census list, Cancer driver = included among the cancer driver genes in PanCan, freqmut = included among the frequently mutated genes in PanCan, Methylation = differentially methylated JIGs in human tumors versus normal tissue, from DiseaseMeth database (hypo = hypomethylated, hyper = hypermethylated), CCLE = up- or down-regulated in highly-invasive vs. less-invasive human cells from the CCLE, Survival = impact on the survival prognosis of the patients from the PanCancer cohort based on Cox regression analysis, hsa_Metastases = up- or down-regulated in human metastatic vs. primary lesions (GSE21510, GSE2509, GSE25976, GSE43837, GSE468, GSE6919, GSE7929, GSE7930, GSE8401), mmu_metast_driver = included among metastasis driver genes in a mouse model of tumor evolution.

Supplementary Table 4 | JIGs and their effect on patient survival prognosis across different cancer types of TCGA based on Cox regression analysis. Annotations: poor prognosis = 1, favorable prognosis = -1, insignificant = 0.

Supplementary Table 5 | JIG orthologs across pre-gnathostome and gnathostome species. Annotations: green = pregnathostome orthologs, orange: gnathostome-specific orthologs, underlined = network hubs.

Supplementary Table 6 | Comprehensive overview of the preclinical and clinical research studies on the hub JIGs that are deregulated in highly-invasive cell lines of CCLE. The drivers of tumor progression predicted using the key innovation-driven model are in agreement with existing experimental data.

REFERENCES

Abu-Helil, B., and van der Weyden, L. (2019). Metastasis in the wild: investigating metastasis in non-laboratory animals. *Clin. Exp. Metastasis.* 36, 15–28. doi: 10.1007/s10585-019-09956-3

Albuquerque, T. A. F., Drummond do Val, L., Doherty, A., and de Magalhães, J. P. (2018). From humans to hydra: patterns of cancer across the tree of life. *Biol. Rev. Camb. Philos. Soc.* 93, 1715–1734. doi: 10.1111/brv.12415

Altschul, S. F., Gish, W., Miller, W., Myers, E. W., and Lipman, D. J. (1990). Basic local alignment search tool. *J. Mol. Biol.* 215, 403–410.

Amirouchene-Angelozzi, N., Swanton, C., and Bardelli, A. (2017). Tumor evolution as a therapeutic target. *Cancer Discov.* 7, 805–817.

Angelova, M., Mlecnik, B., Vasaturo, A., Bindea, G., Fredriksen, T., Lafontaine, L., et al. (2018). Evolution of metastases in space and time under immune selection. *Cell* 175, 751–765.e16.

Bailey, M. H., Tokheim, C., Porta-Pardo, E., Sengupta, S., Bertrand, D., Weerasinghe, A., et al. (2018). Comprehensive characterization of cancer driver genes and mutations. *Cell* 173, 371–385.e18.

Bamford, S., Dawson, E., Forbes, S., Clements, J., Pettett, R., Dogan, A., et al. (2004). The COSMIC (Catalogue of Somatic Mutations in Cancer) database and website. *Br. J. Cancer* 91, 355–358. doi: 10.1038/sj.bjc.6601894

Barabási, A. L., Gulbahce, N., and Loscalzo, J. (2011). Network medicine: a network-based approach to human disease. *Nat. Rev. Genet.* 12, 56–68. doi: 10.1038/nrg2918

Barber, B. J. (2004). Neoplastic diseases of commercially important marine bivalves. *Aquat. Living Resour.* 17, 449–466. doi: 10.1051/alr:2004052

Barretina, J., Caponigro, G., Stransky, N., Venkatesan, K., Margolin, A. A., Kim, S., et al. (2012). The Cancer Cell Line Encyclopedia enables predictive modelling of anticancer drug sensitivity. *Nature* 483, 603–607.

Billaud, M., and Santoro, M. (2011). Is Co-option a prevailing mechanism during cancer progression? *Cancer Res.* 71, 6572–6575. doi: 10.1158/0008-5472.can-11-2158

Birkbak, N. J., and McGranahan, N. (2020). Cancer genome evolutionary trajectories in metastasis. *Cancer Cell.* 37, 8–19. doi: 10.1016/j.ccell.2019.12.004

Bult, C. J., Blake, J. A., Smith, C. L., Kadin, J. A., Richardson, J. E., and Group, M. G. D. (2019). Mouse Genome Database (MGD) 2019. *Nucleic Acids Res.* 47, D801–D806.

Bussey, K. J., Cisneros, L. H., Lineweaver, C. H., and Davies, P. C. W. (2017). Ancestral gene regulatory networks drive cancer. *Proc. Natl. Acad. Sci. U.S.A.* 114, 6160–6162. doi: 10.1073/pnas.1706990114

Carballal, M. J., Barber, B. J., Iglesias, D., and Villalba, A. (2015). Neoplastic diseases of marine bivalves. *J. Invertebr. Pathol.* 131, 83–106. doi: 10.1016/j.jip.2015.06.004

Cerny, R., Cattell, M., Sauka-Spengler, T., Bronner-Fraser, M., Yu, F., and Medeiros, D. M. (2010). Evidence for the prepattern/cooption model of vertebrate jaw evolution. *Proc. Natl. Acad. Sci. U.S.A.* 107, 17262–17267. doi: 10.1073/pnas.1009304107

Chen, H., Lin, F., Xing, K., and He, X. (2015). The reverse evolution from multicellularity to unicellularity during carcinogenesis. *Nat. Commun.* 6:6367.

Clough, E., and Barrett, T. (2016). The gene expression omnibus database. *Methods Mol. Biol.* 1418, 93–110. doi: 10.1007/978-1-4939-3578-9_5

Cooper, M. D., and Alder, M. N. (2006). The evolution of adaptive immune systems. *Cell* 124, 815–822. doi: 10.1016/j.cell.2006.02.001

Costanzo, V., Bardelli, A., Siena, S., and Abrignani, S. (2018). Exploring the links between cancer and placenta development. *Open Biol.* 8:180081. doi: 10.1098/rsob.180081

Couch, J. A., and Harshbarger, J. C. (1985). Effects of carcinogenic agents on aquatic animals: an environmental and experimental overview. *J. Environ. Sci. Health Pt. C Environ. Carcinog. Rev.* 3, 63–105. doi: 10.1080/10590508509373329

Dawe, C. J. (1969). Phylogeny and oncogeny. *Natl. Cancer Inst. Monogr.* 31, 1–40.

Delsuc, F., Brinkmann, H., Chourrout, D., and Philippe, H. (2006). Tunicates and not cephalochordates are the closest living relatives of vertebrates. *Nature* 439, 965–968. doi: 10.1038/nature04336

Deming, A. C., Colegrove, K. M., Duignan, P. J., Hall, A. J., Wellehan, J. F. X., and Gulland, F. M. D. (2018). Prevalence of urogenital carcinoma in stranded California sea lions (*Zalophus californianus*) from 2005-15. *J. Wildl. Dis.* 54, 581–586. doi: 10.7589/2017-08-208

Diaz-Uriarte, R., and Vasallo, C. (2019). Every which way? On predicting tumor evolution using cancer progression models. *PLoS Comput. Biol.* 15:e1007246. doi: 10.1371/journal.pcbi.1007246

Domazet-Lošo, T., Klimovich, A., Anokhin, B., Anton-Erxleben, F., Hamm, M. J., Lange, C., et al. (2014). Naturally occurring tumours in the basal metazoan Hydra. *Nat Commun.* 5:4222.

Falkmer, S. (1998). "The tumour pathology of *Myxine glutinosa*," in *The Biology of Hagfishes*, 1 Edn, eds J. M. Jørgensen, J. P. Lornholt, R. E. Weber, and H. Malte (London: Chapman and Hall), 101–106. doi: 10.1007/978-94-011-5834-3_7

Falkmer, S., Emdin, S. O., Ostberg, Y., Mattisson, A., Sjöbeck, M. L., and Fänge, R. (1976). Tumor pathology of the hagfish, *Myxine glutinosa*, and the river lamprey, *Lampetra fluviatilis*. A light-microscopical study with particular reference to the occurrence of primary liver carcinoma, islet-cell tumors, and epidermoid cysts of the skin. *Prog. Exp. Tumor. Res.* 20, 217–250. doi: 10.1159/000398701

Falkmer, S., Marklund, S., Mattsson, P. E., and Rappe, C. (1978). Hepatomas and other neoplasms in the atlantic hagfish (*Myxine glutinosa*): a histopathologic and chemical study. *Ann. N. Y. Acad. Sci.* 298, 342–355. doi: 10.1111/j.1749-6632.1977.tb19277.x

Fontaine, A. R. (1969). Pigmented tumor-like lesions in an ophluroid echinoderm. *Natl. Cancer Inst. Monogr.* 31, 255–261.

Fürst, K., Steder, M., Logotheti, S., Angerilli, A., Spitschak, A., Marquardt, S., et al. (2019). DNp73-induced degradation of tyrosinase links depigmentation with EMT-driven melanoma progression. *Cancer Lett.* 442, 299–309. doi: 10.1016/j.canlet.2018.11.009

Gess, R. W., Coates, M. I., and Rubidge, B. S. (2006). A lamprey from the Devonian period of South Africa. *Nature* 443, 981–984. doi: 10.1038/nature05150

Gray, K. A., Yates, B., Seal, R. L., Wright, M. W., and Bruford, E. A. (2015). Genenames.org: the HGNC resources in 2015. *Nucleic Acids Res.* 43, D1079–D1085.

Groff, J. M. (2004). Neoplasia in fishes. *Vet. Clin. North Am. Exot. Anim. Pract.* 7, 705–756. doi: 10.1016/j.cvex.2004.04.012

Hanahan, D., and Weinberg, R. A. (2011). Hallmarks of cancer: the next generation. *Cell* 144, 646–674. doi: 10.1016/j.cell.2011.02.013

Harshbarger, J. C. (1969). The registry of tumors in lower animals. *Natl. Cancer Inst. Monogr.* 31, XI–XVI.

Heimberg, A. M., Cowper-Sal-lari, R., Sémon, M., Donoghue, P. C., and Peterson, K. J. (2010). microRNAs reveal the interrelationships of hagfish, lampreys, and gnathostomes and the nature of the ancestral vertebrate. *Proc. Natl. Acad. Sci. U.S.A.* 107, 19379–19383. doi: 10.1073/pnas.1010350107

Hickman, C. P., Roberts, L. S., and Larson, A. (2001). *Integrated Principles of Zoology*. New York, NY: McGraw-Hill.

Hunter, J. P. (1998). Key innovations and the ecology of macroevolution. *Trends Ecol Evol.* 13, 31–36. doi: 10.1016/s0169-5347(97)01273-1

Iacobuzio-Donahue, C. A., Velculescu, V. E., Wolfgang, C. L., and Hruban, R. H. (2012). Genetic basis of pancreas cancer development and progression: insights from whole-exome and whole-genome sequencing. *Clin. Cancer Res.* 18, 4257–4265. doi: 10.1158/1078-0432.ccr-12-0315

Jacob, L. S., Vanharanta, S., Obenauf, A. C., Pirun, M., Viale, A., Socci, N. D., et al. (2015). Metastatic competence can emerge with selection of preexisting oncogenic alleles without a need of new mutations. *Cancer Res.* 75, 3713–3719. doi: 10.1158/0008-5472.can-15-0562

Jandzik, D., Garnett, A. T., Square, T. A., Cattell, M. V., Yu, J. K., and Medeiros, D. M. (2015). Evolution of the new vertebrate head by co-option of an ancient chordate skeletal tissue. *Nature* 518, 534–537. doi: 10.1038/nature14000

Jensen, M. A., Ferretti, V., Grossman, R. L., and Staudt, L. M. (2017). The NCI genomic data commons as an engine for precision medicine. *Blood* 130, 453–459. doi: 10.1182/blood-2017-03-735654

Jones, D. T., Taylor, W. R., and Thornton, J. M. (1992). The rapid generation of mutation data matrices from protein sequences. *Comput. Appl. Biosci.* 8, 275–282. doi: 10.1093/bioinformatics/8.3.275

Kandoth, C., McLellan, M. D., Vandin, F., Ye, K., Niu, B., Lu, C., et al. (2013). Mutational landscape and significance across 12 major cancer types. *Nature* 502, 333–339. doi: 10.1038/nature12634

Kaucka, M., and Adameyko, I. (2019). Evolution and development of the cartilaginous skull: From a lancelet towards a human face. *Semin. Cell Dev Biol.* 91, 2–12. doi: 10.1016/j.semcdb.2017.12.007

Kerosuo, L., and Bronner-Fraser, M. (2012). What is bad in cancer is good in the embryo: importance of EMT in neural crest development. *Semin Cell Dev. Biol.* 23, 320–332. doi: 10.1016/j.semcdb.2012.03.010

Khan, F. M., Marquardt, S., Gupta, S. K., Knoll, S., Schmitz, U., Spitschak, A., et al. (2017). Unraveling a tumor type-specific regulatory core underlying E2F1-mediated epithelial-mesenchymal transition to predict receptor protein signatures. *Nat. Commun.* 8:198.

Kirienko, N. V., Mani, K., and Fay, D. S. (2010). Cancer models in *Caenorhabditis elegans*. *Dev. Dyn.* 239, 1413–1448.

Kontou, P. I., Pavlopoulou, A., Dimou, N. L., Pavlopoulos, G. A., and Bagos, P. G. (2016). Network analysis of genes and their association with diseases. *Gene* 590, 68–78. doi: 10.1016/j.gene.2016.05.044

Koual, M., Cano-Sancho, G., Bats, A. S., Tomkiewicz, C., Kaddouch-Amar, Y., Douay-Hauser, N., et al. (2019). Associations between persistent organic pollutants and risk of breast cancer metastasis. *Environ. Int.* 132:105028. doi: 10.1016/j.envint.2019.105028

Kumar, S., Stecher, G., Li, M., Knyaz, C., and Tamura, K. (2018). MEGA X: molecular evolutionary genetics analysis across computing platforms. *Mol. Biol. Evol.* 35, 1547–1549. doi: 10.1093/molbev/msy096

Kuratani, S., Kuraku, S., and Murakami, Y. (2002). Lamprey as an evo-devo model: lessons from comparative embryology and molecular phylogenetics. *Genesis* 34, 175–183. doi: 10.1002/gene.10142

Lair, S., Measures, L. N., and Martineau, D. (2016). Pathologic findings and trends in mortality in the Beluga (*Delphinapterus leucas*) Population of the St Lawrence Estuary, Quebec, Canada, From 1983 to 2012. *Vet. Pathol.* 53, 22–36. doi: 10.1177/0300985815604726

Langlet, C., and Bierne, J. (1982). Immune characteristics of graft rejection in nemerteans of the genus *Lineus*. *Eur. J. Immunol.* 12, 705–708. doi: 10.1002/eji.1830120902

Lauby-Secretan, B., Loomis, D., Grosse, Y., El Ghissassi, F., Bouvard, V., Benbrahim-Tallaa, L., et al. (2013). Carcinogenicity of polychlorinated biphenyls and polybrominated biphenyls. *Lancet Oncol.* 14, 287–288.

Letunic, I., and Bork, P. (2018). 20 years of the SMART protein domain annotation resource. *Nucleic Acids Res.* 46, D493–D496.

Levine, M., and Davidson, E. H. (2005). Gene regulatory networks for development. *Proc. Natl. Acad. Sci. U.S.A.* 102, 4936–4942.

Lineweaver, C. H., Davies, P. C., and Vincent, M. D. (2014). Targeting cancer's weaknesses (not its strengths): therapeutic strategies suggested by the atavistic model. *Bioessay.* 36, 827–835. doi: 10.1002/bies.201400070

Lipscomb, T. P., Scott, D. P., Garber, R. L., Krafft, A. E., Tsai, M. M., Lichy, J. H., et al. (2000). Common metastatic carcinoma of California sea lions (*Zalophus californianus*): evidence of genital origin and association with novel gammaherpesvirus. *Vet. Pathol.* 37, 609–617. doi: 10.1354/vp.37-6-609

Liu, J., Lichtenberg, T., Hoadley, K. A., Poisson, L. M., Lazar, A. J., Cherniack, A. D., et al. (2018). An integrated TCGA pan-cancer clinical data resource to drive high-quality survival outcome analytics. *Cell* 173, 400–416.

Logotheti, S., Marquardt, S., Richter, C., Sophie Hain, R., Murr, N., Takan, I., et al. (2020). Neural networks recapitulation by cancer cells promotes disease progression: a novel role of p73 isoforms in cancer-neuronal crosstalk. *Cancers (Basel)* 12:3789. doi: 10.3390/cancers12123789

Loomis, D., Guyton, K., Grosse, Y., El Ghissasi, F., Bouvard, V., Benbrahim-Tallaa, L., et al. (2015). Carcinogenicity of lindane, DDT, and 2,4-dichlorophenoxyacetic acid. *Lancet Oncol.* 16, 891–892. doi: 10.1016/s1470-2045(15)00081-9

Maciel, E. I., and Oviedo, N. J. (2018). "Platyhelminthes: molecular dissection of the planarian innate immune system," in *Advances in Comparative Immunology*, ed. E. L. Cooper (Cham: Springer International Publishing), 95–115. doi: 10.1007/978-3-319-76768-0_4

Martik, M. L., and Bronner, M. E. (2017). Regulatory Logic Underlying Diversification of the Neural Crest. *Trends Genet.* 33, 715–727. doi: 10.1016/j.tig.2017.07.015

Martineau, D., Lemberger, K., Dallaire, A., Labelle, P., Lipscomb, T. P., Michel, P., et al. (2002). Cancer in wildlife, a case study: beluga from the St. Lawrence estuary, Québec, Canada. *Environ. Health Perspect.* 110, 285–292. doi: 10.1289/ehp.02110285

Merlo, L. M., Pepper, J. W., Reid, B. J., and Maley, C. C. (2006). Cancer as an evolutionary and ecological process. *Nat. Rev. Cancer* 6, 924–935. doi: 10.1038/nrc2013

Metzger, M. J., Reinisch, C., Sherry, J., and Goff, S. P. (2015). Horizontal transmission of clonal cancer cells causes leukemia in soft-shell clams. *Cell* 161, 255–263. doi: 10.1016/j.cell.2015.02.042

O'Leary, N. A., Wright, M. W., Brister, J. R., Ciufo, S., Haddad, D., McVeigh, R., et al. (2016). Reference sequence (RefSeq) database at NCBI: current status, taxonomic expansion, and functional annotation. *Nucleic Acids Res.* 44, D733–D745.

Ostrander, G. K., Cheng, K. C., Wolf, J. C., and Wolfe, M. J. (2004). Shark cartilage, cancer and the growing threat of pseudoscience. *Cancer Res.* 64, 8485–8491. doi: 10.1158/0008-5472.can-04-2260

Pavlopoulos, G. A., Kontou, P. I., Pavlopoulou, A., Bouyioukos, C., Markou, E., and Bagos, P. G. (2018). Bipartite graphs in systems biology and medicine: a survey of methods and applications. *Gigascience* 7, 1–31. doi: 10.20429/tag.2020.070202

Randhawa, N., Gulland, F., Ylitalo, G. M., DeLong, R., and Mazet, J. A. K. (2015). Sentinel California sea lions provide insight into legacy organochlorine exposure trends and their association with cancer and infectious disease. *One Health* 1, 37–43. doi: 10.1016/j.onehlt.2015.08.003

Richter, C., Marquardt, S., Li, F., Spitschak, A., Murr, N., Edelhäuser, B. A. H., et al. (2019). Rewiring E2F1 with classical NHEJ via APLF suppression promotes bladder cancer invasiveness. *J. Exp. Clin. Cancer Res.* 38:292.

Rodrigues, P., Patel, S. A., Harewood, L., Olan, I., Vojtasova, E., Syafruddin, S. E., et al. (2018). NF-κB-dependent lymphoid enhancer co-option promotes renal carcinoma metastasis. *Cancer Discov.* 8, 850–865. doi: 10.1158/2159-8290.cd-17-1211

Rousseaux, S., Debernardi, A., Jacquiau, B., Vitte, A. L., Vesin, A., Nagy-Mignotte, H., et al. (2013). Ectopic activation of germline and placental genes identifies aggressive metastasis-prone lung cancers. *Sci. Transl. Med.* 5:186ra66. doi: 10.1126/scitranslmed.3005723

Sauka-Spengler, T., and Bronner-Fraser, M. (2008). A gene regulatory network orchestrates neural crest formation. *Nat. Rev. Mol. Cell Biol.* 9, 557–568. doi: 10.1038/nrm2428

Sayers, E. W., Cavanaugh, M., Clark, K., Ostell, J., Pruitt, K. D., and Karsch-Mizrachi, I. (2019). GenBank. *Nucleic Acids Res.* 47, D94–D99.

Schlumberger, H. G., and Lucke, B. H. (1948). Tumors of fishes, amphibians, and reptiles. *Cancer Res.* 8, 657–753.

Shannon, P., Markiel, A., Ozier, O., Baliga, N. S., Wang, J. T., Ramage, D., et al. (2003). Cytoscape: a software environment for integrated models of biomolecular interaction networks. *Genome Res.* 13, 2498–2504. doi: 10.1101/gr.1239303

Shimeld, S. M., and Donoghue, P. C. (2012). Evolutionary crossroads in developmental biology: cyclostomes (lamprey and hagfish). *Development* 139, 2091–2099. doi: 10.1242/dev.074716

Sievers, F., and Higgins, D. G. (2014a). Clustal omega, accurate alignment of very large numbers of sequences. *Methods Mol. Biol.* 1079, 105–116. doi: 10.1007/978-1-62703-646-7_6

Sievers, F., and Higgins, D. G. (2014b). Clustal omega. *Curr. Protoc. Bioinform.* 48, 3.13.1–6.

Somorjai, I. M., Somorjai, R. L., Garcia-Fernàndez, J., and Escrivà, H. (2012). Vertebrate-like regeneration in the invertebrate chordate amphioxus. *Proc. Natl. Acad. Sci. U.S.A.* 109, 517–522. doi: 10.1073/pnas.1100045109

Stacy, B. A., and Parker, J. M. (2004). Amphibian oncology. *Vet. Clin. North Am. Exot. Anim. Pract.* 7, 673–695.

Subramanian, A., Tamayo, P., Mootha, V. K., Mukherjee, S., Ebert, B. L., Gillette, M. A., et al. (2005). Gene set enrichment analysis: a knowledge-based approach for interpreting genome-wide expression profiles. *Proc. Natl. Acad. Sci. U.S. A.* 102, 15545–15550. doi: 10.1073/pnas.0506580102

Szklarczyk, D., Gable, A. L., Lyon, D., Junge, A., Wyder, S., Huerta-Cepas, J., et al. (2019). STRING v11: protein-protein association networks with increased coverage, supporting functional discovery in genome-wide experimental datasets. *Nucleic Acids Res.* 47, D607–D613.

Tascedda, F., and Ottaviani, E. (2014). Tumors in invertebrates. *Inverteb. Surv. J.* 11, 197–203.

Trigos, A. S., Pearson, R. B., Papenfuss, A. T., and Goode, D. L. (2017). Altered interactions between unicellular and multicellular genes drive hallmarks of transformation in a diverse range of solid tumors. *Proc. Natl. Acad. Sci. U.S.A.* 114, 6406–6411. doi: 10.1073/pnas.1617743114

Van Roten, A., Barakat, A. Z. A., Wouters, A., Tran, T. A., Mouton, S., Noben, J. P., et al. (2018). A carcinogenic trigger to study the function of tumor suppressor genes in *Schmidtea mediterranea*. *Dis. Model. Mech.* 11:dmm032573.

Wellings, S. R. (1969). Neoplasia and primitive vertebrate phylogeny: echinoderms, prevertebrates, and fishes–A review. *Natl. Cancer Inst. Monogr.* 31, 59–128.

Xiong, Y., Wei, Y., Gu, Y., Zhang, S., Lyu, J., Zhang, B., et al. (2017). DiseaseMeth version 2.0: a major expansion and update of the human disease methylation database. *Nucleic Acids Res.* 45, D888–D895.

Ylitalo, G. M., Stein, J. E., Hom, T., Johnson, L. L., Tilbury, K. L., Hall, A. J., et al. (2005). The role of organochlorines in cancer-associated mortality in California sea lions (*Zalophus californianus*). *Mar. Pollut. Bull.* 50, 30–39. doi: 10.1016/j.marpolbul.2004.08.005

Conflict of Interest: The authors declare that the research was conducted in the absence of any commercial or financial relationships that could be construed as a potential conflict of interest.

Copyright © 2021 Marquardt, Pavlopoulou, Takan, Dhar, Pützer and Logotheti. This is an open-access article distributed under the terms of the Creative Commons Attribution License (CC BY). The use, distribution or reproduction in other forums is permitted, provided the original author(s) and the copyright owner(s) are credited and that the original publication in this journal is cited, in accordance with accepted academic practice. No use, distribution or reproduction is permitted which does not comply with these terms.

frontiers in Cell and Developmental Biology

MINI REVIEW
published: 05 July 2021
doi: 10.3389/fcell.2021.701986

p63 and p53: Collaborative Partners or Dueling Rivals?

Dana L. Woodstock[1], Morgan A. Sammons[1] and Martin Fischer[2]**

[1] Department of Biological Sciences, The State University of New York at Albany, Albany, NY, United States, [2] Computational Biology Group, Leibniz Institute on Aging – Fritz Lipmann Institute (FLI), Jena, Germany

The tumor suppressor p53 and its oncogenic sibling p63 (ΔNp63) direct opposing fates in tumor development. These paralog proteins are transcription factors that elicit their tumor suppressive and oncogenic capacity through the regulation of both shared and unique target genes. Both proteins predominantly function as activators of transcription, leading to a paradigm shift away from ΔNp63 as a dominant negative to p53 activity. The discovery of p53 and p63 as pioneer transcription factors regulating chromatin structure revealed new insights into how these paralogs can both positively and negatively influence each other to direct cell fate. The previous view of a strict rivalry between the siblings needs to be revisited, as p53 and p63 can also work together toward a common goal.

Keywords: p53, p63, tumor suppressor, oncogene, transcription factor, pioneer factor

OPEN ACCESS

Edited by:
Brigitte M. Pützer, University Hospital Rostock, Germany

Reviewed by:
Matt Fisher, Cold Spring Harbor Laboratory, United States
Adone Mohd-Sarip, Queen's University Belfast, United Kingdom

****Correspondence:***
Morgan A. Sammons
masammons@albany.edu
Martin Fischer
Martin.Fischer@leibniz-fli.de

Specialty section:
This article was submitted to Molecular Medicine, a section of the journal Frontiers in Cell and Developmental Biology

Received: *28 April 2021*
Accepted: *14 June 2021*
Published: *05 July 2021*

Citation:
Woodstock DL, Sammons MA and Fischer M (2021) p63 and p53: Collaborative Partners or Dueling Rivals? Front. Cell Dev. Biol. 9:701986. doi: 10.3389/fcell.2021.701986

INTRODUCTION

The p53 transcription factor family comprises the three members p53, p63, and p73. Although it is evolutionarily the youngest, p53 is the eponymous member of the family. The transcription factors evolved from an ancestral *p63/p73* gene that can be found in most invertebrates (Belyi et al., 2010; Rutkowski et al., 2010). While the ancestral *p63/p73* gene protects organismal integrity and the germ line by inducing cell death upon DNA damage, higher vertebrates possess all three p53 family members with diversified functions. In particular the intricate relationship between the family members and their overlapping and opposing functions have been subject to intense research and debate.

The family matters are complicated by the fact that p53, p63, and p73 comprise multiple isoforms. The *TP53*, *TP63*, and *TP73* genes encode for major isoform groups that are controlled by distinct promoters leading to transcripts that differ in their N-terminus (Murray-Zmijewski et al., 2006). In the case of *TP63*, these isoforms are highly cell type-dependent. The long isoform TAp63 is mainly expressed in germ cells and the shorter ΔNp63 isoform is predominantly expressed in basal and stratifying epithelia. In contrast, full-length p53 is expressed across essentially all tissues. In addition to different N-termini generated through alternative promoter usage, alternative splicing leads to additional isoforms for each p53 family member that differ in their C-termini, such as α, β, and γ isoforms (Murray-Zmijewski et al., 2006).

The full-length isoforms p53α, TAp63α, and TAp73α function as haplo-insufficient tumor suppressors (Venkatachalam et al., 1998; Flores et al., 2005). In addition, p73 functions in neuronal development, multi-ciliated cell differentiation, and metabolism (Nemajerova et al., 2018). In contrast, ΔNp63 governs epidermis development (Mills et al., 1999; Yang et al., 1999) and is an oncogenic driver that is overexpressed or amplified in squamous cell carcinoma

(Campbell et al., 2018; Gatti et al., 2019). The opposing directions in tumor development driven by the tumor suppressor p53α (p53 hereafter) and the proto-oncoprotein ΔNp63 involve the potential for a serious sibling rivalry. During the past two decades, the relationship between p53 and p63 has been the basis for several hypotheses and debates. Here, we provide an updated view on this relationship with an emphasis on recent genome-wide studies and we discuss whether these siblings might get along as much as they fight.

HISTORY FUELED A SIBLING RIVALRY

In 1998, the discovery of p63 laid the foundation for a history of sibling rivalry with its more famous sibling p53. The first study of p63 found that both its full-length isoform TAp63 and the shorter ΔNp63 can bind to DNA motifs that are similar to those of p53, but only TAp63 harbored a transactivation domain (TAD). In contrast to TAp63, ΔNp63 lacked a canonical TAD and was found to confer negative effects over other p53 family members and its own isoforms (Yang et al., 1998). The function of ΔNp63 as dominant negative regulator of its family members was fueled by the initial and additional reporter assays using exogenous expression of different isoforms of p53 family members (Yang et al., 1998; Westfall et al., 2003). While Yang et al. (1998) used a minimal promoter containing multiple p53 binding sites to drive a β-galactosidase reporter, Westfall et al. (2003) employed promoter regions of *CDKN1A* (p21) containing known p53 binding sites to drive a luciferase reporter. Both studies showed that high expression of ΔNp63 was associated with a reduced ability of p53 to *trans*-activate the reporter genes, highlighting a potential sibling rivalry (**Figure 1A**).

DNA RECOGNITION SEQUENCE SPECIFICITY

The p53 family shares a highly conserved DNA binding domain (DBD) through which its members bind to very similar DNA motifs. Consequently, p53, p63, and p73 share many binding sites, but they also bind to many unique sites (Lin et al., 2009; McDade et al., 2014; Riege et al., 2020). In agreement with their ability to also bind to unique genomic sites, differences in their DBDs have been reported with regard to thermostability, hydrophobic potentials (Enthart et al., 2016), zinc-coordination (Lokshin et al., 2007), and redox sensitivity (Tichý et al., 2013). In addition to small differences in their DBD, the different C-terminal domains of the p53 family may affect their DNA binding specificity (Sauer et al., 2008; Laptenko et al., 2015). For example, p53 is well-established to bind to two decameric half sites that both harbor the sequence RRRCWWGYYY (R = A/G; W = A/T; Y = C/T). The substantial number of unique genomic sites bound by p53 and p63 motivated a series of studies that investigated potential differences in their DNA recognition motifs. Using either systematic evolution of ligands by exponential enrichment (SELEX) (Ortt and Sinha, 2006; Perez et al., 2007) or high-throughput analyses of chromatin immunoprecipitation (ChIP-seq) (Yang et al., 2006; Kouwenhoven et al., 2010; McDade et al., 2012) led to the identification of p63 recognition motifs with high similarity to p53 motifs that sill showed some uniqe characteristics. These unique characteristics, however, differed substantially between the studies. A recent study addressed the question of p53 and p63-specific DNA recognition motifs using a meta-analysis of ChIP-seq datasets combined with an iterative *de novo* motif search approach (Riege et al., 2020). The results imply that p53 relies on one CWWG core motif with flanking regions, while p63 relies on two CNNG (N = A/C/G/T) core motifs with little importance of flanking regions. These findings support and expand one of the models established earlier (McDade et al., 2014) and explain a substantial number of genomic regions that are bound by only p53 or p63 (Riege et al., 2020; **Figure 1B**). DNA recognition motifs alone, however, cannot explain productive binding of p53 or p63, which occurs when p53 or p63 bind to a genomic region that functions as a *cis*-regulatory region to transcriptionally regulate a proximal or distal gene that is linked to it. In fact, p53 and p63 regulate largely non-overlapping gene sets (Gallant-Behm et al., 2012; Riege et al., 2020), which indicates that additional layers of regulation play an important role in p53 and p63-mediated gene regulation.

ENGAGING CHROMATIN – THE PIONEER ROLE OF THE p53 FAMILY

Generally, transcription factors bind to nucleosome-free DNA and are inhibited by nucleosomes. This rule is broken by pioneer transcription factors, which can bind to nucleosomal DNA either sequence-dependent or independent (Zaret and Mango, 2016). Numerous recent studies suggest that the p53 family of transcription factors are pioneer transcription factors (Sammons et al., 2015; Yu and Buck, 2019; Yu et al., 2021; **Figure 2A**). Indeed, differential pioneer activity of p53 and p63 has the potential to explain some of the observed gene regulatory differences between these two siblings.

p53 can bind to nucleosomal DNA, although this strongly depends on the specific location of the response element relative to the nucleosome dyad (Sahu et al., 2010; Yu and Buck, 2019). ChIP-seq studies suggest that about 50% of p53 binding sites are nucleosome-occupied, but to date, the role of nucleosome-bound p53 in transcription has only been studied at a single gene level (Espinosa and Emerson, 2001; Laptenko et al., 2011). A subset of p53 binding sites display *de novo* DNA accessibility and potential enhancer activity upon p53 binding, suggesting a requirement for p53 pioneer activity (Younger and Rinn, 2017), although p53 is not required for accessibility at the majority of its binding sites (Karsli Uzunbas et al., 2019). The full activity of p53-bound regulatory regions depends on other factors, such as SP1 and the AP-1 family (Daino et al., 2006; Catizone et al., 2020), but whether they facilitate DNA accessibility or other aspects of transcriptional activation is not fully understood.

Given the high sequence and functional homology to p53, perhaps it is unsurprising that p63 has also emerged as a pioneer transcription factor with similar nucleosomal constraints

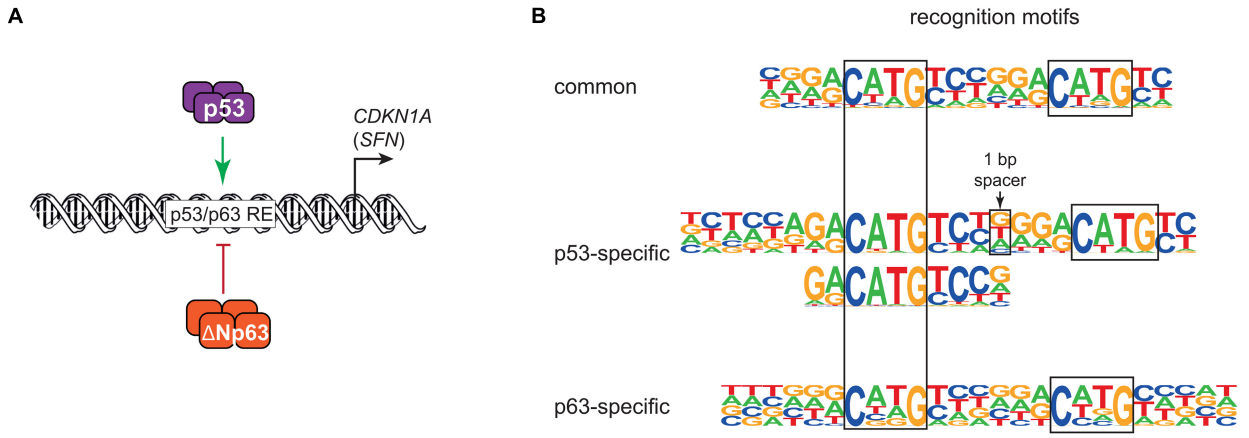

FIGURE 1 | (A) Simplified model of transcriptional repression by ΔNp63 and its dominant negative effect on p53, largely based on Westfall et al. (2003). **(B)** DNA motifs recognized either by both p53 and ΔNp63 (common) or solely by p53 or ΔNp63. Major motifs taken from Riege et al. (2020).

(Yu et al., 2021). Control of cell type-specific chromatin accessibility and gene expression is a feature shared by many other pioneer transcription factors (Iwafuchi-Doi and Zaret, 2014, 2016; Zaret and Mango, 2016). Unlike p53, p63 has a widespread role in establishing and maintaining accessible DNA at transcriptional regulatory regions associated with epithelial cell maturation (Bao et al., 2015; Kouwenhoven et al., 2015; Qu et al., 2018; Li et al., 2019; Lin-Shiao et al., 2019). The identification of p63 as a pioneer factor for epithelial-specific regulatory elements provides a direct molecular connection to the long-known genetic requirement for p63 in epithelial biology. We are just beginning to understand the specific contexts in which p53 and p63 use their pioneer factor activity, or don't (**Figures 2A,B**). Nucleosomes, and chromatin structure in general, remain a potent regulator of transcription factor activity, including the pioneers p53 and p63.

p53 AND p63 – DUELING RIVALS?

The initial model of ΔNp63 functioning as repressor and dominant negative regulator of its siblings was based on its missing TAD (Yang et al., 1998), and was fueled by experiments using reporter gene assays and exogenous expression of p63 or its siblings (Yang et al., 1998; Westfall et al., 2003; **Figure 1A**). Wild-type p53 and p63 are unlikely to form oligomers *in vivo* (Davison et al., 1999; Gaiddon et al., 2001), ruling out the formation of p53:p63 heterotetramers as a mechanism for any dominant negative activity. Notably, ΔNp63 was found to harbor alternative TADs that enable it to *trans*-activate genes (King et al., 2003; Helton et al., 2006). Results from the first integration of ΔNp63 ChIP-seq and transcriptomic data revealed ΔNp63 genome binding to be associated largely with *trans*-activation (Yang et al., 2006). Transcriptome analyses revealed that p63 and p53-regulated genes show only very little overlap (Gallant-Behm et al., 2012), which was inconsistent with ΔNp63 functioning as a negative regulator of its siblings. A broad meta-analysis of ChIP-seq and transcriptomic data corroborated that p63 and p53 regulate largely non-overlapping gene sets, and argue that ΔNp63 is more likely to activate than to repress its target genes (Riege et al., 2020). While genome-wide data revealed an essentially exclusive *trans*-activator function for p53 (Allen et al., 2014; Fischer et al., 2014, 2016a; Sullivan et al., 2018; Sammons et al., 2020), a *trans*-repressor function could not be ruled out for ΔNp63 (Yang et al., 2006; Riege et al., 2020). Interestingly, during epithelial cell maturation, ΔNp63 represses early surface ectoderm gene promoters presumably through chromatin looping-mediated recruitment of repressive histone modifications (Pattison et al., 2018), providing a novel mechanism for p63-mediated repression. The specific impact of this, and the ability of ΔNp63 to recruit negative transcriptional regulators like histone deacetylases and histone variants (LeBoeuf et al., 2010; Ramsey et al., 2011; Gallant-Behm et al., 2012), on p53 activity remains to be fully explored.

The predominant function of ΔNp63 as *trans*-activator and the small overlap between p63 and p53-regulated genes suggest any model of ΔNp63 functioning strictly as a dominant negative regulator of p53 cannot be upheld. p53 and p63 have many opportunities to regulate each other, given the high overlap in genomic binding locations (McDade et al., 2014; Riege et al., 2020). Importantly though, the 180 high-confidence direct ΔNp63 targets and 343 high-confidence direct p53 targets identified by meta-analyses of ChIP-seq and transcriptomic data (Fischer, 2017; Riege et al., 2020) contain an overlap of only 23 genes, 19 (>82%) of which are commonly up-regulated by p53 and Δ Np63.

Having this much organized data at hand, what do we know we about *CDKN1A* and *SFN*, the genes that initially fueled p53 and p63′s history of sibling rivalry (Westfall et al., 2003)? *CDKN1A* has been identified in essentially all p53 ChIP-seq and transcriptome profiling datasets as a direct p53 target gene. While ΔNp63 can bind to the *CDKN1A* promoter, only 4 and 3 out of 16 datasets on ΔNp63-dependent gene regulation identified ΔNp63 to significantly up and down-regulate *CDKN1A*, respectively. *SFN* was identified as a direct p53 and ΔNp63 target that is

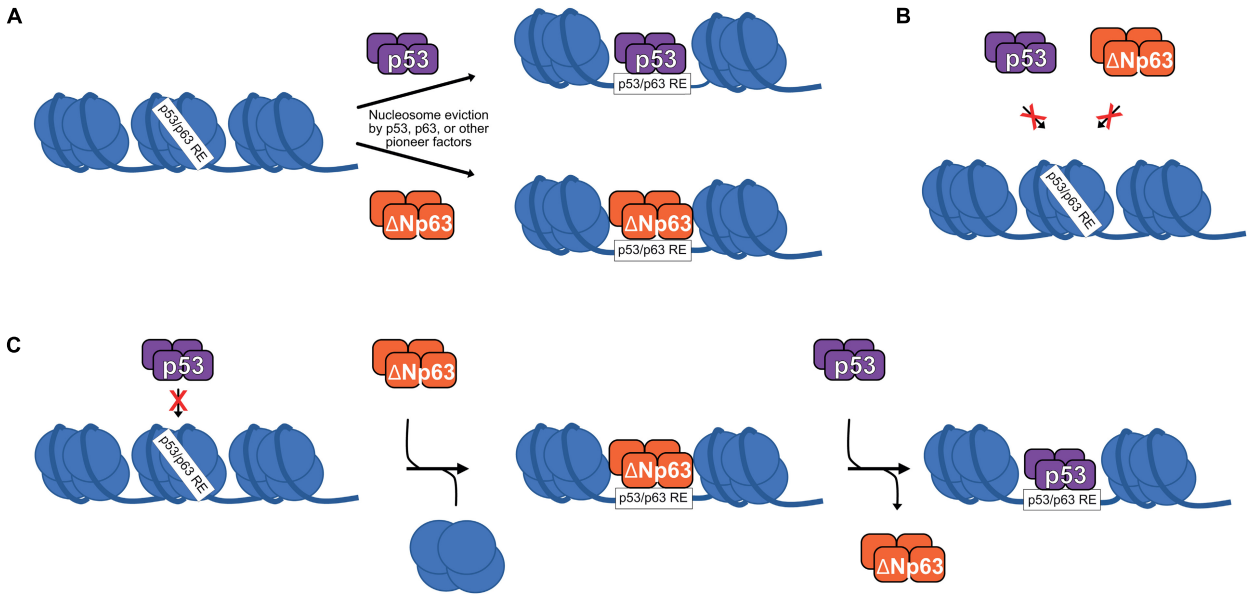

FIGURE 2 | (A) p53 and ΔNp63 can act as pioneer factors to evict/remodel nucleosomes and facilitate DNA accessibility, although other pioneer factors are likely responsible for nucleosome eviction at the majority of p53/ΔNp63 binding sites. **(B)** Certain nucleosome contexts, such as when the p53/p63 RE motif is near the nucleosome dyad, are recalcitrant to p53 and/or ΔNp63 pioneer factor activity and remain unbound (Yu and Buck, 2019; Yu et al., 2021). **(C)** In epithelial cell types, p53 DNA binding can be facilitated by ΔNp63's pioneer factor activity, although specific biochemical mechanisms are still being fully elucidated.

typically up-regulated by both siblings (Fischer, 2017; Riege et al., 2020). Together, these data suggest that the view of ΔNp63 functioning as a potent negative regulator of p53 can be rejected and replaced with a context-dependent model where ΔNp63 functions as either a *trans*-activator or a repressor depending on cell type and binding location. Future work will undoubtedly be focused on better defining the context for these opposing activities.

p53 AND p63 – COLLABORATIVE PARTNERS?

Although they appear to regulate a mostly unique set of target genes and have non-overlapping cellular roles, genetic evidence suggests that p53 and p63 cooperate to regulate DNA damage-induced apoptosis in mouse embryonic fibroblasts (Flores et al., 2002). p53 binds to cell cycle arrest target genes like *CDKN1A* in the absence of p63, but was unable to interact with promoters of the pro-apoptotic genes *NOXA* and *BAX* (Flores et al., 2002). The specific molecular mechanisms regulating this apparent collaborative effort for p53 and p63 are still unknown, but the recent identification of ΔNp63 as a pioneer transcription factor provides one possibility. p53 genomic binding and gene regulatory activity is expanded in epithelial cell types (McDade et al., 2014; Sammons et al., 2015; Nguyen et al., 2018; Karsli Uzunbas et al., 2019). These novel p53 binding sites have epithelial cell-specific DNA accessibility, have chromatin modifications associated with active enhancers, and, importantly, are strongly bound by ΔNp63. Inhibition of ΔNp63 leads to depletion of active transcription-associated hallmarks at these sites and diminishes the ability of p53 to activate nearby genes (Karsli Uzunbas et al., 2019). These sites are nucleosome rich with little to no DNA accessibility in the absence of ΔNp63 (Thurman et al., 2012), and p53 does not bind these sites in non-epithelial cell types (Nguyen et al., 2018; Karsli Uzunbas et al., 2019). Presumably, this is due to the ability of ΔNp63 to mediate local chromatin accessibility with its pioneer factor activity (Sammons et al., 2015; Karsli Uzunbas et al., 2019). Modulation of local and distal chromatin states, be it to facilitate transcriptional activation (Fessing et al., 2011; Bao et al., 2015; Li et al., 2019; Catizone et al., 2020) or repression (Gallant-Behm et al., 2012; Pattison et al., 2018) appears to be a key function of ΔNp63 and paves the way for the field to resolve many of the incongruent observations regarding ΔNp63's influence on p53.

OPPOSING DIRECTIONS IN TUMOR DEVELOPMENT

While current data suggest that p53 and ΔNp63 are more likely to cooperate than to compete at DNA, they remain functionally quite different. Perhaps most importantly, ΔNp63 promotes while p53 restricts cellular growth. As a consequence, ΔNp63 is a key oncogenic driver in squamous cell carcinoma (Campbell et al., 2018; Gatti et al., 2019) while p53 is the best-known tumor suppressor. The context-dependent tumor suppressor role of p63 (Flores et al., 2005; Keyes et al., 2006) appears to be largely reflected by the tumor suppressive function of the TAp63 isoform that induces apoptosis and senescence (Gressner et al., 2005; Suh et al., 2006; Guo et al., 2009). The contrary direction driven by p53 and ΔNp63 in tumor development can be explained on the one

hand by their unique target genes. While unique direct ΔNp63 target genes encode for several proteins that promote squamous cell cancer growth, inflammation, and invasion (Somerville et al., 2018, 2020; Riege et al., 2020), unique p53 target genes encode inducers of cell cycle arrest and apoptosis (Fischer, 2017). On the other hand, there is the large set of cell cycle genes differentially regulated by p53 and ΔNp63 (Riege et al., 2020). p53 employs its direct target gene *CDKN1A*, encoding the cyclin-dependent kinase inhibitor p21, to reactivate the cell cycle *trans*-repressor complexes DREAM and RB:E2F (Fischer et al., 2016a,b; Schade et al., 2019; Uxa et al., 2019). While it is not completely understood how ΔNp63 up-regulates cell cycle genes, it was suggested to inhibit the p21–p130 (DREAM) axis (Truong et al., 2006; McDade et al., 2011) and to *trans*-activate multiple cell cycle genes directly (Riege et al., 2020). We have a detailed picture of how p53 down-regulates cell cycle genes and sustains cell cycle arrest (Schade et al., 2019; Uxa et al., 2019). It remains unresolved, however, whether the regulation of cell cycle genes is cause or consequence of the growth-promoting function of ΔNp63, as it is well established that high expression of cell cycle genes is associated with cancer and worse prognosis (Whitfield et al., 2006). Together, the unique direct p53 and ΔNp63 target genes as well as the differential regulation of cell cycle genes elicited by p53 and ΔNp63 offer a partial, but direct, explanation for their opposing functions in tumor development.

DISCUSSION

Sibling rivalry can happen in any family and it is no different for the p53 transcription factor family. p63 was within p53′s considerably large shadow from the beginning, but p63 has started to step into the light with the discoveries of its clear genetic requirement during development, regulation of a pro-epithelial gene network, and pioneer activity. Now, what are the key questions that need to be addressed regarding the collaboration and competition between p53 and p63?

The other factors and precise context required for p53 and ΔNp63 to elicit productive binding to DNA and to regulate distinct target genes remain unclear. Although ΔNp63 occupies most sites that can be bound by p53, it appears to affect only a very small subset of the associated genes. It is unknown how ΔNp63 distinguishes between the many sites it activates, the smaller number of sites it represses, and the majority of sites it appears to not affect transcriptionally. Along those lines, when and where are p53 and ΔNp63 pioneer factors? The context and the extent to which pioneer activity is required for p53 family function remains an important and active area of investigation. And how collaborative is their oft-forgotten sibling p73?

Despite beginning their relationship as rivals, p53 and ΔNp63 appear to cooperate with each other when mutually beneficial. Identifying the situations when these two transcription factors are collaborators and when they are competitors may provide a blueprint to better understand mechanisms of how transcription factor families that share binding sites and target genes coordinate their efforts.

AUTHOR CONTRIBUTIONS

MS and MF conceptualized the manuscript and prepared the figures. DW, MS, and MF performed the literature review, provided an outline, wrote and edited the manuscript, and approved the submitted version. All authors contributed to the article and approved the submitted version.

FUNDING

This work was supported by grants from the National Institutes of Health (R35 GM138120 to MS and T32 GM132066 to DW). The publication of this manuscript was funded by the Open Access Fund of the Leibniz Association.

REFERENCES

Allen, M. A., Andrysik, Z., Dengler, V. L., Mellert, H. S., Guarnieri, A., Freeman, J. A., et al. (2014). Global analysis of p53-regulated transcription identifies its direct targets and unexpected regulatory mechanisms. *Elife* 3:e02200. doi: 10.7554/eLife.02200

Bao, X., Rubin, A. J., Qu, K., Zhang, J., Giresi, P. G., Chang, H. Y., et al. (2015). A novel ATAC-seq approach reveals lineage-specific reinforcement of the open chromatin landscape via cooperation between BAF and p63. *Genome Biol.* 16:284. doi: 10.1186/s13059-015-0840-9

Belyi, V. A., Ak, P., Markert, E., Wang, H., Hu, W., Puzio-Kuter, A., et al. (2010). The origins and evolution of the p53 family of genes. *Cold Spring Harb. Perspect. Biol.* 2:a001198. doi: 10.1101/cshperspect.a001198

Campbell, J. D., Yau, C., Bowlby, R., Liu, Y., Brennan, K., Fan, H., et al. (2018). Genomic, Pathway Network, and Immunologic Features Distinguishing Squamous Carcinomas. *Cell Rep.* 23, 194–212.e6. doi: 10.1016/j.celrep.2018.03.063

Catizone, A. N., Uzunbas, G. K., Celadova, P., Kuang, S., Bose, D., and Sammons, M. A. (2020). Locally acting transcription factors regulate p53-dependent cis-regulatory element activity. *Nucleic Acids Res.* 48, 4195–4213. doi: 10.1093/nar/gkaa147

Daino, K., Ichimura, S., and Nenoi, M. (2006). Both the basal transcriptional activity of the GADD45A gene and its enhancement after ionizing irradiation are mediated by AP-1 element. *Biochim. Biophys. Acta* 1759, 458–469. doi: 10.1016/j.bbaexp.2006.09.005

Davison, T. S., Vagner, C., Kaghad, M., Ayed, A., Caput, D., and Arrowsmith, C. H. (1999). p73 and p63 Are Homotetramers Capable of Weak Heterotypic Interactions with Each Other but Not with p53. *J. Biol. Chem.* 274, 18709–18714. doi: 10.1074/jbc.274.26.18709

Enthart, A., Klein, C., Dehner, A., Coles, M., Gemmecker, G., Kessler, H., et al. (2016). Solution structure and binding specificity of the p63 DNA binding domain. *Sci. Rep.* 6:26707. doi: 10.1038/srep26707

Espinosa, J. M., and Emerson, B. M. (2001). Transcriptional Regulation by p53 through Intrinsic DNA/Chromatin Binding and Site-Directed Cofactor Recruitment. *Mol. Cell* 8, 57–69. doi: 10.1016/S1097-2765(01)00283-0

Fessing, M. Y., Mardaryev, A. N., Gdula, M. R., Sharov, A. A., Sharova, T. Y., Rapisarda, V., et al. (2011). p63 regulates Satb1 to control tissue-specific chromatin remodeling during development of the epidermis. *J. Cell Biol.* 194, 825–839. doi: 10.1083/jcb.201101148

Fischer, M. (2017). Census and evaluation of p53 target genes. *Oncogene* 36, 3943–3956. doi: 10.1038/onc.2016.502

Fischer, M., Grossmann, P., Padi, M., and DeCaprio, J. A. (2016a). Integration of TP53, DREAM, MMB-FOXM1 and RB-E2F target gene analyses identifies cell cycle gene regulatory networks. *Nucleic Acids Res.* 44, 6070–6086. doi: 10.1093/nar/gkw523

Fischer, M., Quaas, M., Steiner, L., and Engeland, K. (2016b). The p53-p21-DREAM-CDE/CHR pathway regulates G2/M cell cycle genes. *Nucleic Acids Res.* 44, 164–174. doi: 10.1093/nar/gkv927

Fischer, M., Steiner, L., and Engeland, K. (2014). The transcription factor p53: not a repressor, solely an activator. *Cell Cycle* 13, 3037–3058. doi: 10.4161/15384101.2014.949083

Flores, E. R., Sengupta, S., Miller, J. B., Newman, J. J., Bronson, R., Crowley, D., et al. (2005). Tumor predisposition in mice mutant for p63 and p73: evidence for broader tumor suppressor functions for the p53 family. *Cancer Cell* 7, 363–373. doi: 10.1016/j.ccr.2005.02.019

Flores, E. R., Tsai, K. Y., Crowley, D., Sengupta, S., Yang, A., McKeon, F., et al. (2002). p63 and p73 are required for p53-dependent apoptosis in response to DNA damage. *Nature* 416, 560–564. doi: 10.1038/416560a

Gaiddon, C., Lokshin, M., Ahn, J., Zhang, T., and Prives, C. (2001). A Subset of Tumor-Derived Mutant Forms of p53 Down-Regulate p63 and p73 through a Direct Interaction with the p53 Core Domain. *Mol. Cell. Biol.* 21, 1874–1887. doi: 10.1128/MCB.21.5.1874-1887.2001

Gallant-Behm, C. L., Ramsey, M. R., Bensard, C. L., Nojek, I., Tran, J., Liu, M., et al. (2012). ΔNp63α represses anti-proliferative genes via H2A.Z deposition. *Genes Dev.* 26, 2325–2336. doi: 10.1101/gad.198069.112

Gatti, V., Fierro, C., Annicchiarico-Petruzzelli, M., Melino, G., and Peschiaroli, A. (2019). ΔNp63 in squamous cell carcinoma: defining the oncogenic routes affecting epigenetic landscape and tumour microenvironment. *Mol. Oncol.* 13, 981–1001. doi: 10.1002/1878-0261.12473

Gressner, O., Schilling, T., Lorenz, K., Schulze Schleithoff, E., Koch, A., Schulze-Bergkamen, H., et al. (2005). TAp63α induces apoptosis by activating signaling via death receptors and mitochondria. *EMBO J.* 24, 2458–2471. doi: 10.1038/sj.emboj.7600708

Guo, X., Keyes, W. M., Papazoglu, C., Zuber, J., Li, W., Lowe, S. W., et al. (2009). TAp63 induces senescence and suppresses tumorigenesis in vivo. *Nat. Cell Biol.* 11, 1451–1457. doi: 10.1038/ncb1988

Helton, E. S., Zhu, J., and Chen, X. (2006). The unique NH2-terminally deleted (DeltaN) residues, the PXXP motif, and the PPXY motif are required for the transcriptional activity of the DeltaN variant of p63. *J. Biol. Chem.* 281, 2533–2542. doi: 10.1074/jbc.M507964200

Iwafuchi-Doi, M., and Zaret, K. S. (2014). Pioneer transcription factors in cell reprogramming. *Genes Dev.* 28, 2679–2692. doi: 10.1101/gad.253443.114

Iwafuchi-Doi, M., and Zaret, K. S. (2016). Cell fate control by pioneer transcription factors. *Development* 143, 1833–1837. doi: 10.1242/dev.133900

Karsli Uzunbas, G., Ahmed, F., and Sammons, M. A. (2019). Control of p53-dependent transcription and enhancer activity by the p53 family member p63. *J. Biol. Chem.* 294, 10720–10736. doi: 10.1074/jbc.RA119.007965

Keyes, W. M., Vogel, H., Koster, M. I., Guo, X., Qi, Y., Petherbridge, K. M., et al. (2006). p63 heterozygous mutant mice are not prone to spontaneous or chemically induced tumors. *Proc. Natl. Acad. Sci. U. S. A.* 103, 8435–8440. doi: 10.1073/pnas.0602477103

King, K. E., Ponnamperuma, R. M., Yamashita, T., Tokino, T., Lee, L. A., Young, M. F., et al. (2003). deltaNp63alpha functions as both a positive and a negative transcriptional regulator and blocks in vitro differentiation of murine keratinocytes. *Oncogene* 22, 3635–3644. doi: 10.1038/sj.onc.1206536

Kouwenhoven, E. N., Oti, M., Niehues, H., van Heeringen, S. J., Schalkwijk, J., Stunnenberg, H. G., et al. (2015). Transcription factor p63 bookmarks and regulates dynamic enhancers during epidermal differentiation. *EMBO Rep.* 16, 863–878. doi: 10.15252/embr.201439941

Kouwenhoven, E. N., van Heeringen, S. J., Tena, J. J., Oti, M., Dutilh, B. E., Alonso, M. E., et al. (2010). Genome-Wide Profiling of p63 DNA–Binding Sites Identifies an Element that Regulates Gene Expression during Limb Development in the 7q21 SHFM1 Locus. *PLoS Genet.* 6:e1001065. doi: 10.1371/journal.pgen.1001065

Laptenko, O., Beckerman, R., Freulich, E., and Prives, C. (2011). p53 binding to nucleosomes within the p21 promoter in vivo leads to nucleosome loss and transcriptional activation. *Proc. Natl. Acad. Sci. U. S. A.* 108, 10385–10390. doi: 10.1073/pnas.1105680108

Laptenko, O., Shiff, I., Freed-Pastor, W., Zupnick, A., Mattia, M., Freulich, E., et al. (2015). The p53 C Terminus Controls Site-Specific DNA Binding and Promotes Structural Changes within the Central DNA Binding Domain. *Mol. Cell* 57, 1034–1046. doi: 10.1016/j.molcel.2015.02.015

LeBoeuf, M., Terrell, A., Trivedi, S., Sinha, S., Epstein, J. A., Olson, E. N., et al. (2010). Hdac1 and Hdac2 act redundantly to control p63 and p53 functions in epidermal progenitor cells. *Dev. Cell* 19, 807–818. doi: 10.1016/j.devcel.2010.10.015

Li, L., Wang, Y., Torkelson, J. L., Shankar, G., Pattison, J. M., Zhen, H. H., et al. (2019). TFAP2C- and p63-Dependent Networks Sequentially Rearrange Chromatin Landscapes to Drive Human Epidermal Lineage Commitment. *Cell Stem Cell* 24, 271–284.e8. doi: 10.1016/j.stem.2018.12.012

Lin, Y.-L., Sengupta, S., Gurdziel, K., Bell, G. W., Jacks, T., and Flores, E. R. (2009). p63 and p73 transcriptionally regulate genes involved in DNA repair. *PLoS Genet.* 5:e1000680. doi: 10.1371/journal.pgen.1000680

Lin-Shiao, E., Lan, Y., Welzenbach, J., Alexander, K. A., Zhang, Z., Knapp, M., et al. (2019). p63 establishes epithelial enhancers at critical craniofacial development genes. *Sci. Adv.* 5:eaaw0946. doi: 10.1126/sciadv.aaw0946

Lokshin, M., Li, Y., Gaiddon, C., and Prives, C. (2007). p53 and p73 display common and distinct requirements for sequence specific binding to DNA. *Nucleic Acids Res.* 35, 340–352. doi: 10.1093/nar/gkl1047

McDade, S. S., Henry, A. E., Pivato, G. P., Kozarewa, I., Mitsopoulos, C., Fenwick, K., et al. (2012). Genome-wide analysis of p63 binding sites identifies AP-2 factors as co-regulators of epidermal differentiation. *Nucleic Acids Res.* 40, 7190–7206. doi: 10.1093/nar/gks389

McDade, S. S., Patel, D., and McCance, D. J. (2011). p63 maintains keratinocyte proliferative capacity through regulation of Skp2-p130 levels. *J. Cell Sci.* 124, 1635–1643. doi: 10.1242/jcs.084723

McDade, S. S., Patel, D., Moran, M., Campbell, J., Fenwick, K., Kozarewa, I., et al. (2014). Genome-wide characterization reveals complex interplay between TP53 and TP63 in response to genotoxic stress. *Nucleic Acids Res.* 42, 6270–6285. doi: 10.1093/nar/gku299

Mills, A. A., Zheng, B., Wang, X. J., Vogel, H., Roop, D. R., and Bradley, A. (1999). P63 Is a P53 Homologue Required for Limb and Epidermal Morphogenesis. *Nature* 398, 708–713. doi: 10.1038/19531

Murray-Zmijewski, F., Lane, D. P., and Bourdon, J.-C. (2006). P53/P63/P73 Isoforms: an Orchestra of Isoforms To Harmonise Cell Differentiation and Response To Stress. *Cell Death Differ.* 13, 962–972. doi: 10.1038/sj.cdd.4401914

Nemajerova, A., Amelio, I., Gebel, J., Dötsch, V., Melino, G., and Moll, U. M. (2018). Non-oncogenic roles of TAp73: from multiciliogenesis to metabolism. *Cell Death Differ.* 25:144. doi: 10.1038/CDD.2017.178

Nguyen, T.-A. T., Grimm, S. A., Bushel, P. R., Li, J., Li, Y., Bennett, B. D., et al. (2018). Revealing a human p53 universe. *Nucleic Acids Res.* 46, 8153–8167. doi: 10.1093/nar/gky720

Ortt, K., and Sinha, S. (2006). Derivation of the consensus DNA-binding sequence for p63 reveals unique requirements that are distinct from p53. *FEBS Lett.* 580, 4544–4550. doi: 10.1016/j.febslet.2006.07.004

Pattison, J. M., Melo, S. P., Piekos, S. N., Torkelson, J. L., Bashkirova, E., Mumbach, M. R., et al. (2018). Retinoic acid and BMP4 cooperate with p63 to alter chromatin dynamics during surface epithelial commitment. *Nat. Genet.* 50:1658. doi: 10.1038/s41588-018-0263-0

Perez, C. A., Ott, J., Mays, D. J., and Pietenpol, J. A. (2007). p63 consensus DNA-binding site: identification, analysis and application into a p63MH algorithm. *Oncogene* 26, 7363–7370. doi: 10.1038/sj.onc.1210561

Qu, J., Tanis, S. E. J., Smits, J. P. H., Kouwenhoven, E. N., Oti, M., van den Bogaard, E. H., et al. (2018). Mutant p63 Affects Epidermal Cell Identity through Rewiring the Enhancer Landscape. *Cell Rep.* 25, 3490–3503.e4. doi: 10.1016/j.celrep.2018.11.039

Ramsey, M. R., He, L., Forster, N., Ory, B., and Ellisen, L. W. (2011). Physical association of HDAC1 and HDAC2 with p63 mediates transcriptional repression and tumor maintenance in squamous cell carcinoma. *Cancer Res.* 71, 4373–4379. doi: 10.1158/0008-5472.CAN-11-0046

Riege, K., Kretzmer, H., Sahm, A., McDade, S. S., Hoffmann, S., and Fischer, M. (2020). Dissecting the DNA binding landscape and gene regulatory network of p63 and p53. *Elife* 9:e63266. doi: 10.7554/eLife.63266

Rutkowski, R., Hofmann, K., and Gartner, A. (2010). Phylogeny and Function of the Invertebrate p53 Superfamily. *Cold Spring Harb. Perspect. Biol.* 2:a001131. doi: 10.1101/cshperspect.a001131

Sahu, G., Wang, D., Chen, C. B., Zhurkin, V. B., Harrington, R. E., Appella, E., et al. (2010). p53 binding to nucleosomal DNA depends on the rotational positioning of DNA response element. *J. Biol. Chem.* 285, 1321–1332. doi: 10.1074/jbc.M109.081182

Sammons, M. A., Nguyen, T.-A. T., McDade, S. S., and Fischer, M. (2020). Tumor suppressor p53: from engaging DNA to target gene regulation. *Nucleic Acids Res.* 48, 8848–8869. doi: 10.1093/nar/gkaa666

Sammons, M. A., Zhu, J., Drake, A. M., and Berger, S. L. (2015). TP53 engagement with the genome occurs in distinct local chromatin environments via pioneer factor activity. *Genome Res.* 25, 179–188. doi: 10.1101/gr.181883.114

Sauer, M., Bretz, A. C., Beinoraviciute-Kellner, R., Beitzinger, M., Burek, C., Rosenwald, A., et al. (2008). C-terminal diversity within the p53 family accounts for differences in DNA binding and transcriptional activity. *Nucleic Acids Res.* 36, 1900–1912. doi: 10.1093/nar/gkn044

Schade, A. E., Fischer, M., and DeCaprio, J. A. (2019). RB, p130 and p107 differentially repress G1/S and G2/M genes after p53 activation. *Nucleic Acids Res.* 47, 11197–11208. doi: 10.1093/nar/gkz961

Somerville, T. D., Biffi, G., Daßler-Plenker, J., Hur, S. K., He, X.-Y., Vance, K. E., et al. (2020). Squamous trans-differentiation of pancreatic cancer cells promotes stromal inflammation. *Elife* 9:e53381. doi: 10.7554/eLife.53381

Somerville, T. D. D., Xu, Y., Miyabayashi, K., Tiriac, H., Cleary, C. R., Maia-Silva, D., et al. (2018). TP63-Mediated Enhancer Reprogramming Drives the Squamous Subtype of Pancreatic Ductal Adenocarcinoma. *Cell Rep.* 25, 1741–1755.e7. doi: 10.1016/j.celrep.2018.10.051

Suh, E.-K., Yang, A., Kettenbach, A., Bamberger, C., Michaelis, A. H., Zhu, Z., et al. (2006). p63 protects the female germ line during meiotic arrest. *Nature* 444, 624–628. doi: 10.1038/nature05337

Sullivan, K. D., Galbraith, M. D., Andrysik, Z., and Espinosa, J. M. (2018). Mechanisms of transcriptional regulation by p53. *Cell Death Differ.* 25, 133–143. doi: 10.1038/cdd.2017.174

Thurman, R. E., Rynes, E., Humbert, R., Vierstra, J., Maurano, M. T., Haugen, E., et al. (2012). The accessible chromatin landscape of the human genome. *Nature* 489, 75–82. doi: 10.1038/nature11232

Tichý, V., Navrátilová, L., Adámik, M., Fojta, M., and Brázdová, M. (2013). Redox state of p63 and p73 core domains regulates sequence-specific DNA binding. *Biochem. Biophys. Res. Commun.* 433, 445–449. doi: 10.1016/j.bbrc.2013.02.097

Truong, A. B., Kretz, M., Ridky, T. W., Kimmel, R., and Khavari, P. A. (2006). p63 regulates proliferation and differentiation of developmentally mature keratinocytes. *Genes Dev.* 20, 3185–3197. doi: 10.1101/gad.1463206

Uxa, S., Bernhart, S. H., Mages, C. F. S., Fischer, M., Kohler, R., Hoffmann, S., et al. (2019). DREAM and RB cooperate to induce gene repression and cell-cycle arrest in response to p53 activation. *Nucleic Acids Res.* 47, 9087–9103. doi: 10.1093/nar/gkz635

Venkatachalam, S., Shi, Y. P., Jones, S. N., Vogel, H., Bradley, A., Pinkel, D., et al. (1998). Retention of wild-type p53 in tumors from p53 heterozygous mice: reduction of p53 dosage can promote cancer formation. *EMBO J.* 17, 4657–4667. doi: 10.1093/emboj/17.16.4657

Westfall, M. D., Mays, D. J., Sniezek, J. C., and Pietenpol, J. A. (2003). The Np63 Phosphoprotein Binds the p21 and 14-3-3 Promoters In Vivo and Has Transcriptional Repressor Activity That Is Reduced by Hay-Wells Syndrome-Derived Mutations. *Mol. Cell. Biol.* 23, 2264–2276. doi: 10.1128/MCB.23.7.2264-2276.2003

Whitfield, M. L., George, L. K., Grant, G. D., and Perou, C. M. (2006). Common markers of proliferation. *Nat. Rev. Cancer* 6, 99–106.

Yang, A., Kaghad, M., Wang, Y., Gillett, E., Fleming, M. D., Dötsch, V., et al. (1998). P63, a P53 Homolog At 3Q27–29, Encodes Multiple Products With Transactivating, Death-Inducing, and Dominant-Negative Activities. *Mol. Cell* 2, 305–316. doi: 10.1016/S1097-2765(00)80275-0

Yang, A., Schweitzer, R., Sun, D., Kaghad, M., Walker, N., Bronson, R. T., et al. (1999). p63 is essential for regenerative proliferation in limb, craniofacial and epithelial development. *Nature* 398, 714–718. doi: 10.1038/19539

Yang, A., Zhu, Z., Kapranov, P., McKeon, F., Church, G. M., Gingeras, T. R., et al. (2006). Relationships between p63 Binding, DNA Sequence, Transcription Activity, and Biological Function in Human Cells. *Mol. Cell* 24, 593–602. doi: 10.1016/j.molcel.2006.10.018

Younger, S. T., and Rinn, J. L. (2017). p53 regulates enhancer accessibility and activity in response to DNA damage. *Nucleic Acids Res.* 45, 9889–9900. doi: 10.1093/nar/gkx577

Yu, X., and Buck, M. J. (2019). Defining TP53 pioneering capabilities with competitive nucleosome binding assays. *Genome Res.* 29, 107–115. doi: 10.1101/gr.234104.117

Yu, X., Singh, P. K., Tabrejee, S., Sinha, S., and Buck, M. J. (2021). ΔNp63 is a pioneer factor that binds inaccessible chromatin and elicits chromatin remodeling. *Epigenetics Chromatin* 14:20. doi: 10.1186/s13072-021-00394-8

Zaret, K. S., and Mango, S. E. (2016). Pioneer transcription factors, chromatin dynamics, and cell fate control. *Curr. Opin. Genet. Dev.* 37, 76–81. doi: 10.1016/j.gde.2015.12.003

Conflict of Interest: The authors declare that the research was conducted in the absence of any commercial or financial relationships that could be construed as a potential conflict of interest.

Copyright © 2021 Woodstock, Sammons and Fischer. This is an open-access article distributed under the terms of the Creative Commons Attribution License (CC BY). The use, distribution or reproduction in other forums is permitted, provided the original author(s) and the copyright owner(s) are credited and that the original publication in this journal is cited, in accordance with accepted academic practice. No use, distribution or reproduction is permitted which does not comply with these terms.

frontiers in Cell and Developmental Biology

REVIEW
published: 23 July 2021
doi: 10.3389/fcell.2021.716957

p73 as a Tissue Architect

Laura Maeso-Alonso[1], Lorena López-Ferreras[1], Margarita M. Marques[2†] and Maria C. Marin[1*†]*

[1] Departamento de Biología Molecular, Instituto de Biomedicina (IBIOMED), University of León, León, Spain, [2] Departamento de Producción Animal, Instituto de Desarrollo Ganadero y Sanidad Animal, University of León, León, Spain

The *TP73* gene belongs to the p53 family comprised by p53, p63, and p73. In response to physiological and pathological signals these transcription factors regulate multiple molecular pathways which merge in an ensemble of interconnected networks, in which the control of cell proliferation and cell death occupies a prominent position. However, the complex phenotype of the *Trp73* deficient mice has revealed that the biological relevance of this gene does not exclusively rely on its growth suppression effects, but it is also intertwined with other fundamental roles governing different aspects of tissue physiology. p73 function is essential for the organization and homeostasis of different complex microenvironments, like the neurogenic niche, which supports the neural progenitor cells and the ependyma, the male and female reproductive organs, the respiratory epithelium or the vascular network. We propose that all these, apparently unrelated, developmental roles, have a common denominator: p73 function as a tissue architect. Tissue architecture is defined by the nature and the integrity of its cellular and extracellular compartments, and it is based on proper adhesive cell-cell and cell-extracellular matrix interactions as well as the establishment of cellular polarity. In this work, we will review the current understanding of p73 role as a neurogenic niche architect through the regulation of cell adhesion, cytoskeleton dynamics and Planar Cell Polarity, and give a general overview of TAp73 as a hub modulator of these functions, whose alteration could impinge in many of the *Trp73*$^{-/-}$ phenotypes.

Keywords: p53-family, p73, tissue architecture, cell adhesion, actin cytoskeleton, cell polarity, central nervous system development, neurogenic niche

OPEN ACCESS

Edited by:
Brigitte M. Pützer, University Hospital Rostock, Germany

Reviewed by:
Stella Logotheti, University of Rostock, Germany
Xinbin Chen, University of California, Davis, United States

***Correspondence:**
Margarita M. Marques
mmarm@unileon.es
Maria C. Marin
carmen.marin@unileon.es

† These authors have contributed equally to this work and share senior authorship

Specialty section:
This article was submitted to Molecular and Cellular Pathology, a section of the journal Frontiers in Cell and Developmental Biology

Received: *29 May 2021*
Accepted: *28 June 2021*
Published: *23 July 2021*

Citation:
Maeso-Alonso L, López-Ferreras L, Marques MM and Marin MC (2021) p73 as a Tissue Architect. Front. Cell Dev. Biol. 9:716957. doi: 10.3389/fcell.2021.716957

INTRODUCTION

The *TP73* gene belongs to an evolutionary conserved family of transcription factors, the p53 family, with key functions to vertebrate's biology. The genes that constitute this family, *TP53, TP63,* and *TP73*, have evolved from a common ancestor and, consequently, share a similar modular structure which consists of an amino-terminal transactivation domain (TAD), a central DNA binding domain (DBD) and a carboxy-terminal oligomerization domain (OD) (Dötsch et al., 2010). Although *TP53* was the first member of the family to be discovered (Lane and Crawford, 1979; Levine, 2020), *TP63* and *TP73* are the evolutionary older homologs (Kaghad et al., 1997; Yang et al., 1998; Belyi et al., 2010; Chillemi et al., 2017) and differ from *TP53* in that the full-length proteins that they encode contain a carboxy-terminal sterile a-motif (SAM) domain. This C-terminal region, involved in protein–protein interaction, might give p63 and p73 their unique signaling network of regulators and transcriptional targets (Serber et al., 2002; Straub et al., 2010). In addition, due to alternative

splicing of the N-terminal and C-terminal regions and to the use of cryptic promoters, the *TP73* and *TP63* genes can be expressed as transcriptionally competent TA-isoforms or as N-terminally deleted DN-isoforms. Moreover, multiple alternative splicing at the 3′ region of the pre-RNA can give rise to C-terminal isoforms which, in the case of p63 and p73, can include the SAM domain (Vikhreva et al., 2018).

The first studied function of p73 was its p53-like growth suppressor capacity (Jost et al., 1997). Even though p53 is the central regulator of the cellular genomic integrity, TAp73 isoforms can perform similar functions in response to stress. Following DNA damage, TAp73 generates a coordinated response that induces either cell cycle arrest and DNA repair mechanisms, or provokes cell elimination signals leading to apoptosis or senescence (Pflaum et al., 2014). These p53-like responses, executed through the activation of target genes shared with p53, are known as p73-canonical functions. However, elimination of these canonical functions could not account for all the phenotypes observed in the knockout mice lacking all p73 isoforms, the *Trp73*$^{-/-}$ (Yang et al., 2000). These animals display multiple maladies, including gastrointestinal and cranial hemorrhages, rhinitis, hippocampus dysgenesis and enlarged ventricles, female and male infertility, chronic infection and inflammation in lungs, sinus, and ears, and runting (Yang et al., 2000). Several laboratories, including ours, have demonstrated that the biological relevance of p73 does not exclusively rely on its growth suppression effects (Pflaum et al., 2014), but also on p73-non-canonical functions. Some of these functions, like the regulation of cell adhesion establishment, cytoskeleton dynamics, multiciliogenesis and Planar Cell Polarity (PCP) are related to the maintenance of the structural organization and homeostasis of different complex microenvironments, like the neurogenic niche and the ependymal barrier in the central nervous system (CNS), the respiratory and reproductive epithelia, or the vascular network. Thus, important questions arise: How does p73 orchestrate such an ample array of biological processes? Are there some common molecular functions underlying these phenotypes? May this p73 fundamental role be related to the organization of epithelia, a hallmark tissue of metazoans? Could this function represent a primitive p53/p63/p73-ancestor ability kept by p73 throughout evolution, and which is now fundamental in mammals?

DIVERSIFYING BIOLOGICAL ACTIVITIES: THE YING-YANG MODE OF ACTION OF p73 ISOFORMS

As mentioned before, the *Trp73* gene gives raise to functionally different TA and DNp73 isoforms (Candi et al., 2014). TAp73 proteins can transactivate canonical-p53 targets as well as non-p53 related genes involved in development and/or other cell growth associated functions (Engelmann et al., 2015; Wang et al., 2020). TA-isoforms differ in their transactivation efficiency and target gene specificity depending on their carboxy terminus (De Laurenzi et al., 1998; Ueda et al., 1999). Thus, TAp73 function will vary in a cell-context dependent manner and greatly depending upon their C-terminal domain (Logotheti et al., 2013; Vikhreva et al., 2018). Conversely, DN-isoforms can act as dominant-negative inhibitors of p53 and TAp73 and thus, have oncogenic properties (Ishimoto et al., 2002; Engelmann and Pützer, 2014), but they also carry out their own distinct p53/TAp73-independent transcriptional activities (Marqués-García et al., 2009; Wetterskog et al., 2009; Niemantsverdriet et al., 2012). The generation of transactivation-deficient DN-isoforms from the *TP73* gene is quite complex and has been reviewed elsewhere (Murray-Zmijewski et al., 2006; Engelmann et al., 2015). Briefly, there are two types of DN-p73 isoforms, the ones that originate from differential splicing events at the 5′-end of P1-derived transcripts (ΔEx2p73, ΔEx2/3p73, ΔN′p73; generally called ΔTA), and DN-isoforms, *per se*, which arise from the alternative P2 promoter within intron 3 (Stiewe et al., 2002; Buhlmann and Pützer, 2008; Engelmann et al., 2015). Even though most DN-isoforms are transcriptionally inactive, there are reports indicating that the 13 unique residues of DNp73 β and γ, together with the N-terminal PXXP motifs, constitute a novel activation domain capable of inducing some p53 target genes (Liu et al., 2004).

A detailed analysis of the total *Trp73*$^{-/-}$ mice revealed a wide range of novel p73 physiological roles governing different aspects of cell and tissue physiology. However, p73 bimodal function has difficulted the identification of the responsible isoform for each of the observed phenotypes. The generation of isoform-specific knockout mice has provided a useful tool to disentangle some of the p73 isoforms-specific activities in various tissues and cellular processes, endorsing the proposed isoform-based model of p73 function.

Beginning with p73 tumor suppressor function, TAp73 deficient mice revealed an increased predisposition to spontaneous tumorigenesis (Tomasini et al., 2008), demonstrating the role of TAp73 as a tumor suppressor and substantiating previous reports of enhanced rate of spontaneous tumors in *Trp73* ± mice (Flores et al., 2005). On the other hand, elimination of DNp73 greatly inhibits tumor-forming capacity *in vivo* (Wilhelm et al., 2010). In this Ying-Yang model, while DNp73 possesses oncogenic properties that include impairment of the DNA damage-response pathway, cellular immortalization, as well as a dominant negative function of the p53/TAp73-canonical functions (Petrenko et al., 2003; Wilhelm et al., 2010; Billant et al., 2016), TAp73 tumor suppressor activity mainly relies on p53-canonical functions, like its ability to induce cell cycle arrest, apoptosis or regulation of DNA damage response, as well as other functions like immune cell regulation (Tomasini et al., 2008; Costanzo et al., 2014; Wolfsberger et al., 2021). It is noteworthy that TAp73, unexpectedly, activates anabolic pathways compatible with proliferation and promotion of cancer cells by regulating glucose metabolism to control cellular biosynthetic pathways and antioxidant capacity (Du et al., 2013; Fets and Anastasiou, 2013; Amelio et al., 2014). However, whether this metabolic effect reflects cancer-associated metabolic changes, or instead suggests a role for TAp73 in promoting adaptative cellular mechanisms to stress conditions (Agostini et al., 2014; Marini et al., 2018), remains to be determined and has been reviewed elsewhere (Nemajerova et al., 2018). Nevertheless,

the lack of these p73-associated functions could not explain many of the cytoarchitecture alterations resulting from p73 deficiency *in vivo*.

In morphologically complex animals such as mammals, the establishment and maintenance of tissue structure and function, known as tissular architecture (Hagios et al., 1998), regulates the development and functionality of organs such as the digestive, respiratory, reproductive, neural, sensory, and vascular systems (Rodriguez-Boulan and Macara, 2014). Consequently, it would be expected that the disruption of a gene involved in tissue architecture could result in a plethora of developmental defects, such as the ones observed in the *Trp73*$^{-/-}$ mice. Thus, we propose that some of the, apparently unrelated, phenotypes showed by these mice could reflect p73 requirement in the maintenance of functional tissue organization and we ask whether this task could represent one of the original roles of the p53/p63/p73-ancestor.

EVOLUTION OF THE p53 GENE FAMILY AND THE EMERGENCE OF TISSULAR ARCHITECTURE

Identifying the original p53/p63/p73-ancestor functions might be elusive since data on the molecular characterization or function of most of these proteins are lacking. However, a canvass of the published data regarding consensus phylogenetic trees, together with the evidence of the p53 family presence spanning the early Metazoa through the primates, can lead to propose that the organization of the epithelia could be a primitive p73-function, since the appearance of the ancestral p73 paralogs seems to coincide with the phylogenetic emergence and organization of the epithelia (Belyi et al., 2010; Rutkowski et al., 2010; Åberg et al., 2017; **Figure 1**).

Within the animal kingdom, p53-family sequences are encoded in almost all sequenced genomes. The most primitive multicellular organisms encoding p53/p63/p73-ancestor-like proteins are the cnidaria starlet sea anemone *Nematostella vectensis,* and the placozoa *Trichoplax adherens* (Rutkowski et al., 2010). In these basal animals with radial symmetry, the ancestral gene is most closely related to a combined p63/p73-like gene (Belyi et al., 2010), and one or more ancestor sequences are found, while the radiation into p53, p63, and p73 protein coding genes has been described as a vertebrate event (Rutkowski et al., 2010; **Figure 1**).

It is precisely in placozoa where the p53/p63/p73-ancestor's TAD first appeared and thus, the transactivation function (Åberg et al., 2017). Based on the presence of the conserved SAM domain and the greater sequence similarity between the vertebrate p63 and invertebrate p53/p63/p73-ancestor, an initial study suggested that the ancestral and invertebrate function of p53/p63/p73 mainly resembled the p63 vertebrate function (Rutkowski et al., 2010). However, a subsequent detailed phylogenetic analysis with a particular focus on the TAD led to the hypothesis that, since all three family members are equally evolutionarily close to the p53/p63/p73-ancestor, some of its primitive functions would be similar to that of p63, while others would resemble typical p53-functions and still others, not yet identified, could be p73-related functions (Åberg et al., 2017). So, which are these p73-related functions?

In *N. vectensis*, an invertebrate model susceptible to genetic analysis, it was shown that the p53/p63/p73-ancestor gene responds to DNA damage, causing apoptosis in its gametes (Pankow and Bamberger, 2007). These experiments prompted the idea that one of the functions of the p53/p63/p73-ancestor could be to trigger apoptosis in response to DNA damage to eliminate damaged germ cells (Pankow and Bamberger, 2007). This role, preserving genome stability of female germ cells, has been kept in mammals by p63 (Suh et al., 2006; Tomasini et al., 2008; Deutsch et al., 2011) where it serves as a quality control (QC) factor that ensures elimination of damaged oocytes before they can be recruited for ovulation (Suh et al., 2006; Livera et al., 2008). This QC function probably evolved into p53 tumor suppression function when more complex organisms required preservation of the somatic cells genome to prevent cancer (Levine, 2020).

Interestingly, p73, which is also involve in orchestrating germ cell maintenance, appears to exert this function not only through a QC mechanism, but also through the maintenance of the cytoarchitecture that provides the nurturing environment required during spermatogenesis (Holembowski et al., 2014; Inoue et al., 2014) and during the ovarian follicle development (Santos Guasch et al., 2018). This is in accordance with the idea that the regulation of tissue architecture could be one of the functions of the p53/p63/p73-ancestor that has been kept in vertebrate-p73. Nevertheless, whether p53/p63/p73-ancestor is required for epithelial organization in *N. vectensis*, or if the knockdown of the protein would result in defects in germ line maturation of this organism, remains unknown and further functional experiments are required.

The p53/p63/p73-ancestor role as a tissue organizer is supported by its apparent coincidental emergence with the primitive "true" epithelium, which first evolved in Placozoan and Cnidaria (Cereijido et al., 2004; Srivastava et al., 2008; Adams et al., 2010; **Figure 1**). True occluding epithelia are defined by cells that display an aligned polarity, are connected by belt-forming junctions that anchor the cytoskeleton and are associated with extracellular matrix (ECM) basal lamina (Fahey and Degnan, 2010). The placozoa *Trichoplax adhaerens*, which encodes the p53/p63/p73-ancestor like protein, is considered to have true occluding epithelia (Srivastava et al., 2008; Adams et al., 2010). It has an asymmetric epithelial bilayer with cells joined by apical junctions that manifest features of the Eumetazoa's epithelia (Smith and Mayorova, 2019). In addition, its genome also encodes cell-surface adhesion proteins, all polarity complex members, a diverse set of genes that code for putative ECM proteins, as well as cytoskeleton linker proteins (Srivastava et al., 2008; Belahbib et al., 2018). Moreover, the ZO genes, which encode the ZO1-3 scaffold proteins of the tight junction, surge in Placozoa and are expanded in the Craniata (González-Mariscal et al., 2011).

The epithelium constitutes the core tissues of all metazoans, and it is the fundamental building block of all animal's body structural design and function (Miller et al., 2013). The

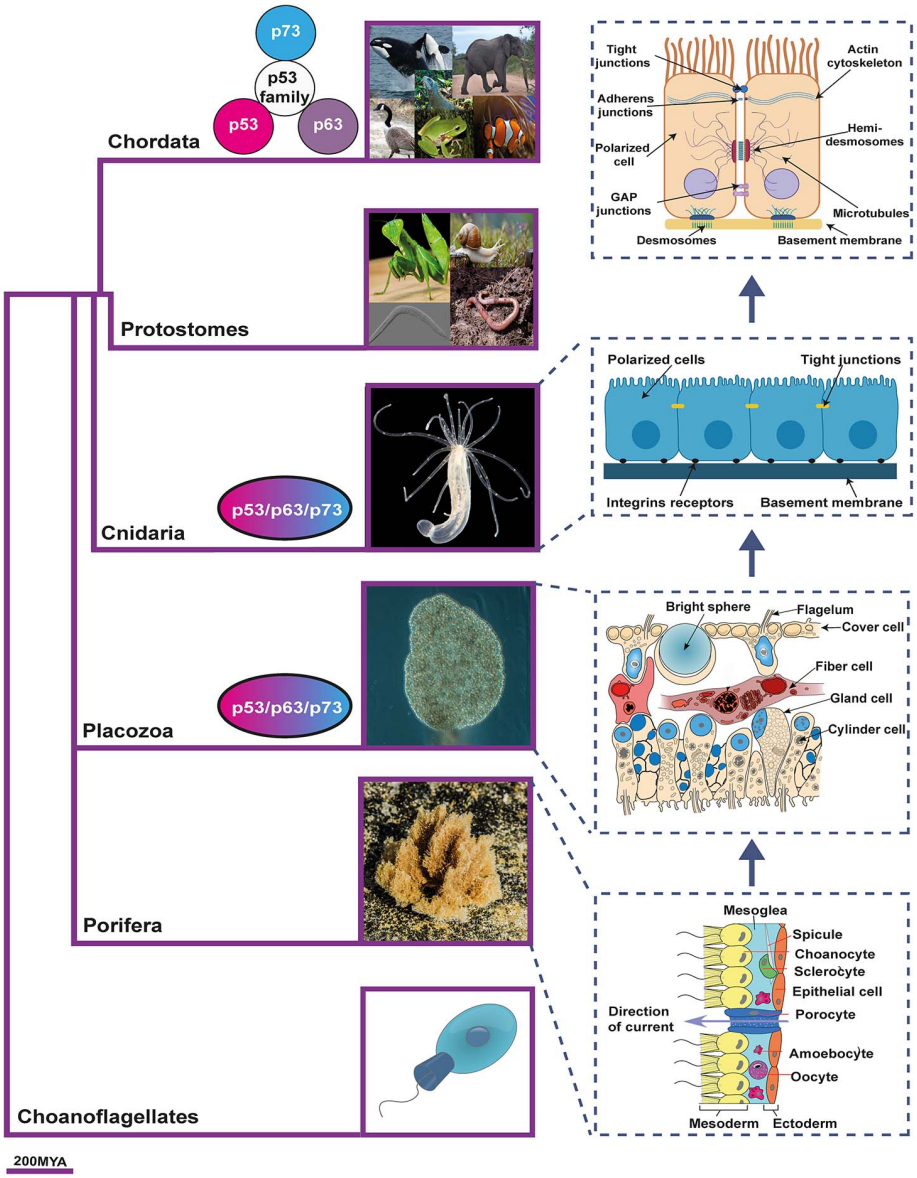

FIGURE 1 | The emergence of epithelia and the proposed relationship with p53 family members phylogeny. p53/p63/p73-ancestor proteins appear for the first time in Placozoan and Cnidaria. Coincidentally, these organisms are the first ones to fulfill the three criteria that distinguish the "true" epithelial phenotype: i) cells displaying aligned polarity; ii) cells connected by belt-forming junctions; and iii) cells associated with extracellular matrix, with a basal lamina. As vertebrates develop, the p53/p63/p73-ancestor gave rise to the three members of the p53 family. The phylogenetic tree is based on Timetree public knowledge-base. The pictures were created with BioRender.com. Photos were a courtesy of Robert Aguilar, Smithsonian Environmental Research Center, United States (https://commons.wikimedia.org/wiki/File:Nematostella_vectensis_(l1419)_999_(30695685804).jpg) and Bernd Schierwater, Institute of Animal Ecology and Cell Biology, Hannover (Germany). https://commons.wikimedia.org/wiki/File:Trichoplax_adhaerens_photograph.png.

establishment and maintenance of tissular architecture requires the correct arrangement of the epithelial cells maintaining their central features: apico-basal cell polarity, cell-cell junctions and basal lamina, as well as their associated signaling complexes. Hence, architecture depends upon the organization of cell adhesion complexes, which hold epithelial cells together and connect them with the environment, as well as on the establishment and maintenance of an epithelial polarity program, including cellular cytoskeleton polarity. All these processes have been associated to p73 function in a variety of *in vitro* and *in vivo* models and could constitute the groundwork for its role as tissue organizer in several microenvironments (Zhang et al., 2012; Medina-Bolívar et al., 2014; Gonzalez-Cano et al., 2016; Fuertes-Alvarez et al., 2018; Santos Guasch et al., 2018). In this work, we will review the current understanding of p73 role as a brain architect. In particular, we will focus on the architecture of the subventricular neurogenic niche, which is of crucial importance for the maintenance of

neural stem cell identity and for their neurogenic potential (Morante-Redolat and Porlan, 2019).

p73 FUNDAMENTAL ROLE IN MOUSE BRAIN DEVELOPMENT

The role of p73 in the development of the CNS was recognized early on based on the profound defects of the total *Trp73*$^{-/-}$ mice (Yang et al., 2000). These animals suffer from severe progressive *ex vacuo* hydrocephalus, hippocampal dysgenesis with abnormalities in the pyramidal cell layers (CA1 and CA3) and in the dentate gyrus, and loss of Cajal-Retzius (CR) neurons (Killick et al., 2011). However, the distinct elimination in the isoform-specific knockouts (TAp73KO and DNp73KO), generates subtle effects, and some of the phenotypes detected in the *Trp73*$^{-/-}$ mice do not even appear in them (Tomasini et al., 2008; Tissir et al., 2009; Wilhelm et al., 2010). This is likely the reflection of either compensatory or redundant mechanisms in the absence of one of the isoforms, and/or possible differences in the genetic background of the mice models (Murray-Zmijewski et al., 2006). This, together with the ability of some isoforms to interact and regulate each other (Murray-Zmijewski et al., 2006), makes the study of the biological functions of this gene extremely complicated.

TAp73 is the predominant isoform expressed in embryonic neural stem cells (NSCs) (Tissir et al., 2009; Agostini et al., 2010; Gonzalez-Cano et al., 2010) and has been shown to regulate NSCs stemness and differentiation *in vitro* (Hooper et al., 2006; Agostini et al., 2010; Fujitani et al., 2010; Gonzalez-Cano et al., 2010; Talos et al., 2010). In accordance with TAp73 predominant role in neurogenesis, TAp73KO mice show hippocampal dysgenesis, but not ventricle enlargement or hydrocephalus (Tomasini et al., 2008). On the other hand, the DNp73KO mice display signs of neurodegeneration and a small reduction in cortical thickness and neuron number in older mice but do not show hippocampal abnormalities nor hydrocephalus (Tissir et al., 2009; Wilhelm et al., 2010). This led to propose that while DNp73 carries out neural protection functions, TAp73-isoforms are the main contributor to the development of the CNS. A recently developed mice model, with a selective knockout of the C-terminus of the full-length alpha isoform (*Trp73*Δ13/Δ13 mice), has shed new light on the role of p73 isoforms in the development of the murine brain (Amelio et al., 2020). These mice, which express the TAp73 beta isoforms at physiological levels, but lack the alfa-isoforms, suffer from a depletion of CR neurons in embryonic stages, leading to aberrant hippocampal architecture, reduced synaptic functionality and impaired learning and memory capabilities, altogether resembling the *Trp73*$^{-/-}$ mice phenotype (Amelio et al., 2020). The authors concluded that the hippocampal dysgenesis was a consequence of deprivation of the CR cells, whose early function is the secretion of reelin that will orchestrate the arrival, size and stratification of all pyramidal neurons of the neocortex gray matter (Marín-Padilla, 2015). Interestingly, several groups have reported a link between cell adhesion and reelin-induced functions in corticogenesis (Sanada et al., 2004; Soriano and del Río, 2005; Sekine et al., 2012; Matsunaga et al., 2017). In the subventricular zone (SVZ), reelin controls the behavior of SVZ-derived migrating neurons, triggering them to leave prematurely the rostral migratory stream (Pujadas et al., 2010; Courtès et al., 2011). However, could lack of CR cells alone explain the severe structural defects of the SVZ in p73-deficient mice?

p73 AS AN ARCHITECT OF THE SVZ AND THE EPENDYMA

Neurogenesis in the mammalian brain is complex and requires specialized microenvironments called "niches" (Scadden, 2006). In the adult brain, two niches haven been identified, the subventricular zone of the lateral walls of the ventricles (Alvarez-Buylla and Garcìa-Verdugo, 2002) and the subgranular zone of the dentate gyrus of the hippocampus (Doetsch et al., 1997). In the SVZ ventricular surface, multiciliated ependymal cells (EpCs) surround monociliated NSCs (B1 cells) forming a unique pinwheel architecture that is essential to maintain neurogenesis (Kuo et al., 2006; Mirzadeh et al., 2010; Paez-Gonzalez et al., 2011). In these pinwheels, the EpCs are polarized within the plane of the tissue, a process that is known as PCP. This essential feature of animal tissues (Butler and Wallingford, 2017) makes feasible that EpCs coordinate cilia beating and direct the cerebrospinal fluid circulation; therefore, PCP disruption results in ciliopathies and hydrocephalus (Marques et al., 2019).

One of the most striking features of the *Trp73*$^{-/-}$ mice is the complete lack of cytoarchitecture in the SVZ neurogenic niche (Gonzalez-Cano et al., 2016; Fuertes-Alvarez et al., 2018; Marques et al., 2019). TAp73, but not DNp73, is expressed in the EpCs and its precursors, the radial glia cells (Tissir et al., 2009; Hernández-Acosta et al., 2011; Medina-Bolívar et al., 2014; Fujitani et al., 2017), and it is essential for the ependymal cell assembly into neurogenic pinwheels (Gonzalez-Cano et al., 2016). Total p73 deficiency results in altered pinwheels where the EpCs have an aberrant membrane morphology with waves and pleats (**Figure 2A**), reflecting severe defects on the intercellular junctions at the apical surface of these cells (Gonzalez-Cano et al., 2016). These cell-junction defects also compromise the integrity of the ependymal barrier (**Figure 2B**), all pointing toward a TAp73 role in the establishment of intercellular junctions.

Compiled evidence indicates that the combination of alterations in vesicle trafficking, cell junction defects and loss of ependymal barrier integrity constructs a common pathway leading to ventricular zone disruption (Ferland et al., 2009). All these processes, as we will discuss later on, have been associated to TAp73 transcriptional regulation. Moreover, it is now accepted that abnormal junction complexes in the cells of the ventricular zone, including NPC, may lead to disruption of the ventricular and subventricular zones, resulting in hydrocephalus and abnormal neurogenesis (Rodríguez et al., 2012; Guerra

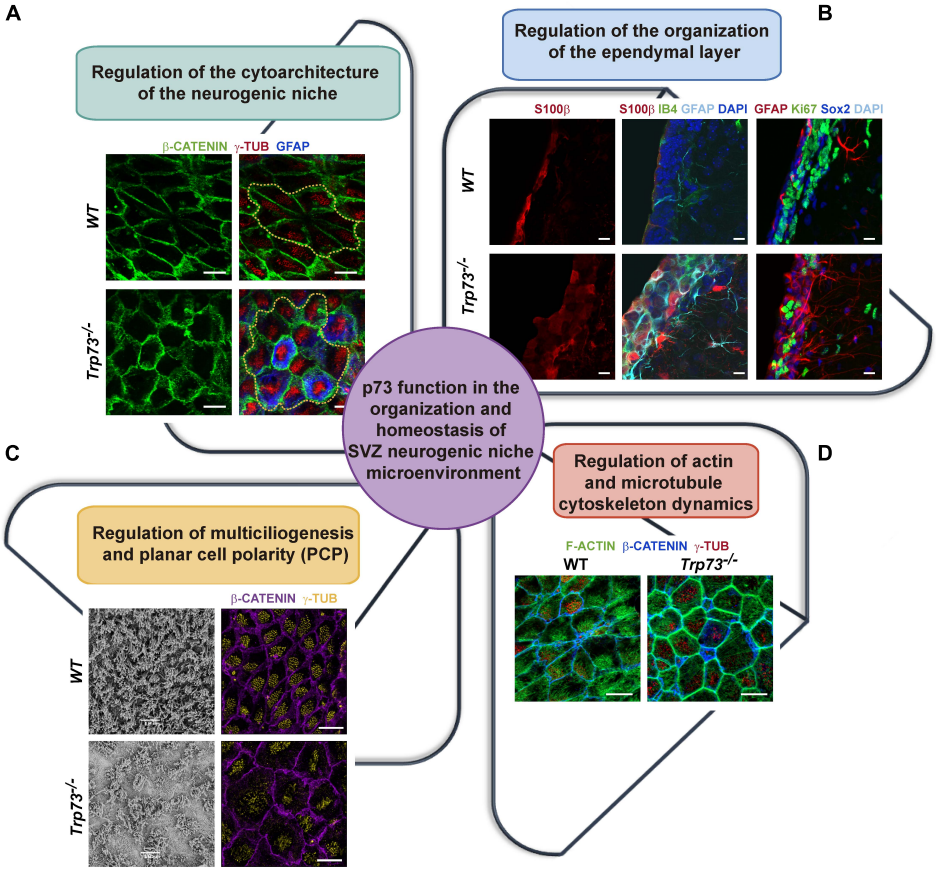

FIGURE 2 | p73 role as an architect of the SVZ neurogenic niche. **(A)** p73 is essential for the formation of the neurogenic pinwheels. In the absence of p73, EpCs show an aberrant membrane morphology and fail to organize into pinwheels, disrupting SVZ niche cytoarchitecture. Analysis of lateral ventricle wall whole-mounts of the indicated genotypes at postnatal day P160 immunostained for b-catenin (green), g-tubulin (red), and GFAP (blue). Pinwheel structures are marked by dotted yellow lines. Scale bars: 10 mm. **(B)** p73-deficient EpCs cell-junction defects compromise the integrity of the ependymal layer and halt the formation of the mono-stratified epithelium. In addition, cells with abnormal marker expression profiles are observed in p73KO brains. Coronal sections of the lateral wall of the lateral ventricle from P15 WT and p73KO mice were stained with the indicated antibodies and analyzed by confocal microscopy. Scale bars: 10 mm. **(C)** p73 is required for ciliogenesis and planar cell polarity establishment. p73KO cells displayed an abnormal cilia organization and basal body-cluster displacement. SEM (P7 mice) and confocal microscopy analysis (P15 mice, γ-tubulin, yellow; β-catenin, purple) of WT and p73KO lateral ventricle wall wholemounts. **(D)** p73 is also necessary for the formation of the polarized apical and sub-apical actin lattices in EpCs. Confocal images of WT and p73KO P15 wholemounts displaying as indicated: actin cytoskeleton (phalloidin, green), basal bodies (γ-tubulin, red) and the cell membrane (β-catenin, blue). Images from Dr. Marin's research group (Gonzalez-Cano et al., 2016, Fuertes-Alvarez et al., 2018).

et al., 2015). Thus, the "cell junction pathology," resulting from p73 ablation, might be underneath some of the functional and structural alterations of the *Trp73*$^{-/-}$ mice in the CNS, but also in other organs.

Trp73 function in the establishment of intercellular junctions has been strongly demonstrated in the reproductive epithelia. In the multilayered epithelia of the seminiferous tubules, lack of total p73 or TAp73 results in defective cell-cell adhesion of germ cells with Sertoli cells, leading to the premature detachment of the developing spermatids and concomitant cell death (Holembowski et al., 2014; Inoue et al., 2014). Interestingly, Sertoli cells do not express p73, but they are also affected by the loss of germ cell adhesion in *Trp73*$^{-/-}$ testes, losing their characteristic morphology as well as the inter-Sertoli cell adhesions that form the blood-testis barrier (Holembowski et al., 2014). Furthermore, in the developing ovary, p73 regulates a set of core genes involved in biological adhesion, thus acting as a regulator of intercellular adhesion, ECM interactions, and cell migration processes required for proper follicle development (Santos Guasch et al., 2018).

However, there are other pathological features of the *Trp73*$^{-/-}$ mice in which the possible link with cell junctional defects has not been addressed. That is the case of the chronic respiratory and gastrointestinal infections that these animals suffer from Yang et al. (2000). While p73 signaling has been associated to the epithelial cell response to infections caused by, for example, *H. pylori* (Wei et al., 2008), the cause of the increased susceptibility to infections, *per se*, in p73-deficient animals is not understood. Interestingly, loss of epithelial integrity has been widely demonstrated to be central to pathogen infection, since disruption of junctional integrity facilitates viral or bacterial entry and spread (Lu et al., 2014). Thus, it would be interesting to

address whether the aforementioned "cell junction pathology" resulting from p73-deficiency is at the root of the susceptibility to chronic infections in these mice.

Another interesting scenario are the defects in the vascular network described in the *Trp73*$^{-/-}$ mice. These mice exhibit extensive gastrointestinal and cranial hemorrhages (Yang et al., 2000) which are suggestive of vascular fragility or other defects in their vascular compartment. Our group reported that *Trp73* deficiency *in vivo* results in aberrant retinal vascular morphology, while *in vitro* ablation of p73 in 3D mESC and iPSC models impairs the early stages of vasculogenesis, demonstrating the essential role of *Trp73* in vascular development (Fernandez-Alonso et al., 2015). Compiled data from several groups supports the idea that this function is, at least in part, due to DNp73 modulation of pro-angiogenic signaling pathways (Dulloo et al., 2015a; Fernandez-Alonso et al., 2015; Stantic et al., 2015). As for TAp73, its role in vascular morphogenesis is unclear, especially regarding tumor angiogenesis. Collectively, several studies have demonstrated that TAp73 can act as both a positive and negative regulator of tumor angiogenesis under different spatio-temporal contexts and therefore, a bi-functional role for TAp73 in angiogenesis has been proposed (Amelio et al., 2015; Dulloo et al., 2015b; Stantic et al., 2015, reviewed in Sabapathy, 2015). However, TAp73 physiological function in vascular morphogenesis still needs to be addressed. Regarding the latter, Stantic et al. reported that TAp73-deficient tumor cells produce and secrete factors that disrupt intercellular contacts in endothelial cells cultured with the tumor cells-conditioned media (Stantic et al., 2015). However, whether the absence of TAp73 in endothelial cells leads to junctional defects, *in vivo* and/or *in vitro,* and the possible consequences of this in vascular morphogenesis remains an important open question.

p73 REGULATION OF CYTOSKELETON DYNAMICS AT THE CENTER STAGE OF PCP AND MULTICILIOGENESIS ESTABLISHMENT

An in-depth analysis of the SVZ of *Trp73*$^{-/-}$, TAp73KO, and DNp73KO mice revealed that the lack of total p73 results in profound alterations of ependymal multiciliogenesis and PCP establishment (Gonzalez-Cano et al., 2016; Fuertes-Alvarez et al., 2018). The role of p73 on ciliogenesis is complex and has been reviewed elsewhere (Marques et al., 2019; Nemajerova and Moll, 2019). p73-deficiency affects different stages of the process depending on the absence of one or both isoforms. EpCs with total lack of p73 have severe ciliary defects, with many cells lacking ciliary axoneme and others displaying disorganized and aberrant cilia (Gonzalez-Cano et al., 2016; **Figure 2C**). TAp73 role in cilia formation has been demonstrated in other systems such as in the respiratory and reproductive epithelia, where TAp73 was found to function as a master transcriptional regulator governing motile multiciliogenesis (Marshall et al., 2016; Nemajerova et al., 2016).

TAp73 isoform elimination in TAp73KO mice does not recapitulate total *Trp73*$^{-/-}$ phenotype in ependymal cells but rather results in a mild phenotype. In these mice, most EpCs display ciliary axoneme but with defective basal body docking and a "disheveled" appearance (Fuertes-Alvarez et al., 2018; Wildung et al., 2019). These defects are most likely due to the observed alterations -linked to TAp73 deficiency- in the sub-apical actin cytoskeleton dynamics and microtubule polarization, which regulates basal body docking and spacing (Vladar and Axelrod, 2008; Werner et al., 2011). On the other hand, DNp73-deficient EpCs do not display any ciliary defects indicating that, in the presence of TAp73, DNp73 is not necessary to orchestrate ciliogenesis. These data suggest that redundant ciliary programs are induced in the absence of TAp73 but that cannot compensate total p73 deficiency. In the same line, the *Trp73*Δ13/Δ13 mice do not display any apparent alteration in the airway ciliated epithelium, neither in the EpCs, suggesting that p73β or other redundant mechanisms can substitute the function of the longer isoform p73α (Buckley et al., 2020).

The spatial and temporal frame of TAp73 expression in the developing brain is an important question to pinpoint its physiological function. In mice, the transition of neuroepithelial cells to radial glial cells occurs between the embryonic days (E) 10 and 12, when the tight junctions that couple neuroepithelial cells convert into adherens junctions, and the cells acquire features associated with glial cells (Fuentealba et al., 2015). It is noteworthy that TAp73 expression in the *Trp73*Δ13/Δ13 mice was detected in the neuroepithelium from E11.5 to E16.5 (Amelio et al., 2020). This is an important stage during CNS development in mice, since birth dating experiments suggest that the majority of telencephalic EpC are produced between E14 and E16 (Spassky et al., 2005). By E16 the primary cilia of many transforming radial glial cells have become asymmetrically displaced within its apical surface, a key step in the ependymal cell's differentiation and in the establishment of the organizations of the SVZ neurogenic niche (Redmond et al., 2019). Moreover, Fujitani and colleagues proposed that p73 regulates embryonic primary ciliogenesis, since disruption of p73 (both TA and DNp73) during early postnatal EpC development (P1-P5) did not cause hydrocephalus (Fujitani et al., 2017). Nevertheless, compiled data strongly support the idea that p73 functions at several stages during radial glial cell transformation into EpC (Marques et al., 2019). Thus, considering the reported early expression of TAp73 during development (Amelio et al., 2020), should we expect the cytoarchitecture of the SVZ in these mice to be maintained? or by the contrary, would sustained expression of TAp73 will be required for organization? Do these mice display PCP defects related to cell-junctions and cytoskeleton alterations as the TAp73KO mice do?

The coordinated polarization of EpC motile cilia within the plane of the tissue allows the synchronized beating that drives directional fluid flow and is required for EpC functionality (Ohata and Alvarez-Buylla, 2016). Multiciliated ependymal cells display two types of PCP, translational PCP (tPCP) and rotational (rPCP). While tPCP is unique to EpCs and is defined by the asymmetric localization of the cilia cluster at the anterior apical surface, rPCP refers to the unidirectional orientation of the

motile cilia within the cell (Mirzadeh et al., 2010). PCP is established by asymmetric localization of PCP-core regulatory proteins complexes at opposite sides of the apical membrane (Boutin et al., 2014; Ohata et al., 2014) and it is driven by multiple global cues that guide the subcellular enrichment of PCP-core proteins such as Frizzled, Vangl, Celsr, Disheveled and Prickle (Butler and Wallingford, 2017). PCP-core components then self-assemble into mutually exclusive complexes at opposite sides of a cell to communicate polarity between neighboring cells and direct polarized cell behaviors. *Trp73* is necessary for the efficient establishment of both types of PCP (Gonzalez-Cano et al., 2016; Fujitani et al., 2017; Fuertes-Alvarez et al., 2018). In the absence of p73, or even TAp73, PCP-core complexes fail to assembly at opposite intercellular junctions of EpCs, and therefore, polarity is not established, suggesting that p73 might regulate early upstream events of PCP establishment (Gonzalez-Cano et al., 2016; Fujitani et al., 2017; Fuertes-Alvarez et al., 2018).

But how do the cells, and for that matter TAp73, establish this asymmetry? Several processes have been involved in PCP-core complex's asymmetry, from cilia-driven fluid flow to cellular rearrangements dependent on cytoskeletal polarity (Takagishi et al., 2017). It is important to bear in mind that asymmetry can be established independently of cilia, through the intrinsic chirality of the actomyosin cytoskeleton (Juan et al., 2018). Polarity in epithelial tissues is known to be influenced by cell-cell junctions, cytoskeletal elements, and by cell-cell signaling. Our group has demonstrated that p73 regulates PCP, at least in part, through TAp73-modulation of actin and microtubule dynamics (Fuertes-Alvarez et al., 2018). The actin cytoskeleton of multiciliated ependymal cells is organized into a cortical network, implicated in cell shape changes, and two interconnected apical and subapical networks that enclose the basal bodies contributing to their spacing and to the synchronization of cilia beating (Werner et al., 2011). p73 is required for the localization and organization of these actin networks, as p73-deficiency results in the complete lack of polarized apical and sub-apical lattices, in the formation of a thick actin cortex and the disposition stress fibers, all with a concurrent change in cell morphology (Fuertes-Alvarez et al., 2018; **Figure 2D**).

In recent years it has become apparent that actin-microtubule crosstalk is particularly important for the establishment of neuronal and epithelial cell shape and function (Dogterom and Koenderink, 2019). Microtubules crosstalk with PCP at two stages (Vladar et al., 2012; Werner and Mitchell, 2012; Takagishi et al., 2017). First, at the initial polarization establishment, when the microtubule-network grows asymmetrically from the center of the cell toward the anterior region of the apical cell cortex, contacting the plasma membrane at the intercellular microtubule-anchoring points which are polarized at tissue level. Second, when these polarized microtubules asymmetrically transport the PCP-core proteins to the correct anterior/posterior cell boundary (Shimada et al., 2006; Harumoto et al., 2010). Lack of p73 blunts the formation of polarized microtubule-anchoring points at cell junctions, suggesting that impairment of microtubule-dynamics is at the root of the defect in p73-deficient cells (Boutin et al., 2014; Takagishi et al., 2017).

As we will discuss below, the role of p73 as a regulator of cellular cytoskeleton dynamics has been shown in several systems. Thus, we should ask whether p73 regulation of PCP is a general function operating in various tissues and organs, or, on the contrary, it is limited to ependymal cells. Emerging data assign new roles for PCP in postnatal contexts, including formation of functional organs such as lungs and kidneys (Henderson et al., 2018), all highlighting the need of polarized cellular behaviors for proper development and function of diverse organs. In particular, asymmetric distribution of PCP-core complexes at intercellular junctions is required for the correct cilia orientation in other epithelia, like the trachea, oviduct and the organ of Corti. TAp73-deficiency results in ciliary defects in trachea and the oviduct in $Trp73^{-/-}$ and TAp73KO mice (Marshall et al., 2016; Nemajerova et al., 2016). However, the planar organization of these epithelia has not been addressed. Furthermore, defects in PCP have been implicated in human pathologies, leading to the obvious and interesting question of whether alterations in p73 expression or mutations could be implicated in these diseases.

TAp73 AS A CENTRAL HUB THAT MODULATES TRANSCRIPTIONAL PROGRAMS INVOLVED IN CYTOSKELETON DYNAMICS AND CELLULAR ADHESION

The main question that arises is: how does TAp73 modulate all this variety of biological processes? The mechanism of TAp73 role in NSC stemness and neural differentiation is complex and relies on p73 regulation of different transcriptional profiles. In recent years, several genes involved in proliferation, differentiation and/or self-renewal of NSC, like *Sox-2, Hey-2, Trim32, and Notch*, have been postulated as TAp73 transcriptional targets (Hooper et al., 2006; Agostini et al., 2010; Fujitani et al., 2010; Gonzalez-Cano et al., 2010, 2016; Talos et al., 2010). TAp73 is also implicated in the regulation of post-mitotic neuron function by modulating the expression of p75NTR or GLS2, which are associated to axonal growth and dendritic arborization and neuronal metabolism, respectively (Niklison-Chirou et al., 2017). However, the profound structural alterations observed in the SVZ architecture of the $Trp73^{-/-}$ mice cannot exclusively be explained by defects in cellular proliferation, differentiation, self-renewal or even metabolic defects. Regarding the regulation of multiciliogenesis, the compiled data identified over 100 putative p73 target genes that regulate multiciliated cell differentiation and homeostasis and revealed *Foxj1* as a direct TAp73 target, supporting a model in which p73 acts as a regulator of multiciliogenesis through direct and indirect regulation of key genes (Marshall et al., 2016; Nemajerova et al., 2016). TAp73 undoubtedly acts as a master regulator of ciliogenesis and *Trp73* total loss results in dramatic ciliary defects in EpCs, oviduct, middle ear and respiratory tract (Gonzalez-Cano et al., 2016; Marshall et al., 2016; Nemajerova et al., 2016; Fujitani et al., 2017). Still, the elimination of this ciliary function alone could not

explain the abovementioned structural alterations. Interestingly, lack of TAp73 in EpCs results in defective actin and microtubule networks with a concomitant loss of PCP even though the ciliary axonemal growth remains unaffected, suggesting that TAp73 uncouples ciliogenesis from PCP establishment and regulates multiple independent, but interrelated, transcriptional programs to orchestrate these processes. In this regard, our group has demonstrated that mechanistically, TAp73 modulates actomyosin dynamics, at least in part by the transcriptional regulation of the myosin light chain kinase (MLCK), the activator of non-muscle myosin II (NMII) (Fuertes-Alvarez et al., 2018), which functions as a cortical organizer to concentrate E-cadherin to the *zonula adherens* (Smutny and Yap, 2010). TAp73 also activates transcriptional programs involved in the regulation of microtubule-dynamics and Golgi organization signaling pathways, both necessary for PCP establishment (Fuertes-Alvarez et al., 2018). Along the same lines, some of the genes significantly bound and regulated by p73 in multiciliated trachea cells, like *Traf3ip1* and *Tubb4b* (Marshall et al., 2016), are known to regulate the acetylation, polymerization and stabilization of microtubules (Berbari et al., 2011; Bizet et al., 2015; Sobierajska et al., 2019) or to be involved in vesicle trafficking, like *Sec24b,* that selectively sorts Vangl2 to regulate PCP (Merte et al., 2010).

A growing body of work indicates that the functional interaction between cell junctions and actin and microtubule cytoskeleton is critical for epithelial morphogenesis (Robinson, 2015; Adil et al., 2021). As discussed before, a possible common denominator to many of the p73-deficient phenotypes is the cell junctional defect and cytoskeleton dynamics alterations, suggesting a general function of TAp73 as a central hub that modulates transcriptional programs involved in these processes. To address whether this is the case, we revisited some of the transcriptomic studies that have been used to identify TAp73 target genes. We selected the genome-wide studies from Koeppel et al. (2011), Santos Guasch et al. (2018), and López-Ferreras et al. (2021). In their work, Koeppel et al. used the p53-deficient, TAp73β-inducible, osteosarcoma cell line Saos2-Tet-On to characterize the molecular basis for the different physiological functions of p73. In the second study, the authors measured global gene expression changes by RNA-seq after ectopic expression of TAp73β in mouse granulosa cells (MGCs) isolated from *Trp73*$^{-/-}$ female mice. They express TAp73β basing their decision on previously published data showing that TAp73β exhibits the highest level of transcriptional activity among p73 isoforms (Lee and La Thangue, 1999; Ueda et al., 1999). Lastly, López-Ferreras et al. (2021) characterized the transcriptomic profile of E14TG2α mouse embryonic stem cells (mESCs) in which they specifically inactivated the TAp73-isoform (E14-TAp73KO) using the CRISPR/Cas9 system. In particular, we selected the analysis performed by the authors under differentiation conditions, since this approach offers the advantage of investigating p73 regulation in a physiological context that recapitulates early developmental stages where p53 family members are known to be upregulated (Medawar et al., 2008; Wang et al., 2017). Using the published RNA-seq data, we focus on the differentially expressed genes (DEGs) that were upregulated upon TAp73-expression in MGCs and Saos-2-Tet-On, or downregulated in E14-TAp73KO. To limit our analysis to genes that are potentially direct TAp73 targets, we compared those DEGs lists with a compilation of candidate genes with p73 genomic binding sites identified through ChIP-seq-studies (Koeppel et al., 2011; Marshall et al., 2016; Santos Guasch et al., 2018) and analyzed them with DAVID Bioinformatics Resources 6.8 (Huang et al., 2008, 2009) to identify enriched biological GO terms and obtain a functional annotation clustering.

Highlighting the significance of p73 non-canonical functions, one of the clusters with the highest enrichment score for the three analyzed models was related to "Development" (GO:0048731∼system development, GO:0048513∼animal organ development, GO:0048869∼cellular developmental process, etc.), even ahead of p73 role in controlling cell death/cell proliferation (**Figures 3A–C**). Also consistent with the expected behavior for a tissular architect, functions related to "Cell-cell adhesion" and "Actin cytoskeleton" were significantly enriched in all the selected gene lists. The preservation of tissue function not only relies on biophysical cues, but also on the correct biochemical communication between cells and with the ECM to relay positional information. Accordingly, clusters like "Cell communication" and "Vesicular transport" (GO:1903561∼extracellular vesicle; GO:0070062∼extracellular exosome) showed a highly significant enrichment score. This coupling at molecular level between different aspects of tissue architecture reinforces p73 role as a key regulator of the organization and homeostasis of complex microenvironments. On a similar note, other annotation clusters like "Cell migration," "Neuron projection," or "Blood vessel development" were also highly significant. These findings are consistent with previous reports of p73 regulation of cell migration (Landré et al., 2016), and with the essential p73 function in neural and vascular development previously discussed in this review, altogether indicating that the cellular systems analyzed here are excellent models to identify and study putative TAp73 target genes.

To gain insight into p73 regulation of cell adhesion and actin cytoskeleton dynamics we explored, for each cell type, the overlapping genes within the main GO terms included in these clusters (**Figures 3A'–C'** and **Supplementary Table 1**). Regarding cell adhesion, we focused on p73 putative targets that were common to the terms "GO:0005912∼adherens junction," "GO:0050839∼cell adhesion molecule binding" and "GO:0098631∼protein binding involved in cell adhesion." Within these, we found: (i) genes encoding integrins such as Itga2 and Itga6, or the *Zonula occludens* protein ZO2, a scaffold protein that physically links transmembrane tight junction proteins to the apical cytoskeleton of actomyosin (Raya-Sandino et al., 2017), in Saos2 cells; (ii) the LIM domain and actin binding 1 protein LIMA1, a demonstrated direct transcriptional target of TAp73 whose activity is counteracted by DNp73 (Steder et al., 2013), or the cytoskeleton-related protein PDLIM5, also known as ENH (Enigma homolog) (Huang et al., 2020), in MGCs; and (iii) genes encoding E-cadherin or plectin-one of the major cytoskeletal linker proteins- (Wiche et al., 2015), in E14TG2α cells. Some of these DEGs were shared between cell models, although it should be noted that there was only one DEG associated to the

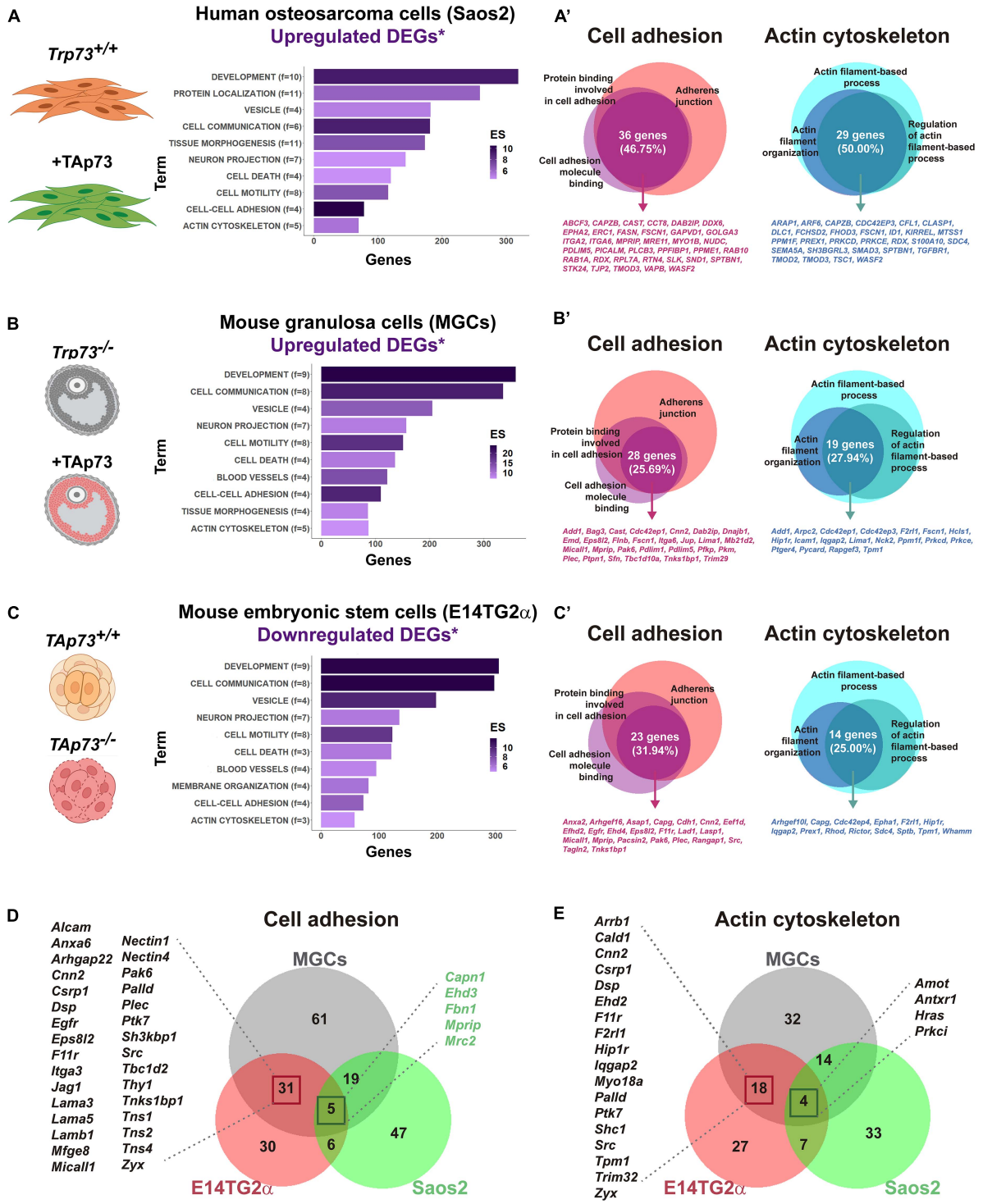

FIGURE 3 | p73 is a central hub of cellular adhesion and cellular cytoskeleton dynamics. For the indicated cell models, putative TAp73 target genes (DEGs*) were obtained by comparison of differentially expressed genes (DEGs) derived from RNA-seq studies with candidate genes containing p73 binding peaks (*) according to ChIP-seq studies by Koeppel et al. (2011), Marshall et al. (2016), and Santos Guasch et al. (2018). A total number of 736 genes for Saos-2-Tet-On cells, 679 genes for MGCs, and 709 genes for E14-TAp73KO were analyzed with DAVID Bioinformatics Resources 6.8. Functional annotation clustering was performed and enriched biological GO terms for Saos2-Tet-On cells **(A)**, MGCs **(B)** and E14-TAp73KO **(C)** are represented. Overlapping genes within GO terms related to "Cell-cell adhesion" and "Actin cytoskeleton" were furthered identified and represented for the three cell models **(A'–C')**. Comparison of the whole list of DEGs assigned to these clusters between the three cell models is shown **(D,E)**. Publicly available datasets were analyzed in this study and can be found here: GSE15780, PRJNA310161; PRJNA437755. The pictures were created with BioRender.com.

analyzed GO terms that was common to the three cell types. This gene encoded the myosin phosphatase Rho-interacting protein MPRIP, a scaffold protein that associates with the actomyosin cytoskeleton, regulating myosin light chain phosphatase (MLCP), and that has been involved in the regulation of stress fibers (Koga and Ikebe, 2005). Whether this gene is a true p73 transcriptional target remains to be validated.

A similar situation occurred for genes related to actin cytoskeleton regulation. In this case, we draw our attention to the functional annotation terms "GO:0030029∼actin filament-based process," "GO:0032970∼regulation of actin filament-based process" and "GO:0007015∼actin filament organization." Among the DEGs shared within cell models, we could find some genes playing relevant roles for cytoskeleton dynamics, like *Fscn1* (DEG in Saos-TetOn and MGCs) or *Scd4* (DEG in Saos-TetOn and E14TG2α). FSCN1 is an actin binding-protein involved in the formation of essential cell structures for migration, cell-to-cell interactions and cell-matrix adhesion (Lamb and Tootle, 2020); therefore, different studies have highlighted its importance for tissue architecture, particularly when it is disrupted in tumor microenvironments (Liu et al., 2021). Syndecans are transmembrane proteins which act as communicators between intracellular, cell surface and ECM components (Elfenbein and Simons, 2013). Loss of Syn-4 alters the actin network and affects focal adhesions, decoupling vinculin from the actin filaments (Cavalheiro et al., 2017). Finding several genes related to cell-ECM interactions when collectively analyzing these transcriptomic studies may imply that the role of p73 as a tissue architect goes far beyond than anticipated and points to p73 involvement in integrin associated-signaling, as already suggested by Xie et al. (2018) or López-Ferreras et al. (2021).

The DEG analysis of cell adhesion and cytoskeleton dynamics clusters for the individual models led as to ask whether we could define a more global transcriptional profile by comparing the whole list of DEGs assigned to these clusters in Saos2-TetOn, MGCs, and mESCs (**Figures 3D,E**). For both biological functions, the cell models with a stronger epithelial component (MGCs and E14TG2α) shared a core set of genes regulated by p73 (36 genes for "Cell-cell adhesion" and 22 genes in the case of "Actin cytoskeleton"), supporting the existence of a "p73 gene signature" associated to tissue architecture. Interestingly, Koeppel et al. (2011) proposed that TAp73β seems to induce target genes that fall into KEGG functional categories linked to metastasis, such as focal adhesion, ECM–receptor interaction and actin cytoskeleton regulation. On the other hand, the p53-signaling pathway is the first functional category that appears in the KEGG pathway analysis for TAp73β, although biological process such as "cell adhesion" and "biological adhesion" were included in their GO functional analysis. In agreement, other GO studies demonstrate that overexpression of TAp73β can also regulate these functions in diverse cellular contexts (Fuertes-Alvarez et al., 2018; Santos Guasch et al., 2018; López-Ferreras et al., 2021). It is worth noting that the molecular networks involved in cell-to-cell adhesion revealed by Santos Guasch et al. (2018) in a total *Trp73* knockout scenario are further supported by the recent study of López-Ferreras et al. (2021), with specific inactivation of TAp73 in mESCs, emphasizing the interest of this fine-tuned cellular model to decipher the role of the *Trp73* gene isoforms. Altogether, the analyzed studies indicate that the integration of -omics data could be a very valuable strategy to provide a more comprehensive dissection of p73 regulated molecular networks and, overall, they place p73 as a central hub in the regulation of cell adhesion and cytoskeleton dynamics, two cornerstones for tissue architecture.

CONCLUSION

TP73 belongs to one of the most intensively studied gene families in molecular oncology. The considerable interest stems from the fact that most human tumors have subverted the function of the founding member of this family, the p53 protein. Thus, since its serendipitous discovery (Kaghad et al., 1997), p73 tumor suppression function was expected by virtue of its homology with p53 and its localization to chromosome 1p36, a region that is frequently deleted in a variety of tumors (Ichimiya et al., 1999). However, this function has been a matter of controversy, fueled by the fact that inactivation of the *TP73* gene is a very rare event in cancers involving chromosome 1p (Han et al., 1999; Inoue and Fry, 2014). Moreover, the observation that viral oncoproteins discriminate between p53 and p73 suggests that the functions of these two proteins may differ under physiological conditions (Marin et al., 1998).

The discovery of the TA- and DN-p73 isoforms with antagonist anti- and pro-oncogenic functions, and the TAp73KO mice predisposition to spontaneous tumorigenesis, demonstrated TAp73 role as a tumor suppressor gene (Tomasini et al., 2008). However, there is growing evidence indicating that while TAp73 has a role in tumor suppression, it is likely to be secondary (reviewed in Wang et al., 2020). The complex phenotype of the *Trp73* deficient mice have revealed that p73 function is essential for the organization and homeostasis of different complex microenvironments governing various aspects of tissue physiology. Altogether, this has raised the idea that TAp73 was not evolved for tumor suppression, but rather to perform unique functions in regulating developmental processes through p53-independent mechanisms (Wang et al., 2020). We propose that some of the, apparently unrelated, phenotypes observed in $Trp73^{-/-}$ mice are the reflection of the p73 requirement for the establishment and/or maintenance of tissue organization (**Figure 4**). This function as a tissular architect might represent one of the original roles of the p53/p63/p73-ancestor. Furthermore, it is important to bear in mind that this function might reconnect with TAp73 tumor suppressor function, since a recent report proposes that the metastatic programs arise from the reactivation, outside of its homeostatic context, of normal embryonic developmental transcriptional modules (Logotheti et al., 2020). Thus, in a similar way, deregulation of p73 expression during tumor progression could result in alterations of the transcriptional nodes that p73 regulates as a tissue architect, playing a pivotal role during metastasis establishment.

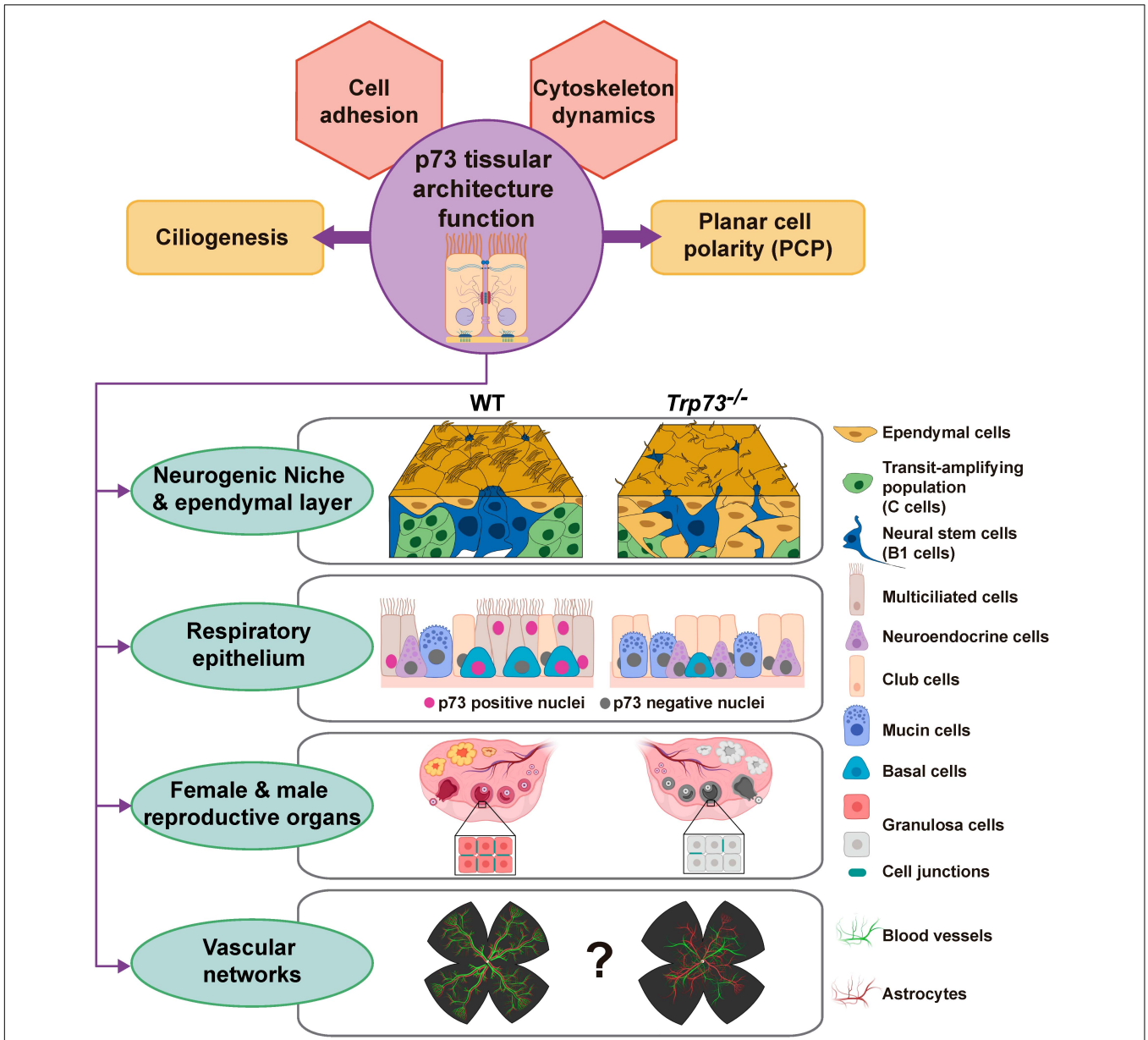

FIGURE 4 | Overview of the proposed p73 novel role as a tissue architect. We present a model in which p73 would act as a tissue architect by regulating transcriptional hubs involved in cellular adhesion and cytoskeleton dynamics. In determined spatio-temporal contexts, TAp73 will interplay with other transcriptional programs to orchestrate morphogenic processes like ciliogenesis and/or PCP, ensuring the correct overall tissular architecture in complex microenvironments such as neurogenic niche, the respiratory and reproductive epithelium and, maybe, the vascular network. The pictures were created with BioRender.com.

In this model, p73 regulates distinct transcriptional nodes in a hierarchical manner that would functionally interact with each other in a cell context and time dependent manner. Cell adhesion mechanisms are responsible for assembling cells together and, along with their connections to the internal cytoskeleton, determine the overall architecture of the tissue (Gumbiner, 1996). In this way, TAp73-regulated transcriptional hubs, involved in cytoskeleton dynamics and cellular adhesion, will constitute the basement of p73 function as a tissue architect. In a context dependent manner, TAp73 will combine the regulation of this basic transcriptional model with other tissue specific transcriptional profiles to orchestrate complex morphogenic processes like ciliogenesis and/or PCP (**Figure 4**). In turn, the coordinated orchestration of these processes (cell adhesion, cytoskeleton dynamic ciliogenesis and PCP) by p73 impinges on the cellular activities, leading to tissue and organ scale functionality of complex microenvironments such as neurogenic niche, the respiratory and reproductive epithelium and, maybe, the vascular network. Thus, based in the compiled data available on p73 physiological function, we propose that p73 might function as a tissue architect, and not just as another p53-Doppelgänger (Kaelin, 1998).

AUTHOR CONTRIBUTIONS

MCM and MMM conceived the review and took the lead in writing. LM-A performed data analysis and crafted the figures. LL-F performed a critical revision of the article. All authors provided critical feedback and contributed to the final manuscript.

FUNDING

This work was supported by Grant PID2019-105169RB-I00 from Spanish Ministerio de Ciencia e Innovación cofinanced by FEDER funds (to MCM). LM-A was a holder of a predoctoral scholarship from the Asociación Española contra el Cáncer (AECC) and was funded by a postdoctoral contract from Junta de Castilla y León.

SUPPLEMENTARY MATERIAL

The Supplementary Material for this article can be found online at: https://www.frontiersin.org/articles/10.3389/fcell.2021.716957/full#supplementary-material

REFERENCES

Åberg, E., Saccoccia, F., Grabherr, M., Ore, W. Y. J., Jemth, P., and Hultqvist, G. (2017). Evolution of the p53-MDM2 pathway. *BMC Evol. Biol.* 17:177. doi: 10.1186/s12862-017-1023-y

Adams, E. D. M., Goss, G. G., and Leys, S. P. (2010). Freshwater sponges have functional, sealing epithelia with high transepithelial resistance and negative transepithelial potential. *PLoS One* 5:e15040. doi: 10.1371/journal.pone.0015040

Adil, M. S., Narayanan, S. P., and Somanath, P. R. (2021). Cell-cell junctions: structure and regulation in physiology and pathology. *Tissue Barriers* 9:1848212. doi: 10.1080/21688370.2020.1848212

Agostini, M., Niklison-Chirou, M. V., Catani, M. V., Knight, R. A., Melino, G., and Rufini, A. (2014). TAp73 promotes anti-senescence-anabolism not proliferation. *Aging* 6, 921–930. doi: 10.18632/aging.100701

Agostini, M., Tucci, P., Chen, H., Knight, R. A., Bano, D., Nicotera, P., et al. (2010). p73 regulates maintenance of neural stem cell. *Biochem. Biophys. Res. Commun.* 403, 13–17. doi: 10.1016/j.bbrc.2010.10.087

Alvarez-Buylla, A., and Garcìa-Verdugo, J. M. (2002). Neurogenesis in adult subventricular zone. *J. Neurosci.* 22, 629–634. doi: 10.1523/JNEUROSCI.22-03-00629.2002

Amelio, I., Inoue, S., Markert, E. K., Levine, A. J., Knight, R. A., Mak, T. W., et al. (2015). TAp73 opposes tumor angiogenesis by promoting hypoxia-inducible factor 1α degradation. *Proc. Natl. Acad. Sci. U.S.A.* 112, 226–231. doi: 10.1073/pnas.1410609111

Amelio, I., Markert, E. K., Rufini, A., Antonov, A. V., Sayan, B. S., Tucci, P., et al. (2014). p73 regulates serine biosynthesis in cancer. *Oncogene* 33, 5039–5046. doi: 10.1038/onc.2013.456

Amelio, I., Panatta, E., Niklison-Chirou, M. V., Steinert, J. R., Agostini, M., Morone, N., et al. (2020). The C terminus of p73 is essential for hippocampal development. *Proc. Natl. Acad. Sci. U.S.A.* 117, 15694–15701. doi: 10.1073/pnas.2000917117

Belahbib, H., Renard, E., Santini, S., Jourda, C., Claverie, J.-M., Borchiellini, C., et al. (2018). New genomic data and analyses challenge the traditional vision of animal epithelium evolution. *BMC Genomics* 19:393. doi: 10.1186/s12864-018-4715-9

Belyi, V. A., Ak, P., Markert, E., Wang, H., Hu, W., Puzio-Kuter, A., et al. (2010). The origins and evolution of the p53 family of genes. *Cold Spring Harb. Perspect. Biol.* 2:a001198. doi: 10.1101/cshperspect.a001198

Berbari, N. F., Kin, N. W., Sharma, N., Michaud, E. J., Kesterson, R. A., and Yoder, B. K. (2011). Mutations in Traf3ip1 reveal defects in ciliogenesis, embryonic development, and altered cell size regulation. *Dev. Biol.* 360, 66–76. doi: 10.1016/j.ydbio.2011.09.001

Billant, O., Léon, A., Le Guellec, S., Friocourt, G., Blondel, M., and Voisset, C. (2016). The dominant-negative interplay between p53, p63 and p73: a family affair. *Oncotarget* 7, 69549–69564. doi: 10.18632/oncotarget.11774

Bizet, A. A., Becker-Heck, A., Ryan, R., Weber, K., Filhol, E., Krug, P., et al. (2015). Mutations in TRAF3IP1/IFT54 reveal a new role for IFT proteins in microtubule stabilization. *Nat. Commun.* 6:8666. doi: 10.1038/ncomms9666

Boutin, C., Labedan, P., Dimidschstein, J., Richard, F., Cremer, H., André, P., et al. (2014). A dual role for planar cell polarity genes in ciliated cells. *Proc. Natl. Acad. Sci. U.S.A.* 111, E3129–E3138. doi: 10.1073/pnas.1404988111

Buckley, N., Panatta, E., Morone, N., Noguchi, M., Scorrano, L., Knight, R. A., et al. (2020). P73 C-terminus is dispensable for multiciliogenesis. *Cell Cycle* 19, 1833–1845. doi: 10.1080/15384101.2020.1783055

Buhlmann, S., and Pützer, B. M. (2008). DNp73 a matter of cancer: mechanisms and clinical implications. *Biochim. Biophys. Acta* 1785, 207–216. doi: 10.1016/j.bbcan.2008.01.002

Butler, M. T., and Wallingford, J. B. (2017). Planar cell polarity in development and disease. *Nat. Rev. Mol. Cell Biol.* 18, 375–388. doi: 10.1038/nrm.2017.11

Candi, E., Agostini, M., Melino, G., and Bernassola, F. (2014). How the TP53 family proteins TP63 and TP73 contribute to tumorigenesis: regulators and effectors. *Hum. Mutat.* 35, 702–714. doi: 10.1002/humu.22523

Cavalheiro, R. P., Lima, M. A., Jarrouge-Bouças, T. R., Viana, G. M., Lopes, C. C., Coulson-Thomas, V. J., et al. (2017). Coupling of vinculin to F-actin demands Syndecan-4 proteoglycan. *Matrix Biol.* 63, 23–37. doi: 10.1016/j.matbio.2016.12.006

Cereijido, M., Contreras, R. G., and Shoshani, L. (2004). Cell Adhesion, polarity, and epithelia in the dawn of metazoans. *Physiol. Rev.* 84, 1229–1262. doi: 10.1152/physrev.00001.2004

Chillemi, G., Kehrloesser, S., Bernassola, F., Desideri, A., Dötsch, V., Levine, A. J., et al. (2017). Structural evolution and dynamics of the p53 proteins. *Cold Spring Harb. Perspect. Med.* 7:a028308. doi: 10.1101/cshperspect.a028308

Costanzo, A., Pediconi, N., Narcisi, A., Guerrieri, F., Belloni, L., Fausti, F., et al. (2014). TP63 and TP73 in cancer, an unresolved "family" puzzle of complexity, redundancy and hierarchy. *FEBS Lett.* 588, 2590–2599. doi: 10.1016/j.febslet.2014.06.047

Courtès, S., Vernerey, J., Pujadas, L., Magalon, K., Cremer, H., Soriano, E., et al. (2011). Reelin controls progenitor cell migration in the healthy and pathological adult mouse brain. *PLoS One* 6:e20430. doi: 10.1371/journal.pone.0020430

De Laurenzi, V., Costanzo, A., Barcaroli, D., Terrinoni, A., Falco, M., Annicchiarico-Petruzzelli, M., et al. (1998). Two New p73 splice variants, γ and δ, with different transcriptional activity. *J. Exp. Med.* 188, 1763–1768. doi: 10.1084/jem.188.9.1763

Deutsch, G. B., Zielonka, E. M., Coutandin, D., Weber, T. A., Schäfer, B., Hannewald, J., et al. (2011). DNA damage in oocytes induces a switch of the quality control factor TAp63α from dimer to tetramer. *Cell* 144, 566–576. doi: 10.1016/j.cell.2011.01.013

Doetsch, F., Garcìa-Verdugo, J. M., and Alvarez-Buylla, A. (1997). Cellular composition and three-dimensional organization of the subventricular germinal zone in the adult mammalian brain. *J. Neurosci.* 17, 5046–5061. doi: 10.1523/JNEUROSCI.17-13-05046.1997

Dogterom, M., and Koenderink, G. H. (2019). Actin–microtubule crosstalk in cell biology. *Nat. Rev. Mol. Cell Biol.* 20, 38–54. doi: 10.1038/s41580-018-0067-1

Dötsch, V., Bernassola, F., Coutandin, D., Candi, E., and Melino, G. (2010). p63 and p73, the Ancestors of p53. *Cold Spring Harb. Perspect. Biol.* 2:a004887. doi: 10.1101/cshperspect.a004887

Du, W., Jiang, P., Mancuso, A., Stonestrom, A., Brewer, M. D., Minn, A. J., et al. (2013). TAp73 enhances the pentose phosphate pathway and supports cell proliferation. *Nat. Cell Biol.* 15, 991–1000. doi: 10.1038/ncb2789

Dulloo, I., Hooi, P. B., and Sabapathy, K. (2015a). Hypoxia-induced DNp73 stabilization regulates Vegf-A expression and tumor angiogenesis similar to TAp73. *Cell Cycle* 14, 3533–3539. doi: 10.1080/15384101.2015.1078038

Dulloo, I., Phang, B. H., Othman, R., Tan, S. Y., Vijayaraghavan, A., Goh, L. K., et al. (2015b). Hypoxia-inducible TAp73 supports tumorigenesis by regulating the angiogenic transcriptome. *Nat. Cell Biol.* 17, 511–523. doi: 10.1038/ncb3130

Elfenbein, A., and Simons, M. (2013). Syndecan-4 signaling at a glance. *J. Cell Sci.* 126(Pt 17), 3799–3804. doi: 10.1242/jcs.124636

Engelmann, D., and Pützer, B. M. (2014). Emerging from the shade of p53 mutants: N-terminally truncated variants of the p53 family in EMT signaling and cancer progression. *Sci. Signal.* 7:re9. doi: 10.1126/scisignal.2005699

Engelmann, D., Meier, C., Alla, V., and Pützer, B. M. (2015). A balancing act: orchestrating amino-truncated and full-length p73 variants as decisive factors in cancer progression. *Oncogene* 34, 4287–4299. doi: 10.1038/onc.2014.365

Fahey, B., and Degnan, B. M. (2010). Origin of animal epithelia: insights from the sponge genome. *Evol. Dev.* 12, 601–617. doi: 10.1111/j.1525-142X.2010.00445.x

Ferland, R. J., Batiz, L. F., Neal, J., Lian, G., Bundock, E., Lu, J., et al. (2009). Disruption of neural progenitors along the ventricular and subventricular zones in periventricular heterotopia. *Hum. Mol. Genet.* 18, 497–516. doi: 10.1093/hmg/ddn377

Fernandez-Alonso, R., Martin-Lopez, M., Gonzalez-Cano, L., Garcia, S., Castrillo, F., Diez-Prieto, I., et al. (2015). p73 is required for endothelial cell differentiation, migration and the formation of vascular networks regulating VEGF and TGFβ signaling. *Cell Death Differ.* 22, 1287–1299. doi: 10.1038/cdd.2014.214

Fets, L., and Anastasiou, D. (2013). p73 keeps metabolic control in the family. *Nat. Cell Biol.* 15, 891–893. doi: 10.1038/ncb2810

Flores, E. R., Sengupta, S., Miller, J. B., Newman, J. J., Bronson, R., Crowley, D., et al. (2005). Tumor predisposition in mice mutant for *p63* and *p73*: evidence for broader tumor suppressor functions for the *p53* family. *Cancer Cell* 7, 363–373. doi: 10.1016/j.ccr.2005.02.019

Fuentealba, L. C., Rompani, S. B., Parraguez, J. I., Obernier, K., Romero, R., Cepko, C. L., et al. (2015). Embryonic origin of postnatal neural stem cells. *Cell* 161, 1644–1655. doi: 10.1016/j.cell.2015.05.041

Fuertes-Alvarez, S., Maeso-Alonso, L., Villoch-Fernandez, J., Wildung, M., Martin-Lopez, M., Marshall, C., et al. (2018). p73 regulates ependymal planar cell polarity by modulating actin and microtubule cytoskeleton. *Cell Death Dis.* 9, 1183–1183. doi: 10.1038/s41419-018-1205-6

Fujitani, M., Cancino, G. I., Dugani, C. B., Weaver, I. C. G., Gauthier-Fisher, A., Paquin, A., et al. (2010). TAp73 Acts via the bHLH Hey2 to promote long-term maintenance of neural precursors. *Curr. Biol.* 20, 2058–2065. doi: 10.1016/j.cub.2010.10.029

Fujitani, M., Sato, R., and Yamashita, T. (2017). Loss of p73 in ependymal cells during the perinatal period leads to aqueductal stenosis. *Sci. Rep.* 7:12007. doi: 10.1038/s41598-017-12105-z

Gonzalez-Cano, L., Fuertes-Alvarez, S., Robledinos-Anton, N., Bizy, A., Villena-Cortes, A., Fariñas, I., et al. (2016). p73 is required for ependymal cell maturation and neurogenic SVZ cytoarchitecture. *Dev. Neurobiol.* 76, 730–747. doi: 10.1002/dneu.22356

Gonzalez-Cano, L., Herreros-Villanueva, M., Fernandez-Alonso, R., Ayuso-Sacido, A., Meyer, G., Garcia-Verdugo, J. M., et al. (2010). p73 deficiency results in impaired self renewal and premature neuronal differentiation of mouse neural progenitors independently of p53. *Cell Death Dis.* 1:e109. doi: 10.1038/cddis.2010.87

González-Mariscal, L., Quirós, M., and Díaz-Coránguez, M. (2011). ZO Proteins and redox-dependent processes. *Antioxid. Redox Signal.* 15, 1235–1253. doi: 10.1089/ars.2011.3913

Guerra, M. M., González, C., Caprile, T., Jara, M., Vío, K., Muñoz, R. I., et al. (2015). Understanding how the subcommissural organ and other periventricular secretory structures contribute via the cerebrospinal fluid to neurogenesis. *Front. Cell. Neurosci.* 9:480–480. doi: 10.3389/fncel.2015.00480

Gumbiner, B. M. (1996). Cell adhesion: the molecular basis of tissue architecture and morphogenesis. *Cell* 84, 345–357. doi: 10.1016/S0092-8674(00)81279-9

Hagios, C., Lochter, A., and Bissell, M. J. (1998). Tissue architecture: the ultimate regulator of epithelial function? *Philos. Trans. R. Soc. Lond. B Biol. Sci.* 353, 857–870. doi: 10.1098/rstb.1998.0250

Han, S., Semba, S., Abe, T., Makino, N., Furukawa, T., Fukushige, S., et al. (1999). Infrequent somatic mutations of thep73genein various human cancers. *Eur. J. Surg. Oncol.* 25, 194–198. doi: 10.1053/ejso.1998.0626

Harumoto, T., Ito, M., Shimada, Y., Kobayashi, T. J., Ueda, H. R., Lu, B., et al. (2010). Atypical Cadherins Dachsous and fat control dynamics of noncentrosomal microtubules in planar cell polarity. *Dev. Cell* 19, 389–401. doi: 10.1016/j.devcel.2010.08.004

Henderson, D. J., Long, D. A., and Dean, C. H. (2018). Planar cell polarity in organ formation. *Curr. Opin. Cell Biol.* 55, 96–103. doi: 10.1016/j.ceb.2018.06.011

Hernández-Acosta, N. C., Cabrera-Socorro, A., Morlans, M. P., Delgado, F. J. G., Suárez-Solá, M. L., Sottocornola, R., et al. (2011). Dynamic expression of the p53 family members p63 and p73 in the mouse and human telencephalon during development and in adulthood. *Brain Res.* 1372, 29–40. doi: 10.1016/j.brainres.2010.11.041

Holembowski, L., Kramer, D., Riedel, D., Sordella, R., Nemajerova, A., Dobbelstein, M., et al. (2014). TAp73 is essential for germ cell adhesion and maturation in testis. *J. Cell Biol.* 204, 1173–1190. doi: 10.1083/jcb.201306066

Hooper, C., Tavassoli, M., Chapple, J. P., Uwanogho, D., Goodyear, R., Melino, G., et al. (2006). TAp73 isoforms antagonize Notch signalling in SH-SY5Y neuroblastomas and in primary neurones. *J. Neurochem.* 99, 989–999. doi: 10.1111/j.1471-4159.2006.04142.x

Huang, D. W., Sherman, B. T., and Lempicki, R. A. (2008). Bioinformatics enrichment tools: paths toward the comprehensive functional analysis of large gene lists. *Nucleic Acids Res.* 37, 1–13. doi: 10.1093/nar/gkn923

Huang, D. W., Sherman, B. T., and Lempicki, R. A. (2009). Systematic and integrative analysis of large gene lists using DAVID bioinformatics resources. *Nat. Protoc.* 4, 44–57. doi: 10.1038/nprot.2008.211

Huang, X., Qu, R., Ouyang, J., Zhong, S., and Dai, J. (2020). An overview of the cytoskeleton-associated role of PDLIM5. *Front. Physiol.* 11:975. doi: 10.3389/fphys.2020.00975

Ichimiya, S., Nimura, Y., Kageyama, H., Takada, N., Sunahara, M., Shishikura, T., et al. (1999). p73 at chromosome 1p36.3 is lost in advanced stage neuroblastoma but its mutation is infrequent. *Oncogene* 18, 1061–1066. doi: 10.1038/sj.onc.1202390

Inoue, K., and Fry, E. A. (2014). Alterations of p63 and p73 in human cancers. *Subcell. Biochem.* 85, 17–40. doi: 10.1007/978-94-017-9211-0_2

Inoue, S., Tomasini, R., Rufini, A., Elia, A. J., Agostini, M., Amelio, I., et al. (2014). TAp73 is required for spermatogenesis and the maintenance of male fertility. *Proc. Natl. Acad. Sci. U.S.A.* 111, 1843–1848. doi: 10.1073/pnas.1323416111

Ishimoto, O., Kawahara, C., Enjo, K., Obinata, M., Nukiwa, T., and Ikawa, S. (2002). Possible oncogenic potential of ΔNp73. *Cancer Res.* 62, 636–641.

Jost, C. A., Marin, M. C., and Kaelin, W. G. Jr. (1997). p73 is a human p53-related protein that can induce apoptosis. *Nature* 389, 191–194. doi: 10.1038/38298

Juan, T., Géminard, C., Coutelis, J.-B., Cerezo, D., Polès, S., Noselli, S., et al. (2018). Myosin1D is an evolutionarily conserved regulator of animal left–right asymmetry. *Nat. Commun.* 9:1942. doi: 10.1038/s41467-018-04284-8

Kaelin, W. G. (1998). Another p53 Doppelgänger? *Science* 281, 57–58. doi: 10.1126/science.281.5373.57

Kaghad, M., Bonnet, H., Yang, A., Creancier, L., Biscan, J.-C., Valent, A., et al. (1997). Monoallelically expressed gene related to p53 at 1p36, a region frequently deleted in neuroblastoma and other human cancers. *Cell* 90, 809–819. doi: 10.1016/S0092-8674(00)80540-1

Killick, R., Niklison-Chirou, M., Tomasini, R., Bano, D., Rufini, A., Grespi, F., et al. (2011). p73: a multifunctional protein in neurobiology. *Mol. Neurobiol.* 43, 139–146. doi: 10.1007/s12035-011-8172-6

Koeppel, M., van Heeringen, S. J., Kramer, D., Smeenk, L., Janssen-Megens, E., Hartmann, M., et al. (2011). Crosstalk between c-Jun and TAp73α/β contributes to the apoptosis–survival balance. *Nucleic Acids Res.* 39, 6069–6085. doi: 10.1093/nar/gkr028

Koga, Y., and Ikebe, M. (2005). p116Rip decreases myosin ii phosphorylation by activating myosin light chain phosphatase and by inactivating RhoA *. *J. Biol. Chem.* 280, 4983–4991. doi: 10.1074/jbc.M410909200

Kuo, C. T., Mirzadeh, Z., Soriano-Navarro, M., Rasin, M., Wang, D., Shen, J., et al. (2006). Postnatal deletion of Numb/Numblike reveals repair and remodeling capacity in the subventricular neurogenic niche. *Cell* 127, 1253–1264. doi: 10.1016/j.cell.2006.10.041

Lamb, M. C., and Tootle, T. L. (2020). Fascin in cell migration: more than an actin bundling protein. *Biology* 9:403. doi: 10.3390/biology9110403

Landré, V., Antonov, A., Knight, R., and Melino, G. (2016). p73 promotes glioblastoma cell invasion by directly activating POSTN (periostin) expression. *Oncotarget* 7, 11785–11802. doi: 10.18632/oncotarget.7600

Lane, D. P., and Crawford, L. V. (1979). T antigen is bound to a host protein in SV40-transformed cells. *Nature* 278, 261–263. doi: 10.1038/278261a0

Lee, C.-W., and La Thangue, N. B. (1999). Promoter specificity and stability control of the p53-related protein p73. *Oncogene* 18, 4171–4181. doi: 10.1038/sj.onc.1202793

Levine, A. J. (2020). p53: 800 million years of evolution and 40 years of discovery. *Nat. Rev. Cancer* 20, 471–480. doi: 10.1038/s41568-020-0262-1

Liu, G., Nozell, S., Xiao, H., and Chen, X. (2004). ΔNp73β is active in transactivation and growth suppression. *Mol. Cell. Biol.* 24, 487–501. doi: 10.1128/MCB.24.2.487-501.2004

Liu, H., Zhang, Y., Li, L., Cao, J., Guo, Y., Wu, Y., et al. (2021). Fascin actin-bundling protein 1 in human cancer: Promising biomarker or therapeutic target? *Mol. Ther. Oncolytics* 20, 240–264. doi: 10.1016/j.omto.2020.12.014

Livera, G., Petre-Lazar, B., Guerquin, M.-J., Trautmann, E., Coffigny, H., and Habert, R. (2008). p63 null mutation protects mouse oocytes from radio-induced apoptosis. *Reproduction* 135, 3–12. doi: 10.1530/rep-07-0054

Logotheti, S., Marquardt, S., Richter, C., Sophie Hain, R., Murr, N., Takan, I., et al. (2020). Neural networks recapitulation by cancer cells promotes disease progression: a novel role of p73 isoforms in cancer-neuronal crosstalk. *Cancers* 12:3789. doi: 10.3390/cancers12123789

Logotheti, S., Pavlopoulou, A., Galtsidis, S., Vojtesek, B., and Zoumpourlis, V. (2013). Functions, divergence and clinical value of TAp73 isoforms in cancer. *Cancer Metastasis Rev.* 32, 511–534. doi: 10.1007/s10555-013-9424-x

López-Ferreras, L., Martínez-García, N., Maeso-Alonso, L., Martín-López, M., Díez-Matilla, Á., Villoch-Fernandez, J., et al. (2021). Deciphering the nature of Trp73 isoforms in mouse embryonic stem cell models: generation of isoform-specific deficient cell lines using the CRISPR/Cas9 gene editing system. *Cancers* 13:3182. doi: 10.3390/cancers13133182

Lu, R.-Y., Yang, W.-X., and Hu, Y.-J. (2014). The role of epithelial tight junctions involved in pathogen infections. *Mol. Biol. Rep.* 41, 6591–6610. doi: 10.1007/s11033-014-3543-5

Marin, M. C., Jost, C. A., Irwin, M. S., DeCaprio, J. A., Caput, D., and Kaelin, W. G. Jr. (1998). Viral oncoproteins discriminate between p53 and the p53 homolog p73. *Mol. Cell. Biol.* 18, 6316–6324. doi: 10.1128/MCB.18.11.6316

Marini, A., Rotblat, B., Sbarrato, T., Niklison-Chirou, M. V., Knight, J. R. P., Dudek, K., et al. (2018). TAp73 contributes to the oxidative stress response by regulating protein synthesis. *Proc. Natl. Acad. Sci. U.S.A.* 115, 6219–6224. doi: 10.1073/pnas.1718531115

Marín-Padilla, M. (2015). Human cerebral cortex Cajal-Retzius neuron: development, structure and function. A Golgi study. *Front. Neuroanat.* 9:21. doi: 10.3389/fnana.2015.00021

Marques, M. M., Villoch-Fernandez, J., Maeso-Alonso, L., Fuertes-Alvarez, S., and Marin, M. C. (2019). The Trp73 mutant mice: a ciliopathy model that uncouples ciliogenesis from planar cell polarity. *Front. Genet.* 10:154. doi: 10.3389/fgene.2019.00154

Marqués-García, F., Ferrandiz, N., Fernández-Alonso, R., González-Cano, L., Herreros-Villanueva, M., Rosa-Garrido, M., et al. (2009). p73 plays a role in erythroid differentiation through GATA1 induction. *J. Biol. Chem.* 284, 21139–21156. doi: 10.1074/jbc.M109.026849

Marshall, C. B., Mays, D. J., Beeler, J. S., Rosenbluth, J. M., Boyd, K. L., Santos Guasch, G. L., et al. (2016). p73 is required for multiciliogenesis and regulates the Foxj1-associated gene network. *Cell Rep.* 14, 2289–2300. doi: 10.1016/j.celrep.2016.02.035

Matsunaga, Y., Noda, M., Murakawa, H., Hayashi, K., Nagasaka, A., Inoue, S., et al. (2017). Reelin transiently promotes N-cadherin–dependent neuronal adhesion during mouse cortical development. *Proc. Natl. Acad. Sci. U.S.A.* 114, 2048. doi: 10.1073/pnas.1615215114

Medawar, A., Virolle, T., Rostagno, P., de la Forest-Divonne, S., Gambaro, K., Rouleau, M., et al. (2008). ΔNp63 is essential for epidermal commitment of embryonic stem cells. *PLoS One* 3:e3441. doi: 10.1371/journal.pone.0003441

Medina-Bolívar, C., González-Arnay, E., Talos, F., González-Gómez, M., Moll, U. M., and Meyer, G. (2014). Cortical hypoplasia and ventriculomegaly of p73-deficient mice: developmental and adult analysis. *J. Comp. Neurol.* 522, 2663–2679. doi: 10.1002/cne.23556

Merte, J., Jensen, D., Wright, K., Sarsfield, S., Wang, Y., Schekman, R., et al. (2010). Sec24b selectively sorts Vangl2 to regulate planar cell polarity during neural tube closure. *Nat. Cell Biol.* 12, 41–48. doi: 10.1038/ncb2002

Miller, P. W., Clarke, D. N., Weis, W. I., Lowe, C. J., and Nelson, W. J. (2013). The evolutionary origin of epithelial cell-cell adhesion mechanisms. *Curr. Top. Membr.* 72, 267–311. doi: 10.1016/b978-0-12-417027-8.00008-8

Mirzadeh, Z., Doetsch, F., Sawamoto, K., Wichterle, H., and Alvarez-Buylla, A. (2010). The subventricular zone en-face: wholemount staining and ependymal flow. *J. Vis. Exp.* 39:1938. doi: 10.3791/1938

Morante-Redolat, J. M., and Porlan, E. (2019). Neural stem cell regulation by adhesion molecules within the subependymal niche. *Front. Cell Dev. Biol.* 7:102. doi: 10.3389/fcell.2019.00102

Murray-Zmijewski, F., Lane, D. P., and Bourdon, J. C. (2006). p53/p63/p73 isoforms: an orchestra of isoforms to harmonise cell differentiation and response to stress. *Cell Death Differ.* 13, 962–972. doi: 10.1038/sj.cdd.4401914

Nemajerova, A., Amelio, I., Gebel, J., Dötsch, V., Melino, G., and Moll, U. M. (2018). Non-oncogenic roles of TAp73: from multiciliogenesis to metabolism. *Cell Death Differ.* 25, 144–153. doi: 10.1038/cdd.2017.178

Nemajerova, A., and Moll, U. M. (2019). Tissue-specific roles of p73 in development and homeostasis. *J. Cell Sci.* 132:jcs233338. doi: 10.1242/jcs.233338

Nemajerova, A., Kramer, D., Siller, S. S., Herr, C., Shomroni, O., Pena, T., et al. (2016). TAp73 is a central transcriptional regulator of airway multiciliogenesis. *Genes Dev.* 30, 1300–1312. doi: 10.1101/gad.279836.116

Niemantsverdriet, M., Nagle, P., Chiu, R. K., Langendijk, J. A., Kampinga, H. H., and Coppes, R. P. (2012). ΔNp73 enhances promoter activity of TGF-β induced genes. *PLoS One* 7:e50815–e50815. doi: 10.1371/journal.pone.0050815

Niklison-Chirou, M. V., Erngren, I., Engskog, M., Haglöf, J., Picard, D., Remke, M., et al. (2017). TAp73 is a marker of glutamine addiction in medulloblastoma. *Genes Dev.* 31, 1738–1753. doi: 10.1101/gad.302349.117

Ohata, S., and Alvarez-Buylla, A. (2016). Planar organization of multiciliated ependymal (E1) cells in the brain ventricular epithelium. *Trends Neurosci.* 39, 543–551. doi: 10.1016/j.tins.2016.05.004

Ohata, S., Nakatani, J., Herranz-Pérez, V., Cheng, J., Belinson, H., Inubushi, T., et al. (2014). Loss of Dishevelleds disrupts planar polarity in ependymal motile cilia and results in hydrocephalus. *Neuron* 83, 558–571. doi: 10.1016/j.neuron.2014.06.022

Paez-Gonzalez, P., Abdi, K., Luciano, D., Liu, Y., Soriano-Navarro, M., Rawlins, E., et al. (2011). Ank3-dependent SVZ niche assembly is required for the continued production of new neurons. *Neuron* 71, 61–75. doi: 10.1016/j.neuron.2011.05.029

Pankow, S., and Bamberger, C. (2007). The p53 tumor suppressor-like protein nvp63 mediates selective germ cell death in the sea anemone *Nematostella vectensis*. *PLoS One* 2:e782. doi: 10.1371/journal.pone.0000782

Petrenko, O., Zaika, A., and Moll, U. M. (2003). ΔNp73 facilitates cell immortalization and cooperates with oncogenic Ras in cellular transformation *in vivo*. *Mol. Cell. Biol.* 23, 5540–5555. doi: 10.1128/MCB.23.16.5540-5555.2003

Pflaum, J., Schlosser, S., and Müller, M. (2014). p53 family and cellular stress responses in cancer. *Front. Oncol.* 4:285. doi: 10.3389/fonc.2014.00285

Pujadas, L., Gruart, A., Bosch, C., Delgado, L., Teixeira, C. M., Rossi, D., et al. (2010). Reelin regulates postnatal neurogenesis and enhances spine hypertrophy and long-term potentiation. *J. Neurosci.* 30, 4636–4649. doi: 10.1523/JNEUROSCI.5284-09.2010

Raya-Sandino, A., Castillo-Kauil, A., Domínguez-Calderón, A., Alarcón, L., Flores-Benitez, D., Cuellar-Perez, F., et al. (2017). Zonula occludens-2 regulates Rho proteins activity and the development of epithelial cytoarchitecture and barrier function. *Biochim. Biophys. Acta* 1864, 1714–1733. doi: 10.1016/j.bbamcr.2017.05.016

Redmond, S. A., Figueres-Oñate, M., Obernier, K., Nascimento, M. A., Parraguez, J. I., López-Mascaraque, L., et al. (2019). Development of ependymal and postnatal neural stem cells and their origin from a common embryonic progenitor. *Cell Rep.* 27, 429–441.e3. doi: 10.1016/j.celrep.2019.01.088

Robinson, R. (2015). Link between cell junctions and microtubule cytoskeleton is critical for epithelial morphogenesis. *PLoS Biol.* 13:e1002088. doi: 10.1371/journal.pbio.1002088

Rodríguez, E. M., Guerra, M. M., Vío, K., González, C., Ortloff, A., Bátiz, L. F., et al. (2012). A cell junction pathology of neural stem cells leads to abnormal

neurogenesis and hydrocephalus. *Biol. Res.* 45, 231–241. doi: 10.4067/s0716-97602012000300005

Rodriguez-Boulan, E., and Macara, I. G. (2014). Organization and execution of the epithelial polarity programme. *Nat. Rev. Mol. Cell Biol.* 15, 225–242. doi: 10.1038/nrm3775

Rutkowski, R., Hofmann, K., and Gartner, A. (2010). Phylogeny and function of the invertebrate p53 superfamily. *Cold Spring Harb. Perspect. Biol.* 2:a001131. doi: 10.1101/cshperspect.a001131

Sabapathy, K. (2015). p73: a positive or negative regulator of angiogenesis, or Both? *Mol. Cell. Biol.* 36, 848–854. doi: 10.1128/MCB.00929-15

Sanada, K., Gupta, A., and Tsai, L.-H. (2004). Disabled-1-regulated adhesion of migrating neurons to radial glial fiber contributes to neuronal positioning during early corticogenesis. *Neuron* 42, 197–211. doi: 10.1016/s0896-6273(04)00222-3

Santos Guasch, G. L., Beeler, J. S., Marshall, C. B., Shaver, T. M., Sheng, Q., Johnson, K. N., et al. (2018). p73 is required for ovarian follicle development and regulates a gene network involved in cell-to-cell adhesion. *iScience* 8, 236–249. doi: 10.1016/j.isci.2018.09.018

Scadden, D. T. (2006). The stem-cell niche as an entity of action. *Nature* 441, 1075–1079. doi: 10.1038/nature04957

Sekine, K., Kawauchi, T., Kubo, K.-I., Honda, T., Herz, J., Hattori, M., et al. (2012). Reelin controls neuronal positioning by promoting cell-matrix adhesion via inside-out activation of integrin α5β1. *Neuron* 76, 353–369. doi: 10.1016/j.neuron.2012.07.020

Serber, Z., Lai Helen, C., Yang, A., Ou Horng, D., Sigal Martina, S., Kelly Alexander, E., et al. (2002). A C-terminal inhibitory domain controls the activity of p63 by an intramolecular mechanism. *Mol. Cell. Biol.* 22, 8601–8611. doi: 10.1128/MCB.22.24.8601-8611.2002

Shimada, Y., Yonemura, S., Ohkura, H., Strutt, D., and Uemura, T. (2006). Polarized transport of frizzled along the planar microtubule arrays in *Drosophila* Wing Epithelium. *Dev. Cell* 10, 209–222. doi: 10.1016/j.devcel.2005.11.016

Smith, C. L., and Mayorova, T. D. (2019). Insights into the evolution of digestive systems from studies of *Trichoplax adhaerens*. *Cell Tissue Res.* 377, 353–367. doi: 10.1007/s00441-019-03057-z

Smutny, M., and Yap, A. S. (2010). Neighborly relations: cadherins and mechanotransduction. *J. Cell Biol.* 189, 1075–1077. doi: 10.1083/jcb.201005151

Sobierajska, K., Ciszewski, W. M., Wawro, M. E., Wieczorek-Szukała, K., Boncela, J., Papiewska-Pajak, I., et al. (2019). TUBB4B downregulation is critical for increasing migration of metastatic colon cancer cells. *Cells* 8:810. doi: 10.3390/cells8080810

Soriano, E., and del Río, J. A. (2005). The cells of Cajal-Retzius: still a mystery one century after. *Neuron* 46, 389–394. doi: 10.1016/j.neuron.2005.04.019

Spassky, N., Merkle, F. T., Flames, N., Tramontin, A. D., García-Verdugo, J. M., and Alvarez-Buylla, A. (2005). Adult ependymal cells are postmitotic and are derived from radial glial cells during embryogenesis. *J. Neurosci.* 25, 10–18. doi: 10.1523/JNEUROSCI.1108-04.2005

Srivastava, M., Begovic, E., Chapman, J., Putnam, N. H., Hellsten, U., Kawashima, T., et al. (2008). The Trichoplax genome and the nature of placozoans. *Nature* 454, 955–960. doi: 10.1038/nature07191

Stantic, M., Sakil, H. A. M., Zirath, H., Fang, T., Sanz, G., Fernandez-Woodbridge, A., et al. (2015). TAp73 suppresses tumor angiogenesis through repression of proangiogenic cytokines and HIF-1α activity. *Proc. Natl. Acad. Sci. U.S.A.* 112, 220–225. doi: 10.1073/pnas.1421697112

Steder, M., Alla, V., Meier, C., Spitschak, A., Pahnke, J., Fürst, K., et al. (2013). DNp73 exerts function in metastasis initiation by disconnecting the inhibitory role of EPLIN on IGF1R-AKT/STAT3 signaling. *Cancer Cell* 24, 512–527. doi: 10.1016/j.ccr.2013.08.023

Stiewe, T., Theseling, C. C., and Pützer, B. M. (2002). Transactivation-deficient Delta TA-p73 inhibits p53 by direct competition for DNA Binding: IMPLICATIONS FOR TUMORIGENESIS *. *J. Biol. Chem.* 277, 14177–14185. doi: 10.1074/jbc.M200480200

Straub, W. E., Weber, T. A., Schäfer, B., Candi, E., Durst, F., Ou, H. D., et al. (2010). The C-terminus of p63 contains multiple regulatory elements with different functions. *Cell Death Dis.* 1:e5. doi: 10.1038/cddis.2009.1

Suh, E.-K., Yang, A., Kettenbach, A., Bamberger, C., Michaelis, A. H., Zhu, Z., et al. (2006). p63 protects the female germ line during meiotic arrest. *Nature* 444, 624–628. doi: 10.1038/nature05337

Takagishi, M., Sawada, M., Ohata, S., Asai, N., Enomoto, A., Takahashi, K., et al. (2017). Daple coordinates planar polarized microtubule dynamics in ependymal cells and contributes to hydrocephalus. *Cell Rep.* 20, 960–972. doi: 10.1016/j.celrep.2017.06.089

Talos, F., Abraham, A., Vaseva, A. V., Holembowski, L., Tsirka, S. E., Scheel, A., et al. (2010). p73 is an essential regulator of neural stem cell maintenance in embryonal and adult CNS neurogenesis. *Cell Death Differ.* 17, 1816–1829. doi: 10.1038/cdd.2010.131

Tissir, F., Ravni, A., Achouri, Y., Riethmacher, D., Meyer, G., and Goffinet, A. M. (2009). DeltaNp73 regulates neuronal survival *in vivo*. *Proc. Natl. Acad. Sci. U.S.A.* 106, 16871–16876. doi: 10.1073/pnas.0903191106

Tomasini, R., Tsuchihara, K., Wilhelm, M., Fujitani, M., Rufini, A., Cheung, C. C., et al. (2008). TAp73 knockout shows genomic instability with infertility and tumor suppressor functions. *Genes Dev.* 22, 2677–2691. doi: 10.1101/gad.1695308

Ueda, Y., Hijikata, M., Takagi, S., Chiba, T., and Shimotohno, K. (1999). New p73 variants with altered C-terminal structures have varied transcriptional activities. *Oncogene* 18, 4993–4998. doi: 10.1038/sj.onc.1202817

Vikhreva, P., Melino, G., and Amelio, I. (2018). p73 alternative splicing: exploring a biological role for the C-terminal isoforms. *J. Mol. Biol.* 430, 1829–1838. doi: 10.1016/j.jmb.2018.04.034

Vladar, E. K., and Axelrod, J. D. (2008). Dishevelled links basal body docking and orientation in ciliated epithelial cells. *Trends Cell Biol.* 18, 517–520. doi: 10.1016/j.tcb.2008.08.004

Vladar, E. K., Bayly, R. D., Sangoram, A. M., Scott, M. P., and Axelrod, J. D. (2012). Microtubules enable the planar cell polarity of airway cilia. *Curr. Biol.* 22, 2203–2212. doi: 10.1016/j.cub.2012.09.046

Wang, c., teo, c. R., and sabapathy, k. (2020). P53-related transcription targets of TAp73 in cancer cells-bona fide or distorted reality? *Int. J. Mol. Sci.* 21:1346. doi: 10.3390/ijms21041346

Wang, Q., Zou, Y., Nowotschin, S., Kim, S. Y., Li, Q. V., Soh, C.-L., et al. (2017). The p53 family coordinates Wnt and nodal inputs in Mesendodermal differentiation of embryonic stem cells. *Cell Stem Cell* 20, 70–86. doi: 10.1016/j.stem.2016.10.002

Wei, J., O'Brien, D., Vilgelm, A., Piazuelo, M. B., Correa, P., Washington, M. K., et al. (2008). Interaction of *Helicobacter* pylori with gastric epithelial cells is mediated by the p53 protein family. *Gastroenterology* 134, 1412–1423. doi: 10.1053/j.gastro.2008.01.072

Werner, M. E., and Mitchell, B. J. (2012). Understanding ciliated epithelia: the power of *Xenopus*. *Genesis* 50, 176–185. doi: 10.1002/dvg.20824

Werner, M. E., Hwang, P., Huisman, F., Taborek, P., Yu, C. C., and Mitchell, B. J. (2011). Actin and microtubules drive differential aspects of planar cell polarity in multiciliated cells. *J. Cell Biol.* 195, 19–26. doi: 10.1083/jcb.201106110

Wetterskog, D., Moshiri, A., Ozaki, T., Uramoto, H., Nakagawara, A., and Funa, K. (2009). Dysregulation of platelet-derived growth factor β-receptor expression by ΔNp73 in Neuroblastoma. *Mol. Cancer Res.* 7, 2031–2039. doi: 10.1158/1541-7786.mcr-08-0501

Wiche, G., Osmanagic-Myers, S., and Castañón, M. J. (2015). Networking and anchoring through plectin: a key to IF functionality and mechanotransduction. *Curr. Opin. Cell Biol.* 32, 21–29. doi: 10.1016/j.ceb.2014.10.002

Wildung, M., Esser, T. U., Grausam, K. B., Wiedwald, C., Volceanov-Hahn, L., Riedel, D., et al. (2019). Transcription factor TAp73 and microRNA-449 complement each other to support multiciliogenesis. *Cell Death Differ.* 26, 2740–2757. doi: 10.1038/s41418-019-0332-7

Wilhelm, M. T., Rufini, A., Wetzel, M. K., Tsuchihara, K., Inoue, S., Tomasini, R., et al. (2010). Isoform-specific p73 knockout mice reveal a novel role for delta Np73 in the DNA damage response pathway. *Genes Dev.* 24, 549–560. doi: 10.1101/gad.1873910

Wolfsberger, J., Sakil, H. A. M., Zhou, L., van Bree, N., Baldisseri, E., de Souza Ferreira, S., et al. (2021). TAp73 represses NF-κB–mediated recruitment of tumor-associated macrophages in breast cancer. *Proc. Natl. Acad. Sci. U.S.A.* 118:e2017089118. doi: 10.1073/pnas.2017089118

Xie, N., Vikhreva, P., Annicchiarico-Petruzzelli, M., Amelio, I., Barlev, N., Knight, R. A., et al. (2018). Integrin-β4 is a novel transcriptional target of TAp73. *Cell Cycle* 17, 589–594. doi: 10.1080/15384101.2017.1403684

Yang, A., Kaghad, M., Wang, Y., Gillett, E., Fleming, M. D., Dötsch, V., et al. (1998). p63, a p53 homolog at 3q27–29, encodes multiple products with transactivating,

death-inducing, and dominant-negative activities. *Mol. Cell* 2, 305–316. doi: 10.1016/S1097-2765(00)80275-0

Yang, A., Walker, N., Bronson, R., Kaghad, M., Oosterwegel, M., Bonnin, J., et al. (2000). p73-deficient mice have neurological, pheromonal and inflammatory defects but lack spontaneous tumours. *Nature* 404, 99–103. doi: 10.1038/35003607

Zhang, Y., Yan, W., Jung, Y. S., and Chen, X. (2012). Mammary epithelial cell polarity is regulated differentially by p73 isoforms via Epithelial-to-mesenchymal Transition *. *J. Biol. Chem.* 287, 17746–17753. doi: 10.1074/jbc.M112.358143

Conflict of Interest: The authors declare that the research was conducted in the absence of any commercial or financial relationships that could be construed as a potential conflict of interest.

Publisher's Note: All claims expressed in this article are solely those of the authors and do not necessarily represent those of their affiliated organizations, or those of the publisher, the editors and the reviewers. Any product that may be evaluated in this article, or claim that may be made by its manufacturer, is not guaranteed or endorsed by the publisher.

Copyright © 2021 Maeso-Alonso, López-Ferreras, Marques and Marin. This is an open-access article distributed under the terms of the Creative Commons Attribution License (CC BY). The use, distribution or reproduction in other forums is permitted, provided the original author(s) and the copyright owner(s) are credited and that the original publication in this journal is cited, in accordance with accepted academic practice. No use, distribution or reproduction is permitted which does not comply with these terms.

frontiers in Cell and Developmental Biology

REVIEW
published: 29 July 2021
doi: 10.3389/fcell.2021.715974

The p53 Family: A Role in Lipid and Iron Metabolism

*Kyra Laubach, Jin Zhang and Xinbin Chen**

Comparative Oncology Laboratory, Schools of Veterinary Medicine and Medicine, University of California, Davis, Davis, CA, United States

The p53 family of tumor suppressors, which includes p53, p63, and p73, has a critical role in many biological processes, such as cell cycle arrest, apoptosis, and differentiation. In addition to tumor suppression, the p53 family proteins also participate in development, multiciliogenesis, and fertility, indicating these proteins have diverse roles. In this review, we strive to cover the relevant studies that demonstrate the roles of p53, p63, and p73 in lipid and iron metabolism.

Keywords: p53, p63, p73, metabolism, lipid, iron

INTRODUCTION

For over 40 years, p53 has been characterized as a master transcriptional regulator that mediates the expression of various genes to prevent aberrant cell growth (Ko and Prives, 1996). Just before the turn of the century, the *TP63* and *TP73* genes were discovered due to their significant homology to *TP53*, particularly in the DNA-binding domain (Kaghad et al., 1997; Schmale and Bamberger, 1997; Trink et al., 1998; Borremans et al., 2001). These three genes constitute the p53 family.

The *TP53, TP63,* and *TP73* genes are expressed as multiple N- and C-terminal isoforms through two promoters and alternative splicing (**Figure 1**). In *TP53*, promoter 1 (P1) gives rise to two translation initiation start sites, termed ATG1 and ATG40, which produce full-length p53 (FLp53) and Δ40p53, respectively (Courtois et al., 2002; Yin et al., 2002). Both isoforms possess transactivation function even though Δ40p53 contains a truncated form of the conventional transactivation domain (Zhu et al., 1998; 2000; Harms and Chen, 2005). Similarly driven by P1, *TP63/73* express TAp63/73 isoforms, which have a transactivation domain that is comparable to the one found in FLp53 (Arrowsmith, 1999). By using promoter 2 (P2), all family members produce the N-terminally truncated isoforms, termed Δ133p53 and Δ160p53 in *TP53*, which arise from translation initiation start sites ATG133 and ATG160 (Bourdon et al., 2005), and ΔNp63/73 in *TP63/73* (Yang et al., 1998; 2000). Interestingly, despite lacking the conventional transactivation domain, ΔNp63 and ΔNp73 are transcriptionally active and can induce some p53 targets (Liu et al., 2004; Helton et al., 2006). Alternative splicing at the C-terminus of each gene generates additional isoforms. *TP53* produces three (α, β, γ) C-terminal isoforms (Bourdon et al., 2005), *TP63* produces four (α, β, γ, δ) C-terminal isoforms (Yang et al., 1998; Mangiulli et al., 2009), and *TP73* produces at least seven C-terminal isoforms (α, β, γ, δ, ε, ζ, η) (De Laurenzi et al., 1998; 1999). While the N-terminal isoforms of p53, p63, and p73 are well studied, the C-terminal isoforms remain largely uncharacterized.

The biological function of the p53 family proteins has been demonstrated through various mouse models. The very first p53-knockout model showed that mice deficient in p53 were prone to spontaneous tumors, but otherwise developed normally (Donehower et al., 1991). Later, it was discovered that p53 dysregulation, predominantly overexpression, can lead to impaired embryogenesis and other developmental defects (Luna et al., 1995; Sah et al., 1995; Parant et al., 2001; Zhang et al., 2012; Nostrand et al., 2014). Unlike p53, total p63-knockout mice exhibit severe epidermal and craniofacial abnormalities and die shortly after birth (Celli et al., 1999; Mills et al., 1999; Yang et al., 1999). Further studies revealed that ΔNp63 is responsible for the

OPEN ACCESS

Edited by:
Kanaga Sabapathy, National Cancer Centre Singapore, Singapore

Reviewed by:
Koji Itahana, Duke-NUS Medical School, Singapore
Qing Feng, Nanjing Medical University, China

***Correspondence:**
Xinbin Chen
xbchen@ucdavis.edu

Specialty section:
This article was submitted to Molecular and Cellular Pathology, a section of the journal Frontiers in Cell and Developmental Biology

Received: *27 May 2021*
Accepted: *08 July 2021*
Published: *29 July 2021*

Citation:
Laubach K, Zhang J and Chen X (2021) The p53 Family: A Role in Lipid and Iron Metabolism. Front. Cell Dev. Biol. 9:715974. doi: 10.3389/fcell.2021.715974

observed phenotype (Candi et al., 2006; Koster et al., 2007). In contrast, TAp63-knockout mice did not exhibit birth defects, but were prone to spontaneous tumors, indicating that TAp63 functions as a tumor suppressor to maintain genome stability (Suh et al., 2006; Guo et al., 2009; Su et al., 2009). Similarly, total p73-knockout mice were runty and had severe neurological defects, chronic inflammation, fertility issues (Yang et al., 2000), and impaired multiciliogenesis (Marshall et al., 2016; Nemajerova et al., 2016). It was later found that ΔNp73-knockout mice exhibited neurodegeneration (Wilhelm et al., 2010), whereas TAp73-knockout mice were prone to spontaneous tumors (Tomasini et al., 2008).

Continued research efforts into the more nuanced cancer-associated roles of the p53 family proteins is undeniably valuable. However, emerging evidence suggests that these proteins possess additional important functions that can affect various human diseases, such as diabetes mellitus and liver steatosis. This review will focus specifically on the roles of the p53 family in lipid and iron metabolism.

LIPID METABOLISM

Lipids play an important role in various biological processes and serve as an essential building block for many cellular structures. Tight regulation of lipid metabolism is crucial for proper organismal function, and dysregulation has been implicated in numerous diseases, such as Alzheimer's disease and fatty liver disease (Hooijmans and Kiliaan, 2008; Hasson et al., 2016). There are three main sources of lipids: dietary lipids, fatty acids produced by hepatocytes and adipocytes, and lipoproteins produced by hepatocytes (Giammanco et al., 2015). In the lumen of the gastrointestinal tract, dietary lipids become emulsified by combining with bile salts, which allows for lipid hydrolysis and subsequent import to enterocytes (Hussain, 2014). In enterocytes, lipids are processed by the endoplasmic reticulum and packaged into lipoprotein bundles, called chylomicrons (Hussain, 2014; Giammanco et al., 2015), to allow for transport through the circulation (Alekos et al., 2020). Once chylomicrons arrive at a target cell, lipases break them down to permit cellular import of lipids (Alekos et al., 2020). Hepatocytes are then responsible for recycling chylomicron components to allow for later use (Alekos et al., 2020).

At the cellular level, lipids are categorized into three groups: structural lipids, lipid droplets, and bioactive lipids. Structural lipids are comprised of phospholipids and form cell and organelle membranes (Bohdanowicz and Grinstein, 2013), which are important for cellular compartmentalization. Lipids are also a main source of energy and are stored as modified sterols and fatty acids in specialized organelles called lipid droplets, which are predominantly found in adipocytes (Röhrig and Schulze, 2016; Olzmann and Carvalho, 2019). This modification gives sterols and fatty acids a neutral charge to form sterol esters (Korber et al., 2017) and triglycerides (Alves-Bezerra and Cohen, 2018), respectively. Bioactive lipids are unique in that they are involved in signal transduction and are categorized into multiple classes, including sphingolipids (Hannun and Obeid, 2008), diacylglycerols (Peter-Riesch et al., 1988), and eicosanoids (Levy et al., 2001). Sphingolipids are further categorized into several sub-classes, such as sphingomyelin, galactosylceramide, glucosylceramide, and sphingosine (Hannun and Obeid, 2018). Studies have shown that sphingolipids can modulate cell death and survival pathways, including apoptosis, cell growth/inhibition, and migration (Hannun and Obeid, 2018). Diacylglycerols serve as a secondary messenger in many critical cellular processes, such as neurotransmitter release (Ma et al., 2013) and insulin signaling in islet cells (Peter-Riesch et al., 1988). Eicosanoids have been implicated in mediating the inflammatory response (Levy et al., 2001). Lipids are exceedingly important for many cellular processes, from structure to signaling. In this review, we focus on the role of the p53 family proteins in cholesterol and fatty acid metabolism. **Table 1** provides a summary of the p53 family targets that are involved in lipid metabolism, and **Figure 2** briefly outlines cholesterol and fatty acid metabolism pathways.

p53

Cholesterol

Multiple studies have shown that p53 is implicated in regulating the levels of intracellular free cholesterol. Sterol Regulatory Element-Binding Protein 2 (SREBP-2) is a master transcriptional regulator of the mevalonate pathway and responds to sterol depletion by promoting cholesterol synthesis (Brown and Goldstein, 1997). It was found that p53 inhibits SREBP-2 maturation through the upregulation of *ABCA1* (Moon et al., 2019), an ATP-binding cassette transporter that inhibits cholesterol synthesis and drives cholesterol export when cholesterol stores are high (Yamauchi et al., 2015). Additionally, p53 can promote cholesterol export through the upregulation of *CAV1* (Bist et al., 2000), a scaffold protein that binds intracellular free cholesterol and facilitates its efflux (Fielding and Fielding, 1995). To enhance cellular cholesterol storage, p53 transactivates dehydrogenase/reductase member 3 (DHSR3) (Kirschner et al., 2010; Deisenroth et al., 2011), which decreases intracellular free cholesterol by increasing lipid droplet formation (Martin and Parton, 2006). Conversely, p53 has been shown to inhibit cholesterol storage by negatively regulating *SOAT1* (Oni et al., 2020). SOAT1 decreases intracellular free cholesterol by increasing cholesterol storage, thus disrupting the negative feedback loop that prevents cholesterol synthesis when free intracellular cholesterol levels are high (Oelkers et al., 1998). Furthermore, *Cyp19*, an aromatase essential for estrogen synthesis (Thompson and Siiteri, 1974), was found to be upregulated by p53, which prevents intracellular free cholesterol overload and adipocyte formation (Wang et al., 2013). One study revealed a potential link between p53 and *LIMA1*, also called *SREBP3*, in mediating cholesterol absorption in the gastrointestinal tract. p53 was shown to upregulate *LIMA1* through p53-response elements in its promoter (Ohashi et al., 2017), and LIMA1 promotes cholesterol absorption in the intestine (Zhang et al., 2018). Interestingly, there are some conflicting findings regarding p53 regulation of other mevalonate pathway genes. For example, one group showed that p53

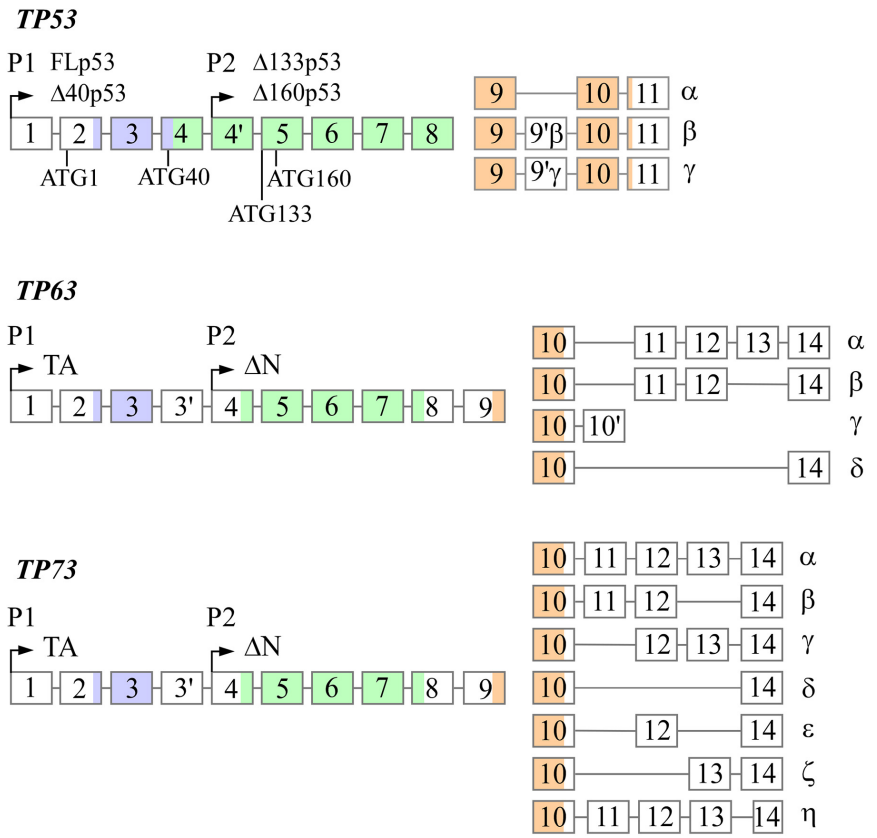

FIGURE 1 | The genomic loci of *TP53*, *TP63*, and *TP73*. All three genes contain two promoters (P1 and P2) through which transcription initiation may occur, resulting in the formation of the N-terminal isoforms. *TP53* contains four alternative translation start sites termed ATG1, ATG40, AG133, and ATG160 that give rise to FLp53, Δ40p53, Δ133p53, and Δ160p53, respectively. Alternative splicing at the 3′ end produces the C-terminal isoforms in each gene with the exception of p63γ, which results from transcriptional termination in intron 10. There exists significantly homology between each gene in the transactivation domains (purple), DNA-binding domains (green), and oligomerization domains (orange).

inhibited expression of mevalonate pathway genes *HMGCR*, *MVK*, *FDPS*, and *FDFT1* (Moon et al., 2019), but another group showed that p53 enhanced expression of these genes (Laezza et al., 2015), suggesting that p53 may regulate some mevalonate pathway genes in a context-dependent manner. Collectively, these findings suggest that multiple targets are regulated by p53 to prevent intracellular free cholesterol accumulation and to maintain the integrity of the negative feedback loop that regulates cholesterol storage and synthesis.

Fatty Acids

Fatty acid oxidation, also known as β-oxidation and hereafter referred to as FAO, is the process of breaking down long-chain fatty acids (LCFAs), primarily in the mitochondria; FAO can be initiated in peroxisomes, but the byproducts undergo complete oxidation in the mitochondria (Qu et al., 2016). LCFAs are metabolized by long-chain acyl-CoA synthetase to form acyl-CoA (Mashek et al., 2007), which is then transported into the mitochondrial matrix by a series of reactions catalyzed by the carnitine palmitoyltransferase system (Rufer et al., 2009). Acyl-CoA is then used as a substrate to initiate FAO (Qu et al., 2016). Each cycle of FAO in the matrix removes two carbons from the fatty acid, until four carbons remain; these are then used to synthesize acetyl-CoA (Qu et al., 2016).

De novo fatty acid synthesis (FAS) is the process by which cells generate fatty acids that are used in various cellular processes (Röhrig and Schulze, 2016). FAS starts with citrate produced by the tricarboxylic acid (TCA) cycle or glutamine metabolism (Akram, 2014; Röhrig and Schulze, 2016). Citrate is then cleaved by ATP-citrate lyase to form acetyl-CoA, which is the starting substrate for FAS (Zaidi et al., 2012). Acetyl-CoA carboxylases convert acetyl-CoA to malonyl-CoA (Abu-Elheiga et al., 2000), at which point fatty acid synthase (encoded by *FASN*) catalyzes the reaction between seven malonyl-CoA molecules and one acetyl-CoA molecule to form palmitate, a long-chain fatty acid (Smith et al., 2003). Palmitate is then modified in length (Jakobsson et al., 2006) and degree of saturation (Igal, 2010) to form additional fatty acids.

p53 has been shown to predominantly promote FAO (Parrales and Iwakuma, 2016). RNA-seq analysis revealed that p53 upregulates *CrOT* (peroxisomal carnitine O-octanoyltransferase) (Goldstein et al., 2012), which is responsible for transporting byproducts of peroxisomal FAO to mitochondria to allow for complete oxidation (Longo et al., 2016). Similarly, another group

showed that p53 pathway activation following γ-irradiation led to increased *CrOT* expression (Hage-Sleiman et al., 2017). In regards to mitochondrial FAO, p53 was found to upregulate *Acad11* (Jiang et al., 2015), which encodes acyl-CoA dehydrogenase and catalyzes the first step of FAO in the mitochondrial matrix (He et al., 2011). p53 can additionally promote FAO through upregulation of *MLYCD* (Liu et al., 2014), which encodes malonyl-CoA decarboxylase and converts the FAO inhibitor malonyl-CoA to acetyl-CoA (Foster, 2004). As evidenced by the name of many FAO intermediates, CoA is a critical molecule in many FAO reactions (Leonardi et al., 2005), and p53 was found to upregulate *PANK1*, which promotes CoA production (Wang et al., 2013). By complexing with FOXO3a, p53 transactivates *SIRT1* (Nemoto et al., 2004), a deacetylase that acts on histones and transcription factors to promote FAO (Rahman and Islam, 2011; Derdak et al., 2013). Activation of p53 in response to DNA damage and glucose starvation results in increased expression of *LPIN1*, a transcriptional co-activator, to promote FAO (Assaily et al., 2011). Lipin-1 also aids in diacylglycerol formation (Donkor et al., 2007), suggesting a role for p53 in diacylglycerol metabolism. There is evidence that p53 directly upregulates *CPT1C,* a neuron-specific carnitine palmitoyltransferase that transfers the acyl group from long chain fatty acyl to carnitine to initiate FAO (Lee and Wolfgang, 2012; Sanchez-Macedo et al., 2013). In addition to CPT1C, there are other tissue-specific carnitine palmitoyltransferase family members, such as CPT1a in the liver and CPT1b in muscle (Greenberg et al., 2009). Thus, it is possible that p53 might regulate FAO through CPT1a and CPT1b. p53 was shown to transactivate *ADRB3* (Kang et al., 2020), which promotes lipolysis, or the breakdown of triglycerides into fatty acids to allow for FAO (Arner and Langin, 2014). Interestingly, a p53 mutant could induce *ADRB3* to a higher degree (Kang et al., 2020). Likewise, studies showed that p53 can prevent lipogenesis through upregulation of *OPN*, which encodes osteopontin (Gómez-Santos et al., 2020). *In vivo* analyses in mouse livers showed that *OPN* levels were increased in response to an increase in p53 (Gómez-Santos et al., 2020). Conversely, a recent report showed that p53 inhibits FAO through *PGC1A* and *APLNR* in response to doxorubicin treatment in cardiomyocytes (Saleme et al., 2020). These data lead us to hypothesize that p53 could have tissue/cell-specific effects on FAO.

p53 has been shown to inhibit FAS (Parrales and Iwakuma, 2016). For example, p53 can negatively regulate transcription of SREBP-1c to inhibit FAS (Yahagi et al., 2003). SREBP-1c, a SREBP family member, is involved in triglyceride and fatty acid synthesis predominantly in the liver, which leads to fat accumulation (Shimano et al., 1997; Shimomura et al., 1998). Additionally, p53 has been implicated in inhibiting FAS through repression of NADPH production, a critical energy source utilized during FAS (Brose et al., 2016). p53 can inhibit NADPH production through negative transcriptional regulation of malic enzyme 1 and 2 (ME1 and 2) (Jiang et al., 2013). ME1/2 catalyze the formation of pyruvate from malate, which produces NADPH (Wise and Ball, 1964). Additionally, p53 prevents NADPH production through inhibition of glucose-6-phosphate dehydrogenase (G6PD) via protein-protein interaction, which requires p53's C-terminus,

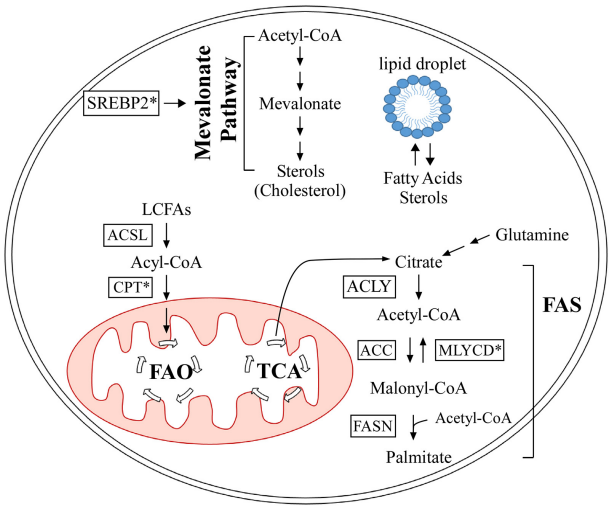

FIGURE 2 | Summary of lipid metabolism, as it pertains to the p53 family. The mevalonate pathway is out lined in the upper half. Fatty acid oxidation and synthesis are portrayed in the lower half. Proteins marked with an asterisk are regulated by the p53 family. FAO, fatty acid oxidation; TCA, tricarboxylic acid cycle; FAS, fatty acid synthesis; ACSL, long-chain acyl-CoA synthetase; CPT, carnitine palmitoyltransferase; ACLY, ATP citrate lyase; MLYCD, malonyl-CoA decarboxylase; ACC, acetyl-CoA carboxylase; FASN, fatty acid synthase; SREBP2, sterol regulatory element-binding protein 2.

DNA-binding domain, and tetramerization domain (Jiang et al., 2011). G6PD is an enzyme that catalyzes the first step of the pentose phosphate pathway (PPP), a major source of NADPH production (Ge et al., 2020). While reports show that p53 predominately inhibits NADPH production, some p53 targets have been identified as promoters of NADPH production. For example, TIGAR, a well-defined p53 target, activates PPP to drive NADPH production, which has been shown to prevent ROS formation (Bensaad et al., 2006). Additionally, it was found that p53 promotes NADPH production through suppression of PFKFB3 expression, which favors glycolysis over PPP (Franklin et al., 2016).

p63 and p73

Several studies have unveiled an important role for p63 in lipid metabolism, although the mechanisms are not fully understood. It was shown that TAp63 deficiency in mice increases the incidence of obesity and liver steatosis and impairs FAO function (Su et al., 2012; Liao et al., 2017). It was found that TAp63 promotes FAO through upregulation of *SIRT1* (a previously described p53 target) and the LKBI/AMPK pathway, the latter of which prevents the conversion of acetyl-CoA to the FAO inhibitor malonyl-CoA (Li et al., 2020). As previously mentioned, p53 promotes the production of acetyl-CoA from malonyl-CoA (Liu et al., 2014), suggesting that the p53 family can transactivate multiple targets to prevent malonyl-CoA formation. Additionally, TAp63 was shown to inhibit FAS by upregulating *CCDC3* (Liao et al., 2017), which encodes a soluble protein that binds to hepatocyte receptors (Kobayashi et al., 2010). While there is limited research on p63 and cholesterol regulation, it

has been shown that p63, like p53, inhibits cellular cholesterol accumulation through *DHSR3* (Kirschner et al., 2010) and promotes intestinal cholesterol absorption through *LIM1A* (Zhang et al., 2018).

Phenotypic similarities between p63- and p73-deficient mice suggest that p73 has an analogous role in regulating lipid metabolism. In response to nutrient deprivation, loss of p73 leads to lipid accumulation in mouse livers (He et al., 2013). Mechanistically, TAp73α/β were shown to modulate lipid metabolism through *ATG5*, a gene that is necessary for autophagy (He et al., 2013). Autophagy is an intracellular process that, among other things, can break down lipid droplets to allow for FAO (Ye et al., 2018; Saito et al., 2019). As such, gene transfer of *ATG5* to p73-knockout mice mitigated the accumulation of lipid droplets in the mouse livers (He et al., 2013). As with p53 and p63, p73β can upregulate *LIM1A* to increase cholesterol absorption (Y. Y. Zhang et al., 2018). These data suggest that p73 prevents lipid accumulation through a mechanism that is quite different from how p53 and p63 regulate this process.

IRON METABOLISM

Iron is an essential element for all living entities and plays an important role in many cellular processes, such as oxygen transport and cell proliferation (Kim and Nemeth, 2015; Wallace, 2019). Additionally, iron is a critical cofactor that is required for various metabolic activities, such as DNA synthesis (Puig et al., 2017). An organism's main source of iron is through dietary intake (Waldvogel-Abramowski et al., 2014). In the gastrointestinal tract, iron exists as non-heme- or heme-iron (Waldvogel-Abramowski et al., 2014); heme is a porphyrin that contains iron (Fiorito et al., 2020). At physiological pH, non-heme iron is present in the ferric (Fe^{3+}) state, but cells can only absorb it in the ferrous (Fe^{2+}) state (Wallace, 2019). Duodenal cytochrome B (Dcytb) reduces Fe^{3+} to Fe^{2+} in the lumen and ferrous iron is absorbed by enterocytes through divalent metal cation transporter 1 (DMCT1) (Wallace, 2019). On the other hand, heme-iron is directly imported by haem carrier protein 1 (HCP1). Once in enterocytes, iron is exported by ferroportin 1 (FPN1), whose function is inhibited by hepcidin (Waldvogel-Abramowski et al., 2014). In the plasma, Fe^{2+} is converted back to Fe^{3+} by ceruloplasmin and binds to transferrin for transport through the circulation (Attieh et al., 1999). A summary schematic of this process is shown in **Figure 3**. Once iron has entered the target cell, it binds ferritin until it is needed (Waldvogel-Abramowski et al., 2014). Regulation of iron metabolism is exceedingly important because iron overload, like in hemochromatosis (Bacon et al., 2011), can lead to heart disease and liver cirrhosis, while deficiency can result in anemia

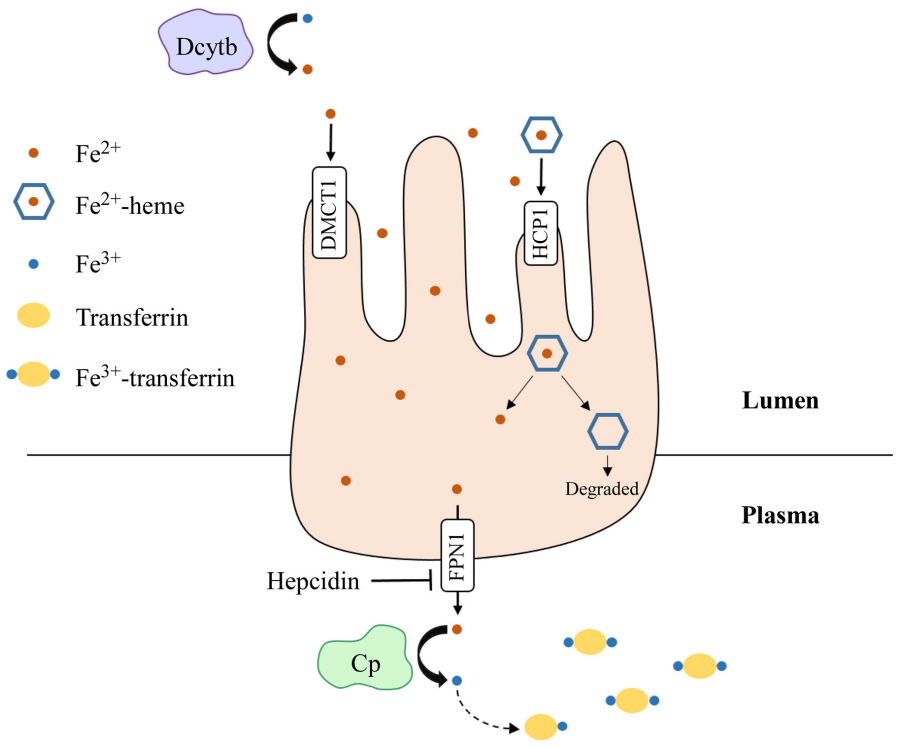

FIGURE 3 | Dietary iron absorption and transport from enterocytes to the plasma. Fe^{3+} is reduced to Fe^{2+} via duodenal cytochrome b (Dcytb) in the intestinal lumen. Non-heme-iron is transported into enterocytes via divalent metal cation transporter 1 (DMCT1), while heme-iron is transported through haem carrier protein 1 (HCP1). Heme dissociates from iron and is degraded. Fe^{2+} is then exported out of enterocytes by ferroportin 1 (FPN1), whose function is inhibited by hepcidin. Once in the plasma, Fe^{2+} is oxidized to Fe^{3+} by ceruloplasmin (Cp), which then binds transferrin for transport through the plasma. Iron is transported into target cells for storage or use.

and developmental impairments (Abbaspour et al., 2014). The p53 family has been implicated in mediating iron metabolism to prevent iron dysregulation.

p53

Iron metabolism exerts regulatory functions over p53 and in turn, p53 can regulate iron metabolism. Excess iron leads to decreased p53 expression (Shen et al., 2014), whereas iron depletion leads to p53 accumulation (Liang and Richardson, 2003; Kim et al., 2007). Additionally, direct binding of heme to p53 protein inhibits p53 transcriptional activity and possibly promotes p53 degradation (Shen et al., 2014). As such, a feedback loop between iron and p53 exists wherein iron overload inhibits p53 activity and p53 inhibits iron accumulation. At the systemic level, p53 upregulates *HAMP* (encoding hepcidin) to inhibit iron efflux from enterocytes (Weizer-Stern et al., 2007) and thus, prevents iron from entering the circulation when it is not needed. To prevent iron overload at the cellular level, p53 directly transactivates several targets, including *FXN* (frataxin) (Shimizu et al., 2014), *FDXR* (ferredoxin reductase) (Hwang et al., 2001; Liu and Chen, 2002), and *ISCU* (iron-sulfur cluster assembly enzyme) (Funauchi et al., 2015). Frataxin is an iron binding protein that regulates mitochondrial iron homeostasis to prevent iron overload (Cavadini et al., 2000) and thus, p53 upregulates frataxin to inhibit mitochondrial iron overload. Additionally, frataxin is necessary for iron-sulfur cluster (ISC) biogenesis (Shimizu et al., 2014) and ISCs are critical for mitochondrial function (Shimizu et al., 2014). In addition to aiding in electron transport during redox reactions (Johnson et al., 2005), ISCs serve as a co-factor for many essential enzymes (Baranovskiy et al., 2012). We also showed that p53 regulates mitochondrial iron metabolism through a FDXR-p53 loop (Liu and Chen, 2002; Zhang et al., 2017). FDXR plays a critical role in ISC biogenesis and steroid hormone synthesis by transferring electrons from NADPH to ferredoxin 1 and 2 (FDX1 and 2) (Brandt and Vickery, 1992; Sheftel et al., 2010). p53 drives the FDXR-p53 loop to upregulate FDXR, which then transfers electrons to FDX2, ultimately preventing iron overload at the cellular level (Zhang et al., 2017). Furthermore, p53 upregulates ISCU, which increases translation of ferritin heavy chain mRNA (*FTH1*) and destabilizes transferrin receptor mRNA (*TFRC*) (Funauchi et al., 2015), therefore increasing cellular iron storage and decreasing cellular iron import. p53 can also regulate iron metabolism through post-transcriptional modifications of Iron Regulatory Protein 1 and 2 (IRP1 and IRP2) (Zhang et al., 2008). IRP1/2 alter the expression of proteins associated with iron transport and storage by binding to conserved iron-regulatory elements (IRE) in target mRNAs (Volz, 2008). Interestingly, the binding of IRP1/2 to a target mRNA has context-dependent outcomes, wherein binding can promote both mRNA degradation and mRNA translation (Volz, 2008). Studies showed that overexpression of p53 led to reduced IRP1 and 2 activity, resulting in increased translation of ferritin mRNA and decreased stability of transferrin receptor mRNA (Zhang et al., 2008). This regulation ultimately leads to an increase in cellular iron stores and a decrease in cellular iron import.

Ferroptosis is a specific form of iron-mediated cell death in which oxidative stress from reactive oxygen species (ROS) leads to the formation of lipid peroxides and accumulation of lipid peroxides triggers the ferroptotic response (Dixon et al., 2012; Lu et al., 2018). Iron has a critical role in promoting ROS formation through several mechanisms. First, iron functions as a co-factor for enzymes that catalyze the formation of ROS (Dixon and Stockwell, 2014). In addition, Fe^{2+} reacts with hydrogen peroxide through the Fenton reaction, resulting in the production of free radicals, a potent form of ROS (Wardman and Candeias, 1996). ROS can then promote lipid peroxidation of cellular membranes, which leads to compromised membrane integrity and cellular damage (Yin et al., 2011). However, several intracellular reducing pathways have been found to block ROS and subsequent accumulation of lipid peroxides (Lu et al., 2018). Import of

TABLE 1 | Targets of the p53 family that are associated with lipid metabolism.

Gene/protein target	Function	Regulation by p53 family member
SREBP-2	Upregulates mevalonate pathway genes	Down by p53 via ABCA1
CAV1	Promotes cellular cholesterol efflux	Up by p53
DHRS3	Promotes lipid droplet formation	Up by p53 and p63
SOAT1	Promotes cholesterol storage	Down by p53
Cyp19	Prevents cholesterol accumulation	Up by p53
LIMA1	Promotes cholesterol absorption in GI tract	Up by p53/p63/p73
HMGCR, MVK, FDPS, FDFT1	Promote mevalonate pathway	Up and Down by p53
CrOT	Transports byproducts of peroxisomal FAO to mitochondria	Up by p53
Acad11	Catalyzes first step of FAO	Up by p53
MLYCD	Converts malonyl-CoA to acetyl-CoA	Up by p53
PANK1	Catalyzes rate-limiting step of CoA production	Up by p53
SIRT1	Modulates histones and transcription factors to promote FAO	Up by p53 and p63
LPIN1	Upregulates FAO-associated genes	Up by p53
CPT1C	Transfers acyl group from long-chain fatty acyl to carnitine	Up by p53
ADRB3	Promotes lipolysis	Up by p53
OPN	Inhibits lipogenesis	Up by p53
PGC1A/APLNR	Inhibits FAO in cardiomyocytes	Up by p53
SREBP-1c	Promotes triglyceride synthesis and FAS	Down by p53
ME1/ME2	Converts malate to pyruvate, which produces NADPH	Down by p53
G6PD	Catalyzes first step of PPP, which produces NADPH	Down by p53 via protein-protein interaction
TIGAR	Promotes PPP activation	Up by p53
PFKFB3	Inhibits PPP activation	Down by p53
LKB1/AMPK	Pathway represses conversion of acetyl-CoA to malonyl-CoA	Pathway activated by p63
CCDC3	Inhibits FAS by binding hepatocyte receptors	Up by p63
ATG5	Promotes lipid droplet degradation	Up by p73

cystine into the cell via system x_c^- (encoded by *SCL7A11*) ultimately results in the synthesis of glutathione, a strong antioxidant (Lu et al., 2018; Sato et al., 2018). GPX4, a member of the glutathione peroxidase family, uses glutathione as a co-activator to reduce lipid peroxides, thus preventing ferroptosis (Lu et al., 2018). Ferroptosis has been implicated in a variety of diseases, such as cell death during ischemia (Gao et al., 2015) and neurodegeneration in Alzheimer's disease (Masaldan et al., 2019). Interestingly, p53 can promote and inhibit ferroptosis in a context-dependent manner (Liu et al., 2020). For example, p53 is able to inhibit ferroptosis through p21, a primary p53 target that inhibits glutathione degradation (Tarangelo and Dixon, 2018). As such, upregulation of p21 by p53 inhibits glutathione degradation and promotes GPX4 activity (Tarangelo and Dixon, 2018). p53 was also shown to prevent ferroptosis by promoting the nuclear, but inhibiting the plasma membrane, accumulation of dipeptidyl-peptidase 4 (DPP4) (Xie et al., 2017). DPP4 in the nucleus upregulates *SLC7A11*, leading to increased GPX4 function and subsequent inhibition of ferroptosis (Xie et al., 2017). Interestingly, p53 can promote ferroptosis by directly inhibiting *SLC7A11* expression (Jiang et al., 2015). Additionally, p53 promotes ferroptosis through upregulation of *SAT1*, which facilitates the production of lipid peroxides (Ou et al., 2016). A recent study showed that Mdm2 and Mdm4 can induce ferroptosis (Venkatesh et al., 2020). Since Mdm2 is a target of p53, it is possible that p53 can act through Mdm2/4 to modulate the induction of ferroptosis. The role of both wild-type and mutant p53 in ferroptosis was discussed comprehensively in a recent review (Liu et al., 2020).

p63 and p73

Recent evidence suggests an important role for p63 and p73 in iron metabolism. Like p53, p63, and p73 can be destabilized by an excess of heme (Shen et al., 2014). Conversely, iron depletion was found to stabilize p73, and possibly p63, to promote apoptosis and cell cycle arrest in a p53-independent manner (Calabrese et al., 2020). These data suggest that iron overload inhibits, whereas iron depletion promotes, p63 and p73 activity, which is similar to the effect of iron overload and depletion on p53. Recent studies in our lab revealed a potential mechanism through which iron overload can influence p63/p73 mRNA stability and protein expression. We showed that TAp63 expression can be repressed by IRP2 and likewise, IRP2 deficiency lead to increased expression of TAp63 (Zhang et al., 2020). Additionally, we showed that IRP2 binds to the IRE in p63 mRNA to regulates its stability (Zhang et al., 2020). Similarly, we found that FDXR regulates p73 mRNA stability through IRP2 (Zhang et al., 2020). These observations represent an important step in understanding how iron metabolism regulates p63 and p73.

Several lines of evidence suggest a role for p63 and p73 in mediating ferroptosis. For example, ferroptosis has been shown to promote liver steatosis and inflammation (Tsurusaki et al., 2019). We and others found that p63-deficient mice were prone to liver steatosis (Jiang et al., 2018). Additionally, both p63- and p73-deficient mice exhibited a high degree of liver inflammation (Jiang et al., 2018; Zhang et al., 2020). Moreover, before the term ferroptosis was coined, we found that p63 inhibited cell death caused by oxidative stress through GPX2 (Yan and Chen, 2006), a member of the same phospholipid peroxidase family as GPX4 (Chu, 1994). Aforementioned, ferroptosis ensues when the cell is unable to overcome oxidative stress. Another study revealed that ΔNp63 promoted glutathione metabolism, thus permitting GPX4 function and inhibiting the ferroptotic pathway (G. X. Wang et al., 2017). These findings suggest that p63 regulates ferroptosis through multiple glutathione peroxidase family members. As previously mentioned, p63 activates the LKB1/AMPK pathway and a group recently showed that this pathway inhibits ferroptosis (Li et al., 2020). While the role of p73 in ferroptosis is less studied, one report showed that TAp73-knockout mouse embryonic fibroblasts were particularly prone to oxidative stress (Agostini et al., 2016). Another study showed that TAp73 is able to mitigate the effect of oxidative stress on mitochondrial integrity (Marini et al., 2018). These data suggest a role for TAp73 in suppressing ferroptosis.

FUTURE DIRECTIONS

There is growing evidence that, in addition to mediating tumor suppression, the p53 family plays an important role in lipid and iron metabolism. However, there is a need for more research on these critical topics. It would be of interest to further explore how p53 is involved in regulating bioactive lipids. Additionally, it would be worthwhile to delve into the mechanisms by which p63/p73 regulate lipid and iron metabolism. While there is evidence that aberrant iron metabolism affects lipid metabolism and ferroptosis, how p53 engages lipid and iron metabolism in ferroptosis needs to be further explored. Moreover, several fundamental questions remain unanswered: Can p63 and p73 function independently of p53 in both lipid and iron metabolism? How does regulation of lipid and iron metabolism differ between the N- and C-terminal isoforms of each protein? Does regulation of lipid and iron metabolism by the p53 family contribute to common diseases associated with these processes, such as diabetes or anemia? Finally, can the p53 family proteins themselves, or the pathways regulated by the p53 family, be manipulated to ameliorate the effect of lipid or iron dysregulation on pathogenesis of diabetes and other diseases? A comprehensive understanding of how the p53 family mediates lipid and iron metabolism will likely provide an insight into the pathways that drive various human diseases.

AUTHOR CONTRIBUTIONS

KL, JZ, and XC wrote the article. All authors contributed to the article and approved the submitted version.

FUNDING

This work was supported in part by the NIH Grants R01 CA081237, CA224433, CA250338, and CA195828 (to XC), T32 HL007013 (to KL), and T31IP1727 (to JZ).

REFERENCES

Abbaspour, N., Hurrell, R., and Kelishadi, R. (2014). Review on iron and its importance for human health. *J. Res. Med. Sci.* 19:2.

Abu-Elheiga, L., Brinkley, W. R., Zhong, L., Chirala, S. S., Woldegiorgis, G., and Wakil, S. J. (2000). The subcellular localization of acetyl-CoA carboxylase 2. *Proc. Natl. Acad. Sci. U. S. A.* 97:4. doi: 10.1073/pnas.97.4.1444

Agostini, M., Annicchiarico-Petruzzelli, M., Melino, G., and Rufini, A. (2016). Metabolic pathways regulated by TAp73 in response to oxidative stress. *Oncotarget*. 7:21. doi: 10.18632/oncotarget.8935

Akram, M. (2014). Citric Acid Cycle and Role of its Intermediates in Metabolism. *Cell Biochem. Biophys.* 68:3. doi: 10.1007/s12013-013-9750-1

Alekos, N. S., Moorer, M. C., and Riddle, R. C. (2020). Dual Effects of Lipid Metabolism on Osteoblast Function. *Front. Endocrinol. (Lausanne).* 11:578194. doi: 10.3389/fendo.2020.578194

Alves-Bezerra, M., and Cohen, D. E. (2018). Triglyceride metabolism in the liver. *Compr. Physiol.* 8:1. doi: 10.1002/cphy.c170012

Arner, P., and Langin, D. (2014). Lipolysis in lipid turnover, cancer cachexia, and obesity-induced insulin resistance. *Trends Endocrinol. Metab.* 25:5. doi: 10.1016/j.tem.2014.03.002

Arrowsmith, C. H. (1999). Structure and function in the p53 family. *Cell Death Differ.* 6:12. doi: 10.1038/sj.cdd.4400619

Assaily, W., Rubinger, D. A., Wheaton, K., Lin, Y., Ma, W., Xuan, W., et al. (2011). ROS-mediated p53 induction of Lpin1 regulates fatty acid oxidation in response to nutritional stress. *Mol. Cell.* 44:3. doi: 10.1016/j.molcel.2011.08.038

Attieh, Z. K., Mukhopadhyay, C. K., Seshadrit, V., Tripoulas, N. A., and Fox, P. L. (1999). Ceruloplasmin ferroxidase activity stimulates cellular iron uptake by a trivalent cation-specific transport mechanism. *J. Biol. Chem.* 274:2. doi: 10.1074/jbc.274.2.1116

Bacon, B. R., Adams, P. C., Kowdley, K. V., Powell, L. W., and Tavill, A. S. (2011). Diagnosis and management of hemochromatosis: 2011 Practice Guideline by the American Association for the Study of Liver Diseases. *Hepatology*. 54:1. doi: 10.1002/hep.24330

Baranovskiy, A. G., Lada, A. G., Siebler, H. M., Zhang, Y., Pavlov, Y. I., and Tahirov, T. H. (2012). DNA polymerase δ and ζ switch by sharing accessory subunits of DNA polymerase δ. *J. Biol. Chem.* 287:21. doi: 10.1074/jbc.M112.351122

Bensaad, K., Tsuruta, A., Selak, M. A., Vidal, M. N. C., Nakano, K., Bartrons, R., et al. (2006). TIGAR, a p53-Inducible Regulator of Glycolysis and Apoptosis. *Cell*. 126:1. doi: 10.1016/j.cell.2006.05.036

Bist, A., Fielding, C. J., and Fielding, P. E. (2000). P53 Regulates Caveolin Gene Transcription, Cell Cholesterol, and Growth By a Novel Mechanism. *Biochemistry*. 39:8. doi: 10.1021/bi991721h

Bohdanowicz, M., and Grinstein, S. (2013). Role of phospholipids in endocytosis, phagocytosis, and macropinocytosis. *Physiol. Rev.* 93:1. doi: 10.1152/physrev.00002.2012

Borremans, B., Hobman, J. L., Provoost, A., and Brown, N. L. (2001). Cloning and functional analysis of human p51, which structurally and functionally resembles p53. *Nat. Med.* 4:7.

Bourdon, J.-C., Fernandes, K., Murray-Zmijewski, F., Liu, G., Diot, A., Xirodimas, D. P., et al. (2005). P53 isoforms can regulate p53 transcriptional activity. *Genes Dev.* 19:18. doi: 10.1101/gad.1339905

Brandt, M. E., and Vickery, L. E. (1992). Expression and characterization of human mitochondrial ferredoxin reductase in *Escherichia coli*. *Arch. Biochem. Biophys.* 294:2. doi: 10.1016/0003-9861(92)90749-M

Brose, S. A., Golovko, S. A., and Golovko, M. Y. (2016). Fatty acid biosynthesis inhibition increases reduction potential in neuronal cells under hypoxia. *Front. Neurosci.* 2016:10. doi: 10.3389/fnins.2016.00546

Brown, M. S., and Goldstein, J. L. (1997). The SREBP pathway: Regulation of cholesterol metabolism by proteolysis of a membrane-bound transcription factor. *Cell*. 89:3. doi: 10.1016/S0092-8674(00)80213-5

Calabrese, C., Panuzzo, C., Stanga, S., Andreani, G., Ravera, S., Maglione, A., et al. (2020). Deferasirox-dependent iron chelation enhances mitochondrial dysfunction and restores p53 signaling by stabilization of p53 family members in leukemic cells. *Int. J. Mol. Sci.* 21:20. doi: 10.3390/ijms21207674

Candi, E., Rufini, A., Terrinoni, A., Dinsdale, D., Ranalli, M., Paradisi, A., et al. (2006). Differential roles of p63 isoforms in epidermal development: Selective genetic complementation in p63 null mice. *Cell Death Differ.* 13:6. doi: 10.1038/sj.cdd.4401926

Cavadini, P., Gellera, C., Patel, P. I., and Isaya, G. (2000). Human frataxin maintains mitochondrial iron homeostasis in Saccharomyces cerevisiae. *Hum. Mol. Genet.* 9:17. doi: 10.1093/hmg/9.17.2523

Celli, J., Duijf, P., Hamel, B. C. J., Bamshad, M., Kramer, B., Smits, A. P. T., et al. (1999). Heterozygous Germline Mutations in the p53 Homolog p63 Are the Cause of EEC Syndrome. *Cell* 1999:99.

Chu, F. F. (1994). The human glutathione peroxidase genes GPX2, GPX3, and GPX4 map to chromosomes 14, 5, and 19, respectively. *Cytogenet. Genome Res.* 66:2. doi: 10.1159/000133675

Courtois, S., Verhaegh, G., North, S., Luciani, M. G., Lassus, P., Hibner, U., et al. (2002). ΔN-p53, a natural isoform of p53 lacking the first transactivation domain, counteracts growth suppression by wild-type p53. *Oncogene*. 21:44. doi: 10.1038/sj.onc.1205874

Deisenroth, C., Itahana, Y., Tollini, L., Jin, A., and Zhang, Y. (2011). P53-inducible DHRS3 is an endoplasmic reticulum protein associated with lipid droplet accumulation. *J. Biol. Chem.* 286:32. doi: 10.1074/jbc.M111.254227

Derdak, Z., Villegas, K. A., Harb, R., Wu, A. M., Sousa, A., and Wands, J. R. (2013). Inhibition of p53 attenuates steatosis and liver injury in a mouse model of non-alcoholic fatty liver disease. *J. Hepatol.* 58:4. doi: 10.1016/j.jhep.2012.11.042

Dixon, S. J., and Stockwell, B. R. (2014). The role of iron and reactive oxygen species in cell death. *Nat. Chem. Biol.* 10:1. doi: 10.1038/nchembio.1416

Dixon, S. J., Lemberg, K. M., Lamprecht, M. R., Skouta, R., Zaitsev, E. M., Gleason, C. E., et al. (2012). Ferroptosis: An iron-dependent form of nonapoptotic cell death. *Cell*. 149:5. doi: 10.1016/j.cell.2012.03.042

Donehower, L. A., Harvey, M., Slagle, B. L., Mcarthurt, M. J., Jrt, C. A. M., Butel, J. S., et al. (1991). Mice deficient for p53 are developmentally normal but susceptible to sponatenous tumors. *Nature* 1991:365.

Donkor, J., Sariahmetoglu, M., Dewald, J., Brindley, D. N., and Reue, K. (2007). Three mammalian lipins act as phosphatidate phosphatases with distinct tissue expression patterns. *J. Biol. Chem.* 282:6. doi: 10.1074/jbc.M610745200

Fielding, P. E., and Fielding, C. J. (1995). Plasma Membrane Caveolae Mediate the Efflux of Cellular Free Cholesterol. *Biochemistry* 34:44. doi: 10.1021/bi00044a004

Fiorito, V., Chiabrando, D., Petrillo, S., Bertino, F., and Tolosano, E. (2020). The Multifaceted Role of Heme in Cancer. *Front. Oncol.* 9:1540. doi: 10.3389/fonc.2019.01540

Foster, D. W. (2004). The role of the carnitine system in human metabolism. *Ann. N. Y. Acad. Sci.* 1033:1. doi: 10.1196/annals.1320.001

Franklin, D. A., He, Y., Leslie, P. L., Tikunov, A. P., Fenger, N., MacDonald, J. M., et al. (2016). P53 coordinates DNA repair with nucleotide synthesis by suppressing PFKFB3 expression and promoting the pentose phosphate pathway. *Sci. Rep.* 6:38067. doi: 10.1038/srep38067

Funauchi, Y., Tanikawa, C., Yi, Lo, P. H., Mori, J., Daigo, Y., et al. (2015). Regulation of iron homeostasis by the p53-ISCU pathway. *Sci. Rep.* 5:16497. doi: 10.1038/srep16497

Gao, M., Monian, P., Quadri, N., Ramasamy, R., and Jiang, X. (2015). Glutaminolysis and Transferrin Regulate Ferroptosis. *Mol. Cell*. 59:2. doi: 10.1016/j.molcel.2015.06.011

Ge, T., Yang, J., Zhou, S., Wang, Y., Li, Y., and Tong, X. (2020). The Role of the Pentose Phosphate Pathway in Diabetes and Cancer. *Front. Endocrinol.* 11:365. doi: 10.3389/fendo.2020.00365

Giammanco, A., Cefalù, A. B., Noto, D., and Averna, M. R. (2015). The pathophysiology of intestinal lipoprotein production. *Front. Physiol.* 6:61. doi: 10.3389/fphys.2015.00061

Goldstein, I., Ezra, O., Rivlin, N., Molchadsky, A., Madar, S., Goldfinger, N., et al. (2012). P53, a novel regulator of lipid metabolism pathways. *J. Hepatol.* 56:3. doi: 10.1016/j.jhep.2011.08.022

Gómez-Santos, B., Saenz, de Urturi, D., Nuñez-García, M., Gonzalez-Romero, F., Buque, X., et al. (2020). Liver osteopontin is required to prevent the progression of age-related nonalcoholic fatty liver disease. *Aging Cell*. 19:8. doi: 10.1111/acel.13183

Greenberg, C. R., Dilling, L. A., Thompson, G. R., Seargeant, L. E., Haworth, J. C., Phillips, S., et al. (2009). The paradox of the carnitine palmitoyltransferase type Ia P479L variant in Canadian Aboriginal populations. *Mol. Genet. Metab.* 96:4. doi: 10.1016/j.ymgme.2008.12.018

Guo, X., Keyes, W. M., Papazoglu, C., Zuber, J., Li, W., Lowe, S. W., et al. (2009). TAp63 induces senescence and suppresses tumorigenesis in vivo. *Nat. Cell Biol.* 11:12. doi: 10.1038/ncb1988

Hage-Sleiman, R., Bahmad, H., Kobeissy, H., Dakdouk, Z., Kobeissy, F., and Dbaibo, G. (2017). Genomic alterations during p53-dependent apoptosis induced by γ-irradiation of Molt-4 leukemia cells. *PLoS One* 12:e0190221. doi: 10.1371/journal.pone.0190221

Hannun, Y. A., and Obeid, L. M. (2008). Principles of bioactive lipid signalling: Lessons from sphingolipids. *Nat. Rev. Mol. Cell Biol.* 9:2. doi: 10.1038/nrm2329

Hannun, Y. A., and Obeid, L. M. (2018). Sphingolipids and their metabolism in physiology and disease. *Nat. Rev. Mol. Cell Biol.* 2018:107. doi: 10.1038/nrm.2017.107

Harms, K. L., and Chen, X. (2005). The C Terminus of p53 Family Proteins Is a Cell Fate Determinant. *Mol. Cell. Biol.* 25:5. doi: 10.1128/mcb.25.5.2014-2030.2005

Hasson, D., Feliú, F., and Gormaz, J. G. (2016). Non-alcoholic fatty liver disease and the metabolic syndrome. *Nonalcoholic Fat. Liver Dis.* 2016, 79–106. doi: 10.2174/138161207781039652

He, M., Pei, Z., Mohsen, A. W., Watkins, P., Murdoch, G., Veldhoven, P. P., et al. (2011). Identification and characterization of new long chain Acyl-CoA dehydrogenases. *Mol. Genet. Metab.* 102:4. doi: 10.1016/j.ymgme.2010.12.005

He, Z., Liu, H., Agostini, M., Yousefi, S., Perren, A., Tschan, M. P., et al. (2013). P73 regulates autophagy and hepatocellular lipid metabolism through a transcriptional activation of the ATG5 gene. *Cell Death Differ.* 20:10. doi: 10.1038/cdd.2013.104

Helton, E. S., Zhu, J., and Chen, X. (2006). The unique NH2-terminally deleted (ΔN) residues, the PXXP motif, and the PPXY motif are required for the transcriptional activity of the ΔN variant of p63. *J. Biol. Chem.* 281:5. doi: 10.1074/jbc.M507964200

Hooijmans, C. R., and Kiliaan, A. J. (2008). Fatty acids, lipid metabolism and Alzheimer pathology. *Eur. J. Pharmacol.* 585:1. doi: 10.1016/j.ejphar.2007.11.081

Hussain, M. M. (2014). Intestinal lipid absorption and lipoprotein formation. *Curr. Opin. Lipidol.* 25:3. doi: 10.1097/MOL.0000000000000084

Hwang, P. M., Bunz, F., Yu, J., Rago, C., Chan, T. A., Murphy, M. P., et al. (2001). Ferredoxin reductase affects p53-dependent, 5-fluorouracil-induced apoptosis in colorectal cancer cells. *Nat. Med.* 7:10. doi: 10.1038/nm1001-1111

Igal, R. A. (2010). Stearoyl-coa desaturase-1: A novel key player in the mechanisms of cell proliferation, programmed cell death and transformation to cancer. *Carcinogenesis.* 31:9. doi: 10.1093/carcin/bgq131

Jakobsson, A., Westerberg, R., and Jacobsson, A. (2006). Fatty acid elongases in mammals: Their regulation and roles in metabolism. *Prog. Lipid Res.* 45:3. doi: 10.1016/j.plipres.2006.01.004

Jiang, D., LaGory, E. L., KenzelmannBrož, D., Bieging, K. T., Brady, C. A., Link, N., et al. (2015). Analysis of p53 Transactivation Domain Mutants Reveals Acad11 as a Metabolic Target Important for p53 Pro-Survival Function. *Cell Rep.* 10:7. doi: 10.1016/j.celrep.2015.01.043

Jiang, L., Kon, N., Li, T., Wang, S. J., Su, T., Hibshoosh, H., et al. (2015). Ferroptosis as a p53-mediated activity during tumour suppression. *Nature.* 520:7545. doi: 10.1038/nature14344

Jiang, P., Du, W., Mancuso, A., Wellen, K. E., and Yang, X. (2013). Reciprocal regulation of p53 and malic enzymes modulates metabolism and senescence. *Nature.* 493:7434. doi: 10.1038/nature11776

Jiang, P., Du, W., Wang, X., Mancuso, A., Gao, X., Wu, M., et al. (2011). P53 regulates biosynthesis through direct inactivation of glucose-6-phosphate dehydrogenase. *Nat. Cell Biol.* 13:3. doi: 10.1038/ncb2172

Jiang, Y., Xu, E., Zhang, J., Chen, M., Flores, E., and Chen, X. (2018). The Rbm38-p63 feedback loop is critical for tumor suppression and longevity. *Oncogene.* 37:21. doi: 10.1038/s41388-018-0176-5

Johnson, D. C., Dean, D. R., Smith, A. D., and Johnson, M. K. (2005). Structure, function, and formation of biological iron-sulfur clusters. *Annu. Rev. Biochem.* 74:1. doi: 10.1146/annurev.biochem.74.082803.133518

Kaghad, M., Bonnet, H., Yang, A., Creancier, L., Biscan, J. C., Valent, A., et al. (1997). Monoallelically expressed gene related to p53 at 1p36, a region frequently deleted in neuroblastoma and other human cancers. *Cell.* 90:4. doi: 10.1016/S0092-8674(00)80540-1

Kang, J. G., Lago, C. U., Lee, J. E., Park, J. H., Donnelly, M. P., Starost, M. F., et al. (2020). A Mouse Homolog of a Human TP53 Germline Mutation Reveals a Lipolytic Activity of p53. *Cell Rep.* 30:3. doi: 10.1016/j.celrep.2019.12.074

Kim, A., and Nemeth, E. (2015). New insights into iron regulation and erythropoiesis. *Curr. Opin. Hematol.* 22:3. doi: 10.1097/MOH.0000000000000132

Kim, B. M., Choi, J. Y., Kim, Y. J., Woo, H. D., and Chung, H. W. (2007). Desferrioxamine (DFX) has genotoxic effects on cultured human lymphocytes and induces the p53-mediated damage response. *Toxicology.* 229:3. doi: 10.1016/j.tox.2006.10.022

Kirschner, R. D., Rother, K., Müller, G. A., and Engeland, K. (2010). The retinal dehydrogenase/reductase retSDR1/DHRS3 gene is activated by p53 and p63 but not by mutants derived from tumors or EEC/ADULT malformation syndromes. *Cell Cycle.* 9:11. doi: 10.4161/cc.9.11.11844

Ko, L. J., and Prives, C. (1996). P53: Puzzle and paradigm. *Genes Dev.* 10:9. doi: 10.1101/gad.10.9.1054

Kobayashi, S., Fukuhara, A., Taguchi, T., Matsuda, M., Tochino, Y., Otsuki, M., et al. (2010). Identification of a new secretory factor, CCDC3/Favine, in adipocytes and endothelial cells. *Biochem. Biophys. Res. Commun.* 392:1. doi: 10.1016/j.bbrc.2009.12.142

Korber, M., Klein, I., and Daum, G. (2017). Steryl ester synthesis, storage and hydrolysis: A contribution to sterol homeostasis. *Biochim. Biophys. Acta - Mol. Cell Biol. Lipids.* 1862:12. doi: 10.1016/j.bbalip.2017.09.002

Koster, M. I., Dai, D., Marinari, B., Sano, Y., Costanzo, A., Karin, M., et al. (2007). P63 Induces Key Target Genes Required for Epidermal Morphogenesis. *Proc. Natl. Acad. Sci. U. S. A.* 104:9. doi: 10.1073/pnas.0611376104

Laezza, C., D'Alessandro, A., Croce, L., Di, Picardi, P., Ciaglia, E., et al. (2015). P53 regulates the mevalonate pathway in human glioblastoma multiforme. *Cell Death Dis.* 6:10. doi: 10.1038/cddis.2015.279

Laurenzi, V., De Catani, M. V., Terrinoni, A., Corazzari, M., Melino, G., Constanzo, A., et al. (1999). Additional complexity in p73: Induction by mitogens in lymphoid cells and identification of two new splicing variants ε and ζ. *Cell Death Differ.* 6:5. doi: 10.1038/sj.cdd.4400521

Laurenzi, V., De Costanzo, A., Barcaroli, D., Terrinoni, A., Falco, M., Annicchiarico-Petruzzelli, M., et al. (1998). Two new p73 splice variants, γ and δ, with different transcriptional activity. *J. Exp. Med.* 188:9. doi: 10.1084/jem.188.9.1763

Lee, J., and Wolfgang, M. J. (2012). Metabolomic profiling reveals a role for CPT1c in neuronal oxidative metabolism. *BMC Biochem.* 13:23. doi: 10.1186/1471-2091-13-23

Leonardi, R., Zhang, Y. M., Rock, C. O., and Jackowski, S. (2005). Coenzyme A: Back in action. *Prog. Lipid Res.* 44, 2–3. doi: 10.1016/j.plipres.2005.04.001

Levy, B. D., Clish, C. B., Schmidt, B., Gronert, K., and Serhan, C. N. (2001). Lipid mediator class switching during acute inflammation: Signals in resolution. *Nat. Immunol.* 2:7. doi: 10.1038/89759

Li, C., Dong, X., Du, W., Shi, X., Chen, K., Zhang, W., et al. (2020). LKB1-AMPK axis negatively regulates ferroptosis by inhibiting fatty acid synthesis. *Signal Transduct. Target. Ther.* 5:187. doi: 10.1038/s41392-020-00297-2

Liang, S. X., and Richardson, D. R. (2003). The effect of potent iron chelators on the regulation of p53: Examination of the expression, localization and DNA-binding activity of p53 and the transactivation of WAF1. *Carcinogenesis.* 24:10. doi: 10.1093/carcin/bgg116

Liao, W., Liu, H., Zhang, Y., Jung, J. H., Chen, J., Su, X., et al. (2017). Ccdc3: A new P63 target involved in regulation of liver lipid metabolism. *Sci. Rep.* 7:1. doi: 10.1038/s41598-017-09228-8

Liu, G., and Chen, X. (2002). The ferredoxin reductase gene is regulated by the p53 family and sensitizes cells to oxidative stress-induced apoptosis. *Oncogene.* 21:47. doi: 10.1038/sj.onc.1205862

Liu, G., Nozell, S., Xiao, H., and Chen, X. (2004). ΔNp73β Is Active in Transactivation and Growth Suppression. *Mol. Cell. Biol.* 24:2. doi: 10.1128/mcb.24.2.487-501.2004

Liu, J., Zhang, C., Wang, J., Hu, W., and Feng, Z. (2020). The regulation of ferroptosis by tumor suppressor p53 and its pathway. *Int. J. Mol. Sci.* 21:21. doi: 10.3390/ijms21218387

Liu, Y., He, Y., Jin, A., Tikunov, A. P., Zhou, L., Tollini, L. A., et al. (2014). Ribosomal protein-Mdm2-p53 pathway coordinates nutrient stress with lipid metabolism by regulating MCD and promoting fatty acid oxidation. *Proc. Natl. Acad. Sci. U. S. A.* 111:23. doi: 10.1073/pnas.1315605111

Longo, N., Frigeni, M., and Pasquali, M. (2016). Carnitine transport and fatty acid oxidation. *Biochim. Biophys. Acta - Mol. Cell Res.* 1863:10. doi: 10.1016/j.bbamcr.2016.01.023

Lu, B., Chen, X. B., Ying, M. D., He, Q. J., Cao, J., and Yang, B. (2018). The role of ferroptosis in cancer development and treatment response. *Front. Pharmacol.* 8:992. doi: 10.3389/fphar.2017.00992

Luna, R. M. D. O., Wagner, D. S., and Lozano, G. (1995). Rescue of early embryonic lethality in mdm2-deficient mice by deletion of p53. *Nature* 378:6553. doi: 10.1038/378203a0

Ma, C., Liging, S., Seven, A. B., Xu, Y., and Rizo, J. (2013). Reconstitution of the Vital Functions of Munc18 and Munc13 in Neurotransmitter Release. *Science* 2013:339.

Mangiulli, M., Valletti, A., Caratozzolo, M. F., Tullo, A., Sbisà, E., Pesole, G., et al. (2009). Identification and functional characterization of two new transcriptional variants of the human p63 gene. *Nucleic Acids Res.* 37:18. doi: 10.1093/nar/gkp674

Marini, A., Rotblat, B., Sbarrato, T., Niklison-Chirou, M. V., Knight, J. R. P., Dudek, K., et al. (2018). TAp73 contributes to the oxidative stress response by regulating protein synthesis. *Proc. Natl. Acad. Sci. U. S. A.* 115:24. doi: 10.1073/pnas.1718531115

Marshall, C. B., Mays, D. J., Beeler, J. S., Rosenbluth, J. M., Boyd, K. L., Santos Guasch, G. L., et al. (2016). P73 Is Required for Multiciliogenesis and Regulates the Foxj1-Associated Gene Network. *Cell Rep.* 14:10. doi: 10.1016/j.celrep.2016.02.035

Martin, S., and Parton, R. G. (2006). Lipid droplets: a unified view of a dynamic organelle. *Mol. Cell* 7:912.

Masaldan, S., Belaidi, A. A., Ayton, S., and Bush, A. I. (2019). Cellular senescence and iron dyshomeostasis in alzheimer's disease. *Pharmaceuticals.* 12:2. doi: 10.3390/ph12020093

Mashek, D. G., Li, L. O., and Coleman, R. A. (2007). Long-chain acyl-CoA synthetases and fatty acid channeling. *Future Lipidol.* 2:4. doi: 10.2217/17460875.2.4.465

Mills, A. A., Zheng, B., Wang, X. J., Vogel, H., Roop, D. R., and Bradley, A. (1999). P63 Is a P53 Homologue Required for Limsb and Epidermal Morphogenesis. *Nature.* 398:6729. doi: 10.1038/19531

Moon, S. H., Huang, C. H., Houlihan, S. L., Regunath, K., Freed-Pastor, W. A., Morris, J. P., et al. (2019). P53 Represses the Mevalonate Pathway to Mediate Tumor Suppression. *Cell.* 176:3. doi: 10.1016/j.cell.2018.11.011

Nemajerova, A., Kramer, D., Siller, S. S., Herr, C., Shomroni, O., Pena, T., et al. (2016). TAp73 is a central transcriptional regulator of airway multiciliogenesis. *Genes Dev.* 30:11. doi: 10.1101/gad.279836.116

Nemoto, S., Fergusson, M. M., and Finkel, T. (2004). Nutrient availability regulates SIRT1 through a forkhead-dependent pathway. *Science* 306:5704. doi: 10.1126/science.1101731

Nostrand, J. L., Van, Brady, C. A., Jung, H., Fuentes, D. R., Kozak, M. M., et al. (2014). Inappropriate p53 activation during development induces features of CHARGE syndrome. *Nature.* 514:7521. doi: 10.1038/nature13585

Oelkers, P., Behari, A., Cromley, D., Billheimer, J. T., and Sturleyt, S. L. (1998). Characterization of two human genes encoding acyl coenzyme A: Cholesterol acyltransferase-related enzymes. *J. Biol. Chem.* 273:41. doi: 10.1074/jbc.273.41.26765

Ohashi, T., Idogawa, M., Sasaki, Y., and Tokino, T. (2017). P53 mediates the suppression of cancer cell invasion by inducing LIMA1/EPLIN. *Cancer Lett.* 390:34. doi: 10.1016/j.canlet.2016.12.034

Olzmann, J. A., and Carvalho, P. (2019). Dynamics and functions of lipid droplets. *Nat. Rev. Mol. Cell Biol.* 20:3. doi: 10.1038/s41580-018-0085-z

Oni, T. E., Biffi, G., Baker, L. A., Hao, Y., Tonelli, C., Somerville, T. D. D., et al. (2020). SOAT1 promotes mevalonate pathway dependency in pancreatic cancer. *J. Exp. Med.* 217:9. doi: 10.1084/jem.20192389

Ou, Y., Wang, S. J., Li, D., Chu, B., and Gu, W. (2016). Activation of SAT1 engages polyamine metabolism with p53-mediated ferroptotic responses. *Proc. Natl. Acad. Sci. U. S. A.* 113:44. doi: 10.1073/pnas.1607152113

Parant, J., Chavez-Reyes, A., Little, N. A., Yan, W., Reinke, V., Jochemsen, A. G., et al. (2001). Rescue of embryonic lethality in Mdm4-null mice by loss of Trp53 suggests a nonoverlapping pathway with MDM2 to regulate p53. *Nat. Genet.* 29:1. doi: 10.1038/ng714

Parrales, A., and Iwakuma, T. (2016). P53 As a Regulator of Lipid Metabolism in Cancer. *Int. J. Mol. Sci.* 17:2074. doi: 10.3390/ijms17122074

Peter-Riesch, B., Fathi, M., Schlegel, W., and Wolheim, C. B. (1988). Glucose and carbachol generate 1,2-diacylglycerols by different mechanisms in pancreatic islets. *J. Clin. Invest.* 81:4. doi: 10.1172/JCI113430

Puig, S., Ramos-Alonso, L., Romero, A. M., and Martínez-Pastor, M. T. (2017). The elemental role of iron in DNA synthesis and repair. *Metallomics.* 9:1483. doi: 10.1039/c7mt00116a

Qu, Q., Zeng, F., Liu, X., Wang, Q. J., and Deng, F. (2016). Fatty acid oxidation and carnitine palmitoyltransferase I: Emerging therapeutic targets in cancer. *Cell Death Dis.* 7:5. doi: 10.1038/cddis.2016.132

Rahman, S., and Islam, R. (2011). Mammalian Sirt1: Insights on its biological functions. *Cell Commun. Signal.* 9:11. doi: 10.1186/1478-811X-9-11

Röhrig, F., and Schulze, A. (2016). The multifaceted roles of fatty acid synthesis in cancer. *Nat. Rev. Cancer.* 16:11. doi: 10.1038/nrc.2016.89

Rufer, A. C., Thoma, R., and Hennig, M. (2009). Structural insight into function and regulation of carnitine palmitoyltransferase. *Cell. Mol. Life Sci.* 66:15. doi: 10.1007/s00018-009-0035-1

Sah, V. P., Attardi, L. D., Mulligan, G. J., Williams, B., Bronson, R. T., and Jacks, T. (1995). A subset of p53-deficient embryos exhibit exencephaly. *Nat Genet.* 10, 175–180. doi: 10.1038/ng0695-175

Saito, T., Kuma, A., Sugiura, Y., Ichimura, Y., Obata, M., Kitamura, H., et al. (2019). Autophagy regulates lipid metabolism through selective turnover of NCoR1. *Nat. Commun.* 10:1. doi: 10.1038/s41467-019-08829-3

Saleme, B., Das, S. K., Zhang, Y., Boukouris, A. E., Lorenzana Carrillo, M. A., Jovel, J., et al. (2020). P53-Mediated Repression of the PGC1A (PPARG Coactivator 1α) and APLNR (Apelin Receptor) Signaling Pathways Limits Fatty Acid Oxidation Energetics: Implications for Cardio-oncology. *J. Am. Heart Assoc.* 9:15. doi: 10.1161/JAHA.120.017247

Sanchez-Macedo, N., Feng, J., Faubert, B., Chang, N., Elia, A., Rushing, E. J., et al. (2013). Depletion of the novel p53-target gene carnitine palmitoyltransferase 1C delays tumor growth in the neurofibromatosis type i tumor model. *Cell Death Differ.* 20:4. doi: 10.1038/cdd.2012.168

Sato, M., Kusumi, R., Hamashima, S., Kobayashi, S., Sasaki, S., Komiyama, Y., et al. (2018). The ferroptosis inducer erastin irreversibly inhibits system xc- and synergizes with cisplatin to increase cisplatin's cytotoxicity in cancer cells. *Sci. Rep.* 8:968. doi: 10.1038/s41598-018-19213-4

Schmale, H., and Bamberger, C. (1997). A novel protein with strong homology to the tumor suppressor p53. *Oncogene.* 15:11. doi: 10.1038/sj.onc.1201500

Sheftel, A. D., Stehling, O., Pierik, A. J., Elsässer, H. P., Mühlenhoff, U., Webert, H., et al. (2010). Humans possess two mitochondrial ferredoxins, Fdx1 and Fdx2, with distinct roles in steroidogenesis, heme, and Fe/S cluster biosynthesis. *Proc. Natl. Acad. Sci. U. S. A.* 107:26. doi: 10.1073/pnas.1004250107

Shen, J., Sheng, X., Chang, Z. N., Wu, Q., Wang, S., Xuan, Z., et al. (2014). Iron metabolism regulates p53 signaling through direct Heme-p53 interaction and modulation of p53 localization, stability, and function. *Cell Rep.* 7:1. doi: 10.1016/j.celrep.2014.02.042

Shimano, H., Horton, J. D., Shimomura, I., Hammer, R. E., Brown, M. S., and Goldstein, J. L. (1997). Isoform 1c of sterol regulatory element binding protein is less active than isoform 1a in livers of transgenic mice and in cultured cells. *J. Clin. Invest.* 99:5. doi: 10.1172/JCI119248

Shimizu, R., Lan, N. N., Tai, T. T., Adachi, Y., Kawazoe, A., Mu, A., et al. (2014). P53 directly regulates the transcription of the human frataxin gene and its lack of regulation in tumor cells decreases the utilization of mitochondrial iron. *Gene.* 551:1. doi: 10.1016/j.gene.2014.08.043

Shimomura, I., Shimano, H., Korn, B. S., Bashmakov, Y., and Horton, J. D. (1998). Nuclear sterol regulatory element-binding proteins activate genes responsible for the entire program of unsaturated fatty acid biosynthesis in transgenic mouse liver. *J. Biol. Chem.* 273:52. doi: 10.1074/jbc.273.52.35299

Smith, S., Witkowski, A., and Joshi, A. K. (2003). Structural and functional organization of the animal fatty acid synthase. *Prog. Lipid Res.* 42:4. doi: 10.1016/S0163-7827(02)00067-X

Su, X., Gi, Y. J., Chakravarti, D., Chan, I. L., Zhang, A., Xia, X., et al. (2012). TAp63 is a master transcriptional regulator of lipid and glucose metabolism. *Cell Metab.* 16:4. doi: 10.1016/j.cmet.2012.09.006

Su, X., Paris, M., Gi, Y. J., Tsai, K. Y., Cho, M. S., Lin, Y. L., et al. (2009). TAp63 Prevents Premature Aging by Promoting Adult Stem Cell Maintenance. *Cell Stem Cell.* 5:1. doi: 10.1016/j.stem.2009.04.003

Suh, E. K., Yang, A., Kettenbach, A., Bamberger, C., Michaelis, A. H., Zhu, Z., et al. (2006). P63 Protects the Female Germ Line During Meiotic Arrest. *Nature.* 444:7119. doi: 10.1038/nature05337

Tarangelo, A., and Dixon, S. (2018). The p53-p21 pathway inhibits ferroptosis during metabolic stress. *Oncotarget.* 9:37. doi: 10.18632/oncotarget.25362

Thompson, E. A., and Siiteri, P. K. (1974). The involvement of human placental microsomal cytochrome P 450 in aromatization. *J. Biol. Chem.* 249:17. doi: 10.1016/s0021-9258(20)79736-x

Tomasini, R., Tsuchihara, K., Wilhelm, M., Fujitani, M., Rufini, A., Cheung, C. C., et al. (2008). TAp73 knockout shows genomic instability with infertility and tumor suppressor functions. *Genes Dev.* 22:19. doi: 10.1101/gad.1695308

Trink, B., Okami, K., Wu, L., Sriuranpong, V., Jen, J., and Sidransky, D. (1998). A new human p53 homologue. *Nat. Med.* 4:7. doi: 10.1038/nm0798-747

Tsurusaki, S., Tsuchiya, Y., Koumura, T., Nakasone, M., Sakamoto, T., Matsuoka, M., et al. (2019). Hepatic ferroptosis plays an important role as the trigger for initiating inflammation in nonalcoholic steatohepatitis. *Cell Death Dis.* 10:6. doi: 10.1038/s41419-019-1678-y

Venkatesh, D., O'Brien, N. A., Zandkarimi, F., Tong, D. R., Stokes, M. E., Dunn, D. E., et al. (2020). MDM2 and MDMX promote ferroptosis by PPARα-mediated lipid remodeling. *Genes Dev.* 34, 7–8. doi: 10.1101/gad.334219.119

Volz, K. (2008). The functional duality of iron regulatory protein 1. *Curr. Opin. Struct. Biol.* 18:1. doi: 10.1016/j.sbi.2007.12.010

Waldvogel-Abramowski, S., Waeber, G., Gassner, C., Buser, A., Frey, B. M., Favrat, B., et al. (2014). Physiology of iron metabolism. *Transfus. Med. Hemotherapy.* 41:3. doi: 10.1159/000362888

Wallace, D. F. (2019). Regulation of Folate Homeostasis. *Clin. Biochem.* 37:2. doi: 10.1515/9783110856262-175

Wang, G. X., Tu, H. C., Dong, Y., Skanderup, A. J., Wang, Y., Takeda, S., et al. (2017). ΔNp63 Inhibits Oxidative Stress-Induced Cell Death, Including Ferroptosis, and Cooperates with the BCL-2 Family to Promote Clonogenic Survival. *Cell Rep.* 21:10. doi: 10.1016/j.celrep.2017.11.030

Wang, S. J., Yu, G., Jiang, L., Li, T., Lin, Q., Tang, Y., et al. (2013). P53-dependent regulation of metabolic function through transcriptional activation of pantothenate kinase-1 gene. *Cell Cycle.* 12:5. doi: 10.4161/cc.23597

Wang, X., Zhao, X., Gao, X., Mei, Y., and Wu, M. (2013). A new role of p53 in regulating lipid metabolism. *J. Mol. Cell Biol.* 5:2. doi: 10.1093/jmcb/mjs064

Wardman, P., and Candeias, L. P. (1996). Fenton Chemistry: An Introduction. *Source Radiat. Res.* Vol. 145:3579270.

Weizer-Stern, O., Adamsky, K., Margalit, O., Ashur-Fabian, O., Givol, D., Amariglio, N., et al. (2007). Hepcidin, a key regulator of iron metabolism, is transcriptionally activated by p53. *Br. J. Haematol.* 138:2. doi: 10.1111/j.1365-2141.2007.06638.x

Wilhelm, M. T., Rufini, A., Wetzel, M. K., Tsuchihara, K., Inoue, S., Tomasini, R., et al. (2010). Isoform-specific p73 knockout mice reveal a novel role for ΔNp73 in the DNA damage response pathway. *Genes Dev.* 24:6. doi: 10.1101/gad.1873910

Wise, E. M., and Ball, E. G. (1964). Malic Enzyme and Lipogenesis. *Proc. Natl. Acad. Sci. U S.* 52:1933. doi: 10.1073/pnas.52.5.1255

Xie, Y., Zhu, S., Song, X., Sun, X., Fan, Y., Liu, J., et al. (2017). The Tumor Suppressor p53 Limits Ferroptosis by Blocking DPP4 Activity. *Cell Rep.* 20:7. doi: 10.1016/j.celrep.2017.07.055

Yahagi, N., Shimano, H., Matsuzaka, T., Najima, Y., Sekiya, M., Nakagawa, Y., et al. (2003). P53 Activation in Adipocytes of Obese Mice. *J. Biol. Chem.* 278:28. doi: 10.1074/jbc.M302364200

Yamauchi, Y., Iwamoto, N., Rogers, M. A., Abe-Dohmae, S., Fujimoto, T., Chang, C. C. Y., et al. (2015). Deficiency in the lipid exporter ABCA1 impairs retrograde sterol movement and disrupts sterol sensing at the endoplasmic reticulum. *J. Biol. Chem.* 290:39. doi: 10.1074/jbc.M115.662668

Yan, W., and Chen, X. (2006). GPX2, a direct target of p63, inhibits oxidative stress-induced apoptosis in a p53-dependent manner. *J. Biol. Chem.* 281:12. doi: 10.1074/jbc.M512655200

Yang, A., Kaghad, M., Wang, Y., Gillett, E., Fleming, M. D., Dötsch, V., et al. (1998). P63, a P53 Homolog At 3Q27-29, Encodes Multiple Products With Transactivating, Death-Inducing, and Dominant-Negative Activities. *Mol. Cell.* 2:3. doi: 10.1016/S1097-2765(00)80275-0

Yang, A., Schweitzer, R., Sun, D., Kaghad, M., Walker, N., Bronson, R. T., et al. (1999). P63 Is Essential for Regenerative Proliferation in Limb, Craniofacial and Epithelial Development. *Nature.* 398:6729. doi: 10.1038/19539

Yang, A., Walker, N., Bronson, R., Kaghad, M., Oosterwegel, M., Bonnin, J., et al. (2000). P73-Deficient mice have neurological, pheromonal and inflammatory defects but lack spontaneous tumours. *Nature.* 404:6773. doi: 10.1038/35003607

Ye, X., Zhou, X. J., and Zhang, H. (2018). Exploring the role of autophagy-related gene 5 (ATG5ATG5) yields important insights into autophagy in autoimmune/autoinflammatory diseases. *Front. Immunol.* 9:2334. doi: 10.3389/fimmu.2018.02334

Yin, H., Xu, L., and Porter, N. A. (2011). Free radical lipid peroxidation: Mechanisms and analysis. *Chem. Rev.* 111:10. doi: 10.1021/cr200084z

Yin, Y., Stephen, C. W., Luciani, M. G., and Fåhraeus, R. (2002). P53 Stability and Activity Is Regulated By Mdm2-Mediated Induction of Alternative P53 Translation Products. *Nat. Cell Biol.* 4:6. doi: 10.1038/ncb801

Zaidi, N., Swinnen, J. V., and Smans, K. (2012). ATP-citrate lyase: A key player in cancer metabolism. *Cancer Res.* 72:15. doi: 10.1158/0008-5472.CAN-11-4112

Zhang, F., Wang, W., Tsuji, Y., Torti, S. V., and Torti, F. M. (2008). Post-transcriptional modulation of iron homeostasis during p53-dependent growth arrest. *J. Biol. Chem.* 283:49. doi: 10.1074/jbc.M806432200

Zhang, J., Kong, X., Zhang, Y., Sun, W., Wang, J., Chen, M., et al. (2020). FDXR regulates TP73 tumor suppressor via IRP2 to modulate aging and tumor suppression. *J. Pathol.* 251:3. doi: 10.1002/path.5451

Zhang, Q., He, X., Chen, L., Zhang, C., Gao, X., Yang, Z., et al. (2012). Synergistic regulation of p53 by Mdm2 and Mdm4 is critical in cardiac endocardial cushion morphogenesis during heart development. *J. Pathol.* 228:3. doi: 10.1002/path.4077

Zhang, Y. Y., Fu, Z. Y., Wei, J., Qi, W., Baituola, G., Luo, J., et al. (2018). A LIMA1 variant promotes low plasma LDL cholesterol and decreases intestinal cholesterol absorption. *Science* 360:6393. doi: 10.1126/science.aao6575

Zhang, Y., Feng, X., Zhang, J., and Chen, X. (2020). Iron regulatory protein 2 exerts its oncogenic activities by suppressing TAp63 expression. *Mol. Cancer Res.* 18:7. doi: 10.1158/1541-7786.MCR-19-1104

Zhang, Y., Qian, Y., Zhang, J., Yan, W., Jung, Y. S., Chen, M., et al. (2017). Ferredoxin reductase is critical for p53-dependent tumor suppression via iron regulatory protein 2. *Genes Dev.* 31:12. doi: 10.1101/gad.299388.117

Zhu, J., Zhang, S., Jiang, J., and Chen, X. (2000). Definition of the p53 functional domains necessary for inducing apoptosis. *J. Biol. Chem.* 275:51. doi: 10.1074/jbc.M005676200

Zhu, J., Zhou, W., Jiang, J., and Chen, X. (1998). Identification of a novel p53 functional domain that is necessary for mediating apoptosis. *J. Biol. Chem.* 273:21. doi: 10.1074/jbc.273.21.13030

Conflict of Interest: The authors declare that the research was conducted in the absence of any commercial or financial relationships that could be construed as a potential conflict of interest.

Publisher's Note: All claims expressed in this article are solely those of the authors and do not necessarily represent those of their affiliated organizations, or those of the publisher, the editors and the reviewers. Any product that may be evaluated in this article, or claim that may be made by its manufacturer, is not guaranteed or endorsed by the publisher.

Copyright © 2021 Laubach, Zhang and Chen. This is an open-access article distributed under the terms of the Creative Commons Attribution License (CC BY). The use, distribution or reproduction in other forums is permitted, provided the original author(s) and the copyright owner(s) are credited and that the original publication in this journal is cited, in accordance with accepted academic practice. No use, distribution or reproduction is permitted which does not comply with these terms.

frontiers in Cell and Developmental Biology

REVIEW
published: 28 September 2021
doi: 10.3389/fcell.2021.737735

Mechanisms of Functional Pleiotropy of p73 in Cancer and Beyond

*Stella Logotheti[1], Christin Richter[1], Nico Murr[1], Alf Spitschak[1], Stephan Marquardt[1] and Brigitte M. Pützer[1,2]**

[1] Institute of Experimental Gene Therapy and Cancer Research, Rostock University Medical Center, Rostock, Germany,
[2] Department Life, Light & Matter, University of Rostock, Rostock, Germany

The transcription factor p73 is a structural and functional homolog of TP53, the most famous and frequently mutated tumor-suppressor gene. The TP73 gene can synthesize an overwhelming number of isoforms via splicing events in 5′ and 3′ ends and alternative promoter usage. Although it originally came into the spotlight due to the potential of several of these isoforms to mimic p53 functions, it is now clear that TP73 has its own unique identity as a master regulator of multifaceted processes in embryonic development, tissue homeostasis, and cancer. This remarkable functional pleiotropy is supported by a high degree of mechanistic heterogeneity, which extends far-beyond the typical mode of action by transactivation and largely relies on the ability of p73 isoforms to form protein–protein interactions (PPIs) with a variety of nuclear and cytoplasmic proteins. Importantly, each p73 isoform carries a unique combination of functional domains and residues that facilitates the establishment of PPIs in a highly selective manner. Herein, we summarize the expanding functional repertoire of TP73 in physiological and oncogenic processes. We emphasize how TP73's ability to control neurodevelopment and neurodifferentiation is co-opted in cancer cells toward neoneurogenesis, an emerging cancer hallmark, whereby tumors promote their own innervation. By further exploring the canonical and non-canonical mechanistic patterns of p73, we apprehend its functional diversity as the result of a sophisticated and coordinated interplay of: (a) the type of p73 isoforms (b) the presence of p73 interaction partners in the cell milieu, and (c) the architecture of target gene promoters. We suppose that dysregulation of one or more of these parameters in tumors may lead to cancer initiation and progression by reactivating p73 isoforms and/or p73-regulated differentiation programs thereof in a spatiotemporally inappropriate manner. A thorough understanding of the mechanisms supporting p73 functional diversity is of paramount importance for the efficient and precise p73 targeting not only in cancer, but also in other pathological conditions where TP73 dysregulation is causally involved.

Keywords: p73, protein–protein interactions(PPI), C-terminus, gene promoter architecture, development and homeostasis, differentiation, neoneurogenesis, cancer progression

OPEN ACCESS

Edited by:
Maria Lina Tornesello, Istituto Nazionale Tumori Fondazione G. Pascale (IRCCS), Italy

Reviewed by:
Shurong Liu, Sun Yat-sen University, China
Federica Verginelli, Fondazione del Piemonte per l'Oncologia, Istituto di Candiolo (IRCCS), Italy

***Correspondence:**
Brigitte M. Pützer
brigitte.puetzer@med.uni-rostock.de

Specialty section:
This article was submitted to Molecular and Cellular Pathology, a section of the journal Frontiers in Cell and Developmental Biology

Received: *07 July 2021*
Accepted: *10 September 2021*
Published: *28 September 2021*

Citation:
Logotheti S, Richter C, Murr N, Spitschak A, Marquardt S and Pützer BM (2021) Mechanisms of Functional Pleiotropy of p73 in Cancer and Beyond. Front. Cell Dev. Biol. 9:737735. doi: 10.3389/fcell.2021.737735

INTRODUCTION

TP53 is a well-known tumor suppressor and a famous "Holy Grail" of anticancer targeting. In 1997, two genes were added in the so-far considered single-membered p53 family: p63 and p73, which present similarities to p53 regarding their basic functional domains and their ability to activate typical p53 targets and participate in common p53 pathways. Nevertheless, both also differ from

p53, since they do not exhibit the characteristics of a classical Knudson-type tumor suppressor gene. p63 and p73 entail three basic functional domains which are homologous to p53, that is the transactivation domain (TA), the core DNA-binding domain (DBD) and the oligomerization domain (OD), with DBD being the most conserved domain. They have an extra SAM (sterile alpha motif) domain in their C-terminus, which confers protein stability (Logotheti et al., 2013). Although *p53* appeared later in evolution, to specifically guard the fidelity of somatic cell divisions and protect from DNA damage-induced cancerous alterations, the ability to regulate DNA damage and apoptosis is primitive within the p53 family. In bony fishes, the *p63*/*p73* and the *p53* genes are separated into distinct entities and undergo positive selection to control different processes: p63 got specialized in the production of epithelial cells and p73 in neuronal development, whereas p53 is better adapted as a tumor suppressor (Belyi and Levine, 2009; Belyi et al., 2010). These functional adaptations were associated with alterations in the gene organization of a single ancestral p53/p63/p73 gene, mainly gain of an alternative promoter that leads to NH2-terminal truncated isoforms, loss of the SAM domain, and ability for formation of additional C-terminal splice variants in *Chordata* and evolutionarily higher organisms (Yang et al., 2002). These changes overall enabled a higher level of functional divergence and specificity for each p53 family member. All three family members synthesize many isoforms, with p73 producing the highest number.

The synthesis of this overwhelmingly large number of p73 isoforms is achieved by (a) use of an extrinsic (P1) and alternative intrinsic promoter (P2) in the 5′ end, generating TA and ΔN classes of isoforms, (b) alternative splicing in the 5′ end, resulting in amino-truncated ΔTA isoforms (ΔEx2p73, ΔEx2/3p73, and ΔN′p73) that partially or entirely lack the transactivation domain and, together with ΔN, constitute the so called DN isoforms, (c) alternative splicing in the 3′ end, putting forth several C-terminal splice variants (α, β, γ, δ, ε, ζ, η, η*, η1, and θ) (Logotheti et al., 2013) (**Figure 1A**). We also detected somatic genomic rearrangements of TP73 that generate an oncogenic TP73ex2/3 (George et al., 2015). In the context of cancer, TAp73 isoforms are considered anti-oncogenic (Stiewe and Pützer, 2000; Malik et al., 2021), while DNp73 forms antagonize TAp73 effects and are oncogenic. The opposing roles of TA versus ΔN classes of isoforms in the context of cancer have been underscored via knockout mice that are selectively deficient for either TAp73 or ΔNp73. TAp73-knockout mice are tumor-prone and more sensitive to carcinogens, and present genomic instability and enhanced aneuploidy, thus highlighting a significant role of TAp73 in the maintenance of genomic integrity (Tomasini et al., 2008). In contrast, mice lacking ΔNp73 show increased apoptosis in response to DNA damage, revealing an oncogenic effect of this isoform in the inhibition of the DNA-damage response (DDR) pathway (Wilhelm et al., 2010). Using kinetic modeling to detect genetic signatures characteristic for cancer drug resistance, we have shown for example that downregulation of miR-205 can be mediated by an imbalance in the TAp73/ΔTA ratio, which leads to increased expression of anti-apoptotic BCL-2 and ABC transporters (Alla et al., 2012; Vera et al., 2013). The ΔTA's that are tumor-specific, are vigorously expressed in advanced stages across a variety of highly aggressive human cancers (Knoll et al., 2011; Steder et al., 2013; George et al., 2015; Meier et al., 2016) and, analogous to Δ*N*'s, promote tumor initiation (Tannapfel et al., 2008) and cancer progression (Engelmann et al., 2015). For instance, DNp73 (p73ΔEx2/3) is a key metastatic driver, which promotes tumor progression via inducing EMT, actin cytoskeletal reorganization, invasion, and stemness in melanoma (Steder et al., 2013; Engelmann and Pützer, 2014; Meier et al., 2016; Fürst et al., 2019). Consistently, p73 isoforms play a key role in the regulation of cancer stemness, epithelial-mesenchymal transition (EMT) and response to therapy across several cancer types (Prabhu et al., 2016; Thakur et al., 2016; Sharif et al., 2019b; Uboveja et al., 2020). For a detailed overview, we refer to Engelmann et al. (2015), Pützer et al. (2017).

The TP73 gene has attracted incredible attention for therapeutic cancer management mainly because it can mimic and/or surrogate for p53 oncosuppressive functions, whereas unlike p53, it is rarely mutated in cancer, a fact that renders this targeting unbiased from intra- and inter-tumoral mutational heterogeneity (Logotheti et al., 2019). Hence, understanding the mechanisms through which p73 isoforms exert their functions are of paramount importance in order to efficiently manipulate these factors in precision medicine. All TA and DNp73 isoforms have intact core DNA-binding and tetramerization domains, via which they can oligomerize and bind to corresponding p53- or p73-responsive elements (RE). The transactivation domain-containing TA's directly activate the transcription of p53/TAp73 target genes. Vice versa, DNp73 lacking a typical N-terminal transactivation domain can act as transdominant inhibitors of TAp73 and p53 (Stiewe et al., 2002a,b) and block their gene regulatory activity either by competing for p53/p73 binding sites or by forming transcriptionally silent TAp73/DNp73 or p53/DNp73 hetero-oligomers (Marabese et al., 2007). The ultimate effect of p73 isoforms on target genes is overall attributed to the TA/DN ratio as opposed to the overexpression of a specific p73 isoform or a specific class of p73 isoforms *per se*. Furthermore, the p53/p63 cell content often influences p73 functions, because p73 can form stable hetero-oligomers with p63 or mutant p53 (Li and Prives, 2007; Nemajerova et al., 2018).

p73 has been initially viewed as a p53 'copycatter,' because of its ability to activate common p53 targets and regulate tumor-suppressive processes, such as cell cycle arrest, senescence, apoptosis and genomic stability. However, it has currently been realized that p73 not only affects a large number of cancer-related pathways, but also regulates disparate processes in embryonic development and tissue homeostasis. More intriguingly, p73 appears to have the potential to activate 'off-context' its non-oncogenic differentiation programs within the cancer cell context to modulate tumor metastasis. This process, whereby a biological function within a specific context may be alternatively used in another context to support a novel function, is termed co-option and consists a recurrent and prevailing pattern during tumor progression (Billaud and Santoro, 2011). The high level of functional pleiotropy in physiological and cancer-related processes cannot be sufficiently supported solely by the typical mode of direct gene transactivation/transrepression that has

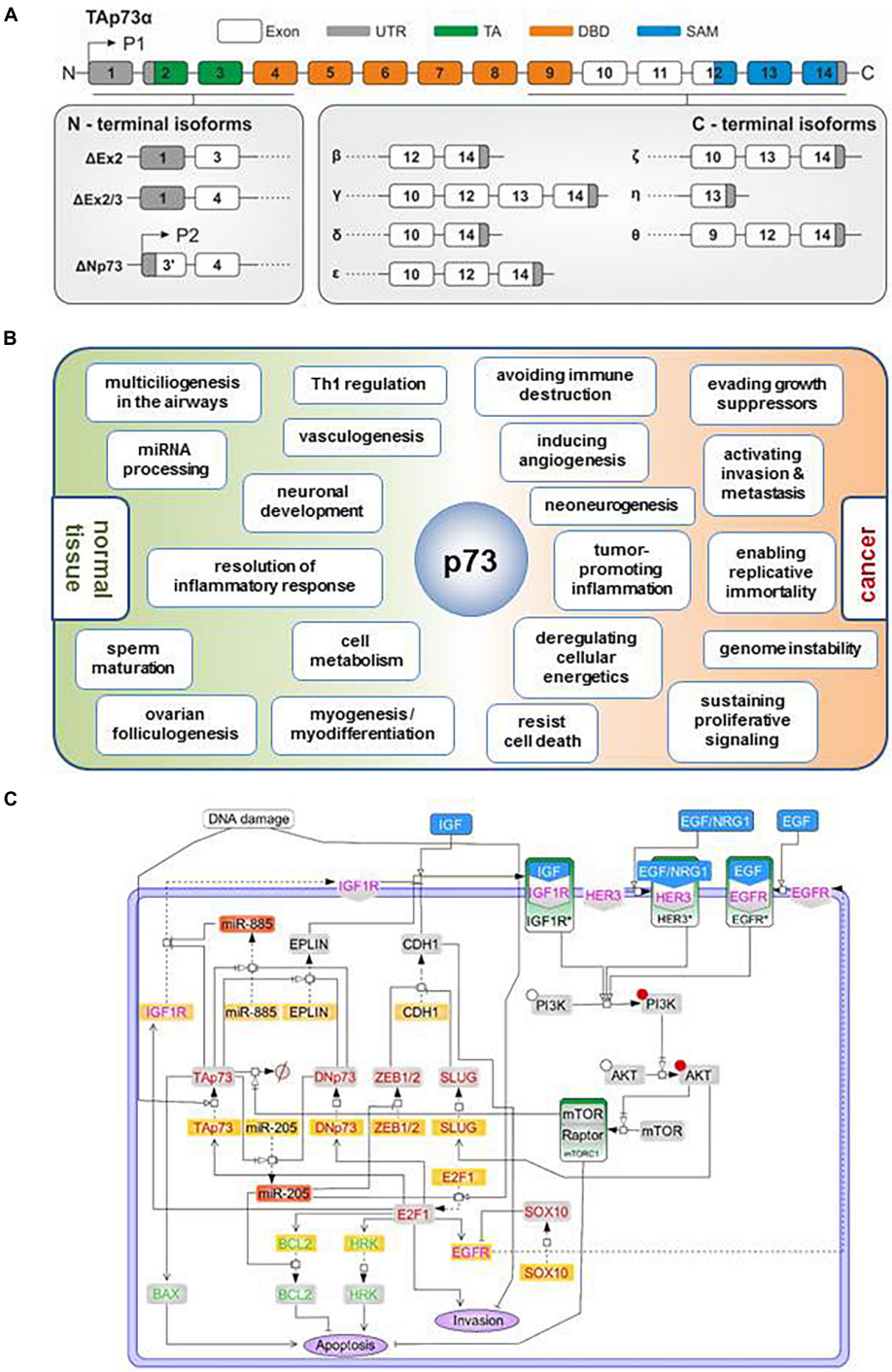

FIGURE 1 | TP73 synthesizes a large number of isoforms contributing to its multifunctionality both in physiological and cancer-related processes. **(A)** Diagram depicting synthesis of p73 isoforms by (i) alternative splicing in the 3′ end, putting forth several C-terminal splice variants; or (ii) the use of an extrinsic (P1) and alternative intrinsic promoter (P2) in the 5′ end, and (iii) alternative splicing in the 5′ end. All isoforms contain a core DNA-binding domain. Different combinations of the N-terminal head with the C-terminal tail give rise to functionally distinct isoforms. TA, transactivation domain; DBD, DNA-binding domain; SAM, sterile alpha motif. **(B)** Overview of the documented and predicted roles of TP73 gene products in normal and cancer tissues. There are analogies in several processes regulated by TP73 in the physiological and cancer context (terms straddling around the p73 node in the scheme) which might represent the aberrant function of p73 regulatory networks of embryonic development, differentiation, and tissue homeostasis within the tumor context. **(C)** Regulatory map of the TAp73/DNp73-controlled pathways depicting their interception with major cascades of extracellular signaling. The model was constructed using SBGN-compliant software Cell Designer. Yellow boxes: RNA; gray boxes: protein; red boxes: mature microRNAs; green boxes: activated signaling complexes; blue boxes: receptor ligands; red font: transcription factors, green font: apoptosis related proteins; magenta font: growth factors. Phosphorylated proteins are marked with a red circle.

been described for p73, but rather suggests more sophisticated mechanisms of action of p73 in multiple levels of gene regulation. This review summarizes the roles of p73 isoforms in physiological and oncogenic processes and describes how its ability to control development and/or differentiation can be hijacked during cancer progression and within the tumor microenvironment (TME). It further sheds light on the mechanistical patterns governing its disparate functions by using the melanoma setting as a paradigm and suggests that a sophisticated and highly coordinated interplay between the p73 C-terminus, the protein interactome, target gene promoter architecture (Rudge et al., 2016) and the subcellular localization of TP73-derived isoforms can support this multifunctionality.

THE EXPANDING FUNCTIONAL REPERTOIRE OF TP73 IN CANCER AND BEYOND

Besides their well-demonstrated roles in DDR and apoptosis (Wilhelm et al., 2010), p73 isoforms also have unique targets (Logotheti et al., 2019; Wang et al., 2020) and exert non-oncogenic functions (Inoue et al., 2014) that are not shared with p53. Understanding their functional pleiotropy has been enabled through the use of DNp73 splice isoform-specific antisense oligonucleotide gapmers (Emmrich et al., 2009) and by knockout mice models with (i) deletion of the entire TP73 gene, (ii) deletion of exons encoding the TAp73 isoforms, (iii) deletion of exons encoding the ΔNp73 isoform, and (iv) deletions of exons encoding the C-terminus of the alpha isoform. These tools in combination with expression and molecular studies, have allowed to uncover the roles of TP73 in cancer and beyond, such as neurodevelopment, ciliogenesis, and metabolism (Melino, 2020). In this chapter, we summarize the non-oncogenic as well as the cancer-related functions of p73 isoforms. We also report that p73 has newly identified roles in regulating the neurogenic potential of tumors by co-opting, in a cancer cell context, its neurodevelopmental/neurodifferentiation programs (Logotheti et al., 2020b).

Roles in Development, Differentiation and Tissue Homeostasis

The generation of the first p73 KO mice unambiguously showed that deletion of all p73 isoforms creates a wide range of neurological, pheromonal and inflammatory defects (Yang et al., 2000). A recurring and predominant phenotypic outcome upon ablation of either global (pan-TP73KO) or isoform class-specific (TAp73 or ΔNp73 KO) knockdown of TP73 products is manifestation of several neurodevelopmental abnormalities. In particular, pan-TP73KO mice display severe hydrocephalus and hippocampal dysgenesis characterized by partial or total loss of the lower blade of the dentate gyrus (DG) and by an impaired organization of CA1 and CA3 regions. TAp73KO mice show a less severe phenotype, but still exert abnormal hippocampal development, whereas ΔNp73 mice demonstrate only marginal reduction of cortical thickness but no hydrocephalus (Nemajerova et al., 2018). In general, TAp73 is required for neuronal differentiation and maintenance of neural stem cells (NSCs), while ΔNp73 is needed for neuronal survival during development and in adult neuronal tissues (Killick et al., 2011). In addition, p73 is essential for maintaining the neurogenic pool in the subventricular (SVZ) and subgranular zone (SGZ) through promoting self-renewal and proliferation, and inhibiting premature senescence of NSCs and/or neural precursor cells (NPCs). Mechanistically, TAp73 either directly or indirectly regulates the expression of genes involved in NSCs maintenance (Sox2, Sox3, TRIM32, and Hey-2), in axonal growth and dendritic arborisation (neurotrophin receptor p75), and in neuronal terminal differentiation (synaptotagmin-1 and syntaxin-1A). The recently described $Trp73^{d13/d13}$ mice, lacking exon 13 in the p73 gene, have revealed a significant contribution of the C-terminus to the brain development. Deletion of exon 13 produces a switch of the longest and most expressed isoform α into β, which in contrast to α lacks the SAM domain. Replacement of α with β substantially affects brain development, producing hippocampal dysgenesis, in particular, progressive depauperation of Cajal-Retzius (CR) cells in the developing brain. Hippocampal dysgenesis appears to be a consequence of deprivation of CR cells that are physiologically deputed to direct brain architecture during embryonic development. These effects appear to be highly isoform-dependent (Killick et al., 2011). Hence, not only the N-terminus of p73 isoforms, but also in their carboxy-terminal sequences have divergent effects on neuronal differentiation, maintenance of NSCs, neuronal survival during development and in adult neuronal tissues (Killick et al., 2011). Overall, p73 is nodal in the regulation of CNS development and function, by modulating NSC self-renewal and differentiation and by promoting terminal neuronal differentiation (Niklison-Chirou et al., 2020). The fact that these phenotypes are non-overlapping with the neurodevelopmental defects caused by the deletion of all p73 isoforms (p73 KO mice), the TAp73 isoforms (TAp73 KO) or the ΔNp73 (ΔNp73 KO mice), indicates indispensable, yet distinct, roles of the N-terminal, core and C-terminal domains of p73 in the regulation of neuronal processes.

In addition to their prevalent role in the central and peripheral nervous system, p73 isoforms have tissue-specific roles in the male and female reproductive organs, the development of respiratory epithelium and the vascular network. A recently discovered function of p73 manifested across several tissues is the differentiation and fate specification of multiciliated cells (MCC), which are vital for respiration, neurogenesis and fertility. Moreover, TAp73 shows a significant ability to regulate cellular metabolism. The abovementioned physiological functions of p73 in these organ systems have been extensively reviewed elsewhere (Nemajerova et al., 2018; Nemajerova and Moll, 2019; Maeso-Alonso et al., 2021). Besides these roles, p73 isoforms are essential for the proper function of the immune system. On one hand, TAp73 is required for macrophage-mediated innate immunity and the resolution of inflammatory response. TAp73 KO alters macrophage polarization such that maintenance of the M1 effector phenotype is prolonged at the expense of the M2 phenotype, thus impairing resolution of

the inflammation (Tomasini et al., 2013). On the other hand, regarding adaptive immunity, Ren et al. (2020) recently identified p73 as a negative regulator of the Th1 immune response via transrepression of IFN gamma transcription and downregulation of IFN gamma production.

Last but not least, several lines of evidence imply a key role of TP73 protein products in the differentiation and homeostasis in several types of muscle tissues. In skeletal muscles, TAp73α but not TAp73β isoform suppresses myogenic differentiation (Li et al., 2005), while ΔNp73α protect differentiated myotubes from DNA damage-induced apoptosis and inhibits the spontaneous apoptosis of satellite skeletal muscle cells that fail to complete their differentiation. Upregulation of the p73 P2 promoter during myogenic differentiation is mediated by a coordinated recruitment and activity of p53/p73 and the master-regulator of muscle cell development, MyoD (Belloni et al., 2006). In smooth muscles, p73 induces apoptosis of vascular smooth muscle cells and is present at high levels in human atherosclerotic plaque (Weiss and Howard, 2001; Davis et al., 2003). In the cardiac tissue, low expression of TP73 products has been observed in cardiomyocytes and other cell types of the heart muscle (data mined from Human Protein Atlas), while others have shown that the directed expression of DNp73 stimulates proliferation of cardiomyocytes via antagonizing p53 (Ebelt et al., 2008). Basal p53 levels are essential for embryonic cardiac development and for maintaining normal heart architecture and physiological function (Men et al., 2021), but it has not been investigated whether p73 isoform(s) participate in these processes. Based on these hints, it would be interesting to explore a so far unnoticed physiological role for p73 isoforms in cardiac development and physiology, a possibility that would further pave new avenues in treatment of cardiovascular diseases and/or cardiac tissue regeneration. The functional diversity of p73 isoforms in embryonic development, differentiation, and tissue homeostasis is depicted in **Figure 1B**. It has been proposed that a common unifying theme among several seemingly divergent p73-regulated physiological functions is that p73 acts as a master-regulator of tissue architecture, and that such a role might have been inherited from a single p53/p63/p73-hybrid gene ancestor at the dawn of epithelial tissue evolution, which is traced back to Placozoans and Cnidaria (Maeso-Alonso et al., 2021).

p73 Involvement in Cancer Hallmarks and Oncogenic Signaling Cascades

Oncogenic transformation occurs through progressive acquisition of key adaptations, the so-called cancer hallmarks, which include sustaining proliferative signaling, resisting cell death, evading growth suppressors, activating invasion, enabling replicative immortality, inducing angiogenesis, reprogramming energy metabolism and evading immune destruction. Transformation is further facilitated by tumor-promoting inflammation and genome instability. Strikingly, TAp73 isoforms inhibit all these hallmarks [reviewed in detail in Logotheti et al. (2013)] and can also enhance responsiveness to standard radio- and chemotherapies (Logotheti et al., 2013) (**Figure 1B**). Their DNp73 counterparts can typically antagonize these functions, thereby drastically influencing cancer promotion, progression and metastasis [reviewed in Logotheti et al. (2013), Engelmann and Pützer (2014), and Engelmann et al. (2015)]. Recently, it was shown that TAp73 regulates macrophage accumulation and tumor infiltration, which is in general a strong driver of cancer progression and predictor of poor outcomes in cancer patients. This occurs via inhibition of the NF-κB pathway, since loss of TAp73 leads to NF-κB hyperactivation and secretion of Ccl2, a known NF-κB target and chemoattractant for monocytes and macrophages. Importantly, TAp73-deficient tumors display an increased accumulation of protumoral macrophages that express the mannose receptor (CD206) and scavenger receptor A (CD204) (Wolfsberger et al., 2021).

It is noteworthy that in some cancer-related processes and cell-contents, TAp73 isoforms show an effect inconsistent with their traditional tumor suppressive function. For example, TAp73 activates anabolic pathways compatible with proliferation and cancer promotion by regulating glucose metabolism to control cellular biosynthetic pathways and antioxidant capacity [reviewed in Nemajerova et al. (2018)]. TAp73 modifies the metabolism and positively regulates growth of cancer stem-like cells in a redox-sensitive manner (Sharif et al., 2019a). Nevertheless, it remains still unclear whether this metabolic effect reflects cancer-associated metabolic changes, or instead a role in promoting adaptative cellular mechanisms to stress conditions [reviewed in Nemajerova et al. (2018) and Maeso-Alonso et al. (2021) and]. Furthermore, p73 proteins regulate angiogenesis, with the ΔNp73 form that has a clear role in promoting this phenomenon, whereas TAp73 isoforms exert both, positive and negative effects, depending on parameters like the strength and spatiotemporal context of its activation (Sabapathy, 2015). It is also not clear if every TAp73 isoform can exhibit such Janus behavior in metastasis-promoting processes, or if this is an attribute of only specific TAp73 C-terminus splice variants.

Using our previous work on melanoma as a representative example of p73's regulation of cancer outcomes via orchestrating molecular networks, we further made the striking observation that TAp73/DNp73-controlled pathways can co-ordinate extracellular changes in the TME and intracellular gene regulation by intercepting with major cellular signaling cascades which respond to growth factors in the TME. These intersections suggest that p73 isoforms internalize the information from extracellular signals that are received by cell surface receptors and convey them to the nucleus, leading to global changes in p73-transcriptome. In particular, we used the melanoma paradigm and constructed a comprehensive regulatory map by exploiting own high-throughput and experimental data from melanoma tissue culture, mouse metastasis models and patient tumor samples. These results were integrated with data from the literature, previous mathematical models describing sections of the map (Vera et al., 2013; Khan et al., 2014), and partial elements of existing IGF1R computational models (Borisov et al., 2009; Bianconi et al., 2012). The reconstructed network demonstrates that TAp73/DNp73-dependent pathways (Alla et al., 2010, 2012) intercept with

cellular receptor-triggered signaling cascades that are relevant for melanoma progression, such as EGFR (Sun et al., 2014; Wang et al., 2015), IGFR (Rosenbluth et al., 2008), and HER3 (Iorio et al., 2009; Tiwary et al., 2014) and portray the potential of p73 isoforms to sense changes in the cell microenvironment and modify the gene regulation programs accordingly (**Figure 1C**).

Regulation of Cancer Neurobiology – p73 and the Emerging Hallmark of Neoneurogenesis

Of particular interest is that neurodevelopmental defects and cancer-related phenotypes co-exist in TAp73 knockout and, to a much lesser extent, in ΔNp73 KO mice. The ability of p73 isoforms to modulate tumor initiation and progression may be relevant to their neurological functions. In particular, it is becoming increasingly evident that cancer and neuronal cells develop reciprocal interactions via mutual production and secretion of neuronal growth factors, neurothrophins and/or axon guidance molecules in the TME. Intriguingly, tumors can stimulate their own innervation during cancer progression, and this phenomenon is termed neoneurogenesis. Tumors produce and excrete neurogenic factors that modulate the TME and induce formation of new nerves that eventually infiltrate tumors (Logotheti et al., 2020b). Recently, Mauffrey et al. (2019) showed that prostate tumors summon neural progenitors from sites as distant as the subventricular zone of the central nervous system (CNS), which break the blood-brain barrier, infiltrate prostate tumors and initiate neurogenesis. This process is essentially distinct from perineural invasion (PNI), which refers to tumor invading into already existing nerves along the perineural space. Besides, cancer cells themselves may acquire brain-like properties as an adaptation for brain colonization (Neman et al., 2014). The nervous system-cancer crosstalk emerges as a crucial regulator of cancer initiation and progression, both systemically and within the local TME. In turn, cancers and cancer therapies can alter nervous system form and function Tumors may induce profound nervous system remodeling and dysfunction by secreting circulating factors which not only locally alter neural activity in the TME, but also have a remote and systemic effect on important brain functions, such as sleep. The interactions between neural and malignant cells are highly relevant for cancer clinical therapy, since they are suspected to be involved, at least in part, in neuronal toxicities induced by radiation and chemotherapies (Monje et al., 2020). The mechanisms that support this enigmatic crosstalk between tumors and the nervous system remain largely unexplored. We have recently provided mechanistic insights that the neurogenic potential of tumors appears to be induced, at least in part, by co-option of neuronal processes within cancer cells. Genes involved in neuronal development and function are reactivated in various tumor types and predict poor patient outcomes. The ectopic activation of neuronal programs in cancer cells and the switch to neurogenic phenotypes does not appear to be a stochastic, random event, but rather provides selective advantages to tumor cells (Logotheti et al., 2020b). Moreover, deregulation of genes that are indispensable for nervous system development and neurological function are associated with long-term survival in adult AML [Yılmaz et al., 2021), accepted for publication]. In this regard, neoneurogenesis might constitute a novel cancer hallmark, comparable to angio- and lymphangiogenesis.

It is possible that the ability of p73 isoforms to regulate several cancer hallmarks may not be independent from their neurological and/or immunomodulatory functions, but instead might imply co-options of relevant p73-governed pathways in a cancer cell context. Looking at the processes regulated by p73 isoforms in normal and cancerous tissues more closely, analogies can be found between some physiological processes and cancer hallmarks. It is well-accepted that ΔNp73 overexpression becomes a positive advantage for tumor progression due to co-option of its pro-angiogenic capacity in tumors that trigger neoangiogenesis (Nemajerova and Moll, 2019). In an analogous manner, it is reasonable to assume that recapitulation of the same p73-regulated neurodevelopmental/neurodifferentiation pathways in cancer cells could promote tumor progression, for example by inducing neoneurogenesis or by altering interactions of cancer cells with neuronal and immune cells (**Figure 1B**). Several p73 isoforms may positively or even negatively regulate cancer invasion and metastasis through activating their nervous system-related target genes within the cancer cell context. In support of this rationale, TAp73 isoforms control cancer cell proliferation, migration and invasion through transactivation of the brain-enriched miRNA gene MIR3158, which targets vimentin (Galtsidis et al., 2017). Similarly, ΔTAp73 (p73ΔEx2/3 α and β) expression in less-invasive melanoma cells enhances stemness and self-renewal capacity through an interplay with MIR885 (Meier et al., 2016), a miRNA with brain/cerebellum-restricted expression [data mined from miRiad database (Hinske et al., 2014)], that targets IGFR (Meier et al., 2016). Again in an IGFR-dependent manner, p73ΔEx2/3 drives EMT phenotypic conversion and initiation of metastasis in melanoma (Steder et al., 2013), along with tyrosinase degradation, depigmentation and loss of melanocyte identity (Fürst et al., 2019). In the presence of p73ΔEx2/3 and persistently high TAp73α levels, melanoma cells lose their original cell-type characteristics, and simultaneously activate stemness (Meier et al., 2016), EMT (Steder et al., 2013), and nervous system-related genes. Upregulation of stemness markers in aggressive melanoma states is accompanied by increased expression of key neurotrophic factors, including BDNF, which was recently shown to foster neoneurogenesis (Logotheti et al., 2020b).

In view of these data, our results suggest that p73 isoforms co-regulate stemness and neurodifferentiation to control tumor progression. The tumor-specific p73ΔEx2/3 isoforms, which are established metastasis inducers and CSC regulators, have the ability to activate key neurodifferentiation players. Increased cancer stemness, together with the loss of original cell identity (de-differentiation), and the acquisition of characteristics of neuronal cell types upon p73 isoform expression, are overall indicative for their ability to switch from a melanocyte to a neuronal-like cell phenotype which would be theoretically able to foster a newly-emerged

dangerous liaison between melanomas and the nervous system (Su et al., 2014; Lu et al., 2017; Logotheti et al., 2020b; Pomeranz Krummel et al., 2021).

DISSECTING THE FUNCTIONAL PLEIOTROPY OF TP73

In light of the overwhelming functional diversity of the products of TP73, it is reasonable to assume that the typical mode of direct transactivation/transrepression that has been described for TAp73 and DNp73's, on its own, is not sufficient to support such high level of functional pleiotropy across several organ systems. Besides the TA/DN ratio, isoforms synthesized by other members of the p53 family, like p53 and p63, also influence p73 activity (Li and Prives, 2007; Nemajerova et al., 2018). However, even distinct p53/p63 backgrounds, wildtype or mutant, cannot explain the plethora of p73 effects in different cellular contexts. The divergent and tissue-specific roles of p73 imply a high degree of complexity and sophistication in relation to its modes of function. Several lines of evidence instead argue for a possible existence of p73 traits complementary to its canonical function as a transcription factor. First of all, global genomic binding studies (Rosenbluth et al., 2008; Koeppel et al., 2011) indicate that only a disproportionally small fraction of p73-responsive genes directly binds p73 to induce p73-mediated functional changes. Second, the ΔNp73 isoforms bear a unique 13-amino acid motif in their N-terminus that possesses transactivation potential (Liu et al., 2004), questioning the dogma that ΔNp73's are transcriptionally inactive at all times. Third, there is a certain degree of controversy, whereby in some cellular contexts, TAp73 isoforms might regulate anti-apoptotic and pro-survival genes (Wang et al., 2020) and ΔNp73 isoforms can activate apoptotic targets (Liu et al., 2004; Toh et al., 2008), a fact that pinpoints toward the cell milieu as a significant determinant of the functional outcome of p73 isoforms. This functional controversy is particularly evident in the context of neoangiogenesis, in which TAp73 manifests a context-dependent dual role, suggesting that other modifiers in the cell milieu co-determine and thus impart its ultimate effect on the process (Sabapathy, 2015). Fourth, TAp73alpha shows a preference for genes with a distinct promoter architecture compared to the ones that specifically respond to TAp73beta, a finding that implies a C-terminus-based selectivity of TAp73 isoforms for target genes (Koeppel et al., 2011). These evidences overall suggest that p73-governed gene regulatory programs may be further orchestrated by indirect mechanisms that extend beyond their canonical role as transcriptional regulators, which compete for occupying gene promoters (Marabese et al., 2007).

In this section we provide compelling evidence to support that p73-regulated functions are a result of a sophisticated combination of at least three parameters: (a) the type of p73 isoforms, (b) the presence of p73 interacting partners in the cellular milieu, and (c) the intrinsic properties of promoters of the target genes. Tissues are characterized by distinct proteomes, hence the expression of the same p73 isoform in one tissue content could lead to functional diversification, since this isoform is able to form protein–protein interactions (PPIs) with a particular set of factors that is contained in one tissue but not in another. In addition, the C-terminus of p73 determines whether PPI occurs, because even if the interactor is present in the cell, the expressed p73 splice variant may not interact with it. Furthermore, p73 isoforms form protein complexes with several other key transcriptional regulators on target gene promoters to fine-tune their transcriptional regulation. Besides, some p73 isoforms appear to have non-transcriptional functions by interacting with proteins other than transcriptional regulators outside the nucleus (Tomasini et al., 2009; Vernole et al., 2009), suggesting that the subcellular localization of p73 isoforms can be an additional co-determinant of the p73 functional repertoire.

The Characteristics of the p73 Protein Interactome

The p73 protein interactome is a decisive parameter of the tissue- and/or cell context-specific p73 activity. Several proteins have been described to physically associate with p73 isoforms, by recognizing the TA domain, the DBD domain, the OD or the C-terminus. These interactions usually take place in the nucleus and regulate the transactivation activity of p73 either positively or negatively. However, in some cases the interactions occur in the cytoplasm (**Table 1**). Another feature of the p73 interactome is that complex feedback loops can be generated among p73 and their binding partners. For example, PIR2 is a direct p73 target gene, and its protein product associates with DNp73 and promotes its proteosomal degradation (Sayan et al., 2010). Sp1 activates transcription from the P1 promoter of TP73 but also has the potential to form Sp1–TAp73 complexes, which can modulate Sp1 binding to corresponding elements on target gene promoters (Logotheti et al., 2010). Another candidate is the p73 transcriptional target NGFR (Logotheti et al., 2020b; Niklison-Chirou et al., 2020) that directly binds p73 isoforms at the DBD to facilitate their proteosomal degradation via chaperone-mediated autophagy (Nguyen et al., 2020).

Several p73 protein binding partners induce post-translational modification, proteolytic degradation, phosphorylation-dependent activation or inhibition, acetylation or gene target co-regulation, often in a p73 C-terminus-dependent manner (Logotheti et al., 2013). Other proteins bind to p73 isoforms and retain them in the cytoplasm, thereby interfering with p73-mediated transcription of its target genes. Moreover, p73 isoforms can interact with non-transcriptional regulators in the nucleus, intimating that they are also involved in processes beyond gene transactivation. For example, TAp73 regulate the spindle assembly checkpoint (SAC) during mitosis and meiosis via physical interaction with components of the SAC complex, such as Bub1, Bub3 and BubR1, the inhibitor of anaphase-promoting complex protein Cdc20, regulating their proper localization (Tomasini et al., 2009). TAp73alpha interacts with the kinetochore-related proteins Bub1 and Bub3, which leads to the alteration of mitotic checkpoint abilities and induction of polyploidy. This association is specific for TAp73alpha but not p53 or any of the other p73 forms (Vernole et al., 2009). Using computational approaches, a previous study predicted that some p73s can interact with DGCR8 (Boominathan, 2010), a nucleus-localized, highly conserved component of the miRNA

TABLE 1 | Interacting partners of p73 isoforms and their outcome on p73 function.

Protein interactor	P73 domain that mediates the PPI	Site of interaction	Outcome	References
MDM2	TA	Nuclear	Blocks p73 transcriptional activity by competing with p300/CBP binding without inducing proteolytic degradation	Bálint et al., 1999; Zeng et al., 1999
Pin1	C-terminus	Nuclear	Stabilizes p73, promotes conformational change of p73 and enhances its proapoptotic activity	Ozaki et al., 2010; Logotheti et al., 2013
YAP1	C-terminus (PPPPY)	Nuclear	p73-coactivator, potentiates p300-mediated acetylation of p73 and promotes stabilization by displacing Itch binding to p73	Ozaki et al., 2010; Logotheti et al., 2013
Itch	C-terminus (PPPPY)	Nuclear	Ubiquitination of p73 and subsequently promoting its proteasome-dependent degradation	Ozaki et al., 2010; Logotheti et al., 2013
FBXO45	C-terminus (SAM)	n.d.	Promotes the proteasome-dependent degradation of p73	Ozaki et al., 2010; Logotheti et al., 2013
PIASγ	C-terminus (OD)	Nuclear	Stabilizes p73 but together with SUMO-1 decreases functional activation of p73 by sumoylation	Ozaki et al., 2010; Logotheti et al., 2013
c-Abl	C-terminus (3K)	Nucleus	c-Abl-mediated phosphorylation of p73 induces p300-mediated acetylation, enhances interaction between Pin1 and p73 and therefore increases its stability and transcriptional as well as proapoptotic activity	Ozaki et al., 2010; Logotheti et al., 2013
NEDL2	C-terminus (PPPPY)	Cytoplasm	Promotes polyubiquitination of p73, stabilizes and enhances its transcriptional activity	Ozaki et al., 2010; Logotheti et al., 2013
JNK	n.d.	Nucleus	JNK-mediated phosphorylation of p73 promotes its stabilization, p300-mediated acetylation and transcriptional activity	Ozaki et al., 2010; Logotheti et al., 2013
IKK	DBD	Nucleus	Stabilizes p73 by inhibiting its polyubiquitination, enhances transcriptional activation and proapoptotic activity of p73	Ozaki et al., 2010
CDK complex	DBD, C-terminus (SAM)	Nucleus	Inhibits transcriptional activity of p73 by phosphorylation of Thr86	Gaiddon et al., 2003; Ozaki et al., 2010
PKA-Cβ(PRKACB)	N- and C-terminus	n.d.	Inhibits transcriptional and apoptotic activity of p73 by phosphorylation	Ozaki et al., 2010
HCK	N-terminus	Cytoplasm	Stabilizes cytoplasmic p73, inhibits transcriptional and apoptotic activity of p73	Ozaki et al., 2010
PLK1/PLK3	TA	Nucleus	Inhibits p73 transcriptional and apoptotic activity	Ozaki et al., 2010
p300	TA	Nucleus	Stabilizes p73 by acetylation at Lys321, Lys327, and Lys331, enhances p73 transcriptional and apoptotic activity	Ozaki et al., 2010; Logotheti et al., 2013
SIRT1	n.d.	n.d.	Inhibits transcriptional and apoptotic activity of p73	Ozaki et al., 2010
HIPK2	OD	Nucleus	Enhances the transcriptional activity of p73	Ozaki et al., 2010
amphiphysin IIb-1	C-terminus (3K)	Cytoplasm	Relocalizes p73 to the cytoplasm, inhibits transcriptional and apoptotic activity of p73	Kim et al., 2001; Ozaki et al., 2010
Wwox	C-terminus (PPPPY)	Cytoplasm	Tumor-suppressor; relocalizes p73 to the cytoplasm, inhibits the transcriptional activity of p73, p73 increases proapoptotic activity of Wwox	Ozaki et al., 2010; Logotheti et al., 2013
ASPP1/ASPP2	DBD	Nucleus	Selectively enhances proapoptotic function of p73	Ozaki et al., 2010
p19ras(HRAS)	DBD	Nucleus	Blocks MDM2-mediated transcriptional repression of p73 and led to the activation of p73	Ozaki et al., 2010
MM1	Extreme C-terminus	Nucleus	Selectively enhances transcriptional and growth-suppressing activity of p73	Ozaki et al., 2010; Logotheti et al., 2013
RanBPM	Extreme C-terminus	Nucleus	Stabilizes p73 by inhibiting its ubiquitination; enhances its transcriptional and proapoptotic activity	Ozaki et al., 2010; Logotheti et al., 2013
WT1	n.d.	Nucleus	Tumor-suppressor; inhibits transcriptional activity of p73	Ozaki et al., 2010
HCV core protein	Extreme C-terminus	Nucleus	Selectively inhibits the transacriptional and proapoptotic activity of p73	Ozaki et al., 2010
E4orf6	OD	n.d.	Inhibits transcriptional and proapoptotic activity of p73	Ozaki et al., 2010
CTF2(CTF/NF-1)	DBD	Nucleus	Inhibits the sequence-specific DNA-binding activity of p73	Ozaki et al., 2010
BAG-1	n.d.	n.d.	Decreases expression of p73 and inhibits its transcriptional activity	Ozaki et al., 2010
TIP60	n.d.	Nucleus	Enhances MDM2 binding affinity to p73 and therefore inhibits its transcriptional and proapoptotic activity	Ozaki et al., 2010
PKP1	C-terminus (SAM)	Cytoplasm	n.d.	Neira et al., 2021
ETS2	C-terminus (SAM)	Nucleus	Forms a complex with DNp73, which directly activates ANGPT1 (angiogenesis and promoting tumor growth) and Tie2 (cell survival and proliferation) gene expression in tumor cells	Cam et al., 2020
NGFR	DBD	Cytoplasm	Inactivates p73 transcriptional activity by promoting its degradation	Nguyen et al., 2020
DGCR8	C-terminus (PPPPY)	Nucleus	Is predicted to interact with p73 and thereby influencing miRNA processing	Boominathan, 2010

(Continued)

TABLE 1 | (Continued)

Protein interactor	P73 domain that mediates the PPI	Site of interaction	Outcome	References
GemC1	n.d.	Nucleus	Recruits p73 to E2F5 to selectively transactivate genes involved in multiciliogenesis as well as p73 itself	Lalioti et al., 2019
Sp1	n.d.	Nucleus	Prevents Sp1 binding to target promoter and subsequently its transcriptional activity	Koutsodontis et al., 2005; Racek et al., 2005
MCL1	OD	Nucleus	Inhibits p73 DNA binding and therefore inhibits its transcriptional activity	Widden et al., 2020
PIR2	n.d.	n.d.	Modulates p73 stability, alters TA/DNp73 ratio by promoting preferential degradation of DNp73	Sayan et al., 2010
Bub1	C-terminus (SAM)	Nucleus	TAp73 regulates SAC protein localization and activities, deregulation of p73 can alter mitotic checkpoint abilities and induce polyploidy	Tomasini et al., 2009; Vernole et al., 2009
Bub3	C-terminus (SAM)	Nucleus	Deregulation of p73 can alter mitotic checkpoint abilities and induce polyploidy	Vernole et al., 2009
BubR1	C-terminus	Nucleus	TAp73 but not DNp73 potentiates BubR1 activity, regulates SAC protein localization and activities	Tomasini et al., 2009
HIF-1α	n.d.	n.d.	p73 affects HIF-1α protein stability and subsequently ubiquitin-dependent proteasomal degradation in an oxygen-independent manner	Amelio et al., 2015
FLASH	C-terminus	n.d.	Regulation of histone gene transcription	De Cola et al., 2012
Cul4A-DDB1	n.d.	Nucleus	Inhibits transcriptional activity of p73	Malatesta et al., 2013
SUMO-1	Extreme C-terminus	Nucleus	Enhances proteosomal degradation of TAp73α	Logotheti et al., 2013
RACK1	Extreme C-terminus	Nucleus	Downregulation of apoptotic targets and inhibition of TAp73α-mediated apoptosis	Logotheti et al., 2013
PTEN	C-terminus (SAM)	Nucleus	Enhances the transcriptional activation of apoptotic genes	Logotheti et al., 2013
UFD2A	C-terminus (SAM)	Nucleus	Ubiquitination of p73 and subsequently promoting its proteasome-dependent degradation	Logotheti et al., 2013

n.d., not determined.

processing machinery which binds pri-miRNA to stabilize it for processing by Yeom et al. (2006). Importantly, DGCR8 is a miRNA-processing protein that is indispensable for miRNA maturation, and its ablation leads to early developmental arrest due to the lack of maturation of pre-miRNA products (Wang et al., 2007). It is therefore possible that p73alpha and p73beta isoforms may crosstalk with the miRNA processing machinery to control the quality and quantity of mature miRNA populations by physically associating with DGCR8. Considering that p73 isoforms can exhibit cytoplasmic localization (Dobbelstein et al., 2005; Nekulová et al., 2010), this raises the possibility of additional functions beyond transcription, in subcellular organelles outside the nucleus. In agreement with this notion, the results of our coIP-MS analyses in Saos-2 cells in which distinct p73 isoforms were exogenously added demonstrated that p73 variants have the ability to bind to proteins in the ER, Golgi apparatus, mitochondria, and endosome. Of particular interest, p73alpha and p73beta can bind to proteins associated with the ruffle membrane, plasma membrane and extracellular region (**Figure 2A**).

The C-Terminus as the Basis for Protein–Protein Interaction Selectivity

While the N-terminus of TP73 has provided a first rule of thumb for the functional characterization and classification of the many gene products based on the presence of TA and the corresponding ability to activate transcription of gene targets, the C-terminus inevitably represents the most variable region of the TP73 gene. A total of eight alternative splicing events in the 3′ end and one alternative termination event in a portion of exon 13 generate 10 different versions of the C-terminus. These carboxy-terminal tails are combined with a main core domain that exerts DNA binding and oligomerization ability, and an N-terminus with or without canonical transactivation activity, giving rise to more than twenty gene products (Logotheti et al., 2013). The significance of the C-terminus for p73-mediated functions is underscored by the recently described $Trp73^{d13/d13}$ mice, in which a switch from the α to β form through knockout of exon 13 results in distinct phenotypic abnormalities that do not overlap with those of other p73 knockout mice (Niklison-Chirou et al., 2020). The C-terminus is a highly active region, both in terms of binding to proteins and DNA. First of all, it carries an electrostatic charge that differs significantly between p73 variants and affects promoter binding and gene transactivation. More importantly, it is particularly enriched in unique motifs and crucial amino acid residues that serve as protein-interacting surfaces. Because of the numerous alternative splicing events in the 3′ end, each C-terminal variant bears its own combination of these motifs. The versatility of the C-terminus can be particularly associated with the many different biological activities of p73 isoforms, as each isoform carries its own unique combinations of functional domains and motifs that are recognized by distinct groups of protein interactors. Overall, the C-terminus may act as a platform for the selection of p73 PPIs that can play a decisive role in both the nature of target genes and the degree of activation, possibly via differential interactions with regulatory proteins.

The functional domains and residues of the C-terminus have been highlighted previously and are shown, along with their corresponding protein interactors in **Figure 2B**. First, the

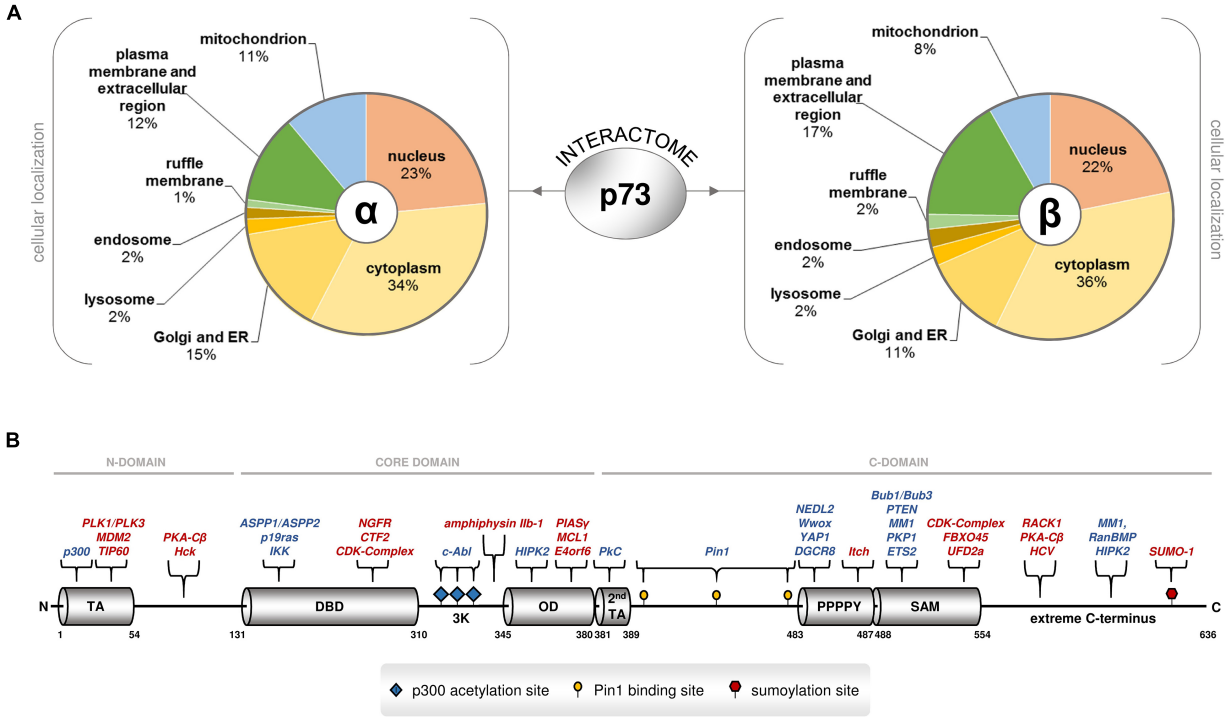

FIGURE 2 | Several proteins physically associate with p73 isoforms inside and outside the nucleus. **(A)** Analysis of the cellular localization of the p73alpha and beta interactome based on high-throughput coIP-MS screening in Saos-2 cells overexpressing TAp73alpha, ΔTAp73alpha, TAp73beta, or ΔTAp73beta. Protein annotation and subcellular distribution was retrieved from UniProt and DAVID GO. **(B)** The TP73 gene encodes a variety of functional motifs and crucial amino acid residues in the N-terminus, the core domain, and the C-terminus that serve as selective interacting surfaces for the p73 proteome. The C-terminus is particularly enriched in such protein-binding sites. Each p73 isoform contains unique combinations of these protein-binding sites. Annotations: TA transactivation domain, DBD DNA binding domain, OD oligomerization domain, 3K p300 acetylation sites, 2nd TA second transactivation domain, SAM sterile alpha motif, extreme: extreme carboxy terminus. The literature-curated protein interactors that recognize the corresponding motifs and residues are also depicted. The proteins with inhibitory effect on p73 stability or activity are highlighted in red.

carboxy-terminal region 380–513 is spanned by Glu/Pro-rich and Pro-rich regions that exhibit transactivation activity. In particular, it entails a glutamine/proline-rich domain within amino residues 381–399 that is phosphorylated by PKCα2 and PKCβ in Ser388, and regulates genes involved in cell cycle progression; three crucial pS/pT-P motifs at residues 412, 442 and 482, which are specifically recognized by the propyl isomerase Pin1, a chaperone that catalyzes the isomerization of peptidyl-propyl bond from *cis*- to *trans*-conformation and regulates transactivation efficiency, stability and subcellular localization; and a highly conserved PPPPY motif in residues 483–491 that is specifically targeted by proteins bearing a WW domain, causing them to develop PPPPY-WW-mediated PPIs. The WW-containing interactors of p73 are (a) the yes-associated protein YAP, a phosphoprotein that interacts with a non-receptor Src tyrosine kinase encoded by the c-yes protooncogene, (b) NEDD4-like ubiquitin protein ligase 2 (NEDL2), (c) cytoplasmic tumor suppressor oxidoreductase (Wwox), and (d) E3 ubiquitin ligase Itch. YAP, NEDL2, and Wwox enhance the transcriptional activity of p73, while Itch is a YAP antagonist, that leads to p73 ubiquitination and degradation and impairs transcriptional activity (Logotheti et al., 2013). DGCR8 was also predicted *in silico* to possess a WW-domain, which may interact with the PPPPY motif of the C-terminal domains of p73α and p73β (Boominathan, 2010).

Additional interacting surfaces downstream of PPPPY render TAp73α susceptible to mediators of ubiquitin-proteasome degradation, as well as other effectors of p73 stability and activity. In detail, the SAM extends between residues 487–554 and is recognized by PTEN, an inducer, and by UFD2A and FBXO45, two attenuators of TAp73α transactivation efficacy. The SAM domain can also bind to the N terminus of MDM2 (Neira et al., 2019). Plakophilin 1 (PKP1), a component of desmosomes, which are key structural components for cell-cell adhesion, also recognizes the SAM domain (Neira et al., 2021). Moreover, residues 555–636, representing the extreme C-terminus of p73 alpha and comprising four conserved sequence motifs (Logotheti et al., 2013), are recognized by RanBPM, a cellular interactor of the nuclear-cytoplasmic transport protein Ran, which stabilizes TAp73alpha and enhances its transactivation activity, most likely by masking C-terminal lysine residues that could be the sites for ubiquitin ligation and/or disrupting the interaction of TAp73alpha with unknown proteins required for ubiquitin-mediated proteolysis. Another protein that physically interacts with TAp73alpha via the extreme C-terminus is MM1, a c-myc binding protein. Upon binding to p73, it

selectively enhances transcription of specific p73 target genes, thereby potentiating growth suppression. MM1 antagonizes the inhibitory effect of c-myc on the extreme C-terminal domain-containing TAp73alpha isoform by preventing the c-myc-p73alpha interaction and/or directly binding to c-myc to inhibit its activity. In addition, the receptor for activated C kinase RACK1 physically interacts through the extreme C-terminus, leading to the downregulation of apoptotic targets and inhibition of TAp73alpha-mediated apoptosis. Finally, small ubiquitin-like modifier 1 (SUMO-1), binds to TAp73alpha through a covalent modification of Lys627, making this isoform more susceptible to proteosomal degradation [reviewed in Logotheti et al. (2013)].

These motifs and residues appear to be important in "finalizing" the effects of the major p73 interactors by recruiting their essential co-factors. For example, it is well-established that TAp73alpha can bind to MDM2 via its OD, but unlike its p53 sibling, this interaction does not lead to protein degradation of p73 (Bálint et al., 1999; Zeng et al., 1999). Only in the presence of Itch, which recognizes PPPPY motifs, can p73 protein degradation finally occur (Bálint et al., 1999; Zeng et al., 1999; Rossi et al., 2005). In a similar manner, c-abl induces phosphorylation of p73 at the NH2-terminus, but additional p73 interactors selective for the C-terminus are needed to enable p73-mediated apoptosis. DNA damage activates c-Abl, which phosphorylates TAp73 directly at site Tyr99 and indirectly, via p38, at Pin1-binding sites 412, 442, and 482. Subsequently, Pin1 targets the phosphorylated residues and catalyzes the conformational change at TAp73. The c-abl phosphorylated YAP1 binds to the PPPPY motif and attracts p300, which in turn acetylates a 3K motif downstream of the OD domain. In this state, the complex selectively binds to transactivate apoptotic versus cell cycle arrest targets (Logotheti et al., 2013). Several of the abovementioned motifs and residues, together with their corresponding interactors, have been conserved within vertebrate clades where p73 has split from its p53/p63/p73-hybrid ancestor. The patterns of co-conservation of the C-terminal motifs and corresponding protein interactors suggest that the corresponding PPIs are required for p73 functions (Logotheti et al., 2013). It is therefore possible that the increase in the number of splice variants reflects the enhanced potential of p73 to evolve PPIs that can support its expanding functional repertoire.

The Promoter Architecture of Direct and Indirect p73 Target Genes

The p73 isoforms show complex patterns of interaction with target gene promoters in addition to their canonical mode of gene transactivation/transrepression (**Figure 3A**). C-terminal variant-specific transcriptional responses have been described previously for TAp73alpha and TAp73beta. The genes responding to TAp73alpha have different binding patterns and gene promoter architectures than TAp73beta-responsive ones. Gene promoters occupied by TAp73alpha are enriched in the AP1 motif, which can bind to Jun/Fos family heterodimers, and this is associated with more frequent upregulation of genes with AP1 motif in comparison to genes lacking this motif. In contrast, promoters occupied by TAp73beta do not exhibit this motif and do not show similar activations of AP1-responsive genes (Koeppel et al., 2011). TAp73 can physically interact with c-Jun of the AP-1 complex on target gene promoters via its carboxyl-terminal region (Subramanian et al., 2015). Taken together, these data underscore a p73 isoform-specific selectivity of target genes that is shaped not only by their intrinsic promoter characteristics but also by PPIs between p73forms and other "extrinsic" transcription factors on these promoters. Based on these findings, we postulate that the interplay of gene promoter architecture with p73 binding partners orchestrates the functional diversity of p73 family members. Target genes may bear typical p73-responsive elements (RE), but there are also cases of indirect p73 targets which lack them. Several p73 isoforms physically associate with other transcriptional regulators at target gene promoters and modify transactivation both in a direct p73-RE-dependent and an indirect p73RE-independent manner (Racek et al., 2005; Beitzinger et al., 2006; Buhlmann et al., 2008). First scenario, p73 isoforms interact with co-regulators at the promoters of p73-responsive genes (**Figure3B**), which induce post-translational modifications to p73 proteins and fine-tune target genes that are eventually transactivated. Such co-activator examples are YAP1 and Pin, which form complexes with TAp73 in response to DNA damage to favor transcription of p73-responsive pro-apoptotic genes (Logotheti et al., 2013). Second, p73 isoforms tether on transcription factors bound to promoters lacking a typical p73RE and modulate their transcriptional activity. For instance, TAp73 interacts with NF-Y bound on the PDGFRB promoter and turns off gene expression, whereas DNp73 interacts with SMAD3/4 bound to SMAD-responsive elements and potentiates activation of the PAI1 and COL1A1 genes (Engelmann et al., 2015) (**Figure 3C**). Similarly, ΔNp73 transcriptionally upregulates both ANGPT1 and Tie2 through conserved ETS-binding sites by interacting with ETS2, resulting in forced angiogenesis and survival of glioblastoma (Cam et al., 2020). Third, p73 isoforms act in a composite manner both by direct binding to p73REs and by physical interaction with transcription factors that bind to adjacent sites. An example is the cooperative activation of PUMA by TAp73beta and Sp1, both of which associate with neighboring responsive elements at the PUMA promoter and physically interact with each other (Ming et al., 2008) (**Figure 3D**).

Using the Promoter Architecture of p73-Responsive Genes as 'Footprint' for Predicting Novel, Functionally Relevant p73 Protein–Protein Interactions

To further explore the idea that the architecture of gene promoters related to p73 PPIs is important for the function of p73 isoforms, we used microarray transcriptomics data that we have produced previously (Steder et al., 2013). Ectopic stable expression of DNp73 in the low-invasive SK-Mel-29 cells causes whole-transcriptome changes and supports metastasis-initiating phenotypes, such as stemness, EMT and invasion, and de-differentiation (Steder et al., 2013; Meier et al., 2016; Fürst et al., 2019). If the hypothesis that the effect of DNp73 on these cancer cell phenotypes is achieved through

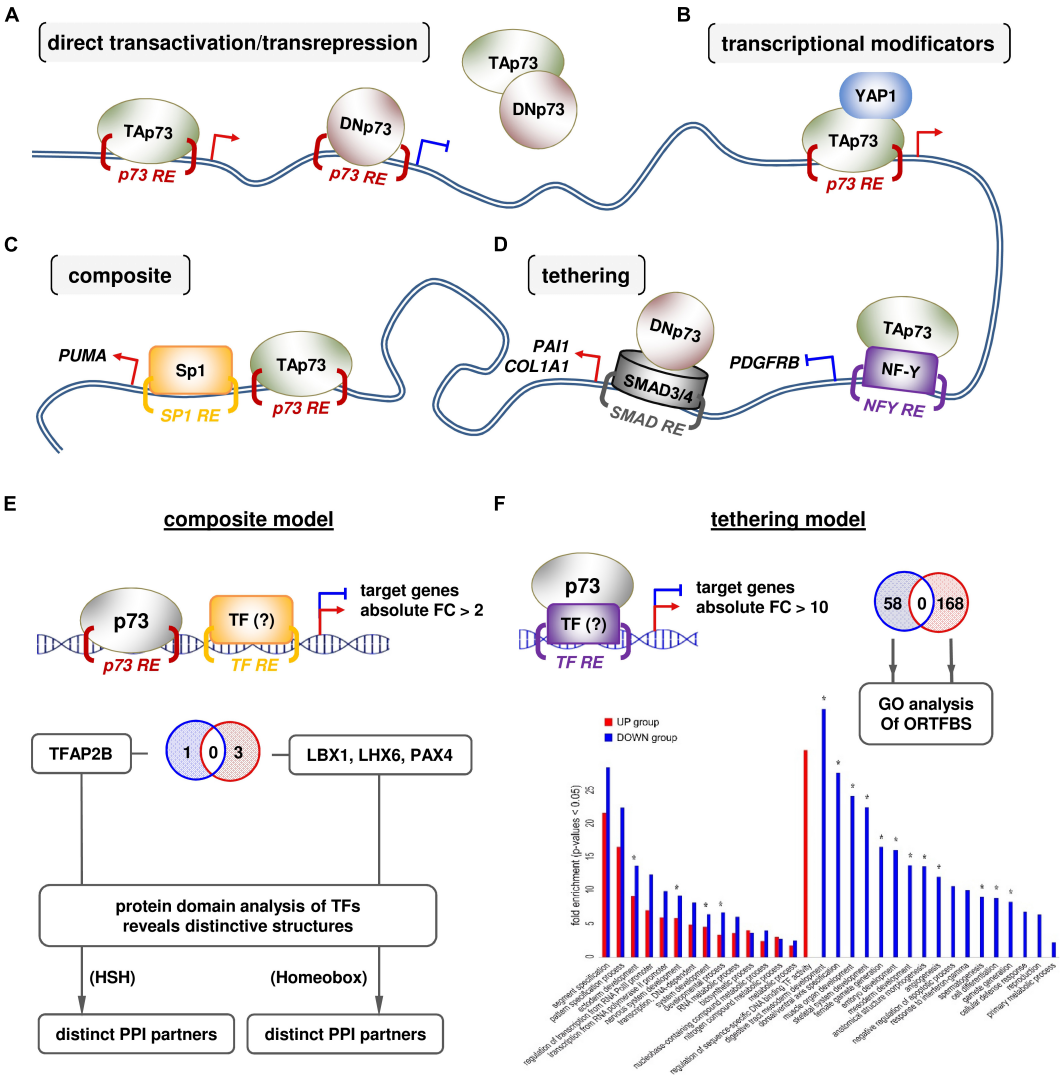

FIGURE 3 | An interplay of gene promoter architecture with p73 binding partners orchestrates the functional diversity of the p73 isoforms. **(A)** Typical transcription factor-based and **(B–D)** PPI-based modes of genomic action of p73 isoforms. **(E,F)** Computational prediction of p73 PPIs relative to the promoter architecture by meta-analysis of extrapolated p73 ChIP-seq and Mel.DNp73 microarray data (Koeppel et al., 2011; Steder et al., 2013). **(E)** *Composite scenario:* the overrepresentation (*Z*-score) of transcription factor binding sites (ORTFBS) in the DNp73-responsive gene groups (using Pscan software): (A1) >2× over-expressed (OE); (A2) >10× OE; (B1) >2× underexpressed (UE); (B2) >10× UE. The groups A1 and B1 were integrated with ChIP-seq data on p73 binding sites. The distance of the p73REs from the selected TFBS in A1 and B1 groups was calculated by Pscan using the "Report Occurrences" function with a PWM-threshold of 0.75. The distance score was set as 1 if the distance was within a range of 15–250 bp and to 0 otherwise. Afterward, the relative number of close TFBS within each group was calculated by setting up the ratio of positive distance hits to the total number of genes in the respective group. This ratio in each group (A1, B1) was compared to the ratio of the same TFBS versus all genes in the microarray to calculate the enrichment of close TFBS. The enriched TFBS were significantly close to the respective p73RE in group B1 (estimated by *t*-test), whereas a significant enrichment in group A1 could only be found for one TF. **(F)** *Tethering scenario:* factors that bind DNp73 were predicted using the A2 and B2 groups of DNp73-responsive genes. The number of TFs recognizing the enriched ORTFBS for A2 and B2 were 58 and 158, respectively. The functions in which TFs are involved were predicted by GO-term analysis.

PPI of DNp73 with nodal molecules on gene promoters is solid, then the architecture of the promoters of the genes that are deregulated upon DNp73 overexpression can serve as a 'footprint' of these PP-interactions. In detail, the DNp73-responsive transcriptome will be enriched of genes which have binding sites for specific and functionally-coherent interactors in their promoter regions. Hence, we sought to meta-analyze this transcriptome data to predict novel, functionally coherent interactors of DNp73 in the promoter regions of these genes. To this end, we integrated the high-throughput mRNAs array of stable SK-Mel-29.DNp73 clones versus its mock counterpart (Steder et al., 2013) with p73 ChIP-seq data (Koeppel et al., 2011) and searched for overrepresentations of binding motifs for transcriptional regulators either near p73REs (composite scenario) or independent of p73REs (tethering scenario) in the promoters of DNp73-responsive

genes. For example, when DNp73 interacts with the transcription factor TF1, the upregulated and downregulated genes in the transcriptome will have over-represented binding sites for TF1. In the case of a composite mechanism, p73REs will be found in close proximity (up to 250 bps) to TF1 REs (Koeppel et al., 2011) to allow physical association between DNp73-TF1. On the other hand, in case of a tethering mechanism, where DNp73 binds independently of p73Res to, e.g., TF2, many significantly up- or downregulated DNp73-responsive genes (more than 10-fold increase) without p73REs would instead have overrepresented binding sites for TF2. As consequence, TF1 and TF2 should have functional relevance to the resulting cell phenotype. With this approach, we were able to predict potential binding partners of DNp73. Our results in detail are:

(a) *Composite scenario:* we found a clear enrichment of TFBS for LBX1, LHX6, and PAX4 in close proximity to p73REs in genes that are downregulated in response to DNp73, whereas in the case of DNp73-upregulated genes, TFAP2B binding sites were significantly enriched. Overall, we predicted that DNp73 binds adjacent to responsive elements for LHX6, PAX4, and/or LBX1 as well as TFAP2B transcription factors and down- or upregulates the corresponding genes, suggesting that these proteins are candidates for p73 co-regulators. Three striking observations were made by this analysis: (Logotheti et al., 2013) candidate p73 co-regulators for downregulated genes differs from predicted p73 co-regulators for upregulated genes. The complete lack of overlap implies a 'deterministic trend' of DNp73 to develop highly "selective" PPIs with the candidate co-regulators; (Belyi and Levine, 2009) candidate p73 co-regulators are important neurodifferentiation/neurodevelopment factors, which suggests the involvement of neurodifferentiation programs in the effect of DNp73 on cancer aggressiveness; and (Belyi et al., 2010) the likely co-regulators for downregulated genes have different structures than those for upregulated genes: LHX6, PAX4, and LBX1 are homeobox proteins, whereas TFAP2B is a basic helix-loop-helix protein. These instances intriguingly imply that DNp73 can select interaction candidates at gene promoters based on structure (**Figure 3E**).

(*b*) *Tethering scenario:* we checked ORTFBS in DNp73 genes that are highly increased (A2, >10-fold) or decreased (B2, <10-fold) and found non-overlapping groups of ORTFBS between both groups (A2 vs. B2) (**Figure 3F**). In A2, genes with binding sites for 58 TFs were significantly enriched, while in B2, 158 TFs behaved in this way. GO-term analysis of the ORTFs of each group revealed that these ORTFs tend to be involved in cellular and embryonic developmental/differentiation processes (**Figure 3F**, annotated with *) in a non-overlapping manner.

In summary, the interplay between p73 isoforms with different C-termini, their interacting partners, and the architecture of the target gene promoter supports a high degree of heterogeneity in the mechanisms underlying tissue-specific p73-driven functions in a variety of organ systems including immunity, neurodevelopment and reproduction. Such sophisticated mechanistical patterns may explain, at least partially, the different and sometimes opposing results across different cell contents and experimental settings. Dysregulation of one or more of the above parameters in tumors could lead to tumor initiation and progression by, at least in some cases, reactivating p73-regulated differentiation programs in a spatiotemporally inappropriate manner.

CONCLUSION AND FUTURE PERSPECTIVES

The main body of research on TP73 has been initially performed in the cancer setting, due to its functional and structural similarity with the tumor-suppressor TP53. In cancer, the networks controlled by the typically anti-oncogenic TAp73 isoforms offer functional redundancy to the intricate circuitries regulated by p53, through activating fully or partially overlapping pathways, which can circumvent blocks attributed to mutations in TP53 or its downstream effectors (Logotheti et al., 2019). Nevertheless, it is now clear that TP73 with the complexity of isoforms is a key regulator of an own unique and wide range of biological aspects in embryonic development, differentiation, homeostasis, and immune response. This pleiotropy has rejuvenated the interest in p73 as a therapeutic target for the management of not only cancer, but also several other complex diseases, such as neurodevelopmental disorders, COPD (Nemajerova and Moll, 2019), sterility (Inoue et al., 2014), metabolic disorders (Jia et al., 2018), and autoimmune disease susceptibility (Ren et al., 2020). Several common unifying themes can be recognized among the diversity of physiological and oncogenic p73 functions, such as the ability of p73 isoforms to act as transcriptional master regulators of motile multiciliogenesis underlying the disparate p73KO phenotypes of airway infections and female and male infertility (Nemajerova and Moll, 2019). Moreover, to determine tissue architecture, through regulating cell adhesion, cytoskeleton dynamics and planar cell polarity, which is essential for the organization and homeostasis of various complex microenvironments, like the neurogenic niche, reproductive organs, respiratory epithelium, or vascular network (Maeso-Alonso et al., 2021).

In view of recent findings, the potential of p73 isoforms to modulate cancer initiation and progression might not be independent from the physiological functions of TP73. Instead, it could reflect the recapitulation of the same p73-regulated developmental/tissue homeostasis pathways within the cancer cell content. Specifically, a new idea proposes that metastatic transcriptional programs arise from *de novo* combinatorial activation of multiple distinct and developmentally distant transcriptional modules (Rodrigues et al., 2018). Although mutations in tumor suppressors and oncogenes predominate during tumor initiation, cancer cells become metastatic at progression stages, often by hijacking gene expression programs of normal embryonic development and reactivating them outside their physiological context. In support of this notion, we have recently shown that p73-driven neurodevelopmental pathways are co-opted in cancer cells to promote the acquisition of neurogenic features in melanoma cells via production of secreted neurotrophins, such as NGF and BDNF (Logotheti et al., 2020b). This process plausibly facilitates cancer cells to gain neurogenic

potential and communicate with neuronal cells, providing overall selective advantages for tumors. More intriguingly, specific factors of the cancer cell secretome force a variety of surrounding cells in the TME, including fibroblasts, endothelial cells, bone marrow-derived cells, immune cells, and neurons to integrate into the stroma, where their activities are redirected to benefit cancer cell progression. Given that BDNF and NGF are recognizable by both, neuronal cells and

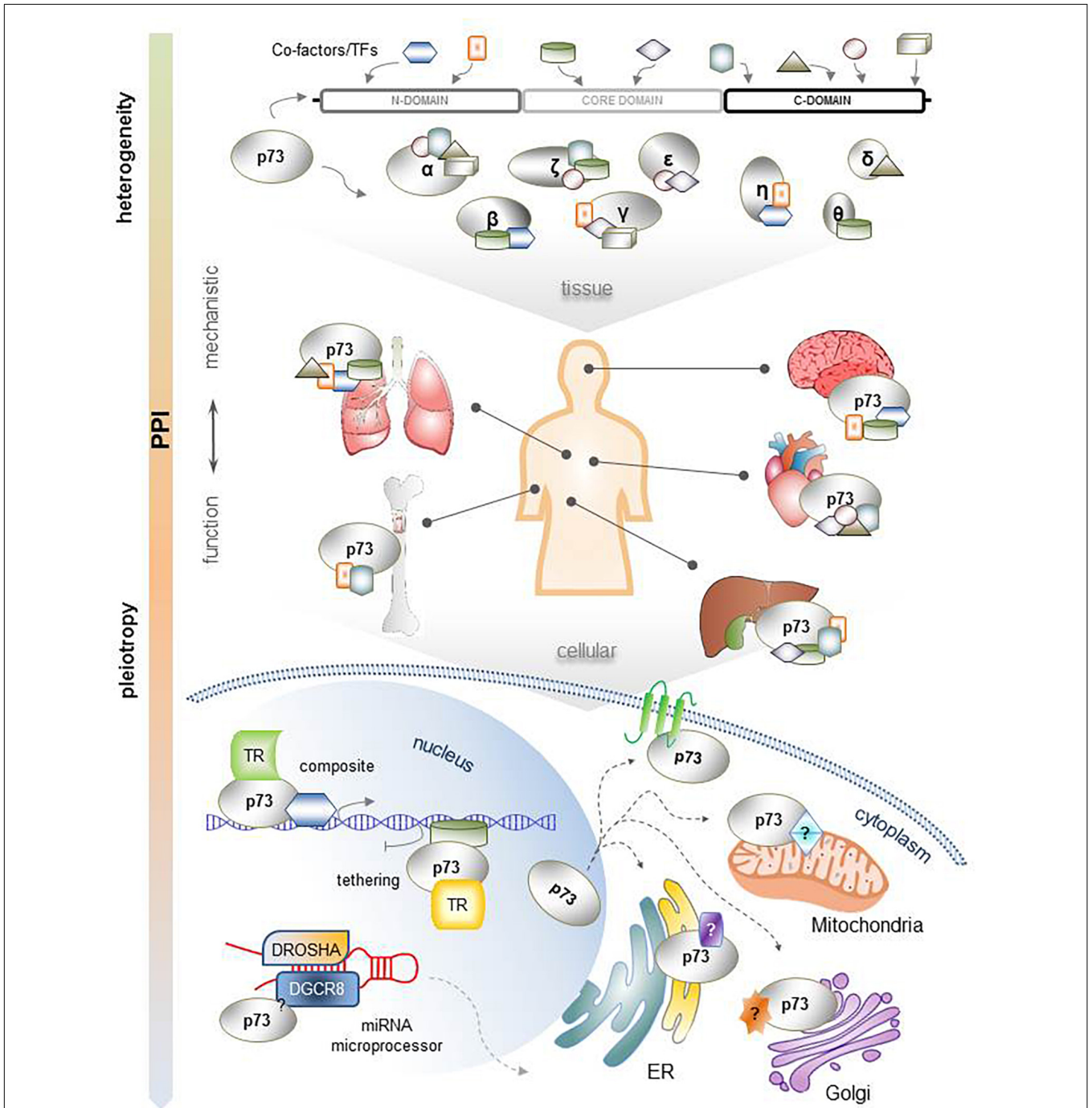

FIGURE 4 | Comprehensive illustration of the mechanistic heterogeneity that supports the functional pleiotropy of TP73. Each p73 isoform has a unique combination of interacting motifs and residues that can develop distinct PPIs. This is particularly important for their function across several organ systems, which present tissue-specific protein contents. The resulting complexes of p73 isoforms with their protein binding partners interact with gene promoters according to composite or tethering mechanisms of gene transcription regulation; are integrated in other multi-protein complexes within the nucleus, such as the miRNA processing complex, to control miRNA maturation; or are localized in the cytoplasm, possibly affecting the function of several subcellular organelles and/or the plasma membrane.

immune cells, an appealing hypothesis is that reactivation of p73 neurodevelopmental networks in cancer cells leading to neurotrophin production and secretion may establish a complex cancer–neuroimmune crosstalk in the TME that alters the dynamics of cellular interactions toward an unfavorable prognosis (Logotheti et al., 2020b).

The functional pleiotropy of TP73 assumes existence of mechanistic heterogeneity that extends beyond its typical transactivation mode of action. The PPI-mode of action of TP73 can provide a basis for its multifunctionality and tissue specificity. We propose that multiple p73 isoforms can establish PPIs with many proteins via several motifs in the N-terminus, core domain, and C-terminus, with the C-terminus being particularly enriched in protein binding motifs and residues. In different tissues, p73 isoforms with different C-termini may have different binding partners that can be recognized by the appropriate interacting regions of 73, causing the formation of a variety of p73 coregulator complexes. The localization of these complexes can also lead to functional diversification. Thus, p73-containing complexes within the nucleus select direct and indirect p73 target genes and regulate them via composite and tethering mechanisms based on a specified promoter architecture. In addition, p73 isoforms may be able to bind to other proteins as transcriptional regulators, such as the miRNA processing complex and SAC. p73 isoforms also physically associate outside the nucleus with proteins localized in a number of subcellular organelles. The ER- and Golgi-related interactome reflects to some extent the well-established tendency of TP73 gene products to undergo post-translational modifications. However, their potential to interact directly with proteins in intracellular compartments, such as the cell membrane, lysosomes, endosomes, and mitochondria might indicate novel, non-transcription-mediated functions of p73 isoforms that are worth unveiling in the future. A comprehensive scheme of the heterogeneity of mechanisms supporting p73 functional pleiotropy and diversity is shown in **Figure 4**. The proposed mechanistic models could explain, at least in part, the different and sometimes conflicting results in different cell contents and experimental settings. Dysregulation of one or more of the above parameters in tumors could lead to cancer progression by reactivating p73-regulated differentiation programs in a spatiotemporally inappropriate manner. Moreover, miRNAs that target and inhibit p73 mRNA at the post-transcriptional level [extensively described in Logotheti et al. (2019)], as well as several protein modificators of the activity and stability of p73 protein in the post-translational label [reviewed in detail in Conforti et al. (2012)] create additional layers of complexity in the mechanisms underlying the p73-mediated functions.

From the therapeutic perspective, these new insights provide a roadmap for efficient and selective manipulation of p73 isoforms toward precision medicine. On the shoulders of structural systems pharmacology (Duran-Frigola et al., 2013; Xie et al., 2014), these mechanisms can be translated into personalized solutions against various complex diseases associated with p73 dysregulation. By applying relative structure-based computational pipelines, which we have recently successfully implemented to design strategies against the metastatic interactome of other key transcription factors such as E2F1 (Babushok et al., 2015; Logotheti et al., 2020a), the p73 isoform-coregulator complexes causally associated with pathological conditions can be identified and 3D models generated to reveal their interacting interfaces. Subsequently, structure-based pharmacophore modeling can be used to identify potential inhibitors that disrupt these PPIs and dissociate the pathological p73 coregulator complexes of interest by destabilizing the bonds at the sites of their physical association. These predicted inhibitors with prognosticating effect can become part of drug discovery programs for the development of next generation p73-based targeted therapeutics.

AUTHOR CONTRIBUTIONS

SL and BP conceived the review and took the lead in writing. SM developed bioinformatics pipelines and analyzed high-throughput data. CR conducted CoIP-MS and data analysis. NM, CR, and SL performed literature search. AS, SM, and SL crafted the illustrations. All authors contributed to and approved the final manuscript.

FUNDING

This work was supported by Grant PU 188/17-1 from Deutsche Forschungsgemeinschaft (DFG), Deutsche Krebshilfe Grant 70112353, and e:Med-MelAutim Grant 01ZX1905D from German Federal Ministry of Education and Research. NM holds a doctoral scholarship from the graduate funding program of the Land Mecklenburg-Vorpommern.

REFERENCES

Alla, V., Engelmann, D., Niemetz, A., Pahnke, J., Schmidt, A., Kunz, M., et al. (2010). E2F1 in melanoma progression and metastasis. *J. Natl. Cancer Inst.* 102, 127–133.

Alla, V., Kowtharapu, B. S., Engelmann, D., Emmrich, S., Schmitz, U., Steder, M., et al. (2012). E2F1 confers anticancer drug resistance by targeting ABC transporter family members and Bcl-2 via the p73/DNp73-miR-205 circuitry. *Cell Cycle* 11, 3067–3078. doi: 10.4161/cc.21476

Amelio, I., Inoue, S., Markert, E. K., Levine, A. J., Knight, R. A., Mak, T. W., et al. (2015). TAp73 opposes tumor angiogenesis by promoting hypoxia-inducible factor 1α degradation. *Proc. Natl. Acad. Sci. U.S.A.* 112, 226–231. doi: 10.1073/pnas.1410609111

Babushok, D. V., Perdigones, N., Perin, J. C., Olson, T. S., Ye, W., Roth, J. J., et al. (2015). Emergence of clonal hematopoiesis in the majority of patients with acquired aplastic anemia. *Cancer Genet.* 208, 115–128.

Bálint, E., Bates, S., and Vousden, K. H. (1999). Mdm2 binds p73 alpha without targeting degradation. *Oncogene* 18, 3923–3929.

Beitzinger, M., Oswald, C., Beinoraviciute-Kellner, R., and Stiewe, T. (2006). Regulation of telomerase activity by the p53 family member p73. *Oncogene* 25, 813–826.

Belloni, L., Moretti, F., Merlo, P., Damalas, A., Costanzo, A., Blandino, G., et al. (2006). DNp73alpha protects myogenic cells from apoptosis. *Oncogene* 25, 3606–3612. doi: 10.1038/sj.onc.1209321

Belyi, V. A., Ak, P., Markert, E., Wang, H., Hu, W., Puzio-Kuter, A., et al. (2010). The origins and evolution of the p53 family of genes. *Cold Spring Harb. Perspect. Biol.* 2:a001198.

Belyi, V. A., and Levine, A. J. (2009). One billion years of p53/p63/p73 evolution. *Proc. Natl. Acad. Sci. U.S.A.* 106, 17609–17610. doi: 10.1073/pnas.0910634106

Bianconi, F., Baldelli, E., Ludovini, V., Crinò, L., Flacco, A., and Valigi, P. (2012). Computational model of EGFR and IGF1R pathways in lung cancer: a systems biology approach for translational oncology. *Biotechnol. Adv.* 30, 142–153. doi: 10.1016/j.biotechadv.2011.05.010

Billaud, M., and Santoro, M. (2011). Is co-option a prevailing mechanism during cancer progression? *Cancer Res.* 71, 6572–6575. doi: 10.1158/0008-5472.CAN-11-2158

Boominathan, L. (2010). The tumor suppressors p53, p63, and p73 are regulators of microRNA processing complex. *PLoS One* 5:e10615. doi: 10.1371/journal.pone.0010615

Borisov, N., Aksamitiene, E., Kiyatkin, A., Legewie, S., Berkhout, J., Maiwald, T., et al. (2009). Systems-level interactions between insulin-EGF networks amplify mitogenic signaling. *Mol. Syst. Biol.* 5:256. doi: 10.1038/msb.2009.19

Buhlmann, S., Racek, T., Schwarz, A., Schaefer, S., and Pützer, B. M. (2008). Molecular mechanism of p73-mediated regulation of hepatitis B virus core promoter/enhancer II: implications for hepatocarcinogenesis. *J. Mol. Biol.* 378, 20–30. doi: 10.1016/j.jmb.2008.02.021

Cam, M., Charan, M., Welker, A. M., Dravid, P., Studebaker, A. W., Leonard, J. R., et al. (2020). ΔNp73/ETS2 complex drives glioblastoma pathogenesis- targeting downstream mediators by rebastinib prolongs survival in preclinical models of glioblastoma. *Neuro Oncol.* 22, 345–356. doi: 10.1093/neuonc/noz190

Conforti, F., Sayan, A. E., Sreekumar, R., and Sayan, B. S. (2012). Regulation of p73 activity by post-translational modifications. *Cell Death Dis.* 3:e285.

Davis, B. B., Dong, Y., and Weiss, R. H. (2003). Overexpression of p73 causes apoptosis in vascular smooth muscle cells. *Am. J. Physiol. Cell Physiol.* 284, C16–C23. doi: 10.1152/ajpcell.00211.2002

De Cola, A., Bongiorno-Borbone, L., Bianchi, E., Barcaroli, D., Carletti, E., Knight, R. A., et al. (2012). FLASH is essential during early embryogenesis and cooperates with p73 to regulate histone gene transcription. *Oncogene* 31, 573–582. doi: 10.1038/onc.2011.274

Dobbelstein, M., Strano, S., Roth, J., and Blandino, G. (2005). p73-induced apoptosis: a question of compartments and cooperation. *Biochem. Biophys. Res. Commun.* 331, 688–693. doi: 10.1016/j.bbrc.2005.03.155

Duran-Frigola, M., Mosca, R., and Aloy, P. (2013). Structural systems pharmacology: the role of 3D structures in next-generation drug development. *Chem. Biol.* 20, 674–684. doi: 10.1016/j.chembiol.2013.03.004

Ebelt, H., Zhang, Y., Köhler, K., Xu, J., Gajawada, P., Boettger, T., et al. (2008). Directed expression of dominant-negative p73 enables proliferation of cardiomyocytes in mice. *J. Mol. Cell Cardiol.* 45, 411–419. doi: 10.1016/j.yjmcc.2008.06.006

Emmrich, S., Wang, W., John, K., Li, W., and Pützer, B. M. (2009). Antisense gapmers selectively suppress individual oncogenic p73 splice isoforms and inhibit tumor growth in vivo. *Mol. Cancer.* 8:61. doi: 10.1186/1476-4598-8-61

Engelmann, D., and Pützer, B. M. (2014). Emerging from the shade of p53 mutants: n-terminally truncated variants of the p53 family in EMT signaling and cancer progression. *Sci. Signal.* 7:re9. doi: 10.1126/scisignal.2005699

Engelmann, D., Meier, C., Alla, V., and Pützer, B. M. (2015). A balancing act: orchestrating amino-truncated and full-length p73 variants as decisive factors in cancer progression. *Oncogene* 34, 4287–4299. doi: 10.1038/onc.2014.365

Fürst, K., Steder, M., Logotheti, S., Angerilli, A., Spitschak, A., Marquardt, S., et al. (2019). DNp73-induced degradation of tyrosinase links depigmentation with EMT-driven melanoma progression. *Cancer Lett.* 442, 299–309. doi: 10.1016/j.canlet.2018.11.009

Gaiddon, C., Lokshin, M., Gross, I., Levasseur, D., Taya, Y., Loeffler, J. P., et al. (2003). Cyclin-dependent kinases phosphorylate p73 at threonine 86 in a cell cycle-dependent manner and negatively regulate p73. *J. Biol. Chem.* 278, 27421–27431. doi: 10.1074/jbc.M300251200

Galtsidis, S., Logotheti, S., Pavlopoulou, A., Zampetidis, C. P., Papachristopoulou, G., Scorilas, A., et al. (2017). Unravelling a p73-regulated network: the role of a novel p73-dependent target, MIR3158, in cancer cell migration and invasiveness. *Cancer Lett.* 388, 96–106. doi: 10.1016/j.canlet.2016.11.036

George, J., Lim, J. S., Jang, S. J., Cun, Y., Ozretić, L., Kong, G., et al. (2015). Comprehensive genomic profiles of small cell lung cancer. *Nature* 524, 47–53.

Hinske, L. C., França, G. S., Torres, H. A., Ohara, D. T., Lopes-Ramos, C. M., Heyn, J., et al. (2014). miRIAD-integrating microRNA inter–and intragenic data. *Database* 2014:bau099. doi: 10.1093/database/bau099

Inoue, S., Tomasini, R., Rufini, A., Elia, A. J., Agostini, M., Amelio, I., et al. (2014). TAp73 is required for spermatogenesis and the maintenance of male fertility. *Proc. Natl. Acad. Sci. U.S.A.* 111, 1843–1848. doi: 10.1073/pnas.1323416111

Iorio, M. V., Casalini, P., Piovan, C., Di Leva, G., Merlo, A., Triulzi, T., et al. (2009). microRNA-205 regulates HER3 in human breast cancer. *Cancer Res.* 69, 2195–2200. doi: 10.1158/0008-5472.CAN-08-2920

Jia, H., Ren, W., Feng, Y., Wei, T., Guo, M., Guo, J., et al. (2018). The enhanced antitumour response of pimozide combined with the IDO inhibitor L-MT in melanoma. *Int. J. Oncol.* 53, 949–960. doi: 10.3892/ijo.2018.4473

Khan, F. M., Schmitz, U., Nikolov, S., Engelmann, D., Pützer, B. M., Wolkenhauer, O., et al. (2014). Hybrid modeling of the crosstalk between signaling and transcriptional networks using ordinary differential equations and multi-valued logic. *Biochim. Biophys. Acta* 1844(1 Pt B), 289–298. doi: 10.1016/j.bbapap.2013.05.007

Killick, R., Niklison-Chirou, M., Tomasini, R., Bano, D., Rufini, A., Grespi, F., et al. (2011). p73: a multifunctional protein in neurobiology. *Mol. Neurobiol.* 43, 139–146. doi: 10.1007/s12035-011-8172-6

Kim, K. C., Kim, T. S., Kang, K. H., and Choi, K. H. (2001). Amphiphysin IIb-1, a novel splicing variant of amphiphysin II, regulates p73beta function through protein-protein interactions. *Oncogene* 20, 6689–6699. doi: 10.1038/sj.onc.1204839

Knoll, S., Fürst, K., Thomas, S., Villanueva Baselga, S., Stoll, A., Schaefer, S., et al. (2011). Dissection of cell context-dependent interactions between HBx and p53 family members in regulation of apoptosis: a role for HBV-induced HCC. *Cell Cycle* 10, 3554–3565. doi: 10.4161/cc.10.20.17856

Koeppel, M., van Heeringen, S. J., Kramer, D., Smeenk, L., Janssen-Megens, E., Hartmann, M., et al. (2011). Crosstalk between c-Jun and TAp73alpha/beta contributes to the apoptosis-survival balance. *Nucleic Acids Res.* 39, 6069–6085. doi: 10.1093/nar/gkr028

Koutsodontis, G., Vasilaki, E., Chou, W. C., Papakosta, P., and Kardassis, D. (2005). Physical and functional interactions between members of the tumour suppressor p53 and the Sp families of transcription factors: importance for the regulation of genes involved in cell-cycle arrest and apoptosis. *Biochem. J.* 389(Pt 2), 443–455. doi: 10.1042/BJ20041980

Lalioti, M. E., Arbi, M., Loukas, I., Kaplani, K., Kalogeropoulou, A., Lokka, G., et al. (2019). GemC1 governs multiciliogenesis through direct interaction with and transcriptional regulation of p73. *J. Cell. Sci.* 132:jcs228684. doi: 10.1242/jcs.228684

Li, C. Y., Zhu, J., and Wang, J. Y. (2005). Ectopic expression of p73alpha, but not p73beta, suppresses myogenic differentiation. *J. Biol. Chem.* 280, 2159–2164.

Li, Y., and Prives, C. (2007). Are interactions with p63 and p73 involved in mutant p53 gain of oncogenic function? *Oncogene* 26, 2220–2225.

Liu, G., Nozell, S., Xiao, H., and Chen, X. (2004). DeltaNp73beta is active in transactivation and growth suppression. *Mol. Cell Biol.* 24, 487–501. doi: 10.1128/MCB.24.2.487-501.2004

Logotheti, S., Marquardt, S., and Pützer, B. M. (2019). p73-Governed miRNA networks: translating bioinformatics approaches to therapeutic solutions for cancer metastasis. *Methods Mol. Biol.* 1912, 33–52. doi: 10.1007/978-1-4939-8982-9_2

Logotheti, S., Marquardt, S., Gupta, S. K., Richter, C., Edelhäuser, B. A. H., Engelmann, D., et al. (2020a). LncRNA-SLC16A1-AS1 induces metabolic reprogramming during bladder cancer progression as target and co-activator of E2F1. *Theranostics* 10, 9620–9643. doi: 10.7150/thno.44176

Logotheti, S., Marquardt, S., Richter, C., Sophie Hain, R., Murr, N., Takan, I., et al. (2020b). Neural networks recapitulation by cancer cells promotes disease progression: a novel role of p73 isoforms in cancer-neuronal crosstalk. *Cancers* 12:3789. doi: 10.3390/cancers12123789

Logotheti, S., Michalopoulos, I., Sideridou, M., Daskalos, A., Kossida, S., Spandidos, D. A., et al. (2010). Sp1 binds to the external promoter of the p73 gene and induces the expression of TAp73gamma in lung cancer. *FEBS J.* 277, 3014–3027. doi: 10.1111/j.1742-4658.2010.07710.x

Logotheti, S., Pavlopoulou, A., Galtsidis, S., Vojtesek, B., and Zoumpourlis, V. (2013). Functions, divergence and clinical value of TAp73 isoforms in cancer. *Cancer Metastasis Rev.* 32, 511–534. doi: 10.1007/s10555-013-9424-x

Lu, R., Fan, C., Shangguan, W., Liu, Y., Li, Y., Shang, Y., et al. (2017). Neurons generated from carcinoma stem cells support cancer progression. *Signal Transduct. Target Ther.* 2:16036.

Maeso-Alonso, L., López-Ferreras, L., Marques, M. M., and Marin, M. C. (2021). p73 as a tissue architect. *Front. Cell Dev. Biol.* 9:716957. doi: 10.3389/fcell.2021.716957

Malatesta, M., Peschiaroli, A., Memmi, E. M., Zhang, J., Antonov, A., Green, D. R., et al. (2013). The cul4A-DDB1 E3 ubiquitin ligase complex represses p73 transcriptional activity. *Oncogene* 32, 4721–4726. doi: 10.1038/onc.2012.463

Malik, N., Yan, H., Yang, H. H., Ayaz, G., DuBois, W., Tseng, Y. C., et al. (2021). CBFB cooperates with p53 to maintain TAp73 expression and suppress breast cancer. *PLoS Genet.* 17:e1009553. doi: 10.1371/journal.pgen.1009553

Marabese, M., Vikhanskaya, F., and Broggini, M. (2007). p73: a chiaroscuro gene in cancer. *Eur. J. Cancer* 43, 1361–1372. doi: 10.1016/j.ejca.2007.01.042

Mauffrey, P., Tchitchek, N., Barroca, V., Bemelmans, A., Firlej, V., Allory, Y., et al. (2019). Progenitors from the central nervous system drive neurogenesis in cancer. *Nature* 569, 672–678.

Meier, C., Hardtstock, P., Joost, S., Alla, V., and Pützer, B. M. (2016). p73 and IGF1R regulate emergence of aggressive cancer stem-like features via miR-885-5p control. *Cancer Res.* 76, 197–205. doi: 10.1158/0008-5472.CAN-15-1228

Melino, G. (2020). Molecular mechanisms and function of the p53 protein family member - p73. *Biochemistry* 85, 1202–1209.

Men, H., Cai, H., Cheng, Q., Zhou, W., Wang, X., Huang, S., et al. (2021). The regulatory roles of p53 in cardiovascular health and disease. *Cell Mol. Life Sci.* 78, 2001–2018.

Ming, L., Sakaida, T., Yue, W., Jha, A., Zhang, L., and Yu, J. (2008). Sp1 and p73 activate PUMA following serum starvation. *Carcinogenesis* 29, 1878–1884. doi: 10.1093/carcin/bgn150

Monje, M., Borniger, J. C., D'Silva, N. J., Deneen, B., Dirks, P. B., Fattahi, F., et al. (2020). Roadmap for the emerging field of cancer neuroscience. *Cell* 181, 219–222. doi: 10.1016/j.cell.2020.03.034

Neira, J. L., Díaz-García, C., Prieto, M., and Coutinho, A. (2019). The C-terminal SAM domain of p73 binds to the N terminus of MDM2. *Biochim. Biophys. Acta Gen. Subj.* 1863, 760–770. doi: 10.1016/j.bbagen.2019.01.019

Neira, J. L., Rizzuti, B., Ortega-Alarcón, D., Giudici, A. M., Abián, O., Fárez-Vidal, M. E., et al. (2021). The armadillo-repeat domain of plakophilin 1 binds the C-terminal sterile alpha motif (SAM) of p73. *Biochim. Biophys. Acta Gen. Subj.* 1865:129914. doi: 10.1016/j.bbagen.2021.129914

Nekulová, M., Zitterbart, K., Sterba, J., and Veselská, R. (2010). Analysis of the intracellular localization of p73 N-terminal protein isoforms TAp73 and ?Np73 in medulloblastoma cell lines. *J. Mol. Histol.* 41, 267–275. doi: 10.1007/s10735-010-9288-0

Nemajerova, A., Amelio, I., Gebel, J., Dötsch, V., Melino, G., and Moll, U. M. (2018). Non-oncogenic roles of TAp73: from multiciliogenesis to metabolism. *Cell Death Differ.* 25, 144–153.

Nemajerova, A., and Moll, U. M. (2019). Tissue-specific roles of p73 in development and homeostasis. *J. Cell Sci.* 132:jcs233338. doi: 10.1242/jcs.233338

Neman, J., Termini, J., Wilczynski, S., Vaidehi, N., Choy, C., Kowolik, C. M., et al. (2014). Human breast cancer metastases to the brain display GABAergic properties in the neural niche. *Proc. Natl. Acad. Sci. U.S.A.* 111, 984–989. doi: 10.1073/pnas.1322098111

Nguyen, D., Yang, K., Chiao, L., Deng, Y., Zhou, X., Zhang, Z., et al. (2020). Inhibition of tumor suppressor p73 by nerve growth factor receptor via chaperone-mediated autophagy. *J. Mol. Cell Biol.* 12, 700–712. doi: 10.1093/jmcb/mjaa017

Niklison-Chirou, M. V., Agostini, M., Amelio, I., and Melino, G. (2020). Regulation of adult neurogenesis in mammalian brain. *Int. J. Mol. Sci.* 21:4869.

Ozaki, T., Kubo, N., and Nakagawara, A. (2010). p73-binding partners and their functional significance. *Int. J. Proteomics* 2010:283863. doi: 10.1155/2010/283863

Pomeranz Krummel, D. A., Nasti, T. H., Kaluzova, M., Kallay, L., Bhattacharya, D., Melms, J. C., et al. (2021). Melanoma cell intrinsic GABA. *Int. J. Radiat. Oncol. Biol. Phys.* 109, 1040–1053. doi: 10.1016/j.ijrobp.2020.10.025

Prabhu, V. V., Hong, B., Allen, J. E., Zhang, S., Lulla, A. R., Dicker, D. T., et al. (2016). Small-molecule prodigiosin restores p53 tumor suppressor activity in chemoresistant colorectal cancer stem cells via c-jun-mediated ΔNp73 inhibition and p73 activation. *Cancer Res.* 76, 1989–1999. doi: 10.1158/0008-5472.CAN-14-2430

Pützer, B. M., Solanki, M., and Herchenröder, O. (2017). Advances in cancer stem cell targeting: how to strike the evil at its root. *Adv. Drug Deliv. Rev.* 120, 89–107. doi: 10.1016/j.addr.2017.07.013

Racek, T., Mise, N., Li, Z., Stoll, A., and Pützer, B. M. (2005). C-terminal p73 isoforms repress transcriptional activity of the human telomerase reverse transcriptase (hTERT) promoter. *J. Biol. Chem.* 280, 40402–40405. doi: 10.1074/jbc.C500193200

Ren, M., Kazemian, M., Zheng, M., He, J., Li, P., Oh, J., et al. (2020). Transcription factor p73 regulates Th1 differentiation. *Nat. Commun.* 11:1475. doi: 10.1038/s41467-020-15172-5

Rodrigues, P., Patel, S. A., Harewood, L., Olan, I., Vojtasova, E., Syafruddin, S. E., et al. (2018). NF-κB-dependent lymphoid enhancer co-option promotes renal carcinoma metastasis. *Cancer Discov.* 8, 850–865. doi: 10.1158/2159-8290.CD-17-1211

Rosenbluth, J. M., Mays, D. J., Pino, M. F., Tang, L. J., and Pietenpol, J. A. (2008). A gene signature-based approach identifies mTOR as a regulator of p73. *Mol. Cell Biol.* 28, 5951–5964. doi: 10.1128/MCB.00305-08

Rossi, M., De Laurenzi, V., Munarriz, E., Green, D. R., Liu, Y. C., Vousden, K. H., et al. (2005). The ubiquitin-protein ligase itch regulates p73 stability. *EMBO J.* 24, 836–848.

Rudge, T. J., Brown, J. R., Federici, F., Dalchau, N., Phillips, A., Ajioka, J. W., et al. (2016). Characterization of intrinsic properties of promoters. *ACS Synth. Biol.* 5, 89–98.

Sabapathy, K. (2015). p73: a positive or negative regulator of angiogenesis, or both? *Mol. Cell Biol.* 36, 848–854.

Sayan, B. S., Yang, A. L., Conforti, F., Tucci, P., Piro, M. C., Browne, G. J., et al. (2010). Differential control of TAp73 and DeltaNp73 protein stability by the ring finger ubiquitin ligase PIR2. *Proc. Natl. Acad. Sci. U.S.A.* 107, 12877–12882. doi: 10.1073/pnas.0911828107

Sharif, T., Martell, E., Dai, C., Singh, S. K., and Gujar, S. (2019b). Regulation of the proline regulatory axis and autophagy modulates stemness in TP73/p73 deficient cancer stem-like cells. *Autophagy* 15, 934–936. doi: 10.1080/15548627.2019.1586321

Sharif, T., Dai, C., Martell, E., Ghassemi-Rad, M. S., Hanes, M. R., Murphy, P. J., et al. (2019a). TAp73 modifies metabolism and positively regulates growth of cancer stem-like cells in a redox-sensitive manner. *Clin. Cancer Res.* 25, 2001–2017. doi: 10.1158/1078-0432.CCR-17-3177

Steder, M., Alla, V., Meier, C., Spitschak, A., Pahnke, J., Fürst, K., et al. (2013). DNp73 exerts function in metastasis initiation by disconnecting the inhibitory role of EPLIN on IGF1R-AKT/STAT3 signaling. *Cancer Cell.* 24, 512–527. doi: 10.1016/j.ccr.2013.08.023

Stiewe, T., and Pützer, B. M. (2000). Role of the p53-homologue p73 in E2F1-induced apoptosis. *Nat. Genet.* 26, 464–469. doi: 10.1038/82617

Stiewe, T., Theseling, C. C., and Pützer, B. M. (2002a). Transactivation-deficient delta TA-p73 inhibits p53 by direct competition for DNA binding: implications for tumorigenesis. *J. Biol. Chem.* 277, 14177–14185. doi: 10.1074/jbc.M200480200

Stiewe, T., Zimmermann, S., Frilling, A., Esche, H., and Pützer, B. M. (2002b). Transactivation-deficient DeltaTA-p73 acts as an oncogene. *Cancer Res.* 62, 3598–3602.

Su, A., Dry, S. M., Binder, S. W., Said, J., Shintaku, P., and Sarantopoulos, G. P. (2014). Malignant melanoma with neural differentiation: an exceptional case report and brief review of the pertinent literature. *Am. J. Dermatopathol.* 36, e5–e9. doi: 10.1097/DAD.0b013e31828cf90a

Subramanian, D., Bunjobpol, W., and Sabapathy, K. (2015). Interplay between TAp73 protein and selected activator protein-1 (AP-1) family members promotes AP-1 target gene activation and cellular growth. *J. Biol. Chem.* 290, 18636–18649. doi: 10.1074/jbc.M115.636548

Sun, C., Wang, L., Huang, S., Heynen, G. J., Prahallad, A., Robert, C., et al. (2014). Reversible and adaptive resistance to BRAF(V600E) inhibition in melanoma. *Nature* 508, 118–122.

Tannapfel, A., John, K., Mise, N., Schmidt, A., Buhlmann, S., Ibrahim, S. M., et al. (2008). Autonomous growth and hepatocarcinogenesis in transgenic mice

expressing the p53 family inhibitor DNp73. *Carcinogenesis* 29, 211–218. doi: 10.1093/carcin/bgm236

Thakur, A. K., Nigri, J., Lac, S., Leca, J., Bressy, C., Berthezene, P., et al. (2016). TAp73 loss favors Smad-independent TGF-β signaling that drives EMT in pancreatic ductal adenocarcinoma. *Cell Death Differ.* 23, 1358–1370. doi: 10.1038/cdd.2016.18

Tiwary, S., Preziosi, M., Rothberg, P. G., Zeitouni, N., Corson, N., and Xu, L. (2014). ERBB3 is required for metastasis formation of melanoma cells. *Oncogenesis* 3:e110. doi: 10.1038/oncsis.2014.23

Toh, W. H., Logette, E., Corcos, L., and Sabapathy, K. (2008). TAp73beta and DNp73beta activate the expression of the pro-survival caspase-2S. *Nucleic Acids Res.* 36, 4498–4509. doi: 10.1093/nar/gkn414

Tomasini, R., Secq, V., Pouyet, L., Thakur, A. K., Wilhelm, M., Nigri, J., et al. (2013). TAp73 is required for macrophage-mediated innate immunity and the resolution of inflammatory responses. *Cell Death Differ.* 20, 293–301. doi: 10.1038/cdd.2012.123

Tomasini, R., Tsuchihara, K., Tsuda, C., Lau, S. K., Wilhelm, M., Rufini, A., et al. (2009). TAp73 regulates the spindle assembly checkpoint by modulating BubR1 activity. *Proc. Natl. Acad. Sci. U.S.A.* 106, 797–802.

Tomasini, R., Tsuchihara, K., Wilhelm, M., Fujitani, M., Rufini, A., Cheung, C. C., et al. (2008). TAp73 knockout shows genomic instability with infertility and tumor suppressor functions. *Genes Dev.* 22, 2677–2691. doi: 10.1101/gad.1695308

Uboveja, A., Satija, Y. K., Siraj, F., Sharma, I., and Saluja, D. (2020). p73 - NAV3 axis plays a critical role in suppression of colon cancer metastasis. *Oncogenesis* 9:12. doi: 10.1038/s41389-020-0193-4

Vera, J., Schmitz, U., Lai, X., Engelmann, D., Khan, F. M., Wolkenhauer, O., et al. (2013). Kinetic modeling-based detection of genetic signatures that provide chemoresistance via the E2F1-p73/DNp73-miR-205 network. *Cancer Res.* 73, 3511–3524. doi: 10.1158/0008-5472.CAN-12-4095

Vernole, P., Neale, M. H., Barcaroli, D., Munarriz, E., Knight, R. A., Tomasini, R., et al. (2009). TAp73alpha binds the kinetochore proteins Bub1 and Bub3 resulting in polyploidy. *Cell Cycle* 8, 421–429. doi: 10.4161/cc.8.3.7623

Wang, C., Teo, C. R., and Sabapathy, K. (2020). p53-related transcription targets of TAp73 in cancer cells-bona fide or distorted reality? *Int. J. Mol. Sci.* 21:1346.

Wang, J., Huang, S. K., Marzese, D. M., Hsu, S. C., Kawas, N. P., Chong, K. K., et al. (2015). Epigenetic changes of EGFR have an important role in BRAF inhibitor-resistant cutaneous melanomas. *J. Invest. Dermatol.* 135, 532–541. doi: 10.1038/jid.2014.418

Wang, Y., Medvid, R., Melton, C., Jaenisch, R., and Blelloch, R. (2007). DGCR8 is essential for microRNA biogenesis and silencing of embryonic stem cell self-renewal. *Nat. Genet.* 39, 380–385.

Weiss, R. H., and Howard, L. L. (2001). p73 is a growth-regulated protein in vascular smooth muscle cells and is present at high levels in human atherosclerotic plaque. *Cell Signal.* 13, 727–733. doi: 10.1016/s0898-6568(01)00195-4

Widden, H., Kaczmarczyk, A., Subedi, A., Whitaker, R. H., and Placzek, W. J. (2020). MCL1 binds and negatively regulates the transcriptional function of tumor suppressor p73. *Cell Death Dis.* 11:946. doi: 10.1038/s41419-020-03068-7

Wilhelm, M. T., Rufini, A., Wetzel, M. K., Tsuchihara, K., Inoue, S., Tomasini, R., et al. (2010). Isoform-specific p73 knockout mice reveal a novel role for delta Np73 in the DNA damage response pathway. *Genes Dev.* 24, 549–560. doi: 10.1101/gad.1873910

Wolfsberger, J., Sakil, H. A. M., Zhou, L., van Bree, N., Baldisseri, E., de Souza Ferreira, S., et al. (2021). TAp73 represses NF-κB-mediated recruitment of tumor-associated macrophages in breast cancer. *Proc. Natl. Acad. Sci. U.S.A* 118:e2017089118. doi: 10.1073/pnas.2017089118

Xie, L., Ge, X., Tan, H., Zhang, Y., Hart, T., Yang, X., et al. (2014). Towards structural systems pharmacology to study complex diseases and personalized medicine. *PLoS Comput. Biol.* 10:e1003554. doi: 10.1371/journal.pcbi.1003554

Yang, A., Kaghad, M., Caput, D., and McKeon, F. (2002). On the shoulders of giants: p63, p73 and the rise of p53. *Trends Genet.* 18, 90–95. doi: 10.1016/s0168-9525(02)02595-7

Yang, A., Walker, N., Bronson, R., Kaghad, M., Oosterwegel, M., Bonnin, J., et al. (2000). p73-deficient mice have neurological, pheromonal and inflammatory defects but lack spontaneous tumours. *Nature* 404, 99–103. doi: 10.1038/35003607

Yeom, K. H., Lee, Y., Han, J., Suh, M. R., and Kim, V. N. (2006). Characterization of DGCR8/Pasha, the essential cofactor for Drosha in primary miRNA processing. *Nucleic Acids Res.* 34, 4622–4629. doi: 10.1093/nar/gkl458

Yılmaz, H., Toy, H., Marquardt, S., Karakülah, G., Küçük, C., Kontou, P., et al. (2021). In silico methods for the identification of diagnostic and favorable prognostic markers in acute myeloid leukemia. *Int. J. Mol. Sci* 22:9601. doi: 10.3390/ijms22179601

Zeng, X., Chen, L., Jost, C. A., Maya, R., Keller, D., Wang, X., et al. (1999). MDM2 suppresses p73 function without promoting p73 degradation. *Mol. Cell Biol.* 19, 3257–3266.

Conflict of Interest: The authors declare that the research was conducted in the absence of any commercial or financial relationships that could be construed as a potential conflict of interest.

Publisher's Note: All claims expressed in this article are solely those of the authors and do not necessarily represent those of their affiliated organizations, or those of the publisher, the editors and the reviewers. Any product that may be evaluated in this article, or claim that may be made by its manufacturer, is not guaranteed or endorsed by the publisher.

Copyright © 2021 Logotheti, Richter, Murr, Spitschak, Marquardt and Pützer. This is an open-access article distributed under the terms of the Creative Commons Attribution License (CC BY). The use, distribution or reproduction in other forums is permitted, provided the original author(s) and the copyright owner(s) are credited and that the original publication in this journal is cited, in accordance with accepted academic practice. No use, distribution or reproduction is permitted which does not comply with these terms.

frontiers in Cell and Developmental Biology

ORIGINAL RESEARCH
published: 02 February 2022
doi: 10.3389/fcell.2021.746359

Multi-Level Computational Modeling of Anti-Cancer Dendritic Cell Vaccination Utilized to Select Molecular Targets for Therapy Optimization

Xin Lai [1,2†], Christine Keller [1†], Guido Santos [1,3], Niels Schaft [2,4], Jan Dörrie [2,4] and Julio Vera [1,2*]*

[1]*Laboratory of Systems Tumor Immunology, Department of Dermatology, Friedrich-Alexander-Universität Erlangen-Nürnberg (FAU) and Universitätsklinikum Erlangen, Erlangen, Germany,* [2]*Deutsches Zentrum Immuntherapie and Comprehensive Cancer Center Erlangen-EMN, Erlangen, Germany,* [3]*Departament of Biochemistry, Microbiology, Cell Biology and Genetics, Faculty of Sciences, University of La Laguna, San Cristóbal de La Laguna, Spain,* [4]*RNA Group, Department of Dermatology, Friedrich-Alexander-Universität Erlangen-Nürnberg (FAU) and Universitätsklinikum Erlangen, Erlangen, Germany*

OPEN ACCESS

Edited by:
Eva Lion,
University of Antwerp, Belgium

Reviewed by:
Yu Zhao,
Capital Medical University, China
Adarsh Kumbhari,
Harvard Medical School, United States

***Correspondence:**
Xin Lai
xin.lai@uk-erlangen.de
Julio Vera
julio.vera-gonzalez@uk-erlangen.de

†These authors have contributed equally to this work

Specialty section:
This article was submitted to Molecular and Cellular Pathology, a section of the journal Frontiers in Cell and Developmental Biology

Received: *23 July 2021*
Accepted: *23 December 2021*
Published: *02 February 2022*

Citation:
Lai X, Keller C, Santos G, Schaft N, Dörrie J and Vera J (2022) Multi-Level Computational Modeling of Anti-Cancer Dendritic Cell Vaccination Utilized to Select Molecular Targets for Therapy Optimization. Front. Cell Dev. Biol. 9:746359. doi: 10.3389/fcell.2021.746359

Dendritic cells (DCs) can be used for therapeutic vaccination against cancer. The success of this therapy depends on efficient tumor-antigen presentation to cytotoxic T lymphocytes (CTLs) and the induction of durable CTL responses by the DCs. Therefore, simulation of such a biological system by computational modeling is appealing because it can improve our understanding of the molecular mechanisms underlying CTL induction by DCs and help identify new strategies to improve therapeutic DC vaccination for cancer. Here, we developed a multi-level model accounting for the life cycle of DCs during anti-cancer immunotherapy. Specifically, the model is composed of three parts representing different stages of DC immunotherapy – the spreading and bio-distribution of intravenously injected DCs in human organs, the biochemical reactions regulating the DCs' maturation and activation, and DC-mediated activation of CTLs. We calibrated the model using quantitative experimental data that account for the activation of key molecular circuits within DCs, the bio-distribution of DCs in the body, and the interaction between DCs and T cells. We showed how such a data-driven model can be exploited in combination with sensitivity analysis and model simulations to identify targets for enhancing anti-cancer DC vaccination. Since other previous works show how modeling improves therapy schedules and DC dosage, we here focused on the molecular optimization of the therapy. In line with this, we simulated the effect in DC vaccination of the concerted modulation of combined intracellular regulatory processes and proposed several possibilities that can enhance DC-mediated immunogenicity. Taken together, we present a comprehensive time-resolved multi-level model for studying DC vaccination in melanoma. Although the model is not intended for personalized patient therapy, it could be used as a tool for identifying molecular targets for optimizing DC-based therapy for cancer, which ultimately should be tested in *in vitro* and *in vivo* experiments.

Keywords: melanoma, immunotherapy, gene networks, kinetic modeling, cellular therapy, bio-distribution, dendritic cell vaccine, systems medicine

INTRODUCTION

Dendritic cells (DCs) are the strongest stimulators of our immune response (Fong and Engleman, 2000). They are the most prevalent antigen-presenting cells in the immune system and regulate the systemic antigen presentation process. The ability to culture DCs *in vitro* and load them with exogenous antigens and their ability to subsequently activate cytotoxic T cell immunity makes them interesting candidates for cancer immunotherapy vaccines (Steinman, 1989; Timmerman and Levy, 1999; Bullock et al., 2003; Michiels et al., 2005; Morandi et al., 2006; Palucka and Banchereau, 2013; Schaft et al., 2013; Sprooten et al., 2019). Currently, two approaches to endow DCs with the antigenic T-cell epitopes are mainly pursued: exogenous peptides can be loaded directly onto the surface of the DCs, where they replace the endogenous peptides within the HLA-molecules. Alternatively, the antigens can be expressed within the DCs by mRNA transfection, to employ the natural antigen-processing machinery of the DCs, which generates epitopes from the encoded antigens and presents them in its HLA molecules (Sprooten et al., 2019). For instance, DCs are pulsed with tumor antigens in form of proteins or peptides (Timmerman and Levy, 1999) or electroporated or transfected with mRNA encoding tumor antigens to generate cancer vaccines (Michiels et al., 2005; Schaft et al., 2013). Specifically, the data showed that successfully transfected DCs express 10 times more antigens than those electroporated with tumor mRNAs and thus can activate more T cells (Schaft et al., 2013). Administered as a vaccine, DCs can induce protective anti-tumor immunity (Timmerman and Levy, 1999). Furthermore, some studies showed that after priming T cells with DCs transfected with tumor mRNA, T cells with both effector and memory phenotypes can be found and both the primary and the recall T-cell response are triggered (Bullock et al., 2003; Morandi et al., 2006).

Compared to other therapy approaches such as adoptive T-cell transfer, the DC therapy shows better tolerance in cancer patients to enhance immune response (Abbas et al., 2018). For example, it has been shown that adoptive transfer with tumor-reactive T cells in melanoma patients can result in tumor regression, but also induce an autoimmune response to normal tissues that led to inflammatory skin lesions (Yee et al., 2000; Dudley et al., 2002). In contrast, Schreurs et al. demonstrated that peptide-loaded DC vaccine can induce strong anti-tumor immunity and reduce toxicity of the immune therapy (Schreurs et al., 2000).

DCs can be derived *in vitro* from blood monocytes, loaded with tumor antigens and matured by cytokine-cocktails including TNFα, IL-1β, and IL-6 combined with PGE2 (Pfeiffer et al., 2014) to be subsequently injected into the patient in the form of a vaccine (Timmerman and Levy 1999; Fong and Engleman, 2000; Abbas et al., 2018). Immature DCs are triggered to mature by stimulation with TNFα or lipopolysaccharide (LPS). Upon maturation, the DCs become motile and travel from the tissue to the T-cell areas of peripheral lymphatic organs for the antigen presentation. They start secreting a variety of cytokines and chemokines (such as IL-6, IL-8, and IL-12) that serve as co-stimulators and attractants for the activation of $CD8^+$ cytotoxic T cells. They also express surface molecules (e.g., CD70) that are used for the specialized interaction with the $CD8^+$ T cells. $CD8^+$ cytotoxic T lymphocytes are important effectors of anti-tumor immunity (Vesely et al., 2011; Abbas et al., 2018), and after the antigen presentation by DCs, successful stimulation of $CD8^+$ T cells depends on the composition of these co-stimulatory factors such as cytokines and chemokines. The NF-κB signaling pathway is crucial for DC maturation (Tas et al., 2005; Morandi et al., 2006; Hernandez et al., 2007; Pfeiffer et al., 2014), and strategies targeting the pathway are continuously being developed to further improve this immunotherapy approach. One promising method, for example, is the electroporation of DCs with mRNA encoding constitutively active IKKβ that can activate the NF-κB signaling pathway and upregulate maturation markers such as CD40, CD70, CD80, OX40L, IL-12, and IL-8 leading to the persistent proliferation of $CD8^+$ T cells with a memory phenotype (Pfeiffer et al., 2014).

In addition to experimental studies, researchers have developed computational models to study dynamic systems accounting for immunity against cancer. Such models not only help to dissect the molecular mechanism underlying immune response against cancer but also to design experiments to improve available anti-cancer immunotherapies. For instance, the model developed by Castiglione et al. describes the dynamics between DCs, $CD8^+$ T cells, and tumor cells using a system of ordinary differential equations (ODEs). The model was used to search for an optimal protocol for the drug treatment, i.e., the optimal amount of DCs per vaccine, the optimal timing for one injection, and the optimal number of injections (Castiglione and Piccoli, 2007). Another work focuses on a personalized application using patient-specific parameters, and therefore, the interaction between immune effector cells and tumor cells was considered in the model (Kogan et al., 2012). Gong et al. used multiscale agent-based modeling to describe the dynamics between cytotoxic T cells and cancer cells and their three-dimensional distribution. The model provides a framework that enables predictions of treatment/biomarker combinations for different cancer types based on patient data (Gong et al., 2017). Mathematical modeling of T cell-macrophage interactions within the tumor microenvironment showed that inhibition of macrophage is the most effective strategy to promote T cell function, and therefore improving the effectiveness of immunotherapies that target macrophages (Cess and Finley, 2020). Arulraj and Barik developed an ODE model to investigate the role of feedback loops in inhibition of T-cell function by PD-1 and identified that the tyrosine kinase Lck is a crucial regulator for PD-1 induced inhibition of T-cell receptor signaling (Arulraj and Barik, 2018). De Pillis and coworkers developed a mathematical model describing the DC vaccination for melanoma and utilized it to propose therapy schedule that can improve the efficacy of the vaccine (DePillis et al., 2013). Santos and coworkers integrated transcriptomic data with mechanistic modeling of DC vaccination for melanoma to detect mechanisms that are related to sensitivity and resistance of the immunotherapy (Santos et al., 2016). So far, most of the published models have considered only cell-to-cell communications through direct contact or the secretion of

cytokines and chemokines. However, intracellular biochemical networks that are crucial for regulating cell function can be tuned to improve immunotherapies (Lai et al., 2021). Therefore, integrating them into multi-level computational models offers the opportunity to simulate and analyze molecular events that can determine the efficiency of anti-cancer immunotherapies.

In this work, we developed a multi-level model accounting for DC-based anti-cancer immunotherapy. By calibrating, simulating, and analyzing the model, we aimed to understand the molecular mechanism and cell-to-cell interactions that are crucial for regulating DC-mediated immunogenic function and therefore identifying molecules that can improve the efficiency of the DC-based immunotherapy. Specifically, the model is composed of three parts representing different stages of the DC immunotherapy – the bio-distribution of the DCs in the human organs, the biochemical reactions regulating the DCs' maturation, and DC-mediated activation of $CD8^+$ T cells. Next, we calibrated the model using several experimental data sets accounting for the dynamics and bio-distribution of intravenously injected DCs in the human body, the kinetics of molecules during DC maturation, and the dynamics of the T cell population after the injection of the DC vaccine, respectively. Then, we performed sensitivity analysis on model parameters to identify molecules and biochemical reactions that are impactful on a DC-mediated T-cell response. We found the NF-κB regulators (i.e., IKKβ and IκBα) and cytokines (i.e., IL-6 and IL-8) are top-ranking molecules for regulating the T-cell response. Finally, we ran simulations to quantify how modulating the expression of the identified molecules can change the number of memory T cells. Such results lay the basis for experimental validation of the effects of the identified molecules for improving the efficiency of DC immunotherapy. Taken together, the modeling approach allows for the effective integration of experimental data into a multi-level model accounting for DC-based anti-cancer immunotherapy. Although the model is not intended for personalized patient therapy, it could be used as a tool for identifying molecular targets for optimizing DC-based therapy for cancer, which ultimately should be tested in *in vitro* and *in vivo* experiments.

MATERIALS AND METHODS

Model Construction and Simulation

We developed a multi-level model accounting for three stages of DC immunotherapy – the spreading and distribution of intravenously injected DCs in the human organs, the biochemical reactions regulating the DCs' maturation and activation, and DC-mediated T-cell responses. The model was implemented using ODEs and simulated in MATLAB R2015b (*see* **Supplementary Material** for details). We used the MATLAB function *ode45* to solve the system accounting for the maturation of DCs. The function is based on the Dormand and Prince Runge-Kutta methods. We used the MATLAB function *dde23* to solve the equations accounting for a DC-mediated T-cell response. This method is based on an explicit Runge-Kutta method pair and especially for delay differential equations with constant delay. We ran simulations on a computer with a four core CPU (3.2 GHz) and 8 GB RAM.

Here, we listed some representative equations for each part of the model. Specifically, we used four ODEs to describe the temporal dynamics of DCs in the blood, the spleen, the liver, and the lung. A representative equation is shown as follows

$$\frac{d}{dt}DC_{Spleen}(t) = \mu_{BS}\frac{Q_{Blood}}{Q_{Spleen}}DC_{Blood}(t) - \mu_{S0}DC_{Spleen}(t) \quad (1)$$

The number of DCs in the spleen (DC_{Spleen}) is determined by the flow of DCs from the blood (DC_{Blood}) into the spleen at the rate (μ_{BS}) and its degradation rate (μ_{S0}). Q_{Blood} and Q_{Spleen} denote the volume of the blood and spleen, respectively.

The maturation of DCs in the spleen is characterized by 20 ODEs that account for the activation of the NF-κB pathway and its downstream targets such as cytokines that are crucial for T-cell responses. The equations accounting for the mRNA and protein of IL-8 are shown below

$$\frac{\mathrm{d}}{\mathrm{dt}}\mathrm{mIL8}(\mathrm{t}) = k^{mIL8}_{transc1} + k^{mIL8}_{trancs2}\cdot \mathrm{NF\kappa B}(t) - k^{mIL8}_{deg}\cdot \mathrm{mIL8}(t) \quad (2)$$

$$\frac{\mathrm{d}}{\mathrm{dt}}\mathrm{IL8_{DC}}(t) = k^{IL8}_{transl}\cdot \mathrm{mIL8}(t) - k^{IL8}_{deg}\cdot \mathrm{IL8_{DC}}(t) - k^{IL8}_{sec}\cdot \mathrm{IL8_{DC}}(t) \quad (3)$$

The transcription of IL-8 mRNA is determined by its basal transcription rate ($k^{mIL8}_{transc1}$) and another term ($k^{mIL8}_{trancs2}\cdot NF\kappa B(t)$) accounting for the regulation by NF-κB. k^{mIL8}_{deg} denotes the degradation of the IL-8 mRNA. The protein expression of IL-8 is determined by its translation from its mRNA (k^{IL8}_{transl}), its degradation (k^{IL8}_{deg}), and its secretion (k^{IL8}_{sec}) from DCs into the spleen.

The activation of T cells is modeled using four ODEs. The equations describe the process of how lymph node T cell activation translates to different phenotypes of T cell subsets such as early effector, short-lived effector, and memory T cells. The equation describing memory T cells is shown as follows

$$\frac{\mathrm{d}}{\mathrm{dt}}M(t) = k^{EE}_{diff2}\cdot EE(t) + 0.1\cdot k^{SLE}_{deg}\cdot SLE(t) \quad (4)$$

The number of memory T cells (M) is translated from early effector (EE) and short-lived effector (SLE) T cells with the rates of k^{EE}_{diff2} and k^{SLE}_{deg}, respectively. The constant 0.1 denotes that in experiments only 10% of the short-lived effector T cells become memory T cells (Badovinac et al., 2002; Mueller et al., 2013).

Structural Identifiability Analysis

Before model calibration, it is useful to investigate whether it is possible to obtain identifiable parameters using experimental data. Global structural identifiability analysis can provide a good indication of this. Therefore, we used the MATLAB toolbox GenSSI to perform structural identifiability analysis (Chis et al., 2011). The algorithm uses Lie derivatives of the ODE model to investigate the structural identifiability of ODE models. Theoretically, if sub-models are structurally identifiable, so is the entire model (Villaverde et al., 2016). Therefore, to reduce computation time we divided our model into separated

parts, including DC distribution, NF-κB activation, NF-κB-mediated secretion of cytokines, and T-cell response, and performed the analysis on each part.

Model Calibration

We used a hybrid method that combines global and local optimization algorithms to perform parameter optimization. Such a method facilitates global exploration of parameter space and fast local convergence (Villaverde et al., 2019). Specifically, we derived 1000 parameter sets using Latin hypercube sampling that not only samples random parameter values but also guarantees a uniformed distribution of parameter values in their defined ranges (Tang, 1993). The 1000 parameter sets are initial values of model parameters and were used for model calibration. We first fit the model to the experimental data using the pattern search algorithm (MATLAB function *patternsearch*) that is a global derivative-free optimization algorithm. The top 100 the solutions of the global optimization results (quantified by the cost function) were used for subsequent local optimization. The local optimization algorithm (MATLAB function *fmincon*) is gradient-based and allows for efficient searching that makes the cost function converge fast. We obtained the optimum parameter set that minimizes the cost function

$$\Phi(p) = \sum_{i,j} \left(\frac{y_i(t_j) - y_i(t_j, p)}{\max_j\left(y_i(t_j)\right) \cdot sd\left(y_i(t_j)\right)} \right)^2, \quad (5)$$

Where $y_i(t_j)$ represents the experimental data that shows the value of the observation $y_i(t_j)$ at time point j. $y_i(t_j, p)$ is the corresponding model simulation with a specific set of parameter values p. The cost function is normalized using the maximum value of each experimental data set (i.e., $\max_j(y_i(t_j))$) to prevent the biased effects caused by different data scaling during parameter estimation. If available, the cost function is additionally weighted by the standard deviation of the experimental data $sd(y_i(t_j))$.

We used the experimental data accounting for *in vitro* differentiated DCs into the liver, the spleen, the lung and other periphery after intravenous injection (Mackensen et al., 1999) to characterize the dynamics of DCs in human organs (**Supplementary Table S1**). We characterized NF-κB pathway activation in DCs (**Supplementary Table S2**), cytokine and chemokine production by DCs (**Supplementary Table S2**), and DC-mediated T cell responses (**Supplementary Table S3**) using the data from our previous publication (Pfeiffer et al., 2014). A detailed description of how each part of the model is calibrated can be found in **Supplementary Material**.

Practical Identifiability Analysis and Confidence Intervals of Parameters

To analyze the uncertainty in parameter estimates, we computed Pearson correlation coefficients to quantify their linear dependence using the top 100 out of 1000 estimates. Among the top 100 parameter estimates, we used the best 15 parameter estimates that show the minimum value in the cost function to calculate the confidence intervals of estimated parameters. Specifically, for each estimated parameter we generated 1000 bootstrap samples using its estimated values in the best 15 parameter estimates. Then, we used the mean value and standard deviation of the 1000 samples to derive the parameters' 95% confidence intervals. We performed the analyses using the MATLAB function *bootci*.

Sensitivity Analysis

We performed global sensitivity analyses to quantify the impact of model parameters on the dynamics of the system. We used the Sobol method that considers variations within the entire variability space of the model parameters (Saltelli et al., 2008; Sarrazin et al., 2016). We computed two types of indices: first-order indices (main-effects) and total-order indices (total-effects). The former measures the direct contribution from a model parameter (e.g., the total amount of NF-κB) to a model variable (e.g., the count of memory T cells), while the latter measures the overall contribution including the direct contribution and the amplification of this contribution due to interactions with all other model parameters (Sarrazin et al., 2016). The analysis was performed using the MATLAB toolbox *SAFE* (Pianosi et al., 2016) and the detailed computation of the sensitivity indices can be found in **Supplementary Material**.

RESULTS

The Multi-Scale Model Accounting for DC-Based Anti-cancer Immunotherapy

We developed a multi-scale model accounting for DC-based anti-cancer immunotherapy. We considered different stages of the DC therapy: *1*) the bio-distribution of DCs in the human body after the treatment, *2*) the biochemical pathways underlying DC maturation, and *3*) the DC-induced immune response such as activation of $CD8^+$ T cells.

We characterized the trafficking and distribution of dendritic cells (DCs) in the human body using published data (Ludewig et al., 2004) (**Figure 1**; *see* **Supplementary Material** for details). Specifically, DCs are administrated into patients through intravenous injection. The injected DCs mainly spread into the liver, the lung, the spleen, and other peripheries. According to the data (Mackensen et al., 1999; Ludewig et al., 2004), after reaching the liver, DCs reside there, while DCs enter quickly into the lung but also decrease to a minimal level. In our model, we used the spleen as a representative lymphoid organ, in which effective, antigen presentation-mediated interactions between T and dendritic cells happen (Mackensen et al., 1999; Barinov et al., 2017; Abbas et al., 2018).

Concerning the pathways underlying DC maturation and activation, we further considered in the model the NF-κB pathway underlying DC maturation; this part of the model was adapted from our previous results (Schulz et al., 2017) (**Figure 1**; *see* **Supplementary Material** for details). In our model, mature DCs secrete a variety of cytokines (e.g., IL-12,

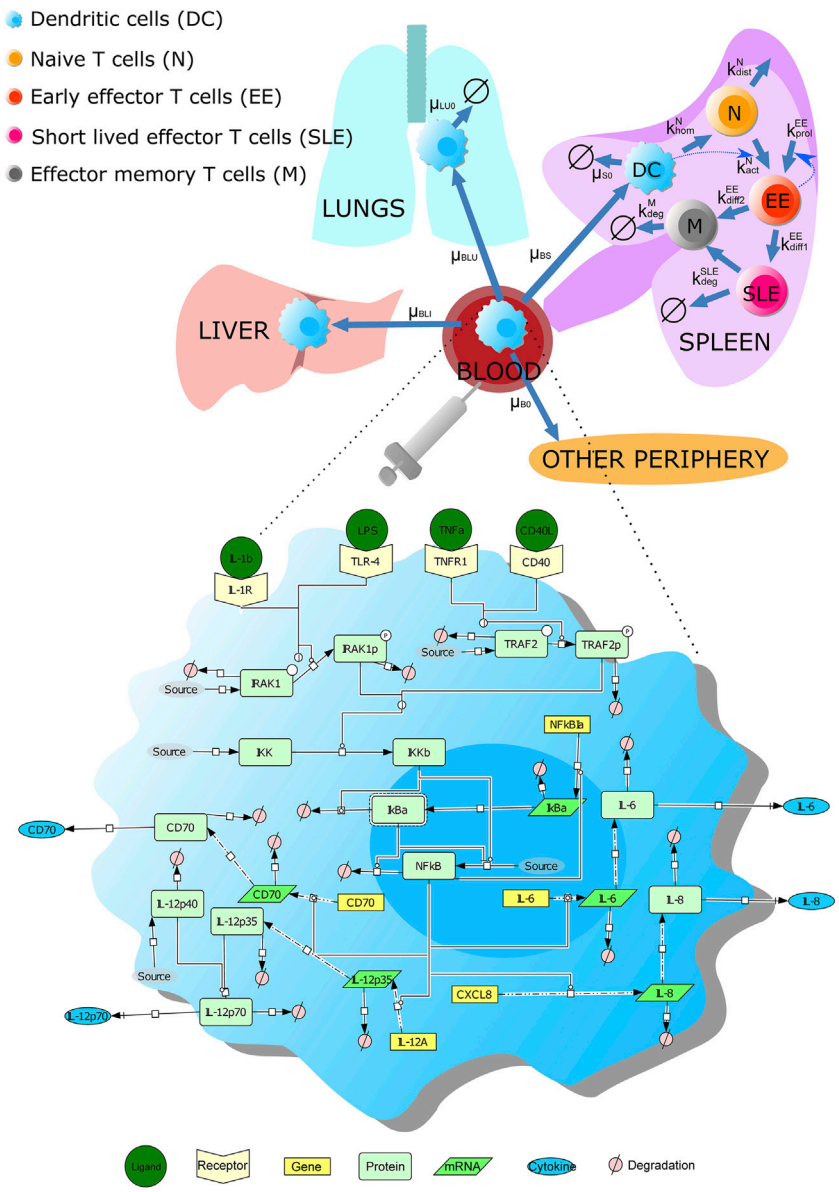

FIGURE 1 | Scheme of the multi-scale model accounting for DC vaccine against cancer. The multi-level model contains three parts: the kinetics and bio-distribution of intravenously injected DCs in human organs (including the liver, the lung, and the spleen), the signaling pathways underlying DC maturation, and DC-mediated T-cell response. The labels next to the blue arrowed lines are the corresponding model parameters. The signaling pathway in DCs is drawn using Systems Biology Graphical Notation. A detailed description of the model can be found in **Supplementary Material**.

IL-6, and IL-8) that can lead to T cell activation. The production of the cytokines is due to the stimulation of receptors (such as TNFα receptor, IL-1 receptor, CD40 receptor, and TLR4), leading to the activation of the NF-κB signaling pathway. Besides, we considered a surface protein CD70 expressed by DCs after stimulation, as the protein can induce the expansion of antigen-specific $CD8^+$ T cells.

Finally, we included a model module accounting for T cell activation by DCs in the spleen. The process was modeled considering three phases: *1*) a short-term interaction between the naive T cells and DCs; *2*) upregulation of activation markers and initiation of IFNγ and IL-2; and *3*) T cell proliferation after contact with DCs.

Taken together, we developed a model accounting for the life cycle of intravenously injected DCs from their spreading in human organs to inducing a T-cell response in the spleen. The resulting model contains 25 variables and 46 parameters (*see* **Supplementary Material** for details). The model includes not only cell population dynamics in human organs but also biochemical reactions that are crucial for DC maturation, making it an *in silico* platform to investigate intracellular manipulation of DCs utilized in vaccination against the tumor.

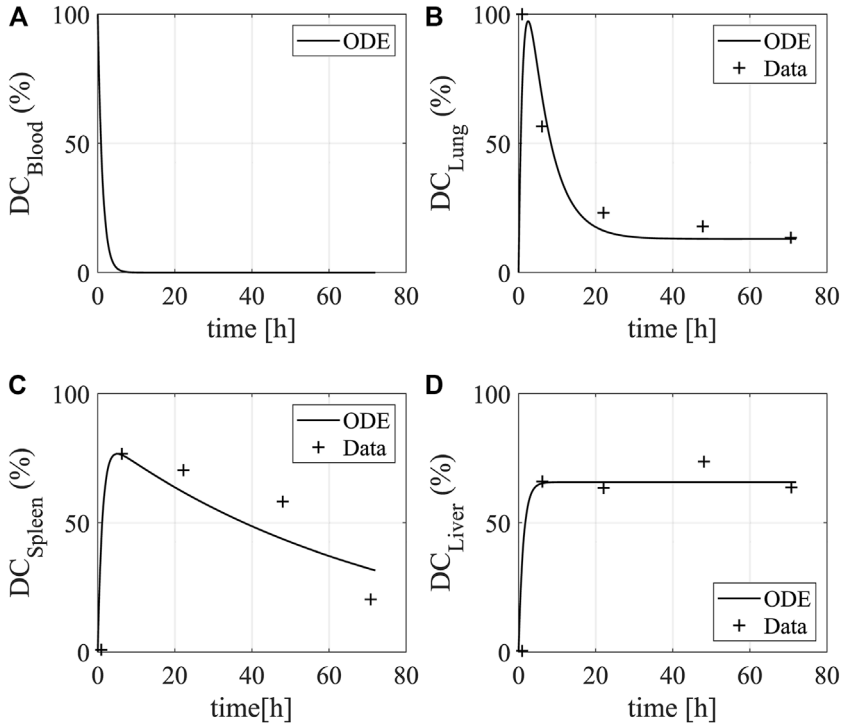

FIGURE 2 | Dynamics of DCs in human organs. The plots show the bio-distribution and kinetics of DCs in **(A)** the blood **(B)** the lung, **(C)** the spleen, and **(D)** the liver. The data show the uptake (y-axis) of intravenously injected DCs over time (x-axis). The lines and star asterisks denote model simulations and experimental data, respectively. The experimental data is from **Figure 2** in Mackensen et al. (1999). The temporal distribution of DCs were quantified by radioactivity in the lung, spleen, and liver of a patient after intravenous injection for 72 h.

Model Calibration Using Experimental Data

After constructing the multi-scale model, we performed structural identifiability analysis to identify whether model parametrizations with different values can produce the same simulations results (*see* **Materials and Methods**). The results showed that the whole model is not structurally identifiable. Specifically, the DC distribution part of the model is structurally non-identifiable, and this is caused by the parameters accounting for volumes of human organs (Q_{Blood}, Q_{Spleen}, Q_{Lung}, and Q_{Liver}), So, we fixed their values using the physiological information (**Supplementary Table S1**). The part accounting for NF-κB activation is structurally non-identifiable, and this is caused by parameters accounting for the phosphorylation rate of IRAK1 (k_{ph2}^{IRAK1}) and TRAF2 (k_{ph2}^{TRAF2}). Hence, we made their values equal to other phosphorylation processes catalyzed by other enzymes (**Supplementary Table S2**). The other model parts are structurally identifiable, and they account for NF-κB-mediated secretion of cytokines and chemokines and T cell response.

Next, we characterized the model parameters using published experimental data sets (*see* **Materials and Methods**). We separately calibrated the model using independent datasets that account for the dynamics of the system at different levels. Such a strategy is suitable and has been used for biological models composed of parts with different structural, time, and space scales (Vera et al., 2013).

We used the data that quantify injected DCs' activities in the lung, liver, spleen, and blood to characterize model parameters associated with the trafficking and distribution of DCs in the human body (Mackensen et al., 1999). The obtained model can reproduce the data available (**Figure 2**). After DCs are injected into the blood, they quickly spread into the other organs and the amount of DCs decreases to zero in the blood. DCs traffic into the lung leading to a temporal increase followed by a quick drop, and afterward, the DCs stay at a low level. DCs enter the liver and remain stable in number for up to 72 h (Mackensen et al., 1999). In the spleen, the amount of DCs rapidly reaches a peak and gradually decreases as they circulate in the body after provoking a T-cell response.

As the model equations accounting for the NF-κB pathway underlying DC maturation were adapted from our previous model, we used their original parameter values as initial values and re-calibrated them by fitting the model simulations to the experimental data measuring NF-κB pathway activation after LPS stimulation (Bode et al., 2009). Using the data, we characterized the dynamics of IκBα mRNA and protein and NF-κB in DCs (**Figure 3**). The LPS stimulation upregulates the expression of free NF-κB, as the increased IKKβ by the stimulation releases NF-κB from the complex formed by NF-κB and IκBα and degrades IκBα through phosphorylation. The free NF-κB promotes the transcription of the IκBα mRNA, leading to the recovery of IκBα that downregulates the expression of free NF-κB through

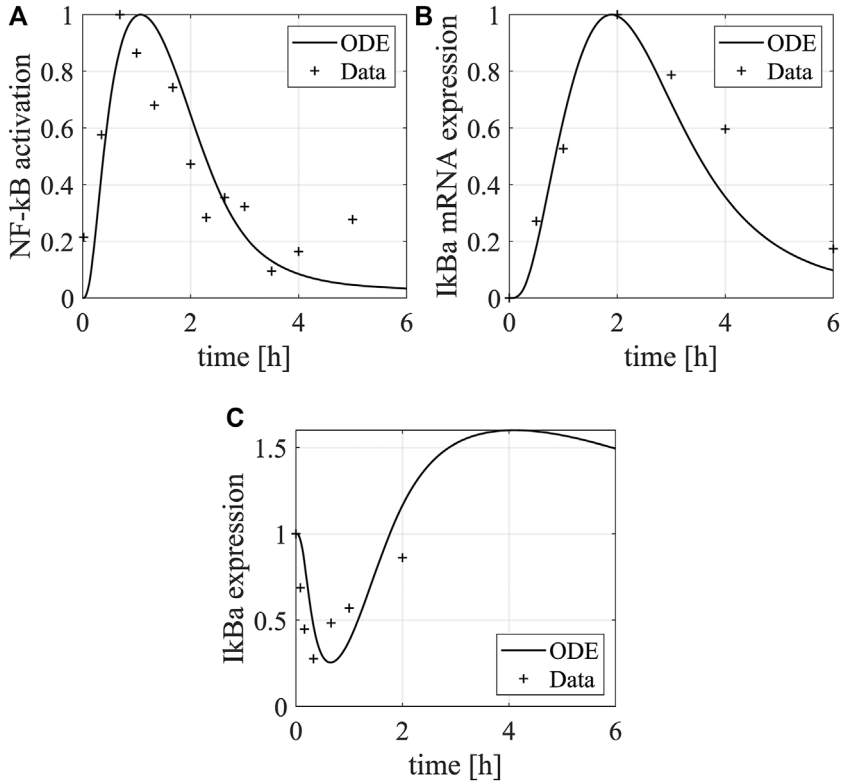

FIGURE 3 | Dynamics of IκBα and NF-κB in DCs. The plots show the dynamics of **(A)** NF-κB protein and **(B)** IκBα mRNA and **(C)** protein in DCs after LPS stimulation. The lines and asterisks denote model simulations and experimental data, respectively. The NF-κB activation was characterized by its binding activity to DNA, and the experimental data were normalized to the maximal binding activity (**Figure 3C** in Bode et al., 2009). The data shown here is a representative of three independent experiments. The IκBα mRNA was measured by qPCR (**Figure 5A** in Bode et al., 2009) and its relative mean expression (normalized to the maximal value) in comparison to the mRNA encoding the house-keeping gene β-actin was shown. The IκBα protein expression was quantified using a representative western blot (**Figure 3A** in Bode et al., 2009) and normalized to the maximal value. The western blot data was quantified using the software ImageJ.

a negative feedback loop. Besides, we used another set of data to characterize the dynamics of cytokines and surface markers after electroporating DCs with RNAs encoding constitutively active IKKα and -β (caIKK) that can activate the NF-κB pathway (Pfeiffer et al., 2014). Such treatment results in upregulation of IL-12, IL-6, IL-8, and CD70 for 72 h (**Figure 4**) and these markers are crucial for priming a T-cell response.

To characterize the model parameters that are associated with T-cell priming by DCs in the spleen, we used the *in vitro* data that show dynamics of the T-cell population after co-culturing them with control DCs or caIKK-DCs (Pfeiffer et al., 2014). Compared to the control DCs, the caIKK-DCs secret more cytokines such as IL-12, IL-8, IL-6, and TNF (Pfeiffer et al., 2014) and increase the production of T cells (**Figure 5**).

Furthermore, we performed practical identifiability analysis in parameter estimates (*see* **Materials and Methods**). This allowed us to examine whether the estimated parameters are practically identifiable – the estimated model parameters have unique values that fit model simulations to experimental data used for model calibration. As shown in **Figure 6A**, the estimated parameters for DC distribution have no correlation with each other suggesting the corresponding parameters are practically identifiable. This is confirmed by the distribution of estimated parameter values in the best 15 parameter estimates that show the minimum cost function value (**Supplementary Figure S1**). All estimated parameters for DC distribution have unique values for the best parameter estimates. In addition, the model parameters accounting for the NF-κB pathway underlying DC maturation show moderate correlations (**Figures 6B,C**). Among the 28 estimated parameters, five are practically non-identifiable and they are k_{ph1}^{TRAF2}, k_{deg}^{TRAF2p}, k_{deg}^{mIL6}, $k_{transc2}^{mIL8}$, and k_{deg}^{IL8} (**Supplementary Figure S2**). The non-identifiable parameters show small variances in their estimated values (**Supplementary Table S2**). This is due to the relatively small number of experimental data that are available for parameter estimation (Raue et al., 2009). The Michaelis-Menten coefficient K_4 is the only parameter estimated to fit model simulations to the data accounting for T-cell dynamics (**Supplementary Table S3**). The estimated value of K_4 is practically identifiable for its unique value in the best parameter estimates (**Supplementary Figure S3**). Taken together, most model parameters are practically identifiable because of their unique estimated values in the best parameter estimates. The practically non-identifiable parameters have confidence intervals with small ranges, suggesting minor influences on their biological interpretability.

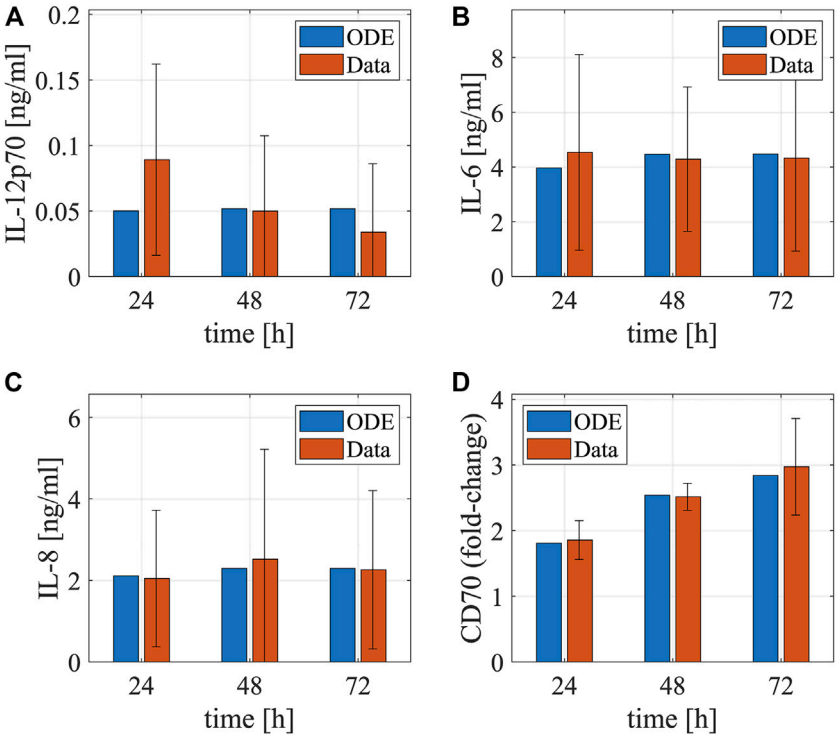

FIGURE 4 | Dynamics of cytokines and membrane proteins in DCs. The bar plots show the temporal concentrations of **(A)** IL-12, **(B)** IL-6, **(C)** IL-8, and **(D)** CD70 after electroporating DCs with mRNAs encoding constitutively active IKKβ. The red and blue bars denote model simulations (the best fitting) and experimental data (mean ± standard deviation), respectively. The experiments were repeated for four times. The cytokine data are from **Figure 3A** in Pfeiffer et al. (Pfeiffer et al., 2014). The matured DCs' cytokine concentrations after electroporation of IKKβ mRNA in the supernatants were determined by cytometric bead array. The data were measured using samples from eight different donors at the respective time points. The CD70 data is from **Figure 1B** in Pfeiffer et al. (Pfeiffer et al., 2014). It was assessed by flow cytometry in matured DCs electroporated with IKKβ mRNA. Fold-changes of CD70 compared to the controls (no electroporation of IKKβ mRNA) were calculated using the mean fluorescence intensity.

Due to the lack of a complete data set that can characterize the dynamics of DCs used as an anti-cancer therapy, we calibrated model modules separately using relevant datasets from different publications. In all cases, the datasets were produced using human material or relevant experimental models that are generally accepted in the context of DC vaccine development (Brossart et al., 2001). We think they are complementary because they characterize the dynamics of the DC vaccination at different levels. This strategy has been used in other data-driven computational models (Sobotta et al., 2017, Hesse et al., 2021, Fey et al., 2015).

Identification of Crucial Parameters Affecting DC-Mediated T-Cell Responses

After finishing calibrating the model with experimental data, we used it to simulate a DC-mediated T-cell response. Before running simulations, we set $DC_{in} = 10^5$ as the data showed that about 10^5 DCs are required for a T-cell response with a 70% probability (Celli et al., 2012). We set $Q_{Spleen} = 10^5$ as the measured volume of a spleen is 10^5 mm^3 (Odorico et al., 1999). Besides, we assumed that the initial number of antigen-specific naive T cells in the spleen is 10^6, so we set $T_0 = 10^6$ (Celli et al., 2012, Henrickson et al., 2008). We simulated the dynamics of different T cells in the spleen after injection with two different DC vaccines: normal DCs and DCs electroporated with caIKKβ-RNA (caIKK-DCs). In the simulations, both types of DCs were injected at $t = 0$ h with different degradation rates of IKKβ that are caused by caIKK in DCs ($k_{deg}^{IKKb} = 0.840$ h^{-1} for normal DCs and $k_{deg,mod}^{IKKb} = 0.216$ h^{-1} for caIKK DCs).

As shown in **Figures 7A–D**, the DC vaccines result in the loss of naive T cells that differentiate into early effector T cells, which show a quick increase after the DC stimulation. The early effector cells gradually differentiate into short-lived effector T cells and memory T cells, both of which saturate at high levels. Compared to the normal DC vaccine, the caIKK-DCs increase the levels of short-lived effector and memory T cells by about 7-fold, demonstrating the enhanced immunogenic potency of the caIKK-DCs. At the molecular level, such improved immunogenic potency is caused by the upregulated activation of NF-κB pathway by IKKβ in DCs (**Figures 7E,F**).

Successful activation of naive T cells depends mainly on successful and strong interaction with antigen-presenting DCs (Timmerman and Levy, 1999, Abbas et al., 2018). The goal of a DC vaccine is to increase the number of the resulting memory T cells that contribute to a rapid immune response upon

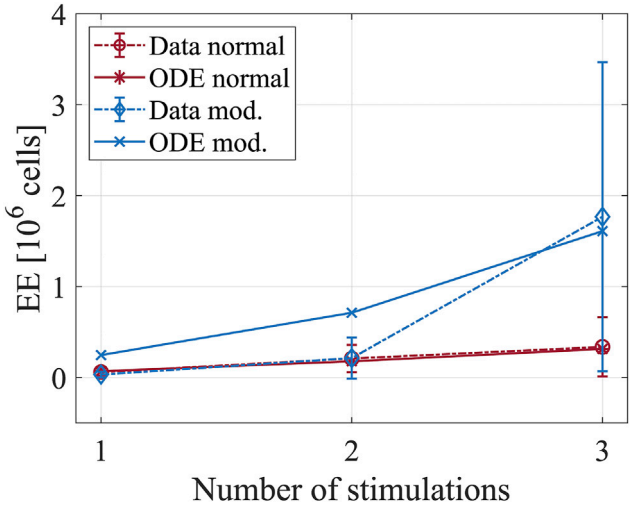

FIGURE 5 | Dynamics of T-cell populations after co-culturing them with DCs. The plot shows the number of short-lived effector cells after priming with mock-electroporated DCs (red lines) and DCs electroporated with mRNAs encoding constitutively active IKKβ (blue lines). The experimental data is from **Figure 4B** in Pfeiffer et al. (Pfeiffer et al., 2014). Four hours after electroporation, the DCs were used to stimulate MelA-specific $CD8^+$ T cells. In total, three stimulations were performed with an interval of 1 week between two subsequent stimulations. After each stimulation, the number of T cells was determined by tetramer-staining.

reactivation and form a long-lasting immunity (Akondy et al., 2017, Ando et al., 2019, Ahmed und Gray, 1996). Therefore, we performed sensitivity analyses to investigate the molecular mechanisms that are crucial for regulating the differentiation from naive T cells into early effectors and thus into memory T cells. Specifically, we used the global sensitivity method Sobol to compute sensitivities of model parameters to the population of memory T cells over the simulation time interval [0, 200] h (*see* **Material and Methods**). As shown in **Figures 8A,B**, the top-ranking 15 parameters show similar patterns in their sensitivity indices – the values are low shortly after the DC stimulation, gradually increase to a higher level, and stays at the high level until the end of the simulations. Among the top-ranking parameters, the most influential ones on the production of memory T cells are k_{deg}^{IKKb}, k_{act}^{N}, and N_{tot} that account for the degradation rate of IKKβ, the activation rate of naive T cells, and the total amount of free NF-κB. The less influential parameters are those associated with the degradation rate of IκBα mRNA (k_{mRNA}^{mIkBa}), the degradation rate of the IKK protein (k_{deg}^{IKK}, short-lived T-cell differentiation (k_{diff2}^{EE}), loss of free IκBα (k_{loss}^{IkBa}), and the production of IκBα mRNA and protein (k_{transc}^{mIkBa} and k_{tranl}^{IkBa}). The least influential parameters are the degradation rate and NF-κB-mediated transcription rate of IL-8 mRNA (k_{deg}^{mIL8} and $k_{transc2}^{mIL8}$), the degradation rate and NF-κB-mediated transcription rate of IL-6 mRNA (k_{deg}^{mIL6} and $k_{transc2}^{mIL6}$), the injected number of DCs (DC_{in}), and the homing rate of DCs into spleen (μ_{BS}). We obtained similar results while computing the sensitivities of model parameters to the total amount of memory T cells (computed by taking the integral over the simulation interval [0, 200] h) (**Figure 8C**). The only difference is that the DC emigration rate from blood to other organs (μ) replaces k_{diff2}^{EE} and appears as the least influencing parameters.

Further analysis showed that the length of simulation time and the variation of estimated parameter values have limited effects on model parameters' sensitivity indices for the total amount of memory T cells over the simulation interval. Specifically, after extending the simulation time to 500 h, the most influential parameters (i.e., k_{deg}^{IKKb}, N_{tot}, k_{act}^{N}, k_{deg}^{mIkBa}, and k_{deg}^{IKK}) remain unchanged (**Supplementary Table S5**). In longer stimulation time, several parameters (i.e., μ, μ_{BS}, DC_{in}, k_{tranl}^{IkBa}, k_{deg}^{mIL6} and $k_{transc2}^{mIL6}$) become less influential and two parameters k_{deg}^{IL6} (the degradation rate of IL-6) and K_4 become more influential. After increasing parameter variations to 90% of their estimated values, most of the top 15 parameters remain in the list but have different ranking (**Supplementary Table S6**). The exceptions are μ_{BS}, $k_{transc2}^{mIL6}$, and k_{deg}^{mIL8} that become less influential and drop out of the top 15 parameters. Besides, k_{deg}^{TRAF2p} (degradation rate of TRAF2), k_{deg}^{IL8}, and k_{diff2}^{EE} (differentiation rate of early effector T cells into memory T cells) become more influential and are new top 15 parameters.

Taken together, the results demonstrated the ability of the multi-scale model to differentiate the ability of different DC vaccines to stimulate a T-cell response and to reveal the molecular mechanisms that are important for $CD8^+$ T-cell activation through sensitivity analysis.

In Silico Experiments to Predict the Effects of Modulation of Selected Molecules on DC-Mediated T-Cell Responses

After identifying influential parameters that can modulate the production of memory T cells, we ran simulations to predict how corresponding biological processes can change the dynamics of the memory T-cell population. From the 15 most influential parameters, we have selected five corresponding to specific genes that could be experimentally manipulated. Specifically, we perturbed those parameters in an interval that decreases and increases their estimated values by 10 folds (i.e., the estimated value × [0.1, 10]) and computed the steady state of memory T cells. As shown in **Figure 9**, the total amount of free NF-κB (N_{tot}) and the degradation rate of IκBα mRNA (k_{deg}^{mIkBa}) can positively affect the population of memory T cells. Decreasing the value of N_{tot} by 90% eliminates the T memory cells while increasing its value leads to an increased cell population. The cell population peaks when the value of N_{tot} increases by about 3–4 folds and slightly decreases when N_{tot} is at its maximum level. Such a phenomenon could be explained by the negative feedback loop formed by NF-κB and IκBα. Free NF-κB activates the transcription of IκBα, whose encoding protein reduces free NF-κB by forming complexes. Thus, when the level of IκBα protein reaches a certain threshold, free NF-κB starts decreasing leading to a reduced number of T cells. In contrast, the decreasing of k_{deg}^{mIkBa} by 90% results in a slight reduction of T memory cells,

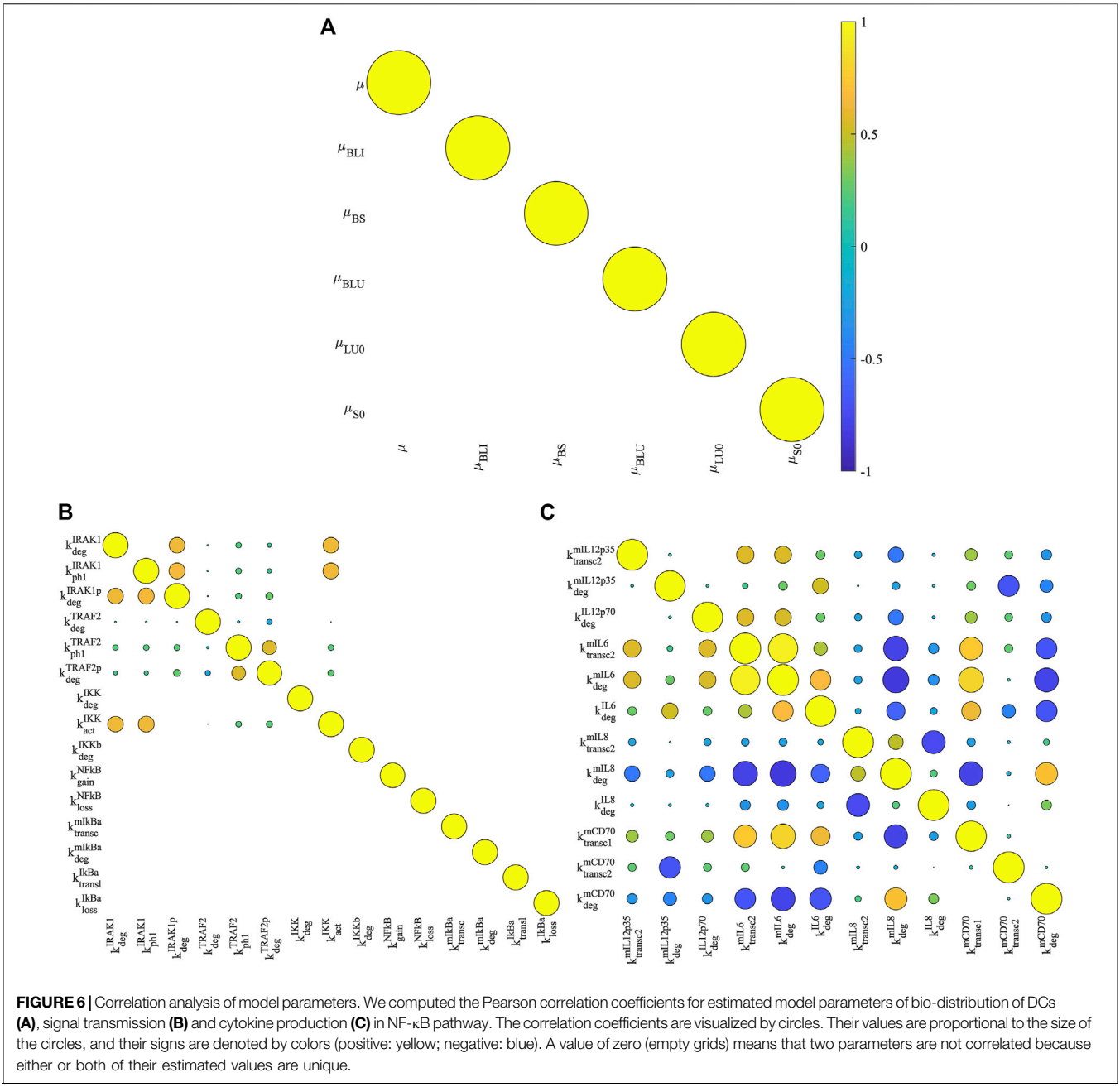

FIGURE 6 | Correlation analysis of model parameters. We computed the Pearson correlation coefficients for estimated model parameters of bio-distribution of DCs **(A)**, signal transmission **(B)** and cytokine production **(C)** in NF-κB pathway. The correlation coefficients are visualized by circles. Their values are proportional to the size of the circles, and their signs are denoted by colors (positive: yellow; negative: blue). A value of zero (empty grids) means that two parameters are not correlated because either or both of their estimated values are unique.

and a 10-fold upregulation in the parameter value leads to about a 3-fold increase in the cell population. Biologically, the IκBα protein is an inhibitor of NF-κB and traps free NF-κB through forming complexes (Hayden and Matthew, 2008), so decreasing the IκBα mRNA results in the reduced level of the protein, thereby releasing more free NF-κB in DCs that is required for T-cell activation.

On the other hand, perturbation of the degradation rates of IKKβ (k_{deg}^{IKKb}), IL-6 mRNA (k_{deg}^{mIL6}), and IL-8 mRNA (k_{deg}^{mIL8}) negatively affect the memory T-cell population. The dynamics of the cell population show similar patterns when the three parameters are perturbed in the specified interval – memory T cells are at the maximum level when the values of the parameters are reduced by 90% and at the minimum level when the values of the parameters increase by 10-folds. Biologically, IKKβ induces degradation of IκBα through phosphorylation (Hayden and Matthew, 2008), thereby releasing NF-κB from the complexes. Therefore, increasing the degradation of IKKβ leads to downregulation of NF-κB in DCs that reduce the induction of memory T cells. IL-6 and IL-8 secreted by DCs are required for differentiation of naive T cells into early effector T cells that further differentiate into short-lived effector T cells and memory T cells (Hunter and Jones, 2017, Taub et al., 1996), thereby increasing the degradation of the cytokines results in the decreased level of memory T cells.

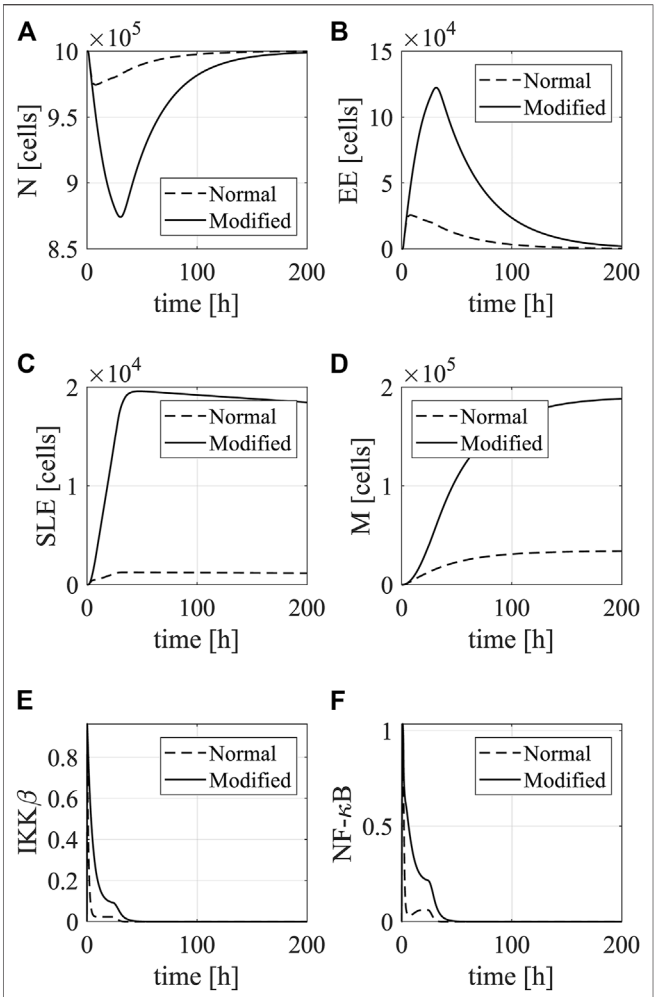

FIGURE 7 | Simulations of DC-mediated T-cell response. The plots show dynamics of **(A)** Naive T cells, **(B)** early effector T cells, **(C)** short-lived effector T cells, and **(D)** memory T cells in the spleen after stimulation with mock-electroporated DCs (dotted line) and caIKKβ-mRNA-electroporated DCs (solid line). Besides, we show the dynamics of **(E)** IKKβ and **(F)** NF-κB in DCs (non-dimensionalized).

Furthermore, we simulated how the population of memory T cells changes when combining two parameters and perturbing them simultaneously. We are particularly interested in modulating the expression levels of genes that can be manipulated in DCs and thereby improving the immunogenic potency of DC vaccines (**Figure 10A**). For instance, one can upregulate the expression level of NF-κB through electroporating DCs with mRNA encoding constitutively active IKKβ. In addition, one could downregulate IκBα using microRNAs that repress gene expression at the post-transcriptional level to increase the level of NF-κB in DCs. One could also increase the levels of DC-secreted cytokines (such as IL-6 and IL-8) that are involved in the T-cell response through electroporation of the corresponding mRNAs into DCs.

As shown in **Figure 10B** left column, directly increasing the expression of free NF-κB shows dominant effects on the upregulation of memory T cells for any combination with other parameters. However, this manipulation is experimentally difficult, as NF-κB is a protein complex and requires the presence of subunits and heterodimerization to be functional. Alternatively, it is experimentally achievable by manipulating the expression of NF-κB regulators. Simultaneously modulating the expression of IKKβ (upregulation) and IκBα (downregulation) can result in an effective increase of memory T cells (**Figure 10B** middle column). Modulating the expression of IκBα has stronger effects than modulating IKKβ. Compared to single modulation of the NF-κB regulators, the combined modulation increases the population of memory T cells by 80–120%. Modulating the levels of IκBα together with DC-secreted cytokines (IL-6 and IL-8) is also an effective regulation of memory T cells but shows different dynamics compared to the modulation of both NF-κB regulators (i.e., IKKβ and IκBα) (**Figure 10B** middle column). The cytokines are less influential than IκBα in regulating the T-cell response, as modulating IκBα directly affects the expression of free NF-κB that can regulate the expression of multiple cytokines and membrane proteins (i.e., IL-6, IL-8, IL-12, and CD70) involved in T-cell activation. When we manipulated the expression level of IKKβ with a cytokine, the effects on increasing memory T cells are mild (**Figure 10B** right column). When both cytokines were simultaneously modulated, the effect on increasing memory T cells is also limited. This is due to the reason that T-cell activation also depends on other proteins (i.e., IL-12 and CD70), and their unchanged levels act as a limiting factor in the increase of memory T cells. This is in line with findings in a biological model system examining CTL-priming and memory formation in the presence or absence of T-cell help, where it was shown that direct cell-cell contact was crucial and soluble factors were not sufficient (Hoyer et al., 2014). Taken together, the simulations predicted that combined manipulation of IκBα and cytokines is an efficient strategy for increasing memory T cells in experiments, and such manipulation shows better performance than manipulating the expression levels of only the NF-κB regulators or the cytokines.

DISCUSSION

Model derivation. In this work, we developed a multi-level model to study DC-based anti-cancer immunotherapy. The model considers three spatiotemporal, different but interlinked stages. The first stage models the bio-distribution of the intravenously injected maturated DCs into key organs of the human body including the lung, liver, and spleen. They are used as a representative immune organ to which DCs are trafficked. Except for intravenous injection, there are other clinical administrations of DC vaccine such as intra-lymph node injection and subcutaneous injection. However, from the physiological point of view, the immune response triggered by DCs may be similar (Mackensen et al., 1999). The rationale to include this mechanism was to achieve a precise quantitative description of how DCs get distributed between organs, how many DCs reach the spleen, and how long DCs remain in the

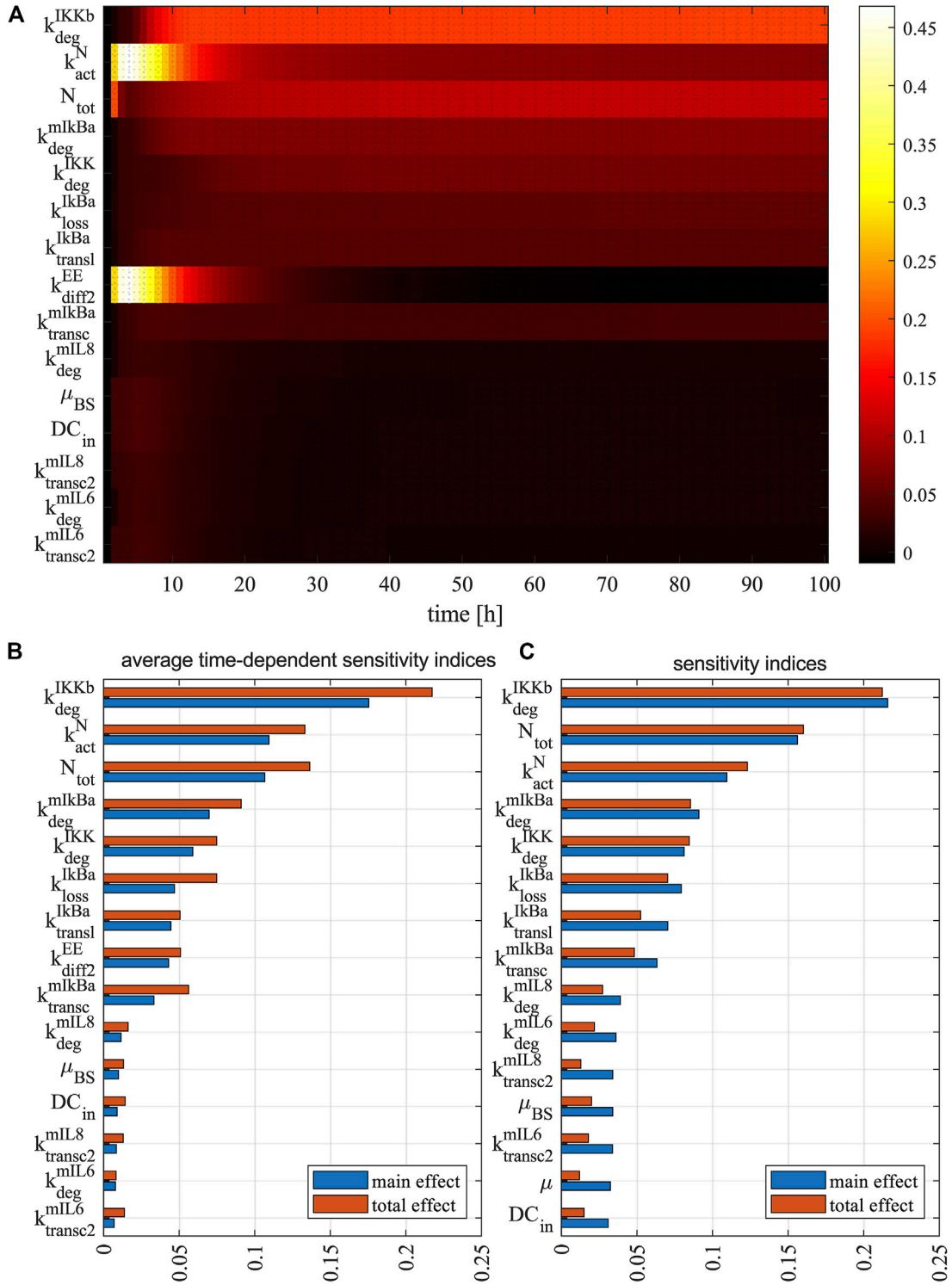

FIGURE 8 | Sensitivity analysis of model parameters. **(A)** The heat map shows the time-dependent sensitivity indices of model parameters. The bar plots show **(B)** average time-dependent sensitivity indices of model parameters and **(C)** sensitivity indices of model parameters to the total amount of memory T cells. The main effect (blue bar) measures the direct contribution from an individual parameter to the model variable, while the total effect (red bar) measures the overall contribution including direct contribution and the amplification of the direct contribution due to interaction with all model parameters. Each graph shows the result for the most 15 sensitive parameters. The sensitivity indices of all parameters can be found in **Supplementary Table S4**.

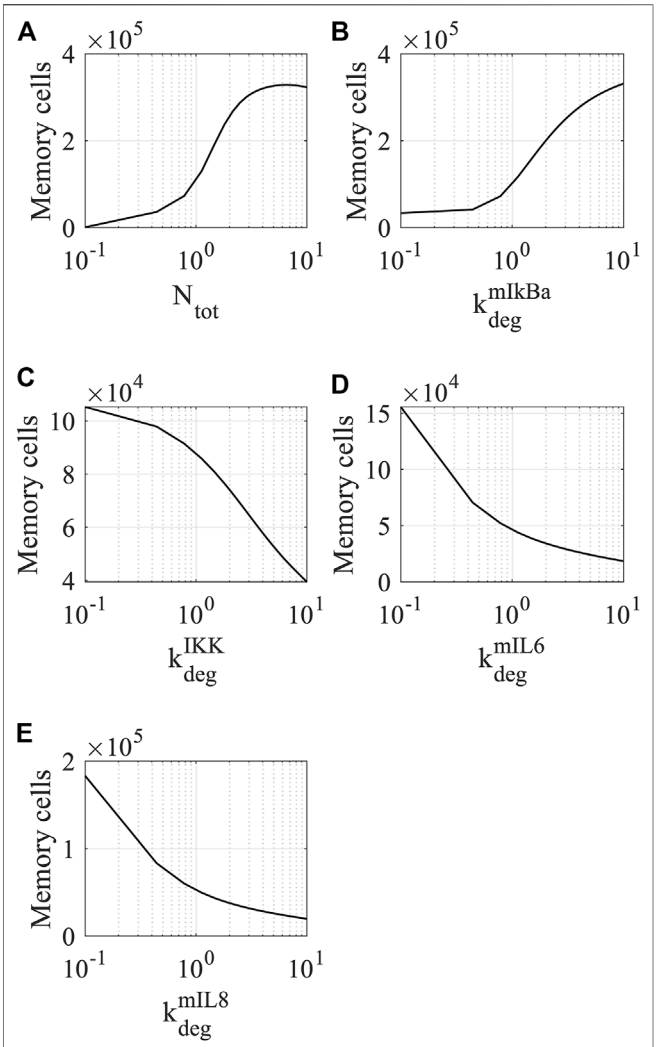

FIGURE 9 | Simulations of memory T-cell dynamics by perturbing the values of sensitive parameters. The response of memory T cells to the modulation of **(A)** total amount of NF-κB, **(B)** degradation rate of IκBα mRNA, **(C)** degradation rate of IKK, **(D)** degradation rate of IL-6 mRNA, and **(E)** IL-8 mRNA. The steady state of memory T cells was determined at $t = 4000$ h. Each parameter was perturbed within the interval (the estimated value × [0.1, 10]).

spleen for stimulating CTL response (Ludewig et al., 2004, Eggert et al., 1999). The second stage of the model accounts for the intracellular processes responsible for the *in vitro* maturation of DCs. This activation is induced by the activation of signaling pathways through ligands like TNFα, IL-1β, or LPS. Then, matured DCs secret cytokines (such as IL-6, IL-8, and IL-12) that are involved in the stimulation of a CTL response. It was important to include this level in the model because our aim was to investigate computationally the effect of molecular modulation of key regulatory pathways. In the last stage, the model simulates interactions between DCs and naive spleen resident T cells. The equations used account for the differentiation of T cells into early effector cells and the transformation of T cells into either short-lived effector cells or memory cells. Specifically, we simulated the effect of tumor antigen presentation, key cytokines secretions, and surface protein markers expression in the interaction of DC and T cells, and therefore the molecular and cell-cell communication are interlinked in the model. The amount of memory T cells is used as an indicator of the effectiveness of the DC-based immunotherapy.

In the literature, there are serval models devoted to understanding DC-mediated T-cell response in the context of immune response or immunotherapy. Most of them have a focus on only the cell populations' interactions and dynamics. For instance, Bianca et al. used ODEs to account for the different stages of the therapy including vaccination, immune cells, and tumor cells. The model includes the dynamics of both humoral and cellular immune responses to associated tumor antigens. The goal was to investigate different vaccination protocols using sensitivity analyses to improve treatment (Bianca et al., 2012). Ludewig et al. (2004) modeled DC distribution after vaccination to determine key parameters that control interactions between DCs and T cells. Furthermore, Serre et al. developed a mathematical model accounting for a cancer treatment combining immunotherapy with radiotherapy. The author used the model to simulate the primary and secondary (or memory) immune response induced by the combined therapy and proposed an optimal schedule for the therapy (Serre et al., 2016). By modeling the interactions between DCs with different types of T cells, Arabameri et al., (2018) showed an optimal configuration of DC vaccine to strengthen DC-T cell interactions, and therefore efficiently reducing tumor size. Castillo-Montiel et al. developed a model with delay differential equations to study cellular mechanisms of DC-based immunotherapy for melanoma. The authors showed the power of the model in reproducing data from experimental trials and predicting possible protocols to improve the immunotherapy while producing them in labs (Castillo-Montiel et al., 2015). Our model not only considers interactions between DCs and T cells but also the effect of signaling pathways governing the triggering of phenotypic changes in DCs, which underlie the efficacy of the CTL response. Such a multi-level model allows for the identification of molecular targets and other therapy parameters (such as vaccination schedules and DC dosage) that can be experimentally manipulated to improve the effectiveness of the therapy. In the future, the model can be expanded by considering the interactions between immune cells and tumor cells, such as the regulatory role of checkpoint proteins (e.g., CTLA-4 and PD-1) on T cell activation. This expansion will make the model suitable for studying the dynamics of immune-tumor interactions in the tumor microenvironment.

Model calibration. To calibrate the multi-level model, we used different data sets accounting for the three stages of the DC immunotherapy because in the literature, we could not find a single, comprehensive data set that measures the dynamics of all different aspects of the DC vaccination. Furthermore, obtaining new data for some of the processes in the model is currently very challenging due to ethical considerations. For example, the data on DC bio-distribution in humans utilized in the model could not be generated *de novo* with the current ethical rules, at least in

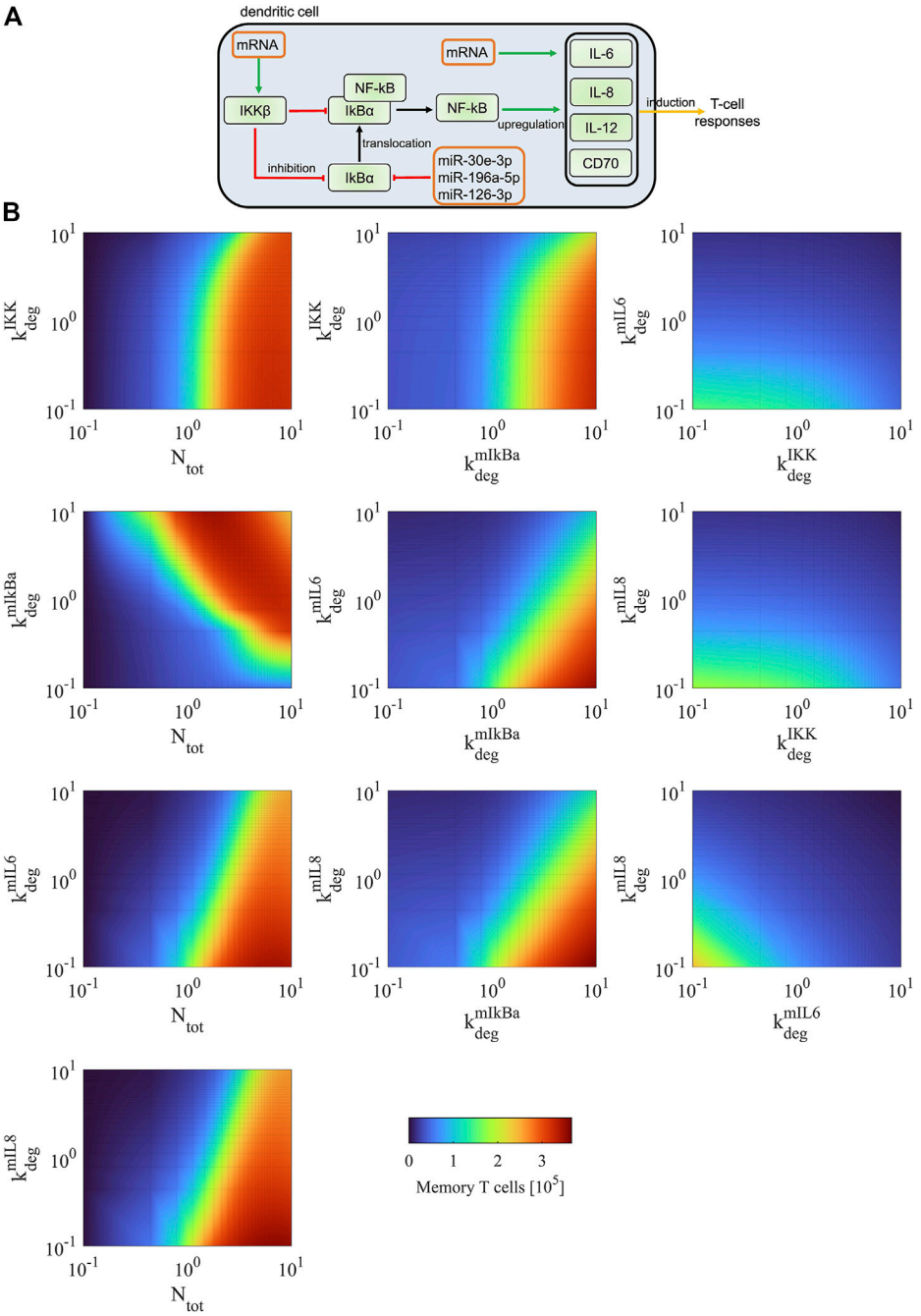

FIGURE 10 | Model predictions of DC-mediated T-cell responses. **(A)** Scheme of experimental strategies to increase T-cell responses. The manipulation of the identified molecules includes upregulation of IKKβ and cytokines using transfected mRNAs encoding the corresponding proteins and downregulation of IκBα using transfected microRNAs. It has been shown that miR-30e, miR-196a, and miR-126 can repress the expression of IκBα (Jiang et al., 2012, Huang et al., 2014, Feng et al., 2012). **(B)** We simulated the dynamics of memory T cells for simultaneous modifying the values of two combined parameters. The number of memory T cells was determined at its steady state (t = 4000 h). Each parameter was perturbed within the interval (the estimated value × [0.1, 10]).

Europe. An alternative is to calibrate the model utilizing mouse data, but we think the animal data could compromise the precision of cell dynamics such as the timing of DC bio-distribution. To circumvent these issues, we selected consistent data sets that represent the dynamics of the DC vaccination at different levels. In such a manner, the data complement each other to characterize the model at all scales.

While performing parameter optimization, we combined global and local optimization methods and fitted different parts of the model to the corresponding data set separately.

This strategy is widely used by the community to deal with complex and large systems whose objective functions are usually multi-modal and non-convex (Villaverde et al., 2019). Alternatively, one can perform parameter optimization using a multi-starting strategy that locally searches for the parameter space from different starting points (Raue et al., 2013). However, such a strategy becomes time-consuming when a model contains many parameters because to ensure reasonable coverage of the parameter space by local searches, the number of starting points will increase exponentially. A solution for such an issue is utilizing parallel computing that can significantly increase the computation efficacy on a high-performance computing cluster (Penas et al., 2017).

The hybrid approach (i.e., global pattern search followed by a gradient-based method) for ensures that the cost function for parameter estimation is not trapped in local minima. The best parameter estimates with the minimum cost function were used to assess practical identifiability of estimated parameters. The analysis showed that a few parameters in the NF-κB pathway underlying DC maturation are practically unidentifiable. Such uncertainties are most likely due to the lack of experimental data and the small variances of the estimated parameter values imply limited impacts on their biological interpretations. More advanced methods are available for analyzing the practical identifiability of estimated parameters (Fröhlich et al., 2014). For instance, the profile likelihood approach perturbs the value of a parameter in a small interval while keeping the other parameters unchanged to draw a profile of the cost function. The shape of the profile is used to identify whether or not the parameter is identifiable (Flassig and Sundmacher, 2012). In a fully clinic-oriented setup for model calibration and to solve the practical identifiability issue of parameters, one can produce additional experimental data for parameter estimation, simplify the model by reducing parameters, or fix the values of unidentifiable parameters using prior knowledge (Villaverde et al., 2021).

Sensitivity analyses to detect key parameters and processes. We performed sensitivity analyses to identify model parameters that are crucial to biological processes. Such a method has been widely used to evaluate the influence of model parameters (e.g., kinetic rate constants) on model outputs (e.g., the steady states of model variables) (Zi, 2011, Nikolov et al., 2010). Depending on strategies used for perturbing model parameters, sensitivity analysis can be classified into local and global analysis. Local sensitivity analysis provides a description of the behavior near a specified operating condition, whereas global sensitivity analysis uses wide ranges of parameter spaces and addresses global behavior of model parameters using statistical methods (Frey and Patil, 2002). We used the Sobol method for performing sensitivity analysis, but there are other methods for computing sensitivity coefficients based on rank transforms (such as partial rank regression coefficient) that show better performance on nonlinear and non-monotonic models (Frey and Patil, 2002). Using both local and global sensitivity analysis, our data showed consistent results in identifying sensitive parameters for affecting the population of memory T cells, implying the significant impact of the corresponding molecules on CTL responses. The results indicated that intracellular or intercellular processes (i.e., DC biodistribution or DC-T cell interaction) influence the efficacy of DC vaccination at inducing memory T cells. Since others investigated cell-cell interactions (*see* (DePillis et al., 2013) for example.), we focused on the wiring of the intracellular DC circuits. The simulations suggested that the activity of several proteins belonging to the network can affect the therapy effectiveness in terms of memory T cell induction.

Predictive model simulations. Our simulations showed that the perturbation of NF-κB and its regulators (i.e., IKKβ and IκBα) have a strong impact on the population of memory T cells. This suggested that enhanced and long-lasting activation of the NF-κB pathway is particularly effective in improving the immunogenic potency of DCs. Since our model accounts for the effect of known negative feedback loops regulating NF-κB activation, the model predictions point to strategies that can help in circumventing the detrimental effect of these loops. However, only improving the population of effective T cells may not be enough to ensure the long-term survival of cancer patients, as T cell subsets and heterogeneity of T cell states in tumors also play a major role in mediating immunotherapy responses (Philip and Schietinger, 2021). In addition, we showed that the cytokines (i.e., IL-6 and IL-8), necessary for the efficient activation of T-cell responses, are also influential on the effectiveness for the DC immunotherapy. It is also worth noting that IL-12 is another important immunostimulatory cytokine and incorporation or endogenous induction of this cytokine is shown to consistently benefit DC-based immunotherapy (Brussel et al., 2012). Furthermore, the production of cytokines by DCs depends not only on the activation of the NF-κB pathway but also on the methods used for isolating human monocytes that can differentiate into DCs (Elkord et al., 2005).

In the current version of the model, the intracellular signaling module is centered on the activation of the NF-κB signaling pathway, which is known to be pivotal in the maturation and activation of DCs. However, other regulatory pathways also play an important role in DC vaccination, and these pathways can crosstalk with each other forming a large regulatory network (Lai et al., 2021). Including these pathways into an intracellular module requires access to time-series data of their activation in DCs. Alternatively, they could be transformed into a Boolean or multi-logic model reproducing the wiring of the network as shown by others in the context of cancer (Khan et al., 2017) and immunity (Saez-Rodriguez et al., 2007). One could also build a hybrid model by combining ODE and Boolean modeling. The ODE model accounts for the core regulatory circuit around NF-κB and the Boolean model for genes and signaling proteins not belonging to the core circuit (Khan et al., 2014). Similarly, one could add spatial details into the interactions between DCs and T cells in the spleen. To do so, one has to develop models in partial differential equations or use agent-based models. Both types of models require detailed spatial information like the one provided by *in vivo* imaging. This is doable and has been implemented in mouse models for characterizing DC-T cell interactions in the lymph nodes (Celli et al., 2012).

Taken together, we demonstrated the potential of our multi-level model in tackling the complexity of DC-based immunotherapy and identifying potential molecules for

improving its effectiveness. Besides, we believe such an approach is adaptable and applicable to optimize other cell-based cancer immunotherapies like CAR-T cells.

DATA AVAILABILITY STATEMENT

The code used for performing model simulations and analyses in this work is accessible at https://doi.org/10.5281/zenodo.5744196. Further details and other data that support the findings of our study are available from the corresponding author upon request.

AUTHOR CONTRIBUTIONS

Concept of the study: XL, GS, and JV. Supervision: XL, GS, and JV. Funding acquisition: JV. Model derivation, calibration, and simulation: XL, CK, and JV. Figures: XL, CK, and GS. Writing of the manuscript: XL and CK. Edition of the manuscript: XL, CK, GS, NS, JD, and JV.

FUNDING

Our work in cancer and immunotherapy modeling is supported by the German Ministry of Education and Research (BMBF) through the e:Med initiatives: MelAutim (01ZX1905A) and KI-VesD (031L0244A). We also acknowledge the funding of our research activities in melanoma from the Manfred Roth-Stiftung, the Staedtler-Stiftung, the Trunk-Stiftung, the Matthias-Lackas-Stiftung, and the Hiege Stiftung.

SUPPLEMENTARY MATERIAL

The Supplementary Material for this article can be found online at: https://www.frontiersin.org/articles/10.3389/fcell.2021.746359/full#supplementary-material

REFERENCES

Abbas, A. K., Lichtman, A. H., and Pillai, S. (2018). *Cellular and Molecular Immunology*, 9. Philadelphia: Elsevier.

Ahmed, R., and Gray, D. (1996). Immunological Memory and Protective Immunity: Understanding Their Relation. *Science* 272, 54–60. doi:10.1126/science.272.5258.54

Akondy, R. S., Fitch, M., Edupuganti, S., Yang, S., Kissick, H. T., Li, K. W., et al. (2017). Origin and Differentiation of Human Memory CD8 T Cells After Vaccination. *Nature* 552, 362–367. doi:10.1038/nature24633

Ando, M., Ito, M., Srirat, T., Kondo, T., and Yoshimura, A. (2019). Memory T Cell, Exhaustion, and Tumor Immunity. *Immunological Med.* 43, 1–9. doi:10.1080/25785826.2019.1698261

Arabameri, A., Asemani, D., and Hajati, J. (2018). Mathematical Modeling of In-vivo Tumor-Immune Interactions for the Cancer Immunotherapy Using Matured Dendritic Cells. *J. Biol. Syst.* 26, 167–188. doi:10.1142/s0218339018500080

Arulraj, T., and Barik, D. (2018). Mathematical Modeling Identifies Lck as a Potential Mediator for PD-1 Induced Inhibition of Early TCR Signaling. *PLoS ONE* 13, e0206232. doi:10.1371/journal.pone.0206232

Badovinac, V. P., Porter, B. B., and Harty, J. T. (2002). Programmed Contraction of CD8+ T Cells After Infection. *Nat. Immunol.* 3, 619–626. doi:10.1038/ni804

Barinov, A., Galgano, A., Krenn, G., Tanchot, C., Vasseur, F., and Rocha, B. (2017). CD4/CD8/Dendritic Cell Complexes in the Spleen: CD8+ T Cells Can Directly Bind CD4+ T Cells and Modulate Their Response. *PLoS ONE* 12, e0180644. doi:10.1371/journal.pone.0180644

Bianca, C., Chiacchio, F., Pappalardo, F., and Pennisi, M. (2012). Mathematical Modeling of the Immune System Recognition to Mammary Carcinoma Antigen. *BMC Bioinformatics* 13, S21. doi:10.1186/1471-2105-13-s17-s21

Bode, K. A., Schmitz, F., Vargas, L., Heeg, K., and Dalpke, A. H. (2009). Kinetic of RelA Activation Controls Magnitude of TLR-Mediated IL-12p40 Induction. *J. Immunol.* 182, 2176–2184. doi:10.4049/jimmunol.0802560

Brossart, P., Wirths, S., Brugger, W., and Kanz, L. (2001). Dendritic Cells in Cancer Vaccines. *Exp. Hematol.* 29, 1247–1255. doi:10.1016/s0301-472x(01)00730-5

Brussel, I. V., Berneman, Z. N., and Cools, N. (2012). Optimizing Dendritic Cell-Based Immunotherapy: Tackling the Complexity of Different Arms of the Immune System. *Mediators Inflamm.* 2012, 1–14. doi:10.1155/2012/690643

Bullock, T. N. J., Mullins, D. W., and Engelhard, V. H. (2003). Antigen Density Presented by Dendritic Cells In Vivo Differentially Affects the Number and Avidity of Primary, Memory, and Recall CD8+ T Cells. *J. Immunol.* 170, 1822–1829. doi:10.4049/jimmunol.170.4.1822

Castiglione, F., and Piccoli, B. (2007). Cancer Immunotherapy, Mathematical Modeling and Optimal Control. *J. Theor. Biol.* 247, 723–732. doi:10.1016/j.jtbi.2007.04.003

Castillo-Montiel, E., Chimal-Eguía, J. C., Tello, J. I., Piñon-Zaráte, G., Herrera-Enríquez, M., and Castell-Rodríguez, A. (2015). Enhancing Dendritic Cell Immunotherapy for Melanoma Using a Simple Mathematical Model. *Theor. Biol. Med. Model.* 12, 11. doi:10.1186/s12976-015-0007-0

Celli, S., Day, M., Müller, A. J., Molina-Paris, C., Lythe, G., and Bousso, P. (2012). How many Dendritic Cells Are Required to Initiate a T-Cell Response? *Blood* 120, 3945–3948. doi:10.1182/blood-2012-01-408260

Cess, C. G., and Finley, S. D. (2020). Multi-Scale Modeling of Macrophage-T Cell Interactions within the Tumor Microenvironment. *Plos Comput. Biol.* 16, e1008519. doi:10.1371/journal.pcbi.1008519

Chis, O.-T., Banga, J. R., and Balsa-Canto, E. (2011). Structural Identifiability of Systems Biology Models: A Critical Comparison of Methods. *PLoS ONE* 6, e27755. doi:10.1371/journal.pone.0027755

De Odorico, I., Spaulding, K. A., Pretorius, D. H., Lev-Toaff, A. S., Bailey, T. B., and Nelson, T. R. (1999). Normal Splenic Volumes Estimated Using Three-Dimensional Ultrasonography. *J. Ultrasound Med.* 18, 231–236. doi:10.7863/jum.1999.18.3.231

DePillis, L., Gallegos, A., and Radunskaya, A. (2013). A Model of Dendritic Cell Therapy for Melanoma. *Front. Oncol.* 3, 56. doi:10.3389/fonc.2013.00056

Dudley, M. E., Wunderlich, J. R., Robbins, P. F., Yang, J. C., Hwu, P., Schwartzentruber, D. J., et al. (2002). Cancer Regression and Autoimmunity in Patients After Clonal Repopulation with Antitumor Lymphocytes. *Science* 298, 850–854. doi:10.1126/science.1076514

Eggert, A. A., Schreurs, M. W., Boerman, O. C., Oyen, W. J., de Boer, A. J., Punt, C. J., et al. (1999). Biodistribution and Vaccine Efficiency of Murine Dendritic Cells Are Dependent on the Route of Administration. *Cancer Res.* 59 (14), 3340–3345.

Elkord, E., Williams, P. E., Kynaston, H., and Rowbottom, A. W. (2005). Human Monocyte Isolation Methods Influence Cytokine Production from In Vitro Generated Dendritic Cells. *Immunology* 114, 204–212. doi:10.1111/j.1365-2567.2004.02076.x

Feng, X., Wang, H., Ye, S., Guan, J., Tan, W., Cheng, S., et al. (2012). Up-Regulation of microRNA-126 May Contribute to Pathogenesis of Ulcerative Colitis via Regulating NF-kappaB Inhibitor IκBα. *PloS One* 7 (12), e52782. doi:10.1371/journal.pone.0052782

Fey, D., Halasz, M., Dreidax, D., Kennedy, S. P., Hastings, J. F., Rauch, N., et al. (2015). Signaling Pathway Models as Biomarkers: Patient-Specific Simulations of JNK Activity Predict the Survival of Neuroblastoma Patients. *Sci. Signal.* 8 (408), ra130. doi:10.1126/scisignal.aab0990

Flassig, R. J., and Sundmacher, K. (2012). Optimal Design of Stimulus Experiments for Robust Discrimination of Biochemical Reaction Networks. *Bioinformatics* 28, 3089–3096. doi:10.1093/bioinformatics/bts585

Fong, L., and Engleman, E. G. (2000). Dendritic Cells in Cancer Immunotherapy. *Annu. Rev. Immunol.* 18, 245–273. doi:10.1146/annurev.immunol.18.1.245

Frey, H. C., and Patil, S. R. (2002). Identification and Review of Sensitivity Analysis Methods. *Risk Anal.* 22, 553–578. doi:10.1111/0272-4332.00039

Fröhlich, F., Theis, F. J., and Hasenauer, J. (2014). "Uncertainty Analysis for Non-identifiable Dynamical Systems: Profile Likelihoods, Bootstrapping and More," in Computational Methods in Systems Biology. CMSB 2014. Lecture Notes in Computer Science, Manchester, November 17–19, 2014. Editors P. Mendes, J. O. Dada, and K. Smallbone (Cham: Springer), 61–72. doi:10.1007/978-3-319-12982-2_5

Gong, C., Milberg, O., Wang, B., Vicini, P., Narwal, R., Roskos, L., et al. (2017). A Computational Multiscale Agent-Based Model for Simulating Spatio-Temporal Tumour Immune Response to PD1 and PDL1 Inhibition. *J. R. Soc. Interf.* 14, 20170320. doi:10.1098/rsif.2017.0320

Hayden, M. S., and Ghosh, S. (2008). Shared Principles in NF-Kb Signaling. *Cell* 132, 344–362. doi:10.1016/j.cell.2008.01.020

Henrickson, S. E., Mempel, T. R., Mazo, I. B., Liu, B., Artyomov, M. N., Zheng, H., et al. (2008). T Cell Sensing of Antigen Dose Governs Interactive Behavior with Dendritic Cells and Sets a Threshold for T Cell Activation. *Nat. Immunol.* 9, 282–291. doi:10.1038/ni1559

Hernandez, A., Burger, M., Blomberg, B. B., Ross, W. A., Gaynor, J. J., Lindner, I., et al. (2007). Inhibition of NF-Kb During Human Dendritic Cell Differentiation Generates Anergy and Regulatory T-Cell Activity for One but Not Two Human Leukocyte Antigen DR Mismatches. *Hum. Immunol.* 68, 715–729. doi:10.1016/j.humimm.2007.05.010

Hesse, J., Martinelli, J., Aboumanify, O., Ballesta, A., and Relógio, A. (2021). A Mathematical Model of the Circadian Clock and Drug Pharmacology to Optimize Irinotecan Administration Timing in Colorectal Cancer. *Comput. Struct. Biotechnol. J.* 19, 5170–5183. doi:10.1016/j.csbj.2021.08.051

Hoyer, S., Prommersberger, S., Pfeiffer, I. A., Schuler-Thurner, B., Schuler, G., Dörrie, J., et al. (2014). Concurrent Interaction of DCs with CD4+and CD8+T Cells Improves Secondary CTL Expansion: It Takes Three to Tango. *Eur. J. Immunol.* 44, 3543–3559. doi:10.1002/eji.201444477

Huang, F., Tang, J., Zhuang, X., Zhuang, Y., Cheng, W., Chen, W., et al. (2014). MiR-196a Promotes Pancreatic Cancer Progression by Targeting Nuclear Factor Kappa-B-Inhibitor Alpha. *PloS One* 9 (2), e87897. doi:10.1371/journal.pone.0087897

Hunter, C. A., and Jones, S. A. (2017). IL-6 as a keystone Cytokine in Health and Disease. *Nat. Immunol.* 16, 448–457. doi:10.1038/ni.3153

Jiang, L., Lin, C., Song, L., Wu, J., Chen, B., Ying, Z., et al. (2012). MicroRNA-30e* Promotes Human Glioma Cell Invasiveness in an Orthotopic Xenotransplantation Model by Disrupting the NF-κB/IκBα Negative Feedback Loop. *J. Clin. Invest.* 122 (1), 33–47. doi:10.1172/JCI58849

Khan, F. M., Marquardt, S., Gupta, S. K., Knoll, S., Schmitz, U., Spitschak, A., et al. (2017). Unraveling a Tumor Type-Specific Regulatory Core Underlying E2F1-Mediated Epithelial-Mesenchymal Transition to Predict Receptor Protein Signatures. *Nat. Commun.* 8 (1), 198. doi:10.1038/s41467-017-00268-2

Khan, F. M., Schmitz, U., Nikolov, S., Engelmann, D., Pützer, B. M., Wolkenhauer, O., et al. (2014). Hybrid Modeling of the Crosstalk Between Signaling and Transcriptional Networks Using Ordinary Differential Equations and Multi-Valued Logic. *Biochim. Biophys. Acta (Bba) - Proteins Proteomics* 1844, 289–298. doi:10.1016/j.bbapap.2013.05.007

Kogan, Y., Halevi–Tobias, K., Elishmereni, M., Vuk-Pavlović, S., and Agur, Z. (2012). Reconsidering the Paradigm of Cancer Immunotherapy by Computationally Aided Real-Time Personalization. *Cancer Res.* 72, 2218–2227. doi:10.1158/0008-5472.CAN-11-4166

Lai, X., Dreyer, F. S., Cantone, M., Eberhardt, M., Gerer, K. F., Jaitly, T., et al. (2021). Network- and Systems-Based Re-Engineering of Dendritic Cells with Non-Coding RNAs for Cancer Immunotherapy. *Theranostics* 11, 1412–1428. doi:10.7150/thno.53092

Ludewig, B., Krebs, P., Junt, T., Metters, H., Ford, N. J., Anderson, R. M., et al. (2004). Determining Control Parameters for Dendritic Cell-Cytotoxic T Lymphocyte Interaction. *Eur. J. Immunol.* 34, 2407–2418. doi:10.1002/eji.200425085

Mackensen, A., Krause, T., Blum, U., Uhrmeister, P., Mertelsmann, R., and Lindemann, A. (1999). Homing of Intravenously and Intralymphatically Injected Human Dendritic Cells Generated In Vitro from CD34 + Hematopoietic Progenitor Cells. *Cancer Immunol. Immunother.* 48, 118–122. doi:10.1007/s002620050555

Michiels, A., Tuyaerts, S., Bonehill, A., Corthals, J., Breckpot, K., Heirman, C., et al. (2005). Electroporation of Immature and Mature Dendritic Cells: Implications for Dendritic Cell-Based Vaccines. *Gene Ther.* 12, 772–782. doi:10.1038/sj.gt.33024710.1038/sj.gt.3302471

Morandi, F., Chiesa, S., Bocca, P., Millo, E., Salis, A., Solari, M., et al. (2006). Tumor mRNA-Transfected Dendritic Cells Stimulate the Generation of CTL that Recognize Neuroblastoma-Associated Antigens, Kill Tumor Cells: Immunotherapeutic Implications. *Neoplasia* 8, 833–842. doi:10.1593/neo.06415

Mueller, S. N., Gebhardt, T., Carbone, F. R., and Heath, W. R. (2013). Memory T Cell Subsets, Migration Patterns, and Tissue Residence. *Annu. Rev. Immunol.* 31, 137–161. doi:10.1146/annurev-immunol-032712-095954

Nikolov, S., Lai, X., Liebal, U. W., Wolkenhauer, O., and Vera, J. (2010). Integration of Sensitivity and Bifurcation Analysis to Detect Critical Processes in a Model Combining Signalling and Cell Population Dynamics. *Int. J. Syst. Sci.* 41, 81–105. doi:10.1080/00207720903147746

Palucka, K., and Banchereau, J. (2013). Dendritic-Cell-Based Therapeutic Cancer Vaccines. *Immunity* 39, 38–48. doi:10.1016/j.immuni.2013.07.004

Penas, D. R., González, P., Egea, J. A., Doallo, R., and Banga, J. R. (2017). Parameter Estimation in Large-Scale Systems Biology Models: A Parallel and Self-Adaptive Cooperative Strategy. *BMC Bioinformatics* 18 (1), 52. doi:10.1186/s12859-016-1452-4

Pfeiffer, I. A., Hoyer, S., Gerer, K. F., Voll, R. E., Knippertz, I., Gückel, E., et al. (2014). Triggering of NF-Kb in Cytokine-Matured Human DCs Generates Superior DCs for T-Cell Priming in Cancer Immunotherapy. *Eur. J. Immunol.* 44, 3413–3428. doi:10.1002/eji.201344417

Philip, M., and Schietinger, A. (2021). CD8+ T Cell Differentiation and Dysfunction in Cancer. *Nat. Rev. Immunol.* [Epub ahead of print]. doi:10.1038/s41577-021-00574-3

Pianosi, F., Beven, K., Freer, J., Hall, J. W., Rougier, J., Stephenson, D. B., et al. (2016). Sensitivity Analysis of Environmental Models: A Systematic Review with Practical Workflow. *Environ. Model. Softw.* 79, 214–232. doi:10.1016/j.envsoft.2016.02.008

Raue, A., Schilling, M., Bachmann, J., Matteson, A., Schelke, M., Kaschek, D., et al. (2013). Lessons Learned from Quantitative Dynamical Modelingin Systems Biology. *PLoS One* 8 (9), e74335. doi:10.1371/journal.pone.0074335

Raue, A., Kreutz, C., Maiwald, T., Bachmann, J., Schilling, M., Klingmüller, U., et al. (2009). Structural and Practical Identifiability Analysis of Partially Observed Dynamical Models by Exploiting the Profile Likelihood. *Bioinformatics* 25, 1923–1929. doi:10.1093/bioinformatics/btp358

Saez-Rodriguez, J., Simeoni, L., Lindquist, J. A., Hemenway, R., Bommhardt, U., Arndt, B., et al. (2007). A Logical Model Provides Insights into T Cell Receptor Signaling. *Plos Comput. Biol.* 3, e163. doi:10.1371/journal.pcbi.0030163

Saltelli, A., Ratto, M., Andres, T., Campolongo, F., Cariboni, J., Gatelli, D., et al. (2008). *Global Sensitivity Analysis: The Primer*, 3. Chichester, United Kingdom: Wiley-Interscience.

Santos, G., Nikolov, S., Lai, X., Eberhardt, M., Dreyer, F. S., Paul, S., et al. (2016). Model-Based Genotype-Phenotype Mapping Used to Investigate Gene Signatures of Immune Sensitivity and Resistance in Melanoma Micrometastasis. *Sci. Rep.* 6, 24967. doi:10.1038/srep24967

Sarrazin, F., Pianosi, F., and Wagener, T. (2016). Global Sensitivity Analysis of Environmental Models: Convergence and Validation. *Environ. Model. Softw.* 79, 135–152. doi:10.1016/j.envsoft.2016.02.005

Schaft, N., Wellner, V., Wohn, C., Schuler, G., and Dörrie, J. (2013). CD8+ T-Cell Priming and Boosting: More Antigen-Presenting DC, or More Antigen Per DC? *Cancer Immunol. Immunother.* 62, 1769–1780. doi:10.1007/s00262-013-1481-z

Schreurs, M. W., Eggert, A. A., de Boer, A. J., Vissers, J. L., van Hall, T., Offringa, R., et al. (2000). Dendritic Cells Break Tolerance and Induce Protective Immunity against a Melanocyte Differentiation Antigen in an Autologous Melanoma Model. *Cancer Res.* 60, 6995–7001.

Schulz, C., Lai, X., Bertrams, W., Jung, A. L., Sittka-Stark, A., Herkt, C. E., et al. (2017). THP-1-Derived Macrophages Render Lung Epithelial Cells Hypo-Responsive to *Legionella P* - a Systems Biology Study. *Sci. Rep.* 7 (1), 11988. doi:10.1038/s41598-017-12154-4

Serre, R., Benzekry, S., Padovani, L., Meille, C., André, N., Ciccolini, J., et al. (2016). Mathematical Modeling of Cancer Immunotherapy and its Synergy with Radiotherapy. *Cancer Res.* 76, 4931–4940. doi:10.1158/0008-5472.can-15-3567

Sobotta, S., Raue, A., Huang, X., Vanlier, J., Jünger, A., Bohl, S., et al. (2017). Model Based Targeting of IL-6-Induced Inflammatory Responses in Cultured Primary Hepatocytes to Improve Application of the JAK Inhibitor Ruxolitinib. *Front. Physiol.* 8, 775. doi:10.3389/fphys.2017.00775

Sprooten, J., Ceusters, J., Coosemans, A., Agostinis, P., De Vleeschouwer, S., Zitvogel, L., et al. (2019). Trial Watch: Dendritic Cell Vaccination for Cancer Immunotherapy. *OncoImmunology* 8, 1638212. doi:10.1080/2162402x.2019.1638212

Steinman, R. M. (1989). Dendritic Cells: Clinical Aspects. *Res. Immunol.* 140, 911–918. doi:10.1016/0923-2494(89)90054-0

Tang, B. (1993). Orthogonal Array-Based Latin Hypercubes. *J. Am. Stat. Assoc.* 88, 1392–1397. doi:10.1080/01621459.1993.10476423

Tas, S. W., de Jongde Jong, E. C., Hajji, N., May, M. J., Ghosh, S., Vervoordeldonk, M. J., et al. (2005). Selective Inhibition of NF-kappaB in Dendritic Cells by the NEMO-Binding Domain Peptide Blocks Maturation and Prevents T Cell Proliferation and Polarization. *Eur. J. Immunol.* 35, 1164–1174. doi:10.1002/eji.200425956

Taub, D. D., Anver, M., Oppenheim, J. J., Longo, D. L., and Murphy, W. J. (1996). T Lymphocyte Recruitment by Interleukin-8 (IL-8). IL-8-Induced Degranulation of Neutrophils Releases Potent Chemoattractants for Human T Lymphocytes Both In Vitro and In Vivo. *J. Clin. Invest.* 97, 1931–1941. doi:10.1172/JCI118625

Timmerman, J. M., and Levy, R. (1999). Dendritic Cell Vaccines for Cancer Immunotherapy. *Annu. Rev. Med.* 50, 507–529. doi:10.1146/annurev.med.50.1.507

Vera, J., Schmitz, U., Lai, X., Engelmann, D., Khan, F. M., Wolkenhauer, O., et al. (2013). Kinetic Modeling-Based Detection of Genetic Signatures that Provide Chemoresistance via the E2F1-p73/DNp73-miR-205 Network. *Cancer Res.* 73, 3511–3524. doi:10.1158/0008-5472.can-12-4095

Vesely, M. D., Kershaw, M. H., Schreiber, R. D., and Smyth, M. J. (2011). Natural Innate and Adaptive Immunity to Cancer. *Annu. Rev. Immunol.* 29, 235–271. doi:10.1146/annurev-immunol-031210-101324

Villaverde, A. F., Pathirana, D., Frohlich, F., Hasenauer, J., and Banga, J. R. (2021). A Protocol for Dynamic Model Calibration. *Water Sci. Technol.* 65, 1172–1178. doi:10.2166/wst.2012.934

Villaverde, A. F., Barreiro, A., and Papachristodoulou, A. (2016). Structural Identifiability of Dynamic Systems Biology Models. *Plos Comput. Biol.* 12, e1005153. doi:10.1371/journal.pcbi.1005153

Villaverde, A. F., Fröhlich, F., Weindl, D., Hasenauer, J., and Banga, J. R. (2019). Benchmarking Optimization Methods for Parameter Estimation in Large Kinetic Models. *Bioinformatics* 35, 830–838. doi:10.1093/bioinformatics/bty736

Yee, C., Thompson, J. A., Roche, P., Byrd, D. R., Lee, P. P., Piepkorn, M., et al. (2000). Melanocyte Destruction after Antigen-Specific Immunotherapy of Melanoma. *J. Exp. Med.* 192, 1637–1644. doi:10.1084/jem.192.11.1637

Zi, Z. (2011). Sensitivity Analysis Approaches Applied to Systems Biology Models. *IET Syst. Biol.* 5, 336–346. doi:10.1049/iet-syb.2011.0015

Conflict of Interest: NS and JD are named as inventors on a patent on caIKK-RNA-electroporated DCs (WO/2012/055551), which is held by the Friedrich-Alexander-Universität Erlangen-Nürnberg.

Publisher's Note: All claims expressed in this article are solely those of the authors and do not necessarily represent those of their affiliated organizations, or those of the publisher, the editors and the reviewers. Any product that may be evaluated in this article, or claim that may be made by its manufacturer, is not guaranteed or endorsed by the publisher.

Copyright © 2022 Lai, Keller, Santos, Schaft, Dörrie and Vera. This is an open-access article distributed under the terms of the Creative Commons Attribution License (CC BY). The use, distribution or reproduction in other forums is permitted, provided the original author(s) and the copyright owner(s) are credited and that the original publication in this journal is cited, in accordance with accepted academic practice. No use, distribution or reproduction is permitted which does not comply with these terms.

Advantages of publishing in Frontiers

OPEN ACCESS
Articles are free to read for greatest visibility and readership

FAST PUBLICATION
Around 90 days from submission to decision

HIGH QUALITY PEER-REVIEW
Rigorous, collaborative, and constructive peer-review

TRANSPARENT PEER-REVIEW
Editors and reviewers acknowledged by name on published articles

Frontiers
Avenue du Tribunal-Fédéral 34
1005 Lausanne | Switzerland

Visit us: www.frontiersin.org
Contact us: frontiersin.org/about/contact

REPRODUCIBILITY OF RESEARCH
Support open data and methods to enhance research reproducibility

DIGITAL PUBLISHING
Articles designed for optimal readership across devices

FOLLOW US
@frontiersin

IMPACT METRICS
Advanced article metrics track visibility across digital media

EXTENSIVE PROMOTION
Marketing and promotion of impactful research

LOOP RESEARCH NETWORK
Our network increases your article's readership